4 A

STRENGTH AND COMPRESSIBILITY OF GRANULAR MATERIALS UNDER GENERALISED STRAIN CONDITIONS

VOLUME II

thesis submitted to the
University of London
Imperial College of Science and Technology

for the degree of

Doctor of Philosophy in the Faculty of Engineering
by

Gordon E. Green, B.Sc. (Durham), M.S. (Northwestern).

March 1969

List of Contents

		Page
	Title Page	i
	Abstract	ii
	Acknowledgements	iv
	List of Contents	v

VOLUME I

Chapter 1	Purpose and extent of the investigation	
1.1	The relevance to field problems of strength and deformation characteristics measured in laboratory tests.	1
1.2	The scope of this investigation.....	2
1.3	The research programme	4
1.4	Some aspects of the notation and method of presentation.	6
Chapter 2	The strength of granular materials under various 3-dimensional stress systems	
2.1	Non-uniformities and errors in conventional triaxial strength tests.	8
2.1.1	Piston friction.....	8
2.1.2	Sample sheath rigidity.....	8
2.1.3	Filter paper drains.....	9
2.1.4	Sample sheath penetration.....	9
2.1.5	Stress measurements.....	10
2.1.6	Pore pressure effects in clays	10
2.1.7	Platten friction	11
2.1.8	Stress and strain variations within a specimen	12
2.1.9	Stress gradients within a specimen	14
2.1.10	Axial loading condition.....	15
2.1.11	Equality of radial and tangential stresses.....	16
2.1.12	Initial non-uniformities due to difficulties in sample preparation.	19
2.1.13	Specimen anisotropy.....	20
2.2	Theories concerning platten friction	21
2.3	Experiments concerning platten friction and sample proportions.	25

2.3.1	Techniques which have been tried with varying degrees of success.	25
2.3.2	Some techniques tried for concrete and rock.....	27
2.3.3	Lubricated plattens and varying H/D ratio.....	28
2.3.3.1	Experiments on sands.....	29
2.3.3.2	Experiments on clays	32
2.4	Failure theories applied to soils	36
2.4.1	Theories based on continuum mechanics.....	37
2.4.1.1	Mohr-Coulomb, extended Tresca and extended von Mises theories.	37
2.4.1.2	Some other theories.....	38
2.4.2	Theories based on particulate mechanics.....	41
2.4.2.1	Some theories based on ordered packings of spheres.....	41
2.4.2.2	Stress-dilatancy theory	42
2.4.2.3	Some other theories.....	44
2.5	Comparative strengths in triaxial compression and extension.	44
2.5.1	Experiments on sands.....	45
2.5.2	Experiments on clays.....	49
2.6	Comparative strengths in triaxial compression and plane strain.	50
2.6.1	Experiments on sands.....	51
2.6.2	Experiments on clays.....	54
2.7	Comparative strengths as σ_2' is varied continuously between σ_1' and σ_3'.	56
2.7.1	Experiments on cuboidal specimens.....	57
2.7.1.1	Sands.....	57
2.7.1.2	Clays.....	61
2.7.2	Experiments on hollow cylindrical specimens.....	62
2.7.2.1	Sands.....	62
2.7.2.2	Clays.....	65
2.7.2.3	Torsion tests on solid cylinders.....	66
2.8	Important factors involved in developing an adequate independent stress control test.	66

Chapter 3	Preliminary study of the mode of deformation of cylindrical triaxial compression test samples	
3.1	Ideal shear test samples.....	69
3.2	Shape factor for a cylindrical triaxial compression sample.	69
3.3	Previous work.....	70
3.4	Test results.....	70
3.5	Review of mode of deformation.....	73
Chapter 4	Design, development and description of apparatus	
4.1	Triaxial cell for cylindrical compression tests.....	75
4.1.1	Introduction.....	75
4.1.2	Enlarged loading plattens.....	75
4.1.3	Sample sheath.....	76
4.1.4	Internal axial proving ring.....	76
4.1.5	Cell design.....	78
4.2	Triaxial cell for cylindrical extension tests.....	79
4.3	Triaxial cell for cuboidal compression and extension tests.	79
4.4	Independent stress control cell.....	80
4.4.1	Important factors in design.....	80
4.4.2	Cell.....	81
4.4.3	Internal axial proving ring.....	82
4.4.4	Axial loading plattens.....	83
4.4.5	Sample sheath.....	84
4.4.6	Independent stress control belt.....	84
4.4.6.1	Proving ring.....	84
4.4.6.2	Hydraulic ram.....	85
4.4.6.3	Belt and plattens.....	85
4.4.6.4	Suspension wires.....	86
4.4.6.5	Encapsulated dial gauges.....	86
4.5	General arrangement of testing apparatus.....	87
Chapter 5	Description of material tested	
5.1	Particle size analysis and specific gravity.....	88
5.2	Particle breakdown.....	89

Chapter 6	Test programme	
6.1	Introduction.....	90
6.2	Cylindrical triaxial compression test series, 4 ins diameter samples.	92
6.2.1	1st series.....	92
6.2.1.1	Type X, Tests X/1 & X/3 to X/13.....	92
6.2.1.2	Type A, Tests A/1 to A/16.....	92
6.2.1.3	Type B, Tests B/1 to B/9.....	92
6.2.1.4	Type C, Tests C/1 to C/7.....	93
6.2.1.5	Type D, Tests D/1 to D/3.....	93
6.2.1.6	Type B1, Tests B1/1 to B1/4.....	93
6.2.1.7	Type E, Tests E/1 to E/4.....	93
6.2.2	2nd series.....	93
6.2.2.1	Type SA, Tests SA/1 to SA/4.....	94
6.2.2.2	Type SB, Tests SB/1 to SB/5.....	94
6.2.2.3	Type SC, Tests SC/1 & SC/2.....	94
6.2.2.4	Type SD, Tests SD/1 & SD/2.....	94
6.2.2.5	Type SD1, Tests SD1/1 & SD1/2.....	94
6.2.2.6	Type SE, Tests SE/1 & SE/2.....	94
6.2.2.7	Type SF, Tests SF/1 & SF/2.....	95
6.3	Cylindrical triaxial compression and extension test series, 4 ins diameter specimens.	95
6.3.1	Type H, Tests H/1 to H/7, triaxial compression.....	95
6.3.2	Type HA, Tests HA/1 to HA/6, triaxial compression, decreasing σ_3'.	95
6.3.3	Type EX, Tests EX/1 to EX/12, triaxial extension.....	96
6.3.4	Type EL, Tests EL/1 to EL/3, triaxial extension	96
6.3.5	Type ELA, Tests ELA/1 to ELA/4, triaxial extension	96
6.4	Cuboidal triaxial compression and extension test series.	97
6.4.1	Type IB, Tests IB/1 to IB/6, cylindrical triaxial compression.	97
6.4.2	Type IA, Tests IA/1 to IA/10, triaxial compression.....	97
6.4.3	Type IC, Tests IC/1 to IC/4, triaxial compression	97
6.4.4	Type ICE, Tests ICE/2 & ICE/4 to ICE/10, triaxial extension.	98
6.5	Independent stress control test series, cuboidal samples.	98

6.5.1	Type ISC.....	98
6.5.1.1	Tests ISC/1 to ISC/3.....	98
6.5.1.2	Tests ISC/4 to ISC/7.....	99
6.5.1.3	Tests ISC/8 to ISC/18.....	99
6.5.1.4	Tests ISC/19 & ISC/20.....	99
6.5.2	Type IC, Tests IC/5 & IC/6.....	99
Chapter 7	Preparation of samples, test procedure and calculations	
7.1	Specimen preparation.....	100
7.1.1	Cylindrical samples.....	100
7.1.1.1	Normal sample.....	100
7.1.1.2	Two halves sample.....	102
7.1.2	Cuboidal samples.....	103
7.2	Test procedure.....	105
7.2.1	Cylindrical triaxial compression tests.....	105
7.2.2	Cylindrical triaxial extension tests.....	107
7.2.3	Cuboidal triaxial compression and extension tests	107
7.2.4	Independent stress control tests.....	108
7.3	Shear test calculations.....	111
7.3.1	All tests.....	111
7.3.2	Cylindrical samples.....	112
7.3.3	Cuboidal triaxial compression and extension samples....	113
7.3.4	Cuboidal independent stress control samples.....	114
Chapter 8	Cylindrical triaxial compression test results and discussion	
8.1	Introduction	115
8.2	1st series of tests.....	116
8.2.1	Type X.....	116
8.2.2	Type A.....	117
8.2.3	Type B.....	118
8.2.4	Type C.....	118
8.2.5	Type D.....	119
8.2.6	Type E.....	119
8.2.7	Type B1.....	120
8.3	2nd series of tests.....	120

8.4	Comparison of stress-strain and volume change curves...	121
8.5	Comparison of residual strengths.....	124
8.6	Comparison of failure characteristics - 1st series of tests.	125
8.6.1	Comparison of peak strengths.....	127
8.6.2	Comparison of axial strains at failure	129
8.6.3	Comparison of volumetric strains at failure	130
8.6.4	Comparison of volumetric strain rates at failure	131
8.7	Comparison of failure characteristics - 2nd series of tests.	131
8.8	Influence of end restraint and H/D ratio	133

Chapter 9	Cylindrical triaxial compression and extension test results and discussion	
9.1	Introduction.....	136
9.1.1	Type H.....	138
9.1.2	Type HA.....	138
9.1.3	Type EX.....	139
9.1.4	Type EL	140
9.1.5	Type ELA	141
9.2	Comparison of stress-strain and volume change curves ..	141
9.3	Comparison of failure characteristics.....	143
9.4	Comparison of peak strengths.....	145
9.5	Comparison of axial and lateral strains at failure	148
9.6	Comparison of volumetric strains at failure	149
9.7	Comparison of volumetric strain rates at failure	149
9.8	Influence of end restraint, H/D ratio and stress path .	150

Chapter 10	Cuboidal triaxial compression and extension test results and discussion	
10.1	Introduction	152
10.1.1	Type IB	154
10.1.2	Type IA	154
10.1.3	Type IC	155
10.1.4	Type ICE	156
10.2	Comparison of stress-strain and volume change curves ..	157
10.3	Comparison of failure characteristics	158

10.4	Comparison of peak strengths	162
10.5	Comparison of axial and lateral strains at failure	165
10.6	Comparison of volumetric strains at failure	166
10.7	Comparison of volumetric strain rates at failure	167
10.8	Influence of end restraint and H/D ratio	167
Chapter 11	Independent stress control test results and discussion	
11.1	Introduction	170
11.2	Plane strain tests: ISC belt plattens fixed, $\Delta B/B_o = 0$.	173
11.3	Belt plattens opening, $\Delta B/B_o < 0$	175
11.4	ISC belt plattens closing, $\Delta B/B_o > 0$	176
11.5	Plane strain tests: axial plattens fixed $\Delta H/H_o \simeq 0$	179
11.6	Control tests, Type IC	179
11.7	Comparison of stress-strain and volume change characteristics.	180
11.8	Comparison of peak strengths	182
11.9	Comparison of axial and lateral strains at failure	187
11.10	Comparison of volumetric strains at failure	190
11.11	Comparison of volumetric strain rates at failure	191
11.12	Variation of the intermediate principal stress	193
11.13	Comparison of results with some failure theory predictions.	200
11.14	Stress paths in σ_3' = constant space	204
11.15	Correlation of stresses and strains	206
Chapter 12	Summary and conclusions	
12.1	Introduction	210
12.2	Preliminary tests	210
12.3	Cylindrical triaxial compression tests	210
12.4	Cylindrical triaxial compression and extension tests...	210
12.5	Cuboidal triaxial compression and extension tests	211
12.6	Independent stress control tests	212
	List of references	215

VOLUME II

Appendix A1	Equivalent coefficient of friction of lubricated plattens	
A1.1	Choice of lubricant and number of membranes	235
A1.2	Theoretical analysis	235
A1.3	Method of measurement of equivalent μ	236
A1.4	Test technique	237
A1.5	Test results	237
A1.6	Comparison with previous work	237
Appendix A2	Non-uniformity of initial sample porosity	
A2.1	Porosity measurements within samples	239
A2.2	Methods of sample preparation	240
A2.3	Porosity measurements using suction probe	240
A2.4	Test technique	240
A2.5	Test results	241
A2.6	Effect of initial porosity variations on shear behaviour.	242
Appendix A3	Calibration of apparatus	
A3.1	Electro-mechanical stability of proving rings ...	243
A3.1.1	Temperature effect	243
A3.1.2	Zero stability	244
A3.1.3	Long term stability	244
A3.2	Load calibration of proving rings and pressure gauge.	245
A3.2.1	Proving rings	245
A3.2.2	Proving ring calibrator	245
A3.2.3	Accuracy of calibration	246
A3.2.4	Calibration curves	247
A3.2.5	Lateral loads	247
A3.2.6	Ambient pressure	247
A3.2.7	Pressure gauge	248
A3.3	Compressibility of proving rings and lubricated membrane sandwiches.	248

A3.3.1 Axial proving ring in the triaxial cell 248
A3.3.2 Axial proving ring in the ISC cell 249
A3.3.3 ISC belt 250

Appendix A4 Isotropic compression of Belgium Sand
A4.1 Introduction 251
A4.2 Testing technique 251
A4.3 Test results 251
A4.4 Relation to previous work 252

Appendix A5 Cylindrical triaxial compression tests on glass ballotini
A5.1 Introduction 254
A5.2 Test programme 254
A5.3 Test results 255

Appendix A6 Sample sheath strength and platten friction corrections
A6.1 Introduction 258
A6.2 Triaxial compression and extension tests 259
A6.3 Independent stress control tests 259

Appendix A7 Typical test computations
A7.1 Cylindrical triaxial compression 262
A7.2 Cuboidal triaxial extension 264
A7.3 Independent stress control 266

Appendix A8 Graphical presentation of cylindrical triaxial compression test results 269

Appendix A9 Graphical presentation of cylindrical triaxial compression and extension test results 270

Appendix A10 Graphical presentation of cuboidal triaxial compression and extension test results 271

Appendix A11 Graphical presentation of independent stress control test results 272

Appendix A1

Equivalent coefficient of friction of lubricated plattens

Tests were made to measure the equivalent coefficient of friction between a polished, flat metal surface and a thin rubber membrane lubricated with silicone grease. Previous measurements by Roscoe (1953), Wood (1958), Freedman (1959), Gray (1960), Blight (1961), Casagrande & Poulos (1964), Rowe & Barden (1964), Barden & McDermott (1965), Duncan & Dunlop (1968) have suggested that a system consisting of a solid platten-lubricant-rubber membrane - soil, has a low equivalent coefficient of friction. Low friction materials such as polytetrafluoroethylene (P.T.F.E., Fluon, Teflon) are so soft that soil particles will become embedded and the resultant scouring of the surface of the platten results in a high coefficient of friction. The material of the solid platten is of little consequence provided it is flat and smooth, Rowe & Barden (1964). Clearly a hard corrosion - free material such as brass or stainless steel will stay smooth longer and would be most suitable.

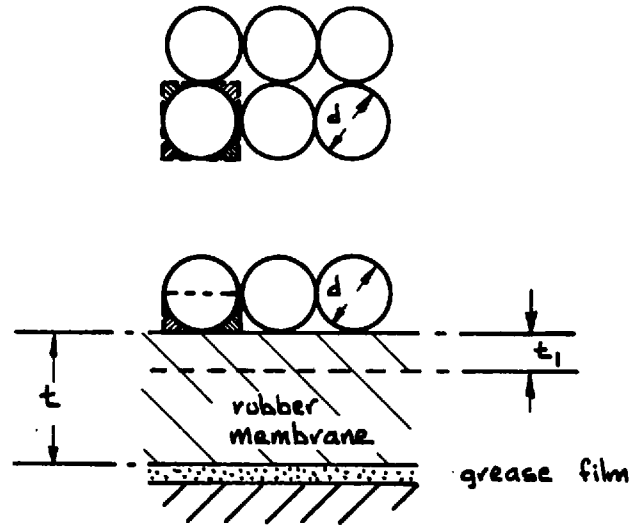
A1.1 Choice of lubricant and number of membranes

A number of lubricants have been tried. The most effective has been found to be silicone grease which, being chemically inert, does not attack natural rubber. In addition, because of its molecular structure, silicone grease is not easily squeezed out from between the rubber membrane and the solid platten under high contact pressure. The criteria for a choice of the number and thickness of rubber membranes appears to have received little or no attention. It is reasonable to expect that the thickness of the membrane should be related to the grain size of the soil. A thin membrane is capable of being squeezed locally into the pore space between adjacent grains. The soil grains may, in the limit, penetrate the rubber membrane and make contact with the platten. Even if this does not occur the silicone grease directly under the grain contacts may be squeezed into the adjacent areas where the stress is theoretically zero, assuming a drained test.

A1.2 Theoretical analysis

If we consider an ordered packing of spheres, as shown in Fig A1.1 we

Consider an ordered single layer of spheres in contact with a lubricated membrane :



Volume of half-sphere $= \frac{1}{12}\pi d^3$

Circumscribing volume $= \frac{1}{2} d^3$

Volume of pore space per sphere available for membrane penetration $= \left(\frac{1}{2} - \frac{\pi}{12}\right) d^3$

$= 0.238\, d^3$

Thickness of membrane that may be forced into the pore-space, t_1 $= \frac{0.238\, d^3}{d^2}$

$= \frac{1}{4} d$

Sphere diameter, m.m.	0.2	0.4
t_1, inches	0.002	0.004

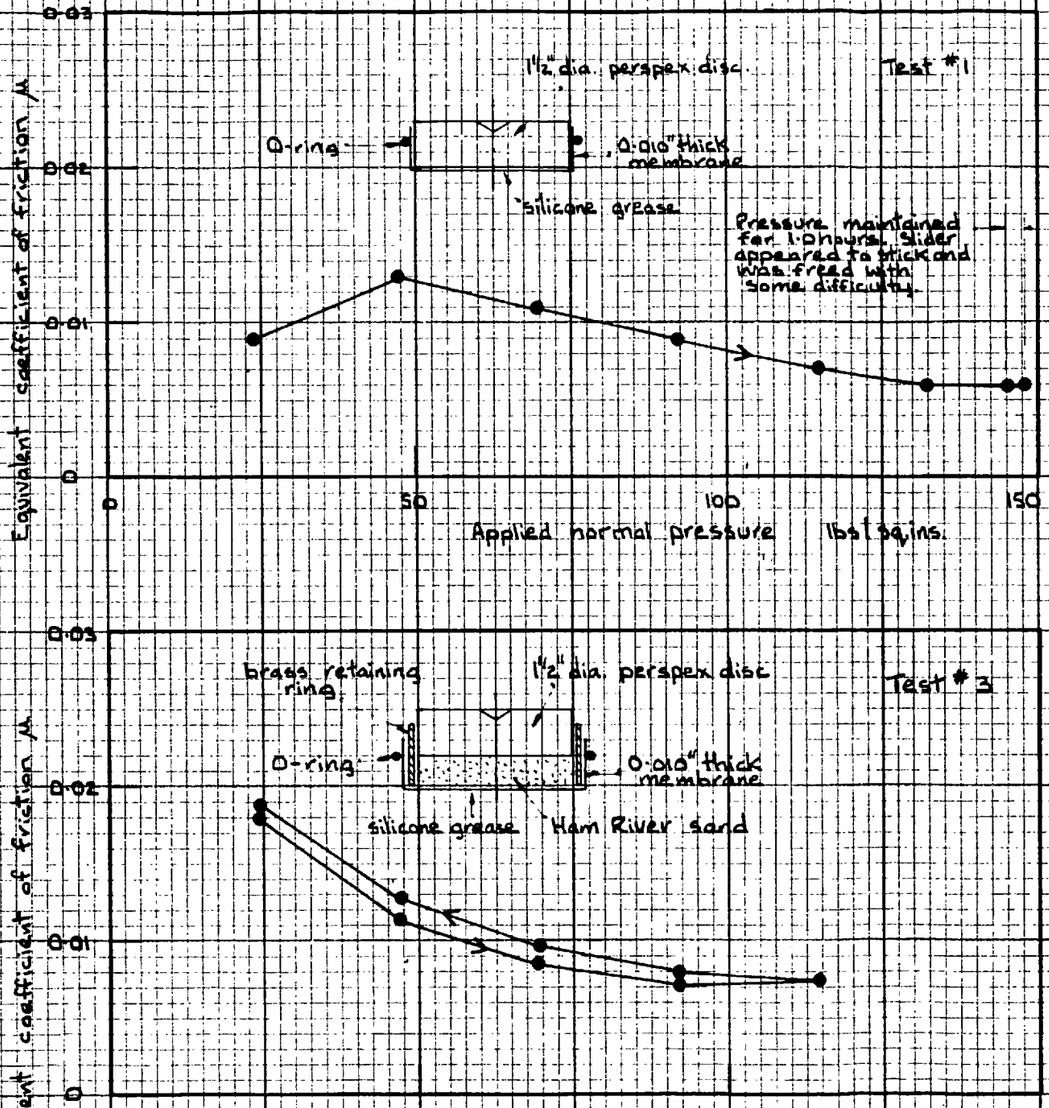
FIG. A1.1

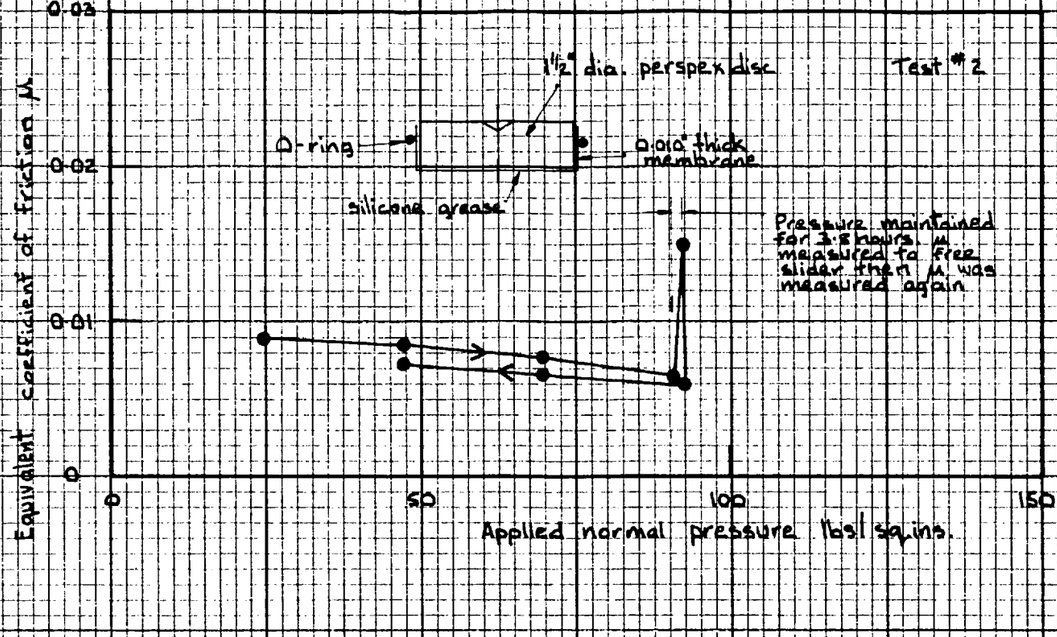
can calculate the thickness of membrane that can be squeezed into, and just fill, the pore space. This thickness, t, is shown to be equal to one quarter of the sphere diameter, d. Hence a membrane 0.002-0.004 ins thick could, theoretically, be completely displaced into the pore space of the Ham River sand used. Clearly a membrane thickness in excess of this is needed. Initially a single 0.009 ins thick membrane was chosen although subsequent triaxial compression tests using a sandwich of 2/0.009 ins thick membranes gave more acceptable results. It is possible that a larger number of thinner membranes would be even better but this remains to be investigated. The membrane in immediate contact with the end of the sample transmits a shear stress, proportional to its thickness, to the sample. This is in addition to any shear stress transmitted across the grease film. Hence it may be advantageous to reduce the thickness of the membrane in immediate contact with the sample.

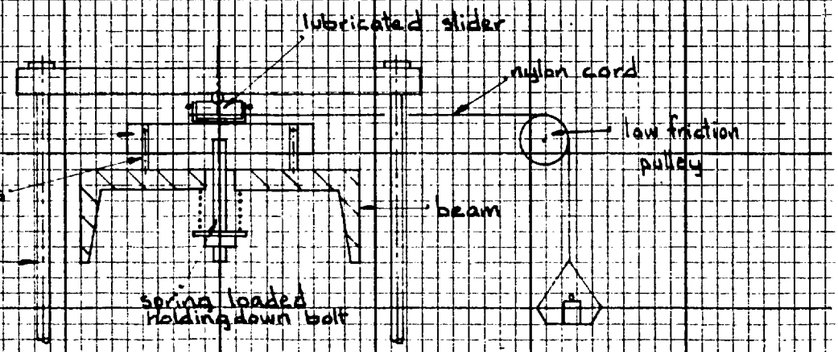
A1.3 Method of measurement of equivalent μ

The equivalent coefficient of friction of a grease film was determined by the friction slider test shown in Fig A1.2. Previous measurements by Wood (1958), Freedman (1959), Gray (1960), Blight (1961), Rowe & Barden (1964), were made using a shear box, whereas Casagrande & Poulos (1964), Duncan & Dunlop (1968), used a friction slider technique. As the equivalent coefficient of friction to be measured is very small (1 degree or less) two important test conditions must be fulfilled. Firstly the surface must be horizontal and secondly there must be no significant additional unknown friction in the system. The apparatus shown in Fig A1.2 fulfills these criteria.

A polished flat brass plate with 3 levelling screws was placed at the mid-point of a simply supported beam. The plate was levelled before a test with a spirit level having a sensitivity of 5 minutes of arc. The level of the plate was checked after application of the normal load. Two types of slider were used. Firstly a polished, flat perspex disk covered with 1/0.010 ins thick lubricated natural rubber membrane and secondly a brass ring retaining Ham River sand and covered with a 1/0.010 ins thick natural rubber membrane, Fig A1.2. The membrane-platten interface was lubricated with silicone grease, Midland Silicone Releasil 7.







MEASUREMENT OF COEFFICIENT OF FRICTION OF SILICONE GREASE FILM.

FIG. A1.2

A1.4 Test technique

In the tests a normal dead load was placed on the hanger and a lateral load was applied to the slider by means of a nylon cord passing over a low friction pulley. The line of action of the nylon cord was adjusted to be as close to the sliding surface as possible. The lateral load was increased until the slider just began to move, as detected by the naked eye. It was found in preliminary tests that if the slider were moved back and forth across the brass plate whilst applying or removing the normal load increments it was possible to induce dry spots on the interface and the equivalent coefficient of friction would increase many times. This should not occur during a shear test.

A1.5 Test results

The 3 tests are consistent and indicate that μ decreases with increasing applied normal pressure and that under a constant normal pressure μ will increase with time if the slider is at rest. However if the slider were moving continuously, as would be the case in a shear test, no increase would appear likely. An equivalent coefficient of friction, $\mu = 0.01$ (0.6°) is deduced from the test data.

A1.6 Comparison with previous work

Wood (1958) obtained a value of $\mu = 0.018$ (1.0°) for Releasil 7 using a 0.010-0.015 ins thick membrane backed up by Glen Shira moraine in a conventional 6cm x 6cm shear box. As the material was a well-graded sandy gravel passing a $\frac{3}{8}$ins B.S. sieve it is probable that minute dry spots occurred on the membrane-platten interface due to the presence of larger particles. The maximum applied normal pressure was 30 psi, which is low compared with the range of the present tests and is also low compared with the range of stresses in Wood's shear tests.

Rowe & Barden (1964) report a value of μ generally less than 0.018 (1.0°) obtained in immediate tests with sand and a silicone grease, Midland Silicone Valve Seal A. Barden & McDermott (1965) obtained a similar value of μ using a more viscous grease, Midland Silicone High Vacuum, which had the additional advantage of being more resistant to being squeezed out under prolonged high stress.

Casagrande and Poulos (1964) were unable to achieve a value of μ lower than 0.052 (3°) using Dow-Corning stopcock grease. However, there is

no reason to presume that all silicone greases posses the same viscous properties, indeed Barden & McDermott's tests indicate they do not.

Appendix A2

Non-uniformity of initial sample porosity

The initial porosity within a shear test specimen may vary due to the inadequacy of the method of sample preparation. During the subsequent application of boundary stresses to the specimen, non-uniform changes in porosity may occur due to the non-uniformity of the applied stresses. At shear failure an instability mechanism may be induced which causes large displacements along a preferential set of planes. A prime object of the present work was to try to develop an experimental technique that would allow a uniform system of boundary stresses to be applied to a sample of saturated sand. It is believed that if a sufficiently uniform sample could be prepared and subjected to a sufficiently uniform stress system then it may be possible to apply very large strains to the sample without the formation of predominant slip zones.

A2.1 Porosity measurements within samples

The preparation of a uniform test specimen of sand has proved extremely difficult if not impossible. A major complication is to find a technique, preferably non-destructive, of measuring the porosity at different points throughout the specimen. Methods used in the past include, (a) freezing the sample, slicing it into segments and measuring their porosity by a volume displacement technique, Shockley (1953), Shockley & Ahlvin (1960), (b) injection of grout, slicing into segments and measuring their porosity by a volume displacement technique (Skipp & Renner (1963) give details of a grouting technique that could be used), (c) careful sampling of a saturated medium-dense or dense sample and calculating the porosity from a water content determination, Cornforth (1961), (this method is not practicable for loose samples). These three methods are all destructive and can only be used to determine the initial porosity of a subsequently tested sample if one accepts that it is possible to prepare two identical specimens. The only non-destructive method known to be presently used is the transmission X-ray technique developed by Roscoe et al (1963c), Arthur et al (1964). This method has proved satisfactory for plane strain conditions where the X-rays are shot through in the σ_2 direction; clearly they would have great difficulty in coping with displacements in 3 directions.

A2.2 Methods of sample preparation

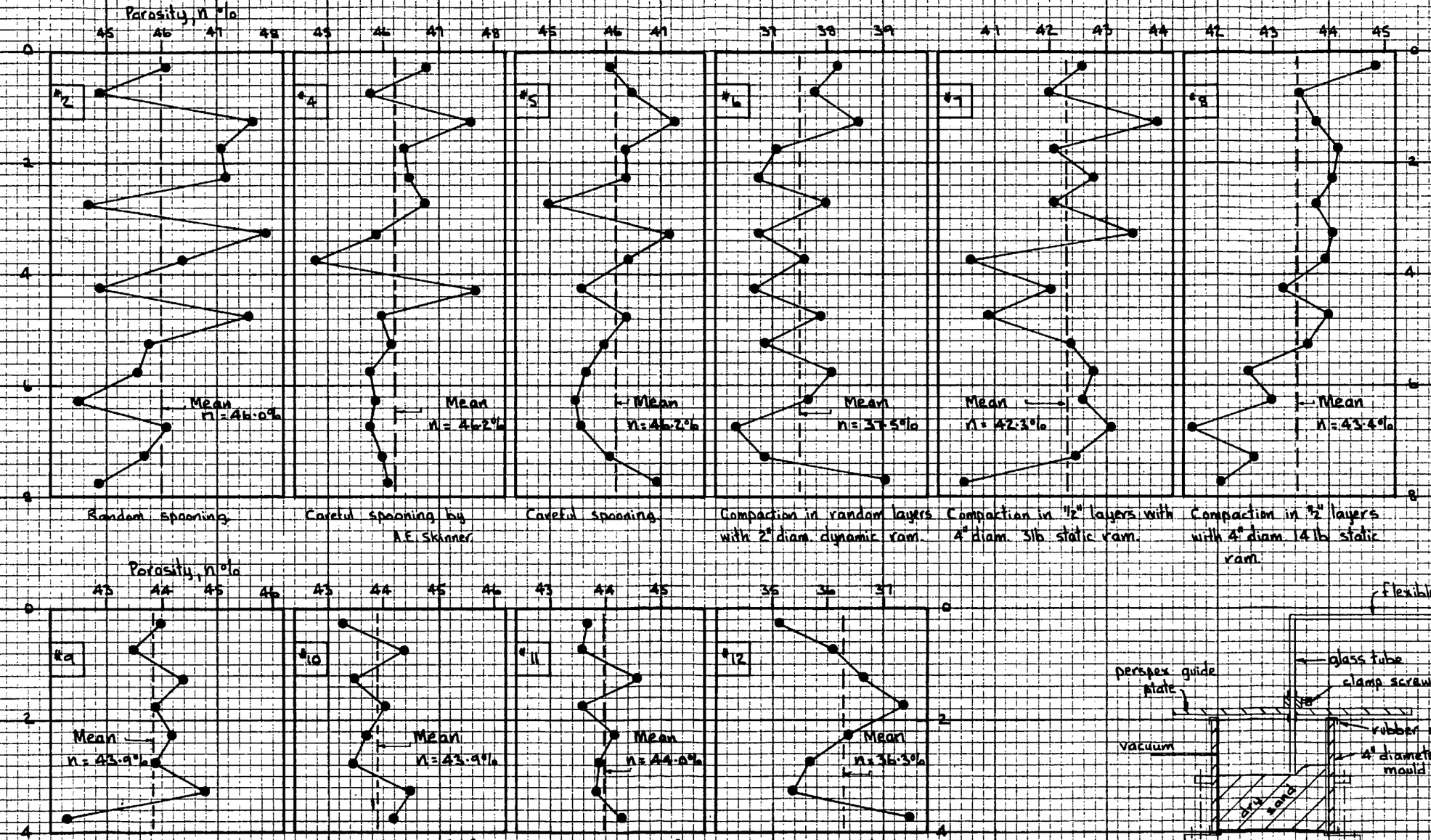
Various sample preparation techniques have been developed. A sample may be prepared from dry sand or from saturated sand. If the sand is initially dry the sample may be subsequently saturated by displacing the air with water but complete saturation is impossible to achieve unless a back pressure is applied to the sample in addition. Alternatively the air may be replaced with ammonia gas which, being very soluble, is more easily replaced by water, Waterways Experimental Station (1950), Casagrande & Wilson (1951). Shockley & Ahlvin (1960) achieved a degree of saturation of 99% or greater using this method. However the very small amount of air remaining in the sample is probably concentrated at the contacts between the sand grains and may have an effect on the shear behaviour. It is therefore better to prepare a specimen from an initially saturated sample to avoid this additional complication. Against this however, it may be easier to prepare a uniform sample of dry sand than of wet sand. The best known method of depositing sand in a uniform manner is by pouring dry sand from a tube, Kolbuszewski (1948a, 1948b), or by means of a roller if the area is large, Walker & Whitaker (1967). By controlling the height and intensity of deposition a wide range of porosities can be obtained. This technique is not suitable for a saturated sand sample which can best be formed by deposition under water with controlled tamping or vibration, Bishop & Henkel (1957). The latter method appears to be the best compromise and was the method used in preparing all the shear test specimens.

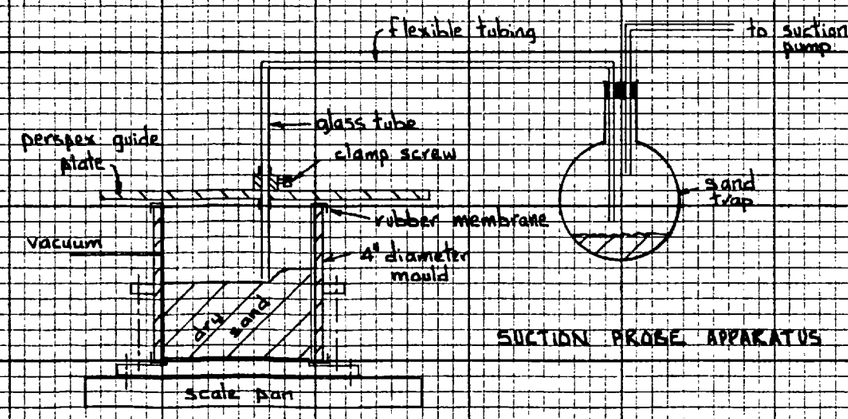
A2.3 Porosity measurements using suction probe

A series of experiments were performed to try to measure the porosity variation in a 4 ins diameter specimen of dry sand using various methods of sample preparation. The sand used was Belgium sand, Sable de Mol, Ladanyi (1960), Wade (1963). The result of these experiments together with the apparatus used is shown in Fig A2.1.

A2.4 Test technique

A 4 ins diameter mould, 4 ins or 8 ins high as required, was lined with a 0.010 ins thick rubber membrane and bolted to the scale pan of a 7kg balance reading to 1gm. The space between the membrane and the mould was completely lined with a rectangular sheet of paper towel and a vacuum





SUCTION PROBE APPARATUS

POROSITY MEASUREMENTS USING SUCTION PROBE

All tests on Belgium sand (Sable de Mol).

FIG. A2.1

applied to hold the membrane securely against the mould. After a sample had been prepared in the mould and carefully levelled off with a straight-edge the weight was recorded. A suction probe consisting of a glass tube about 0.1 ins I.D.connected by a flexible tube to a sand trap was used to remove the prepared sand from the mould in $\frac{1}{2}$ ins layers. The probe was clamped rigidly into a perspex guide plate. The length of probe extending below the guide plate was measured with a vernier caliper reading to 0.001 ins. The depths of the first two $\frac{1}{2}$ ins layers that were removed were measured at 4 points around the rim of the mould with a 1 ins micrometer depth gauge reading to 0.001 ins. From these two sets of readings together with the respective sets of vernier caliper readings a probe 'end correction' was obtained. Provided the suction applied to the probe was constant then the distance from the end of the probe to the sand surface was constant throughout the experiment. After removing each $\frac{1}{2}$ ins layer the depth was recorded together with the weight of the mould and sand remaining. Great care was taken to prevent the scale pan from jarring and disturbing the sand.

A2.5 Test results

Test 2 shows a range in porosity of 3.2% for a randomly placed loose sample with a mean porosity of 46.0%. Test 4, by a second operator using a careful spooning technique, shows a range of 2.7% with a mean of 46.2% and a further sample, Test 5, showed a range of 2.2% and an identical mean porosity. Tests 6,7 & 8 using a dynamic and two static ram techniques all show large ranges in porosity of 2.7%, 3.4% & 3.4% respectively. In all, Tests 2-8 on 8 ins high samples show an excessively wide variation in porosity within each sample. In tests 9,10 & 11 identical methods of sample preparation were used, static compaction in $\frac{1}{2}$ ins layers. The mean porosities were 43.9%, 43.9% & 44.0% respectively with porosity ranges of 2.5%, 1.2% & 1.0% respectively. These three tests suggest that the operator's technique was fairly consistent (the measured porosity range in Test 9 was biased by a very low porosity at the base of the sample which may be in error). In Test 12 the sample was vibrated in random layers and it is seen that the measured porosities can be considered to follow a smooth S-shaped curve. A similar phenomenon has been observed in vibrated dry sand by Mogami & Kubo (1953). Any porosity variations in a vibrated

sample might be expected to be continuous compared with those in a tamped sample. This appears to be the case and gives strong support to the argument that the porosity variations measured are all real and are not significantly affected by testing errors.

A2.6 Effect of initial porosity variations on shear behaviour

An initial variation of 1% within a sample might be considered tolerable whereas a variation of from 2 to 3% appears completely unacceptable for reliable shear test samples. Since all the shear tests reported in this thesis are on saturated samples prepared by deposition under water and subsequently tamped or vibrated one may question the relevance of the above results. Clearly some differences will occur but no fundamentally different principle appears to be involved.

The different series of shear tests over a widely varying porosity range were all self-consistent. Although the lowest porosities were only obtained by vibration there is no apparent discontinuity between the behaviour of vibrated and tamped samples.

In spite of the large measured porosity variations within any one sample the overall consistency of the shear test data is remarkably good. Thus one may postulate that an initially non-uniform sample may, upon application of a uniform all-round stress, and even more so upon application of a subsequent uniform deviator stress, initially tend toward a more uniform state. This postulate does not of course hold at or beyond failure.

Appendix A3

Calibration of apparatus

A3.1 Electro-mechanical stability of proving rings

As the proving rings and associated electrical equipment used to measure the axial load and ISC belt load were new in the laboratory it was considered necessary to devote some effort to determining their behaviour characteristics. The temperature effect, zero stability and long term stability checks were mainly performed on the axial proving ring as this was obtained first.

A3.1.1 Temperature effect

As the commercially available mountings for the ring were unsuitable the fittings described in Chapter 4 were designed and manufactured. The 4-arm differential inductance type displacement transducer, type F52, together with the C61 transducer meter is capable of detecting a linear displacement of 1×10^{-6} ins. Since the coefficient of linear expansion α, of steel is $10 \times 10^{-6}/^{\circ}C$ it is clear that the system may act as an excellent thermometer if mounted on say a 1 ins steel gauge length. Clearly this is most undesirable. Attempts were made to calculate the theoretical expansion per $^{\circ}C$ for various mounting designs. Two sets of mountings were made up, Fig 4.2, one of brass and the other of steel ($\alpha_{brass} = 2.\alpha_{steel}$). The part-assembled ring was placed in a temperature controlled oil-bath and the temperature cycled. The brass mountings gave a temperature coefficient for the ring plus mountings of 9×10^{-6} ins/$^{\circ}C$ whereas the steel mountings gave a temperature coefficient, of from 3 to 5 $\times 10^{-6}$ ins/$^{\circ}C$. However, the calculation of α is subject to major assumptions concerning the construction of the transducer body and its mounting on the proving ring. The phase-sensitive coils are encapsulated in araldite in the transducer body and the radio-metal armature is a push fit in a split brass tube. Clearly the precise behaviour of these components under varying temperature is difficult to assess.

It had been hoped to be able to design temperature compensated mountings but this proved more difficult than was anticipated. Should this type of

proving ring be used in a more variable temperature environment this would be worth pursuing. The brass mountings were selected and the proving ring reassembled and calibrated in a temperature bath, Fig A3.1. The mean temperature coefficient of the assembled ring was 6.5×10^{-6} ins/^{o}C, i.e. 0.8 lbs/^{o}C. The air temperature in the laboratory is not likely to vary over a 3 to 4 hour test period by more than 1^{o}C and in view of the insulating effect of the cell water and oil around the ring the actual variation in ring temperature during a shear test will be much less.

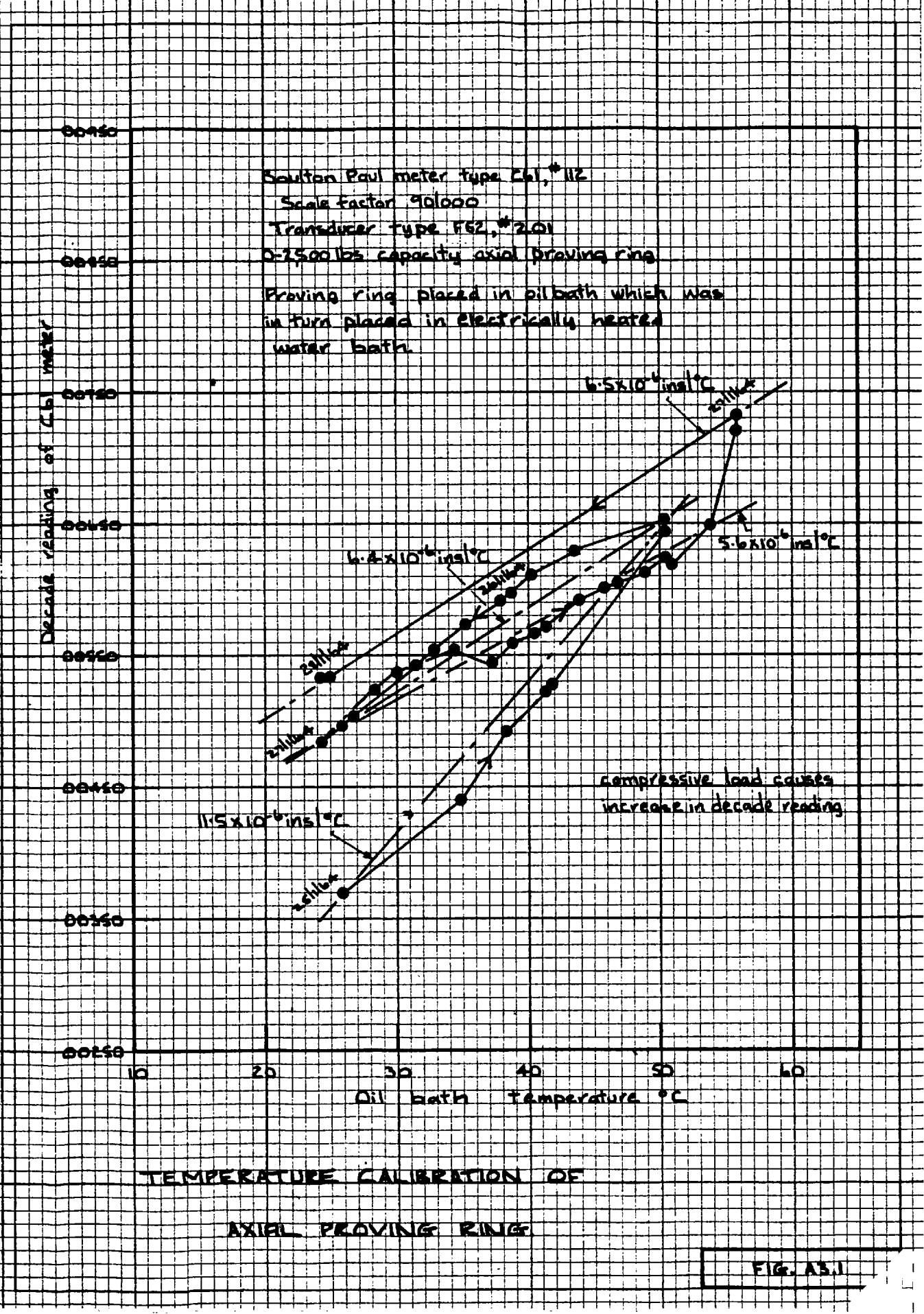
A3.1.2 Zero stability

A check was made on the zero stability of the axial proving ring over a 6-day period. The ring was placed in an oil-bath in the laboratory and the oil-bath temperature adjacent to the ring recorded, Fig A3.2. It is observed that the oil-bath temperature rises during the day-time and falls during the night. The C61 meter readings vary in a random manner and do not correlate well with temperature. Momentarily switching off the power supply to the C61 meter caused a small change in the reading. The overall variation in reading corresponds to a load change of 1.9 lbs, whereas the load change over a 4 to 6 hour period is much less than this. It is this latter change that is significant in the present test programme.

A more limited check was made on the zero stability of the ISC belt proving ring over a 6 day period but nearly 3 years later. The assembled ring, Fig 4.6, was placed on the laboratory bench and the air temperature adjacent to it was recorded, Fig A3.3. The C61 meter readings vary more than for the axial proving ring whereas the temperature variations are significantly less. The reasons for this are not entirely clear, The axial proving ring had a Parkerised finish whereas the ISC belt proving ring was chrome-plated. The makers report that they no longer chrome-plate the rings due to hysteresis problems. Although obtained at a later date the chrome-plated ring was manufactured much earlier than the Parkerised ring and had since been used for demonstration purposes. This may account for the difference in zero stability between the two rings.

A3.1.3 Long term stability

During the test programme the axial proving ring was loaded and unloaded many times. It was used both in compression and extension. Hence it is



TEMPERATURE CALIBRATION OF AXIAL PROVING RING

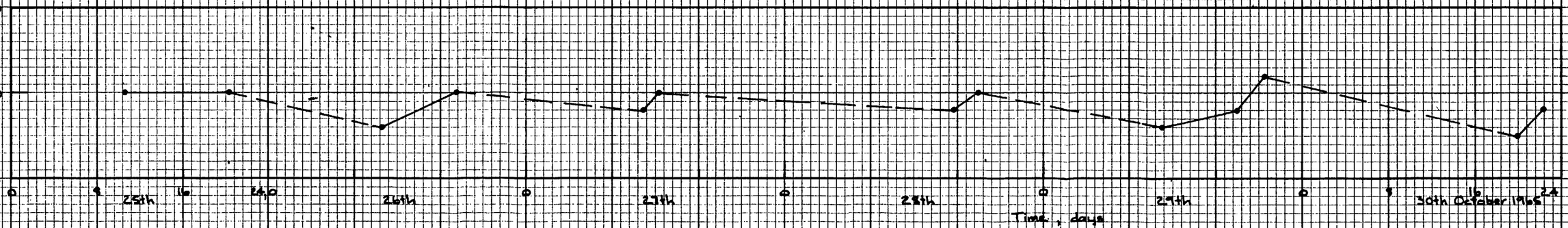
FIG. A3.1



ZERO STABILITY TEST ON AXIAL PROVING RING.

FIG. A3.2.





ZERO STABILITY TEST ON I.S.C. BELT PROVING RING.

FIG. A3.3

of interest to note how the zero reading of the ring varied over the 3 year test period. The decade reading on the C61 meter just before commencing the shear stage is plotted against time in Fig A3.4. Between February 1964 and August 1965 the ring was used in compression only and the zero readings were fairly consistent. From September 1965 to December 1966 the ring was used both in compression and extension and two new mean zero readings were established.

It was established that part of the variation in the zero reading during any test series was due to contamination of the contacts in the line plug and socket in the electrical lead. This was necessary to enable the proving ring and cell to be assembled. It could probably be reduced by using a better quality plug and socket with gold plated contacts. This problem is also discussed by Lovenbury (1969).

Since the load measured in any single test was obtained by subtracting the instantaneous decade reading at any stage in the test from the reading at the commencement of the test the variations shown in Fig A3.4 are largely eliminated.

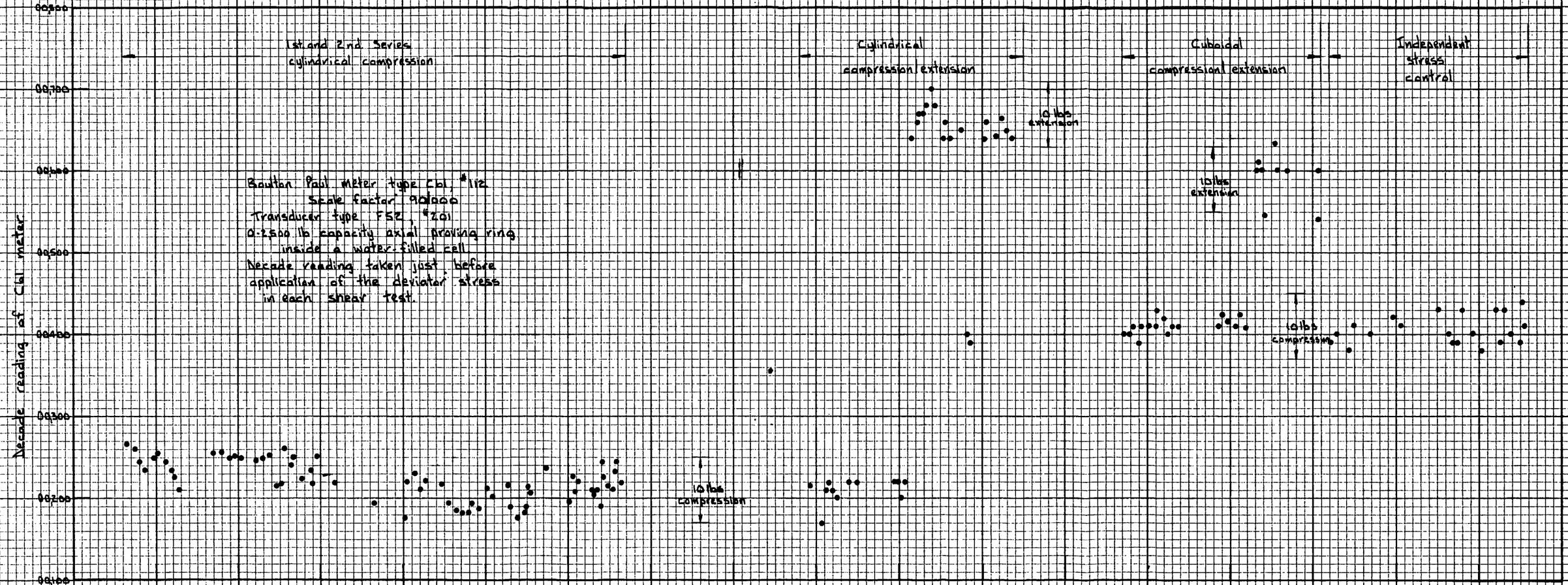
A3.2 Load Calibration of proving rings and pressure gauge

A3.2.1 Proving rings

In attempting to produce a set of self-consistent data over a long period of time it is important to be able to calibrate the proving rings and pressure gauge at reasonable intervals against a relatively invariant standard. It is also desirable that they are each calibrated against the same standard since if not, the computed principal stresses, σ_1', σ_2' & σ_3', may not be comparable. A difficulty in relating compression and extension test results arises because ϕ' obtained in an extension test is very sensitive to errors in the cell pressure, as is well known. The method of calibration is shown in Fig A3.5 and Plate A3.1.

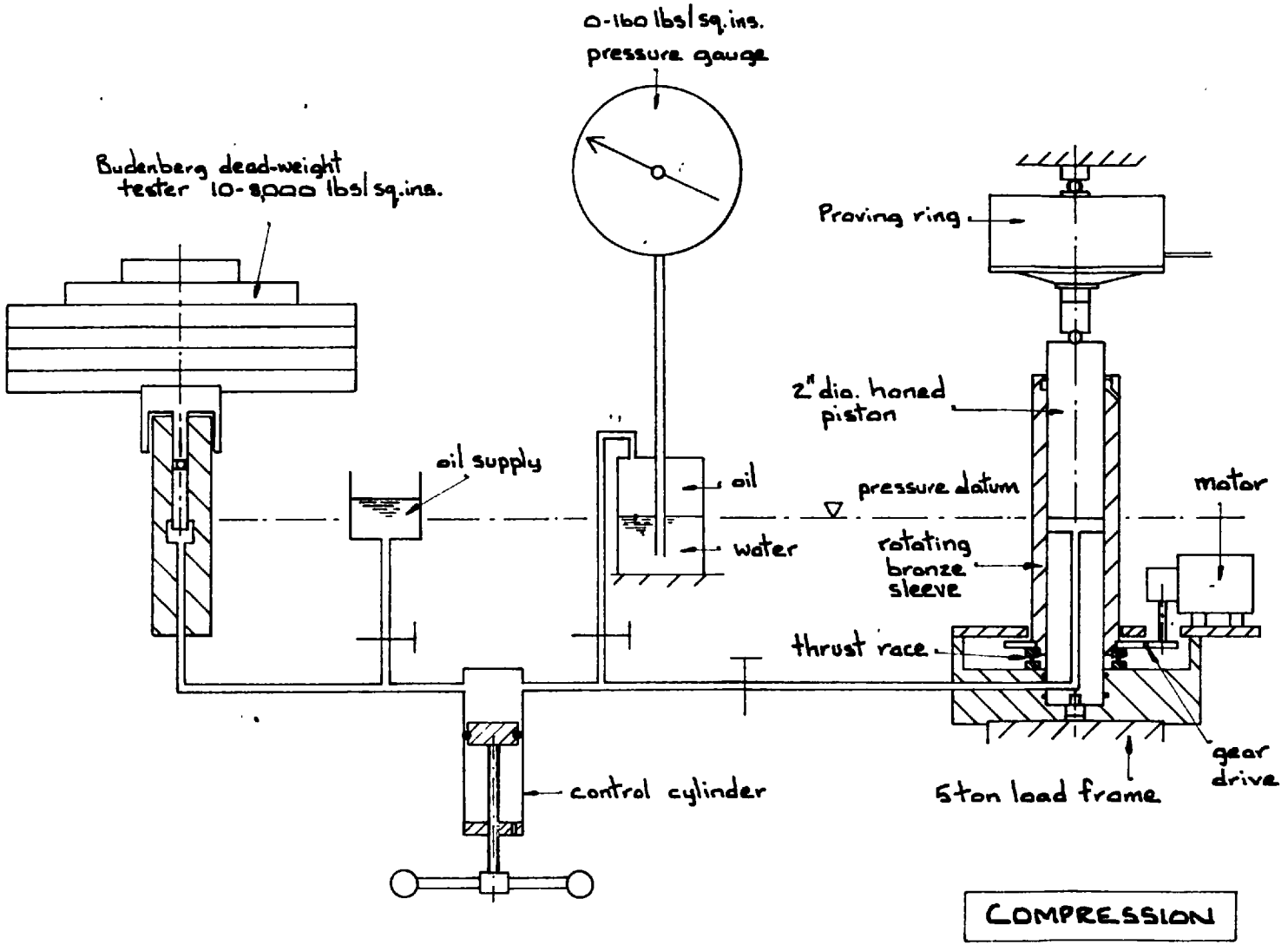
A3.2.2 Proving ring calibrator

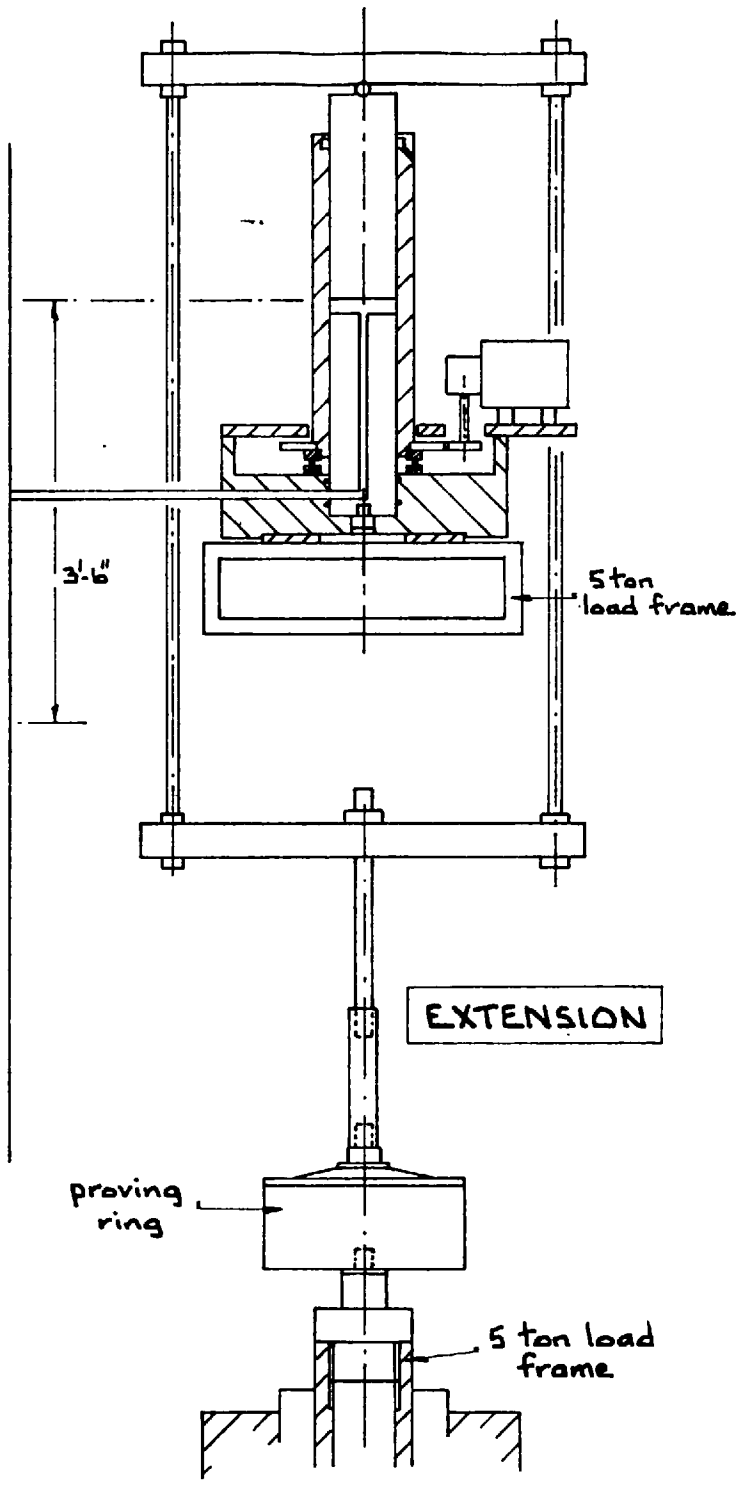
A Budenberg dead-weight tester was used having a range of 10-8000 psi with an accuracy better than 0.03% of the pressure being measured. This incorporated a dual range patented piston unit (not shown in Fig A3.5) designed to reduce the dead load required for so large a pressure range.



STABILITY OF AXIAL PROVING RING OVER THREE YEAR PERIOD

FIG. A5.4





APPARATUS USED TO CALIBRATE PROVING RINGS AND PRESSURE GAUGE.

FIG. A3.5



APPARATUS USED TO CALIBRATE PROVING RINGS

PLATE A3.1

The unit consists of two concentric pistons of areas $\frac{1}{8}$ and 1/80 ins^2 which cover pressure ranges 10-800 and 100-8000 psi respectively. During all calibrations it was necessary to rotate the piston of the dead-weight tester by slowly spinning the weights in order to minimise friction.

To calibrate the proving rings the known fluid pressure supplied from the dead-weight tester was used to lift a 2 ins diameter honed stainless steel piston running in a phosphor bronze bushing. To minimise friction errors the bushing was rotated at about 1 rpm by an electric motor through a gear box. The self-weight of the bushing was carried on a ball thrust race. For a compression calibration the proving ring calibrator together with the proving ring were placed on the pedestal of a 5-ton triaxial compression machine to provide a rigid reaction and to ensure good alignment (Plate A3.1 shows the proving ring calibrator together with a conventional 3000 lb ring installed in a lighter triaxial compression machine). For an extension calibration the proving ring calibrator was placed on top of the crosshead of the 5 ton triaxial machine. The proving ring was screwed via an adapter to the pedestal and was connected to the calibrator by a hanger system.

Whereas the dead-weight tester worked best with a light oil (SAE 20) the 2 ins diameter piston and bushing had been poorly honed so that the upper end of the bushing was belled and caused excessive oil loss under the higher pressures. It was therefore necessary to use a heavier oil (SAE 50) in the system.

A3.2.3 Accuracy of calibration

The effective piston area used in the computation was the mean of the diameter of the piston and the inside diameter of the bushing. These were obtained with precise instruments reading to 0.00001 ins and 0.0001 ins respectively. The average piston diameter was 1.99545 ins and the average diametral clearance was 0.001 ins. Since an error in the measured effective piston diameter of 0.001 ins represents a loss of 0.1% accuracy it is probable that an accuracy better than 0.05% was obtained. In addition there is an error due to the increase in piston diameter and bushing diameter under pressure. Theoretically the phospor bronze bushing will increase in diameter by about 0.0003 ins under an internal pressure of 1000 psi. This corresponds to an error of about 0.03% and was neglected. An error of

0.1% corresponds to an error of 2 lbs in a measured deviator load of 2000 lbs. This problem is considered in detail by Johnson et al (1957).

A3.2.4 Calibration curves

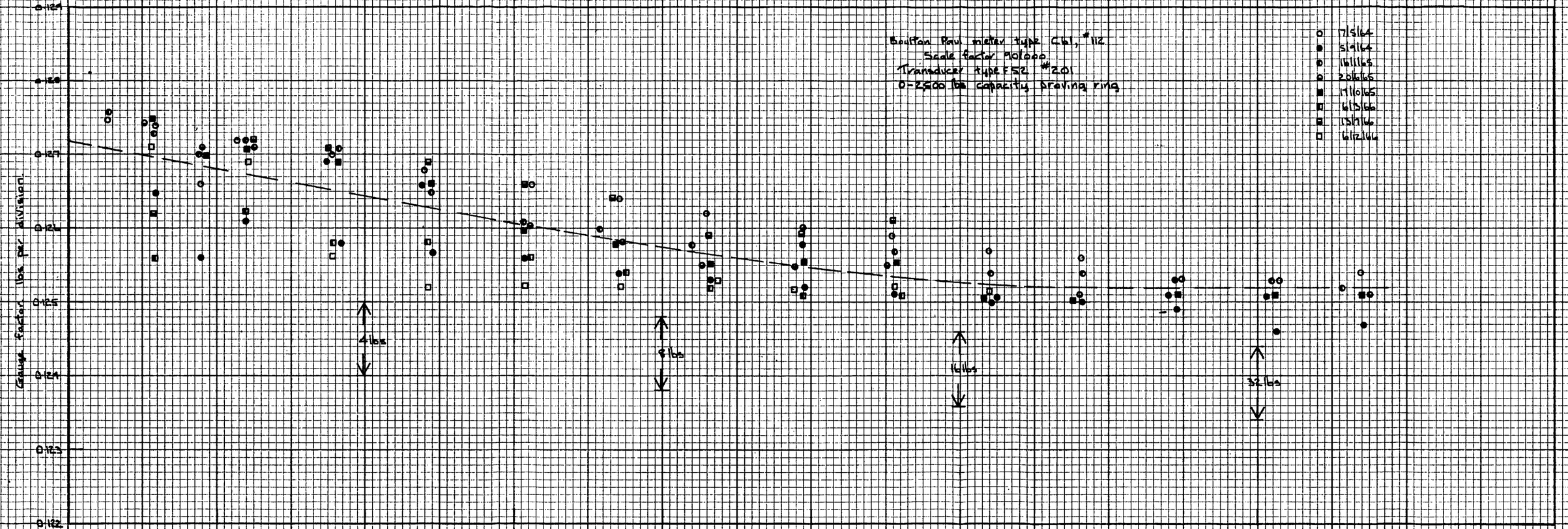
The compression and extension calibrations of the axial proving ring and the compression calibration of the ISC belt proving ring are shown in Figs A3.6, A3.7 & A3.8 respectively. The compression curve for the axial proving ring indicates that the gauge factor for the ring decreasesfrom about 0.127 lbs/division to 0.125 lbs/division as the load increases and is fairly flat in the upper 50% of the load range. The extension curve for the axial proving ring shows a decrease in gauge factor from about 0.127 lbs/division to 0.124 lbs/division and is similarly flat in the upper 50% of the load range. The scatter in the points is, in part, random but does show a reduction in gauge factor with time. The compression curve for the ISC belt proving ring indicates that the ring is 18-21% more sensitive than the axial proving ring and the gauge factor decreases slightly with time. As a check on the calibration a 50 lb dead load was applied to the ISC belt proving ring and the agreement is seen to be excellent. The mean curves were used in the computations.

A3.2.5 Lateral loads

In view of the possibility of lateral loads being applied to the proving rings due to distortion of the sample the lateral stability of the axial proving ring was determined. The ring was clamped in a vertical position by means of the tapped hole in the loading anvil (Fig 4.2) and a lateral load applied by a steel wire. Care was taken to maintain the steel wire in a horizontal position, the load being recorded on a proving ring in tension. The axial proving ring was tested under zero normal load. The results are given in Fig A3.9 and suggest that the errors due to possible lateral loads will be very small and will not materially affect the interpretation of the results. Based on observations by Webb (1966) this error is likely to be less than 0.4% of the axial load on long samples with unlubricated plattens and therefore to be much smaller in all tests with lubricated plattens.

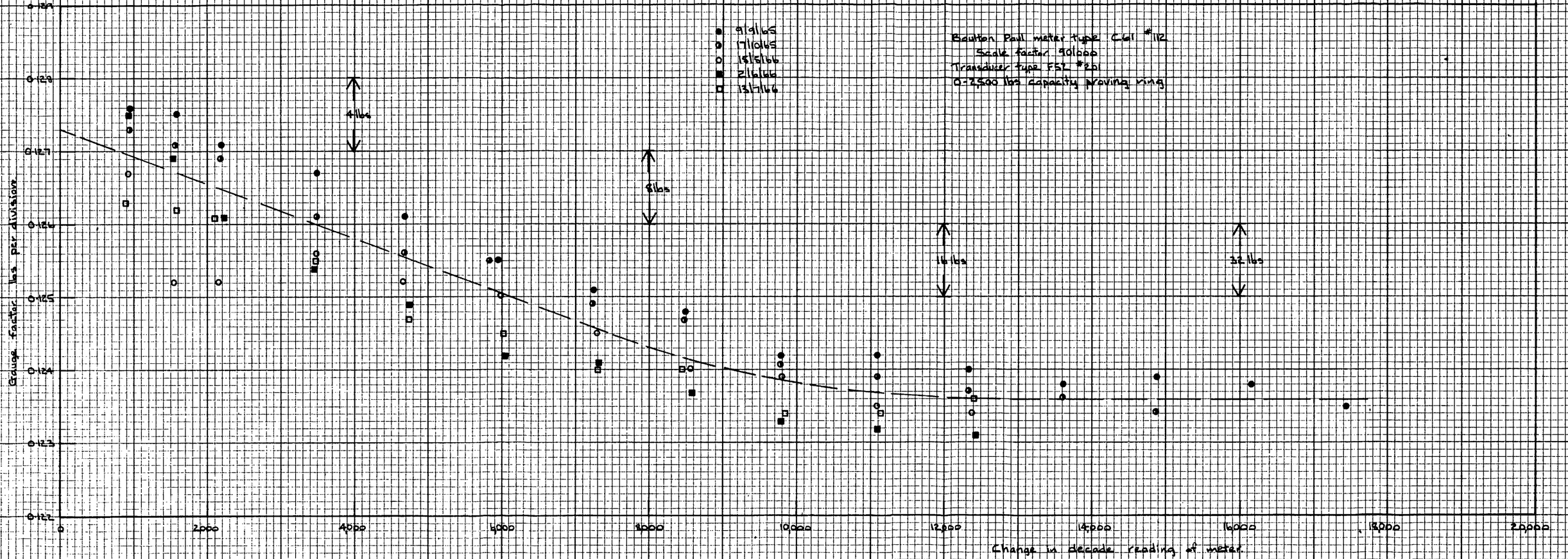
A3.2.6 Ambient pressure

It was observed that the zero load reading of the proving rings was



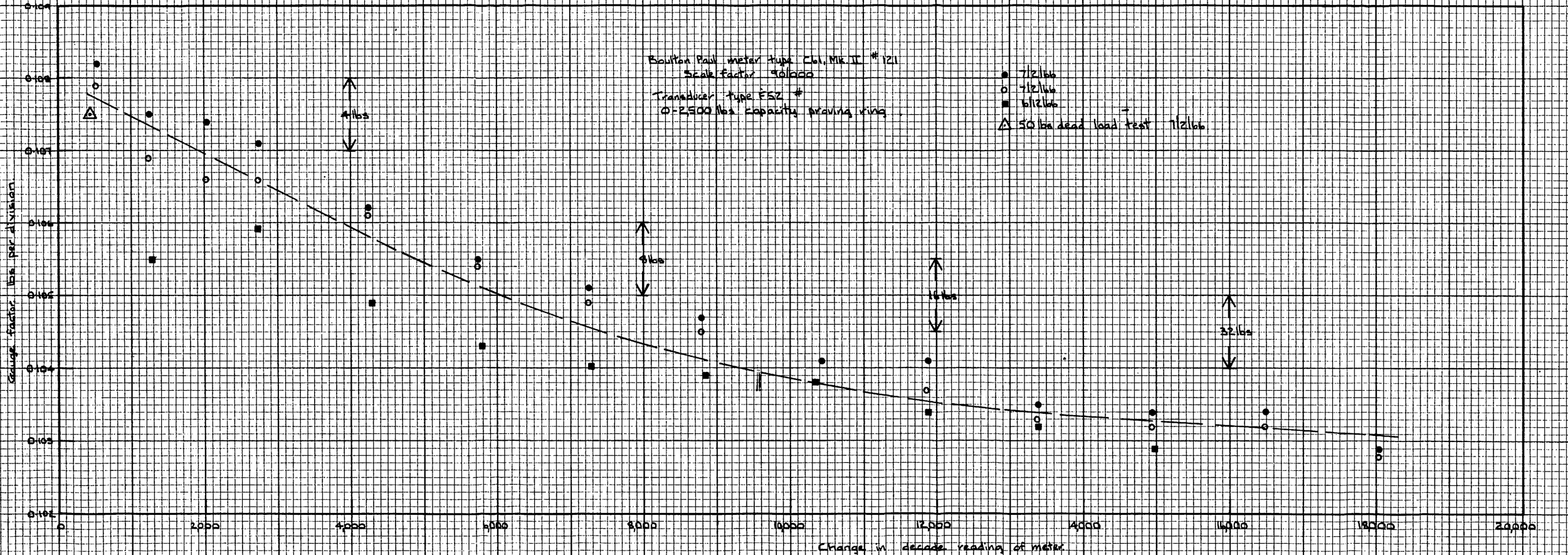
COMPRESSION CALIBRATION OF AXIAL PROVING RING.

FIG. A5.6



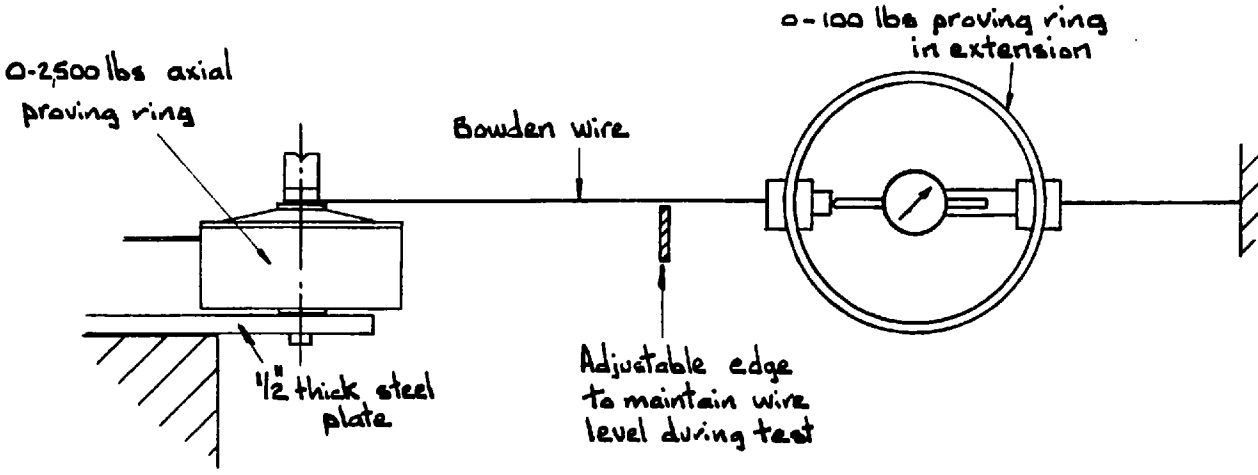
EXTENSION CALIBRATION OF AXIAL PROVING RING

FIG. A3.1



COMPRESSION CALIBRATION OF I.S.C. BELT PROVING RING.

FIG. A3.1



Result of applying lateral load whilst under zero normal load:

Direction of pull.	Applied horizontal load. lbs.	Load equivalent of change in decade reading of C61 meter. lbs.
Parallel to plane of ring.	75	1
Perpendicular to plane of ring.	75	6

15/1/66

LATERAL LOAD CALIBRATION OF AXIAL PROVING RING.

FIG. A3.9

unaffected by changes in the ambient cell pressure. It is possible, but very unlikely, that when the proving ring is under load a variation in cell pressure might have a small effect on the ring. As a check on this a cell was assembled with a rotating bush and an additional external proving ring, Fig A3.10. The ambient pressure was raised with no contact between the internal proving ring and the steel dummy samples. An initial axial load of about 1400 lbs was then applied and the ambient pressure increased again. During this second stage it was observed that there was no significant change in the decade reading on the C61 meter. Secondly the changes in dial gauge reading on the external proving ring correspond almost exactly to those in the first stage of the test for corresponding cell pressures. Clearly those tests show that the internal proving ring only records stresses in excess of the ambient pressure.

A3.2.7 Pressure gauge

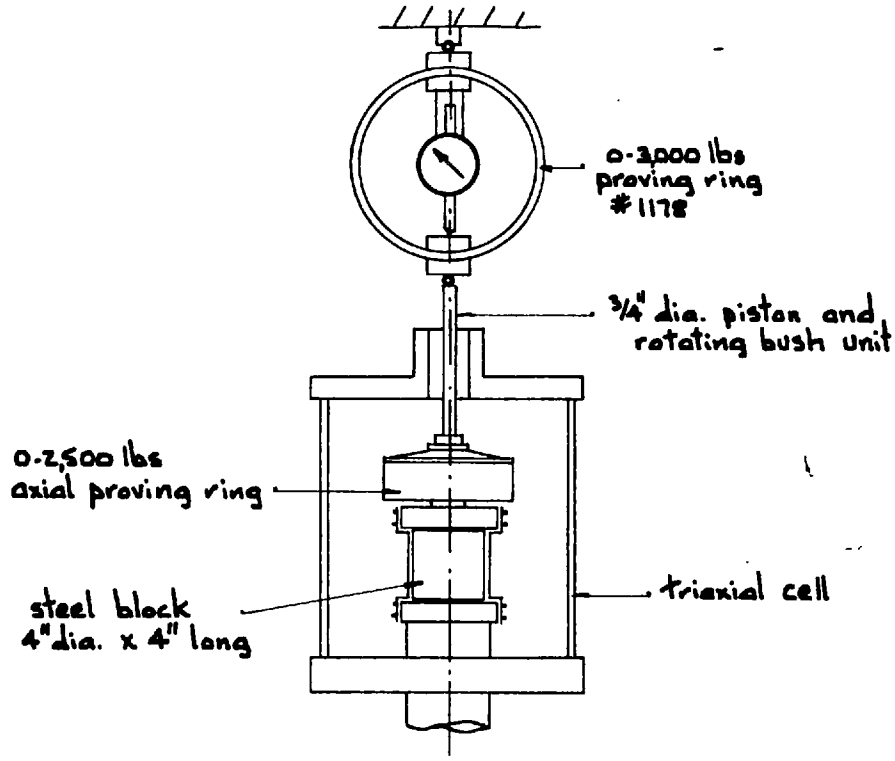
The pressure gauge was calibrated directly through an oil-water interchange vessel. The pressure gauge calibration may easily be upset if, by inadvertently opening the wrong valve, the pressure gauge is vented to atmosphere whilst under load. A pressure snubber was not fitted to the gauge. The calibrations, Fig A3.11, show that this probably occurred between 15/1/64 and 11/11/64. Some difficulty arose in detecting exactly when this occurred, see Chapter 8. The individual corrections were applied to the tests performed between one calibration and another rather than using an average value over the whole period of the test programme. In view of the possible change mentioned above this appears to be most logical.

The gauge used covered a pressure range 0-160 psi. For cell pressures in excess of this range, i.e. extension tests, the Budenberg dead-weight tester was connected directly into the system, Fig 4.8.

A3.3 Compressibility of proving rings and lubricated membrane sandwiches

A3.3.1 Axial proving ring in the triaxial cell

The compressibilities of the axial proving ring and various lubricated membrane sandwiches were obtained as required, Figs A3.12 - A3.15. The sample was replaced by a steel block whose calculated longitudinal compress-



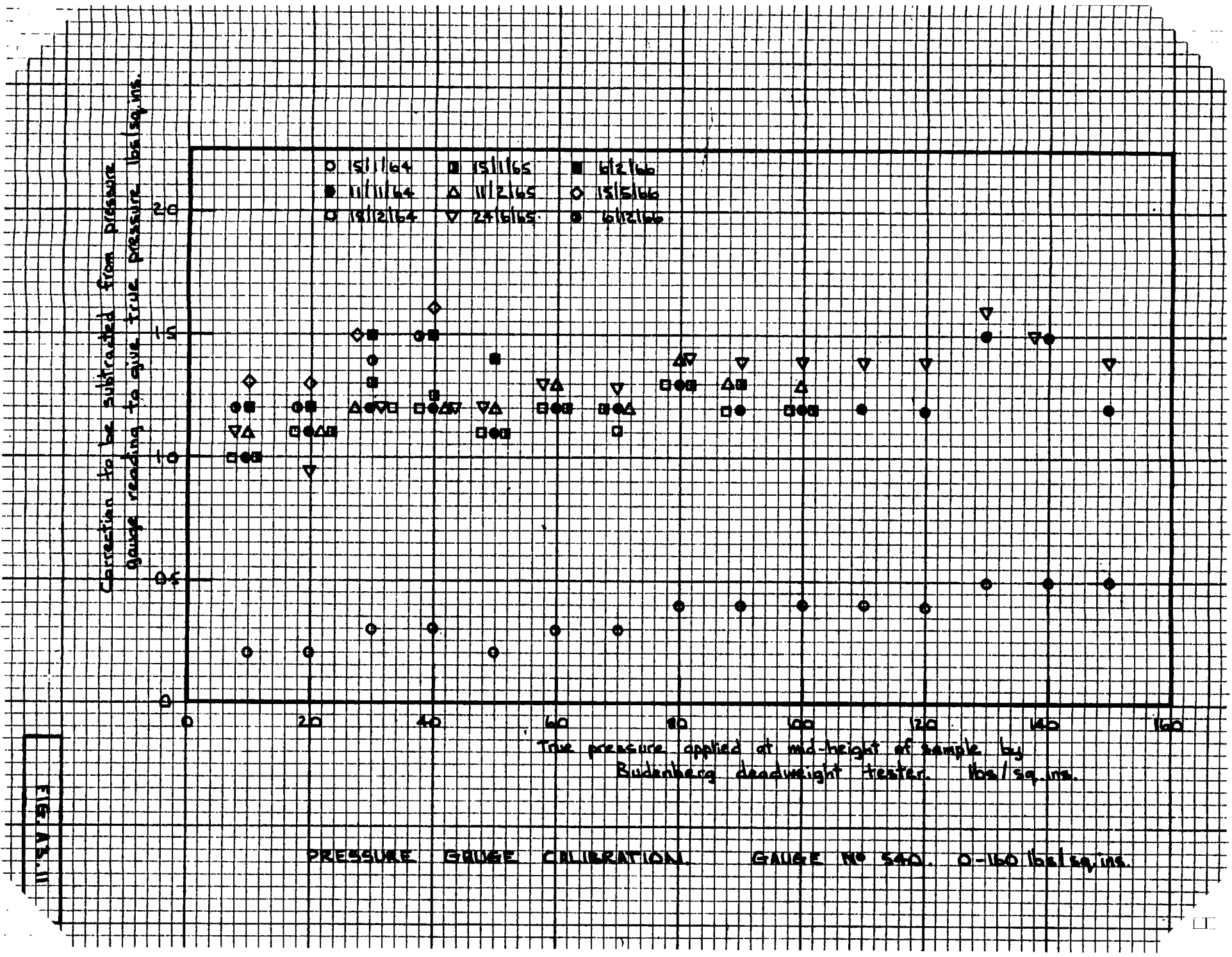
10/12/64

Cell pressure lbs/sq.ins.	Dial gauge reading on P.R. #1178. No contact between internal proving ring and sample. ins. x 10^{-4}	Dial gauge reading on P.R. #1178. Initial load on P.R. #1178 equivalent to approx 1400 lbs. ins. x 10^{-4}	Decade reading on Cbl meter.
10	0.2	500.0	11238
20	1.9	501.5	11238
30	3.2	503.0	11244
40	4.8	504.5	11240
50	6.3	506.0	11241
60	7.8	507.5	11238
70	9.3	509.0	11234
80	10.7	510.5	11236
90	12.2	512.0	11235
100	13.7	513.6	11238

CALIBRATION OF AXIAL PROVING RING

UNDER VARYING AMBIENT PRESSURE.

FIG. A3.10


15/1/64
11/1/64
18/2/64
15/1/65
11/2/65
24/6/65
6/2/66
15/5/66
6/12/66
Correction to be subtracted from pressure gauge reading to give true pressure lbs/sq.ins.
2·0
1·5
1·0
0·5
0
0
20
40
60
80
100
120
140
160
True pressure applied at mid-height of sample by Budenberg deadweight tester. lbs/sq.ins.
PRESSURE GAUGE CALIBRATION. GAUGE No 540. 0-160 lbs/sq.ins.
FIG 11

Axial load measured on proving ring. lbs.

0 500 1000 1500 2000 2500

Correction to be subtracted from measured axial deflection. ins x 10^{-3}

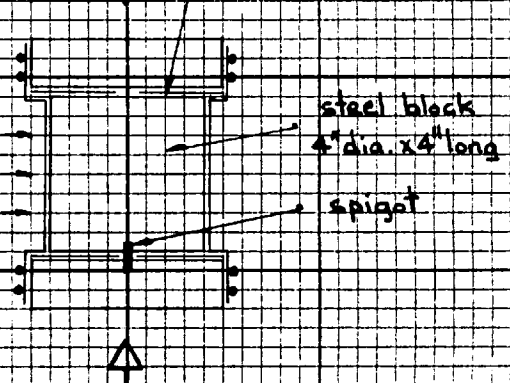
140 130 120 110 100 90 80 70 60 50 40 30 20 10 0

5/0.024" thick membranes at each end of sample
[2 0/9/64] σ_3 = 40 lbs/sq.ins.

3/0.024" thick membranes at each end of sample
[14/9/64] σ_3 = 40 lbs/sq.ins.

3/0.024" thick membranes at each end of sample
[30/6/64]
▽ ▽ σ_3 = 0
▽ ▽ σ_3 = 40 lbs/sq.ins.

lubricated membranes



1/0.009" thick membrane at each end of sample
[10/2/64] σ_3 = 0

direct contact between platens and sample
[20/5/64] σ_3 = 0

2/0.009" thick membranes at each end of sample
[3/6/64] σ_3 = 0

0 5000 10000 15000 20000

Change in decade reading of meter

FIG. A5.12

COMPRESSION CALIBRATION OF AXIAL PROVING RING AND LUBRICATED MEMBRANE SANDWICHES.

TRIAXIAL CELL.

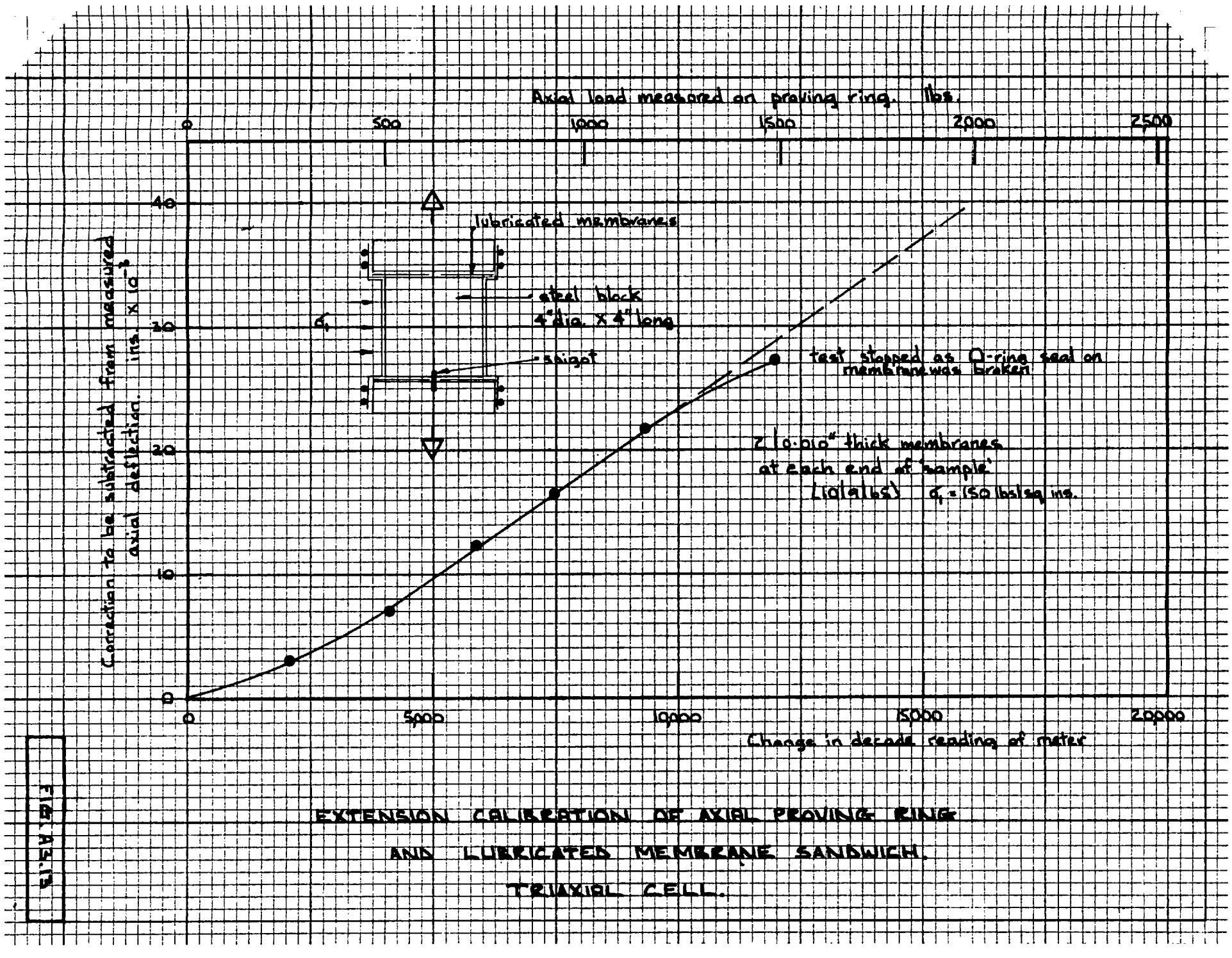


FIG. 13

EXTENSION CALIBRATION OF AXIAL PROVING RING AND LUBRICATED MEMBRANE SANDWICH. TRIAXIAL CELL.

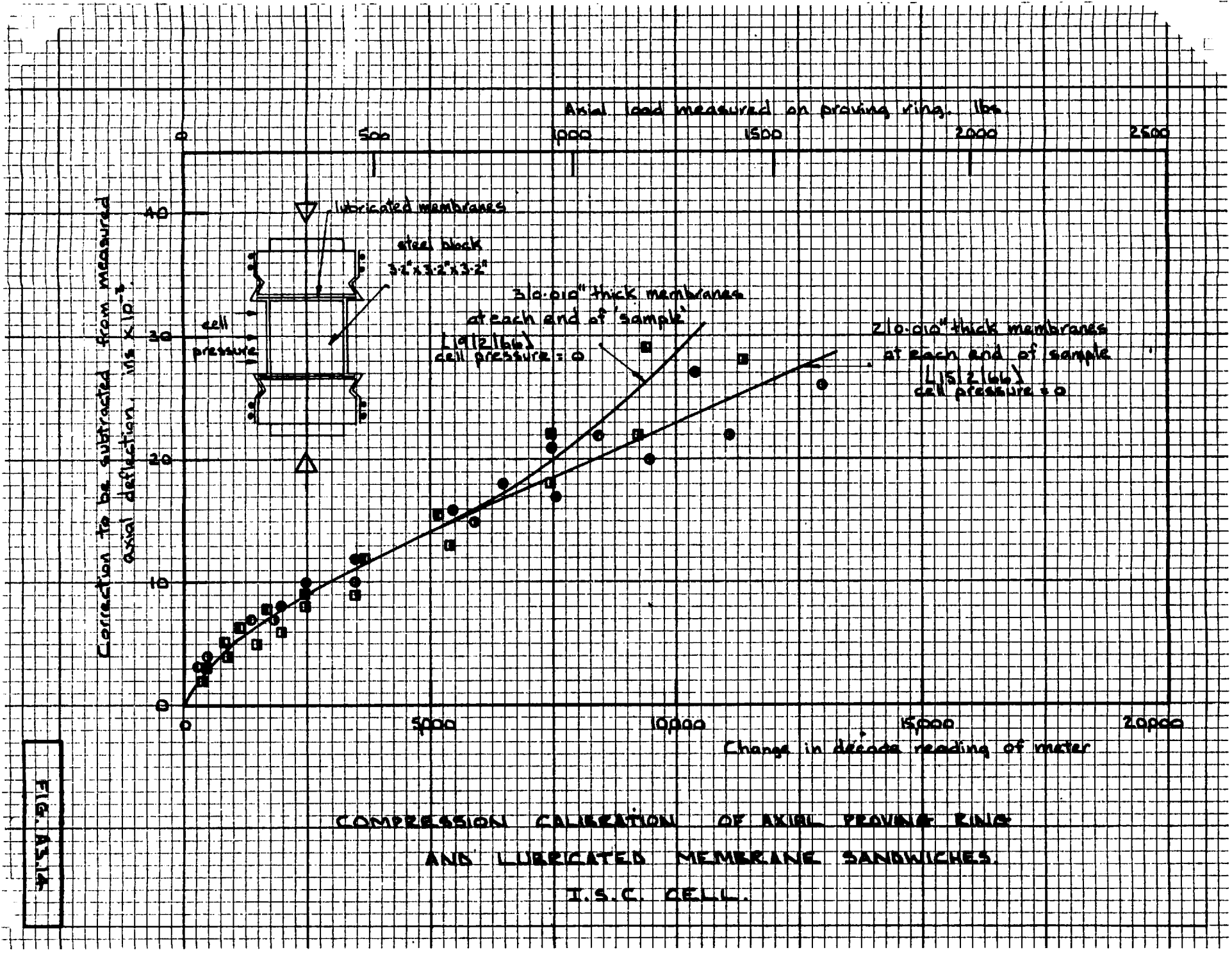
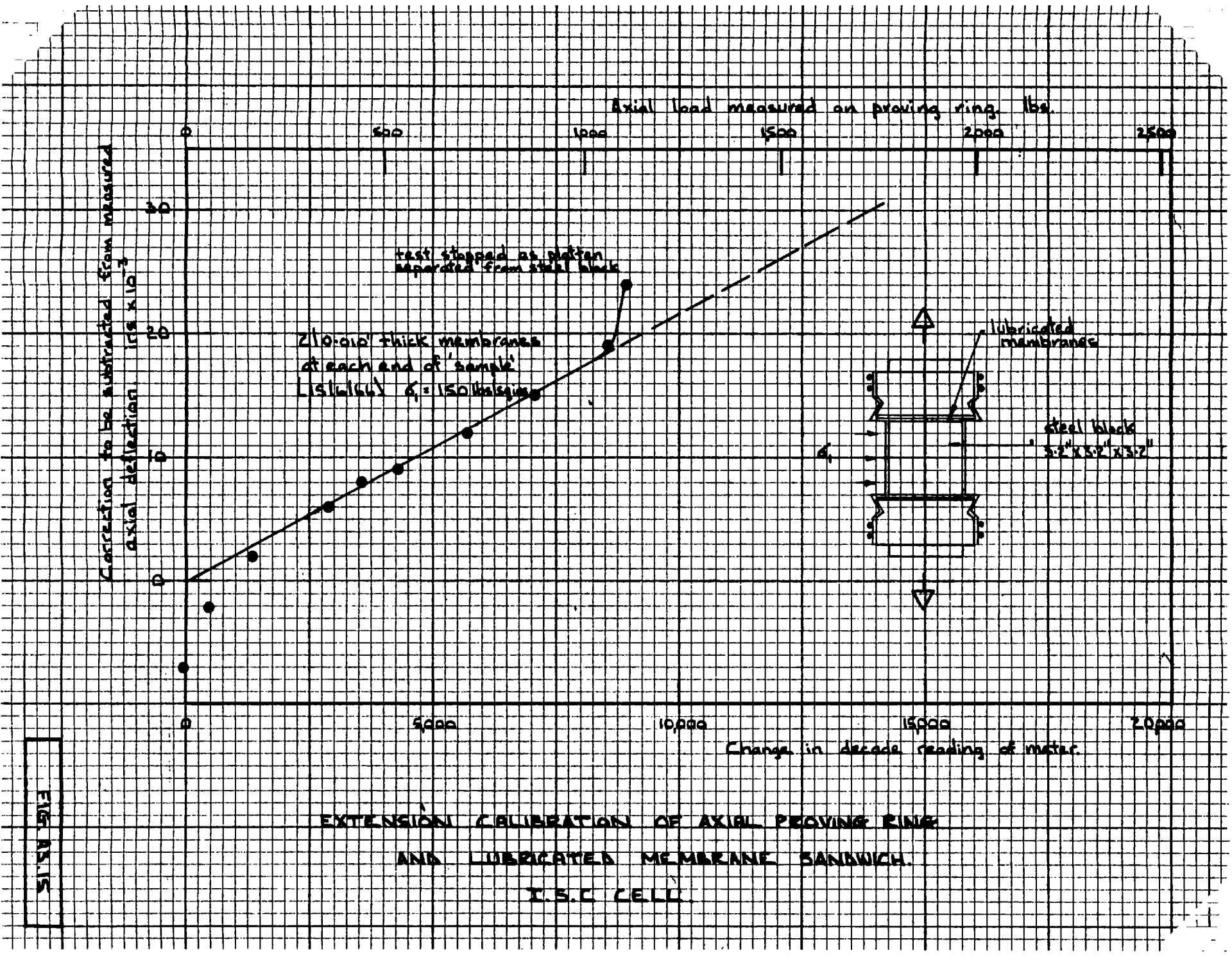


FIG. A3.4

COMPRESSION CALIBRATION OF AXIAL PROVING RING AND LUBRICATED MEMBRANE SANDWICHES. I.S.C. CELL.



EXTENSION CALIBRATION OF AXIAL PROVING RING AND LUBRICATED MEMBRANE SANDWICH.

T.S.C CELL.

FIG. A.15

ion under a 2,500 lb load is about 0.00002 ins, clearly negligible.

Preliminary tests with the cylindrical plattens showed that the steel block slid out sideways under load, due to instability, so that a spigot was inserted in the central drainage hole in the bottom loading platten. The compressibility calibrations were generally performed in an air-filled triaxial cell at atmospheric pressure but a few were carried out in a water-filled cell pressurised at 40 psi.

The 4 compressioh loading cycles for 3/0.024 ins thick lubricated membranes on 30/6/64 indicate that the measured compressibility is independent of the ambient pressure, Fig A3.12. The compression curve for the axial proving ring alone i.e. direct contact between the plattens and the steel dummy, is a straight line through the origin and the maximum deflection under a 2,500 lb load is 0.023 ins, which agrees with the manufacturers rating of approximately 0.025 ins. The compression curves for 1/0.009 ins and 2/0.009 ins thick lubricated membranes lie close to the curve for the axial proving ring alone. The compression curves for 3/0.024 ins and 5/0.024 ins thick lubricated membranes indicate much larger deflections due to the much greater membrane thickness and the consequent squeezing out of the membranes under load which was observed. There is some scatter in the results as the correction to be applied does not vary directly with the number and thickness of membranes used. Measurements indicated that the grease film thickness at the interface between two membranes was consistently about 0.001 ins. The differences referred to are therefore unlikely to be due to a varying grease film thickness.

The extension calibration of the axial proving ring together with 2/0.010 ins thick lubricated membranes, Fig A3.13, was curtailed due to the top loading platten lifting off the steel dummy sample. However it was considered reasonable to extrapolate the curve the short distance required to cover the load range used in the subsequent tests.

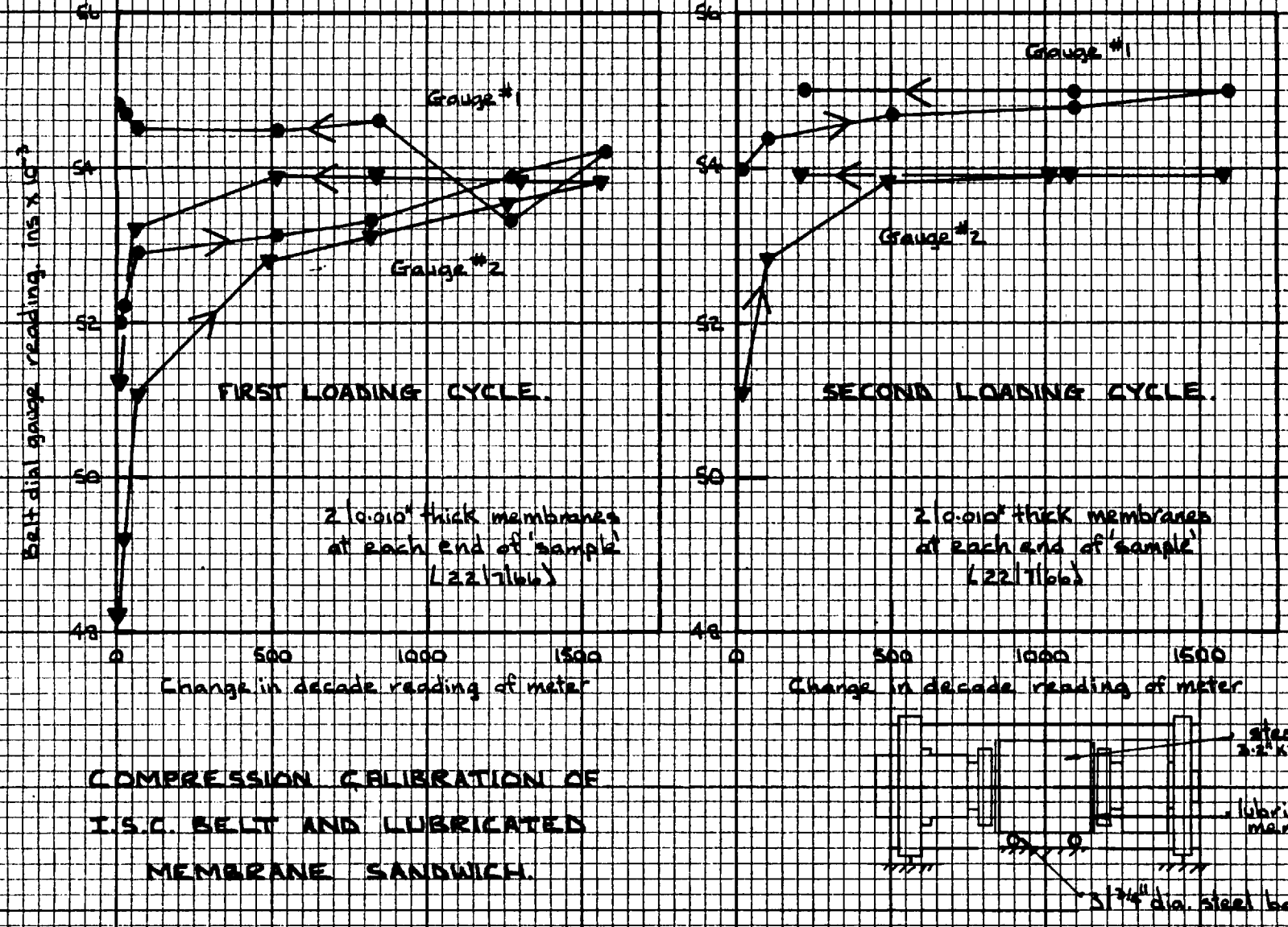
A3.3.2 Axial proving ring in the ISC cell

The compression and extension calibration for the axial proving ring were repeated when it was transfered to the ISC cell. The compression curves for 2/0.010 ins thick lubricated membranes were generally similar to those for the 3/0.010 ins thick lubricated membranes but diverged slightly above an axial load of 1000 lb, Fig A3.14. The extension calibration was again terminated prematurely as the top loading platten assembly separated

from the steel block, Fig A3.15.

A3.3.3 ISC belt

The measured deformation in the ISC belt direction is only in error by an amount corresponding to the compressibility of the lubricated membrane sandwich since the deformation is measured directly between the belt loading plattens. The assembled belt was supported horizontally at 3 points on a level bench. A steel block, 3.2 ins cube, was supported between the plattens on 3 balls, Fig A3.16. As it was not convenient to incorporate a locating spigot on the steel block only a limited load could be applied before the block began to slide out sideways from between the plattens. Clearly the inherent instability of the hydraulic piston would encourage this. Sufficient load was applied to indicate that a load of about 20 lbs was adequate to overcome the initial bedding of 2/0.010 ins thick lubricated membranes and thereafter the dial gauge readings were essentially constant. In the shear tests in which the ISC belt was used the belt was brought into contact with the sample after the cell pressure had been applied, and a small preload applied. The subsequently measured deformations were taken as being correct.



COMPRESSION CALIBRATION OF I.S.C. BELT AND LUBRICATED MEMBRANE SANDWICH.

FIG. A5.16

Appendix A4

Isotropic compression of Belgium Sand

A4.1 Introduction

During the early part of the investigation limited measurements were made of the compressibility of Belgium Sand, Sable de Mol, Ladanyi (1960), Wade (1963). The primary purpose of the tests was to ascertain whether a variation in the strain between different elements within a standard cylindrical triaxial sample could be measured by a relatively simple technique. Secondly, it was of interest to know whether the compressibility was essentially elastic or not and to what extent the strains were uniform throughout the sample.

A4.2 Testing technique

The loading piston and bushing were removed from the triaxial cell and the cell blanked off. A 4 ins diameter, 8 ins high sample in direct contact with enlarged loading plattens was tested. A reference mark mounted on a tripod was placed inside the cell. The axial strains were measured by sighting through the perspex cell wall with a cathetometer reading to 0.0004 ins. By sighting along a cell and sample diameter refraction errors, Escario & Uriel (1961), are avoided.

An increment of pressure was applied and after about 10 minutes readings were taken with the cathetometer. In Test 1, one set of readings were taken, sighting back onto the reference point each time. In Test 2, three sets of readings were taken in an attempt to reduce the scatter in the results, again sighting back onto the reference point each time. Reference to Fig A4.1 suggests that this was marginally successful. In Test 1, the overall axial strain was measured whereas in Test 2 the axial strain over the middle half of the sample was also measured. To facilitate the latter measurement, two small brass targets were cemented to the sample sheath at the sample quarter points. The measured overall axial strains include an unknown bedding error at the two sample-platten interfaces.

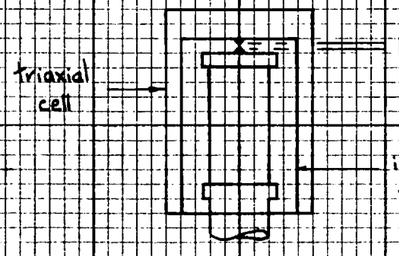
A4.3 Test results

The results clearly show that on first loading and unloading, large non-reversible strains occur. Subsequent loading cycles are more nearly

Test #1

n_c = 44·7%

Overall axial strain



Ambient pressure, lbs/sq.ins

0 20 40 60 80 100 120 140

0 0·1 0·2 0·3 0·4 0·5 0·6 0·7

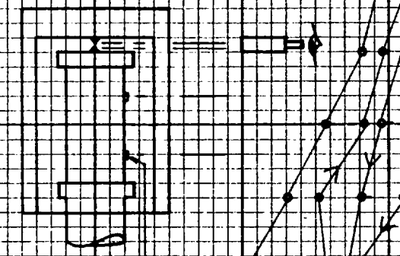
Axial strain, %

Test #2

n_c = 44·8%

Overall axial strain

Axial strain over middle half of sample



Ambient pressure, lbs/sq.ins

0 20 40 60 80 100 120 140

0 0·1 0·2 0·3 0·4 0·5 0·6 0·7

Axial strain, %

COMPRESSIBILITY OF BELGIUM SAND (SABLE DE MOL) UNDER INCREASING AMBIENT PRESSURE

Sample, 4"ins diam. 8ins high.
Direct contact between sample and plattens.
Sample sheath 0·023 ins thick.

FIG. A4.1

reversible. That the initial large non-reversible overall strain is not due to bedding errors at the two sample-platten interfaces is shown by the results of Test 2. The axial strain over the middle half of the sample is, on first loading, similarly large and non-reversible; indeed its magnitude is about 50% greater than the overall strain. The slopes of the overall axial strain curves on first loading are significantly different whereas their slopes on reloading are quite similar. The initial loading curves may be greatly affected by small non-uniformities within the sample and will probably never be exactly reproducible. In both tests the samples were initially loose (n_i = 45%) and one would expect the small-scale non-uniform behaviour, if it exists, to be quite marked.

A4.4 Relation to previous work

The slope of the reloading curves for the middle half of the sample, Test 2, is about 40% lower than that of the reloading curves for the overall axial strain due to the effect of end restraint. This is in accordance with the findings of Shockley (1953), Shockley & Ahlvin (1960), Truesdale & Rusin (1963), Roscoe et al (1963a), Januskevicius & Vey (1965), Amirsoleymani (1966a,b).

The two tests clearly show that the initial loading is non-reversible whereas the subsequent loading is. This is contrary to the findings of Fatt (1957), Roscoe et al (1963), McMurdie & Day (1958), Bell (1965), Ko (1966), Ko & Scott (1967a,b). However the respective authors interpretation of their test data and, in the case of McMurdie & Day, their testing technique, is open to question. The data contained in these papers, generally, appears to show a non-reversible first loading cycle followed by essentially reversible subsequent reloading cycles. The extent of non-reversibility is, as one would expect, dependent on whether the sample is initially dense or loose. A dense sample exhibits almost complete reversibility during the first loading cycle whereas a loose sample does not. However the authors do not make it clear to which of the cycles or density states they refer in drawing their conclusions or alternatively, their conclusions are, in the writer's opinion, false. For example Ko & Scott (1967b) state in their paper, "During the first cycle of loading and unloading, there was a certain amount of irreversible volumetric compression which was smaller for the denser soil. During the second cycle, the amount

of irreversible compression was considerably reduced, especially for the dense soil in HC-1, where all the compression was recoverable at the datum pressure of 4 psi." Then follows a discussion explaining this by invoking unstable soil grains and the absence of grain crushing, which is very reasonable. However in their conclusions they state, "The volumetric compression of a sand stressed hydrostatically is non-linear but nearly elastic". Since, for the case of a loose sand, their Fig 13, only 58% of the volumetric strain is recoverable on first loading it is difficult to see how they justify this statement.

Appendix A5

Cylindrical triaxial compression tests on glass ballotini

A5.1 Introduction

During the initial phases of the research it was thought that it would be appropriate if in addition to the Ham River sand at least one other material were tested in a second, more limited, series of tests. Glass ballotini is an almost ideal material as the particles are nearly spherical (they are in fact slightly egg-shaped due to their method of manufacture).

Previous tests, Fraser (1957), Gray (1960), Rowe (1962), all show that glass ballotini has a low Coulomb ϕ' in the range 25-34° as measured in triaxial compression. However its stick-slip behaviour during shear may make it difficult to define a satisfactory stress-strain curve. This can be largely overcome by using a material of sufficiently fine particle size relative to the specimen size tested.

Ideal spherical particles feature in a number of theories concerned with the mechanics of the irreversible behaviour of regular or random packings of discrete particles, Thurston & Deresiewicz (1959), Rennie (1959), Dantu (1961), Rowe (1962, 1963), Parkin (1964, 1965), Horne (1965). The complexities of a theory capable of including irregularly shaped particles e.g.sand, are formidable and it is clearly easier to consider only spherical particles. The theories contained in the above mentioned references can only cope with spherical particles. Even after making this simplifying assumption the remaining theoretical difficulties are considerable. Some indication of the extent of these difficulties is given by the length and authorship of the subsequent discussion to Rowe's 1963 paper, Gibson & Morgenstern (1963), Trollope & Parkin (1963), Scott (1964), Roscoe & Schofield (1964), Rowe (1964b), which extended to over two and a half times the length of the original paper.

A5.2 Test programme

It became clear at an early stage of the present work that it would only be feasible to test one material, the Ham River sand, and a complete series of tests on glass ballotini were, therefore, excluded from the scope of this thesis. A few tests, on glass ballotini were carried out during

the first series of cylindrical triaxial compression tests and are included for completeness.

Two samples of clear lead glass ballotini were tested, firstly a 14-25 B.S.Sieve size fraction and secondly a sample of a similar grading to the first batch of Ham River sand. As the quantity of ballotini available at the time was limited, only 4 ins diameter, 4 ins high samples could be tested.

The specific gravities of the two types of glass ballotini used were

(a) 14-25 B.S.sieve size, G = 2.943

(b) grading similar to Ham River sand, Batch No.1, G = 2.915 made up as follows:

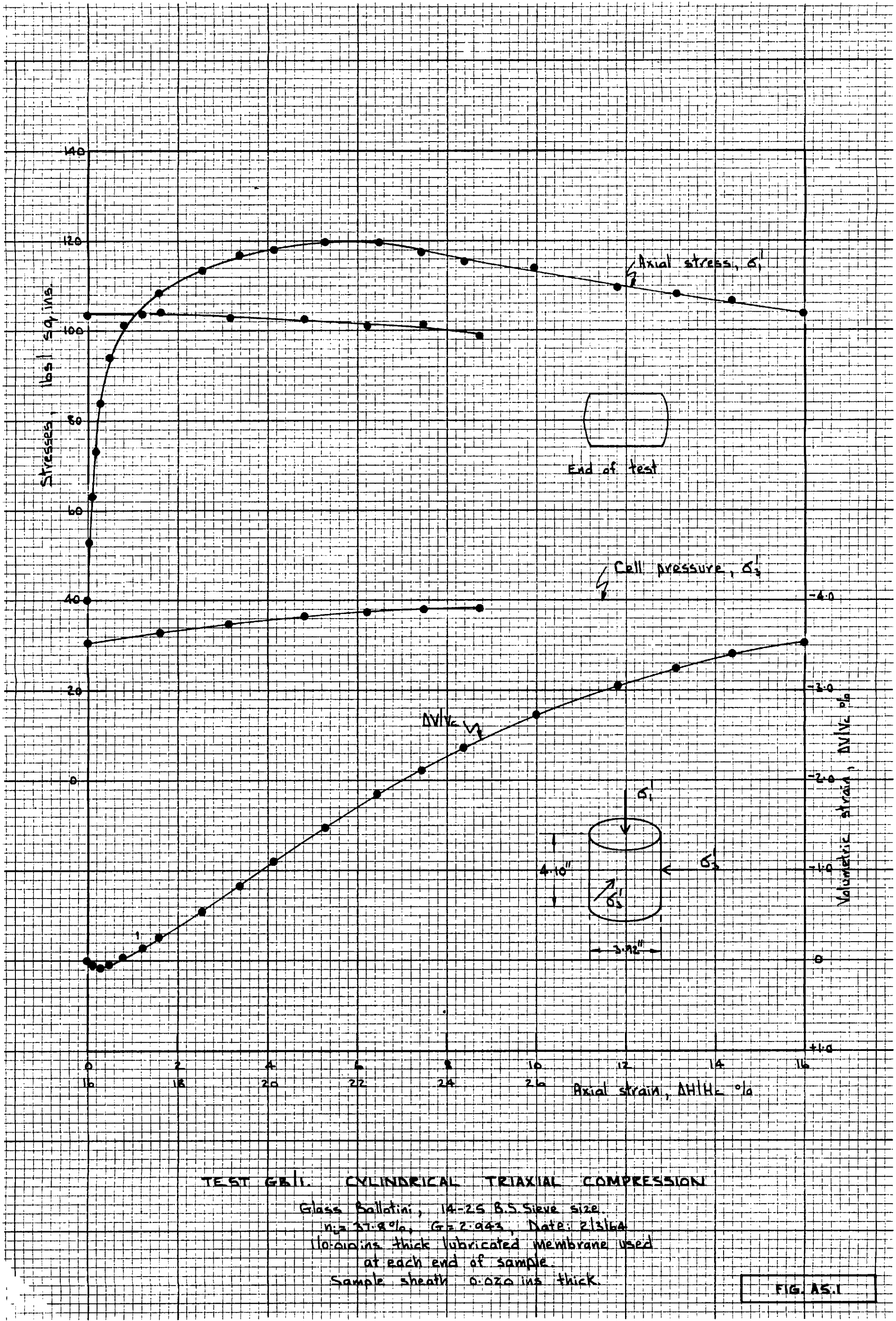
B.S.Sieve size fraction	52	52-72	72-100	100-200
G	2.922	2.924	2.905	2.905

The general experimental procedure was identical to that used in similar tests on Ham River sand.

A5.3 Test results

A single test, GB/1, was performed on the 14-25 B.S.sieve sized material, Fig A5.1. The limiting porosities of the glass ballotini were not determined but as the sample was prepared by spooning saturated ballotini into the mould under water a loose sample was to be expected. The shape of the stress-strain curve substantiates this hypothesis. A stick-slip action was observed throughout the test, σ_1' falling by about 10% and then rapidly increasing again, these drop-offs not being recorded (see Skinner (1969)). The stick-slip action was distinctly audible and each time a shock wave passed through the testing machine which was easily sensed by touch. There appeared to be no expansion at the top or bottom of the specimen and no preferential slip zones were visible. However at the end of the test it was possible to distinguish layers of balls having moved over one another at the ends of the specimen. An ordered pattern appeared to be emerging not unlike that observed by Bernal et al (1964).

Tests GB/2-5 were performed on samples having a similar grading to the first batch of Ham River sand. This reduced the stick-slip action but did not completely eliminate it. Tests GB/2 & 3 were intended to be identical



TEST GB11. CYLINDRICAL TRIAXIAL COMPRESSION

Glass Ballotini, 14-25 B.S. Sieve size.
n_i = 37.8%, G = 2.943, Date: 2/3/64
Two 0.010 ins. thick lubricated membrane used at each end of sample.
Sample sheath 0.020 ins thick.

FIG. A5.1

tests on medium dense samples and superposition of the stress-strain and volume change curves, not shown, shows them to be almost indistinguishable up to 10% axial strain and to deviate only very slightly beyond this point, Figs A5.2 & A5.3. The samples for Tests GB/1 & 2 were built in a normal manner. In Test GB/2 no stick-slip action occurred up to 15% axial strain whereafter σ_1' oscillated slightly. These oscillations were not of the catastrophic type observed in Test GB/1. The sample expanded predominantly at the base and numerous preferential slip zones were visible.

The sample for Test GB/3 was made in a normal manner but inverted. The mould was placed on the upturned top loading platten and a sample was built. The cell base was upturned and placed on the sample, the rubber membrane turned back and O-rings secured. After clamping the mould to the cell base and applying a suction to the sample it was possible to invert the whole assembly by sliding it off the edge of the bench whilst supporting the top loading platten by hand. The sample expanded across the top loading platten, there being little or no movement at the bottom loading platten (top and bottom refer to the as tested condition). The failed sample is shown in Plate A5.1, numerous preferential slip zones are to be seen. This clearly demonstrates again that the large strain behaviour of the sample is dependent on the method of sample preparation and not gravity as suggested by Haythornthwaite (1963a).

The sample for Test GB/4, again medium dense, was made in two halves. The sample appeared to remain cylindrical up to about 8-10% axial strain, i.e. beyond failure, after which it expanded predominantly at the top, Fig A5.4. Some stick-slip action was observed well beyond peak but again it was not pronounced. Measurements taken at the end of the test indicated that the base diameter had increased by about 8%. A number of well defined preferential slip zones were visible.

The final test, GB/5, was similar to Test GB/4 but on a loose sample, Fig A5.5. Slight stick-slip action was observed early on in the test which increased significantly later in the test. Lines scribed on the membrane did not detect the presence of any preferential slip zones within the sample. The sample remained cylindrical initially but later in the test it expanded predominantly at the top. The test was carried to an axial strain of 28.8% and it may be noted that the stress-strain curve is remarkably flat beyond peak σ_1', whereas the volumetric strain rate was

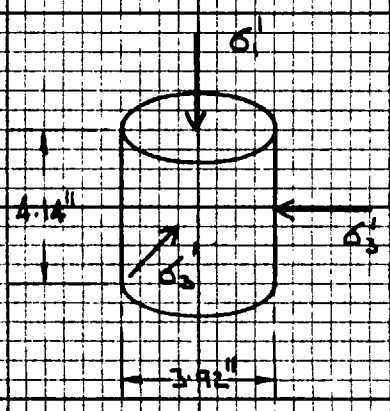
Stresses, lbs/sq.ins.

Axial stress, σ_1'

Cell pressure, σ_3'

$\Delta V/V_c$ %

End of test



Volumetric strain, $\Delta V/V_c$ %

Axial strain, $\Delta H/H_c$ %

TEST GB12. CYLINDRICAL TRIAXIAL COMPRESSION

Glass Ballotini, Grading similar to Ham River Sand, Batch#1
n_i = 36.1% G = 2.915 Date: 8/3/64
Two 0.010 ins. thick lubricated membrane used at each end of sample.
Sample sheath 0.020 ins. thick

FIG. A5.7

Stresses, lbs sq ins

Axial stress, σ_1'

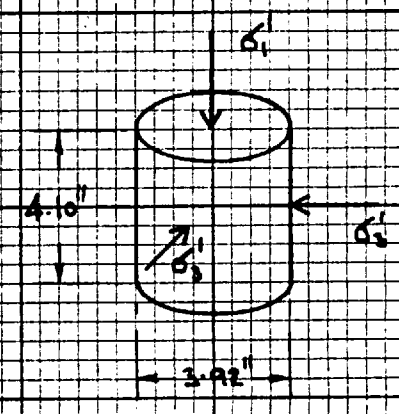
Slip planes first observed

Cell pressure, σ_3'

$\Delta V/V_c$

Volumetric strain, $\Delta V/V_c$ %

Axial strain, $\Delta H/H_c$ %



TEST GB13. CYLINDRICAL TRIAXIAL COMPRESSION

Glass Ballotini, Grading similar to Ham River Sand, Batch #1

n_i = 35.9 %, G: 2.915, Date: 12/3/64

1/a.010 ins. thick lubricated membrane used at each end of sample.

Sample sheath 0.020 ins. thick.

FIG A5.3



TEST GB13.

glass ballotini,
cylindrical compression,
n_i = 35·9 %, 4·1 ins high,
1/0·009 ins thick membrane,
test stopped at $\Delta H/H_c$ = +24·3%,
$(\Delta H/H_c)_f$ = +2·3%.

PLATE A5.1

Axial stress, σ_1'

Cell pressure, σ_3'

$\Delta V/V_c$

Stresses, lbs/sq. ins.

Volumetric strain $\Delta V/V_c$ %

Axial strain, $\Delta H/H_c$ %

4.13"
4.13"
4.13"
4.14"

End of test

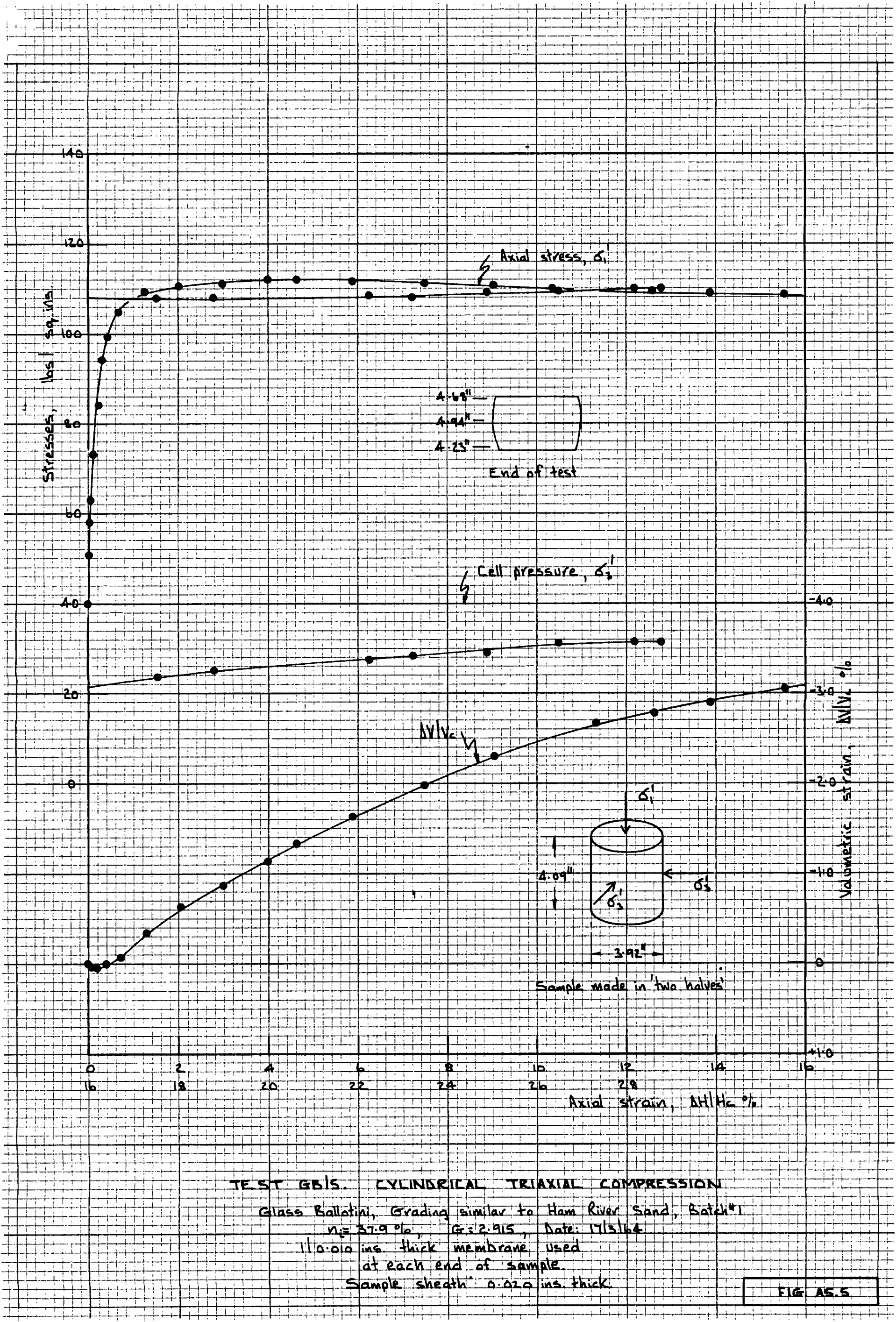
σ_1'
4.19"
σ_3'
σ_3'
3.92"

Sample made in 'two halves'

TEST GB14. CYLINDRICAL TRIAXIAL COMPRESSION

Glass Ballotini, Grading similar to Ham River Sand, Batch*1.
n_i = 35.2 %, G_s = 2.915, Date: 15/3/64.
No. 0.010 ins. thick lubricated membrane used at each end of sample.
Sample sheath 0.020 ins. thick.

FIG. A5.4



TEST GB15. CYLINDRICAL TRIAXIAL COMPRESSION

Glass Ballotini, Grading similar to Ham River Sand, Batch#1
n_i = 37.9 %, G = 2.915, Date: 17/3/64
1/0.010 ins. thick membrane used
at each end of sample.
Sample sheath 0.020 ins. thick.

FIG A5.5

certainly not zero. This stress-strain curve could be idealised to that of a perfectly plastic material, Prager & Hodge (1951), with a relatively smaller error, however the dilatancy effect still remains.

A comparison of the failure characteristics is drawn, Fig A5.6. The data is very limited and it is assumed that Tests GB/4 & 5 are reliable results. The comparable Ham River sand data were also used for guidance. The failure characteristics of Tests GB/2 & 3 are consistent and suggest that any initial structure built into the sample is not changed significantly when inverting the sample-mould-cell base assembly in Test GB/3. In view of the inherent difficulty in the latter this is perhaps surprising. The shape of the $\phi' - n_i$ plot is established by Tests GB/4 & 5 and is steeper than the comparable Ham River sand plot (1.4°/1% porosity and 1.1°/1% porosity, respectively). The difference in ϕ' between a sample made in a normal manner and one made in two halves is slightly larger than for the Ham River sand.

The line through Tests GB/4 & 5 probably does not represent the true lower limit $\phi' - n_i$ relationship since only 1/0.010 ins thick lubricated membrane was used rather than two or more. The lower limit is probably about 1° lower. Since the particle size of the material used in Test GB/1 is larger than that used in Tests GB/2-5, a higher strength would appear likely as the end conditions were similar, but not sufficiently 'free' to give the lower limit $\phi' - n_i$ relationship; based on the Ham River sand data. However the particle size difference in the two materials precludes a firmer comparison of the failure characteristics.

The axial strains at failure are very much lower than those of comparable tests on Ham River sand, see Figs 8.8 & 8.9. Whereas comparable Ham River sand samples, Type X, failed at axial strains greater than 10%, the glass ballotini samples failed at an axial strain of only 2 to 5%. The volumetric strains at failure were similar to those for Ham River sand whereas the volumetric strain rates were higher for the medium dense glass ballotini samples.

The measured ϕ' values compare favourably with previously published data on glass ballotini. Fraser (1957) tested 4 ins diameter, 8 ins high samples and obtained:

saturated, loose	$\phi' = 24.3^\circ$
saturated, dense	$\phi' = 33.8^\circ$
dry, loose	$\phi' = 24.9^\circ$

Maximum angle of shearing resistance, ϕ'

GB13 GB12 GB14 GB11 GB15

$\phi'_{1/2}$

Volumetric strain at failure, $\Delta V/V_c$ %

$\Delta H/H_c$

$\Delta V/V_c$

Axial strain at failure, $\Delta H/H_c$ %

$\frac{d(\Delta V/V_c)}{d(\Delta H/H_c)}$

Sample, 4 ins. diam, 4 ins high
10.010 ins thick lubricated membrane used at each end of sample.

Sample type / Grading	Sample made in two halves	Normal
Grading similar to Ham River Sand	●	□
14-25 B.S. Sieve size		○

$\frac{dL}{dL}\frac{(\Delta V/V_c)}{(\Delta H/H_c)}$ at failure, Volumetric strain rate at failure

Initial porosity, n_i %

CYLINDRICAL TRIAXIAL COMPRESSION

GLASS BALLOTINI

COMPARISON OF FAILURE CHARACTERISTICS

FIG. A5.6

Appendix A6

Sample sheath strength and platten friction corrections

A6.1 Introduction

The rubber sheath enclosing the specimen contributes to the measured strength since it may act as a thin shell in compression or extension. Sample sheath strength corrections may be made based on the results given by Henkel & Gilbert (1952). Since this thesis is primarily concerned with peak strength it may reasonably be assumed that the sample sheath deforms uniformly up to that point and that their approach is valid.

Assuming that the rubber sample sheath is held against the sample to prevent buckling then, for a conventional undrained test on a saturated sand, as the Poissons ratio of the sample is the same as that of the rubber, $\frac{1}{2}$, no hoop tension will be set up in the sample sheath. In which case the sample sheath may be considered as a right cylindrical shell in compression or extension and, in the case of a triaxial compression or extension test, would only influence the axial stress. In a drained test, hoop stresses would occur due to volume changes (Poissons ratio $\neq \frac{1}{2}$) but, according to Bishop & Henkel (1957) the corrections determined from the results of undrained tests may be applied to drained tests with little error. A more rigorous analysis than that given by Henkel & Gilbert, not reported herein, shows this to be true. Further it may be assumed that the results can be extended to rectangular cross-sectioned samples, Wood (1958), Cornforth (1961), Wade (1963).

Consider a triaxial compression or extension test sample,

Sample sheath strength correction to be applied to the measured deviator stress at failure, psi $= \dfrac{L.M.e}{A}$ .....(1)

where M = extension modulus of the membrane, lbs/ins

L = initial perimeter of sample, ins

e = axial strain at failure

A = cross-sectional area of sample at failure, ins^2

For the rubber latex sample sheaths used M = 175t, where t is the thickness of the membrane in inches.

For a circular cross-sectioned sample $L = \pi D$, where D is the initial diameter of the sample.

For a rectangular cross-sectioned sample $L = 2(B+C)$, where B and C are the widths in the belt and cell directions respectively.

A6.2 Triaxial compression and extension tests

The sample sheath strength corrections for selected triaxial compression and extension tests over a range of porosities are shown in Fig A6.1. Since the sample sheath strength is independent of the height of the sample it is of little consequence in the comparison of cylindrical triaxial compression test results on samples of differing heights. It has a possible effect on the comparison of compression and extension test results and in relating test data on cylindrical and cuboidal samples.

It is clear that the sample sheath correction has an insignificant effect on both the cylindrical and cuboidal triaxial compression test results. The maximum sample sheath strength correction is 0.4 psi, Test C/1, whereas a change in $(\sigma_1' - \sigma_3')$ of 0.6 psi is required to change ϕ' by 0.1 degrees.

The sample sheath strength has a small but significant effect on the measured strength in triaxial extension, especially on the loose samples which fail at up to -10% axial strain. However compared with the other uncertainties in interpreting the extension test results, particularly in defining the cross-sectional area of the sample at failure, this effect is small and could be neglected. The effect of the choice of area used in calculating the strength in an extension test is discussed in Chapter 9. It will be noted from the data given in Fig A6.1 that the extension test results are much more sensitive to a variation in $(\sigma_1' - \sigma_3')$, as is well-known.

A6.3 Independent stress control tests

A sample sheath strength correction may be applied to $(\sigma_1' - \sigma_3')$ and $(\sigma_2' - \sigma_3')$ in a similar manner to that applied to the triaxial compression and extension test results. In calculating the sample sheath strength correction to be applied to the belt stress the lubricated rubber membranes in immediate contact with the sample on the axial plattens are considered to act in a similar manner to the sample sheath.

	Cylindrical triaxial						Cuboidal triaxial			
	Compression			Extension			Compression		Extension	
Test number	B|6	C|3	C|1	EX|6	EX|5	EX|8	IA|5	IA|7	ICE|4	ICE|8
Porosity, n_i %	38·1	41·9	45·5	39·1	42·5	45·9	38·8	39·6	39·1	40·0
Density	dense	medium	loose	dense	medium	loose	dense	dense	dense	dense
Compression, σ_3' lbs|sq.in. Extension, σ_1' lbs|sq.ins.	40·0	40·0	40·0	180·0	150·0	130·0	30·0	30·0	140·0	140·0
$(\sigma_1' - \sigma_3')$, lbs|sq.ins.	157·9	123·0	98·2	139·5	110·7	90·7	107·8	102·2	113·0	112·0
Sheath correction, lbs|sq.ins.	0·2	0·3	0·4	0·2	0·2	0·4	0·1	0·1	0·2	0·1
Corrected $(\sigma_1' - \sigma_3')$, lbs|sq. ins.	157·7	122·7	97·8	139·3	110·5	90·3	107·7	102·1	112·8	111·9
Measured ϕ', degrees	41·6	37·2	33·4	39·2	35·7	32·4	39·9	39·0	42·5	41·7
Corrected ϕ', degrees	41·6	37·2	33·3	39·1	35·6	32·2	39·9	39·0	42·3	41·6
Change in $(\sigma_1' - \sigma_3')$ required for a change in ϕ' of 0·1° lbs|sq. ins.	0·9	0·7	0·6	0·2	0·2	0·2	0·6	0·6	0·1	0·1

CYLINDRICAL AND CUBOIDAL TRIAXIAL COMPRESSION AND EXTENSION TESTS
TYPICAL CORRECTIONS TO MEASURED ϕ' FOR SAMPLE SHEATH STRENGTH

FIG. A6.1

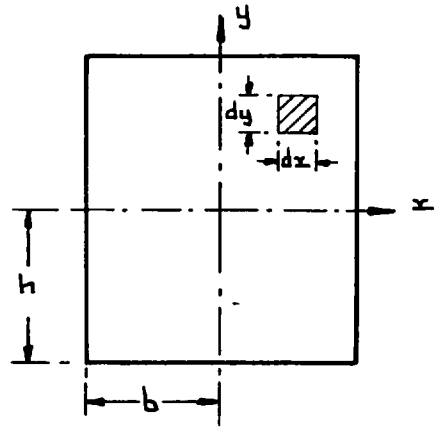
Following the analyses used by Wood (1958), Cornforth (1961), Wade (1963), an additional correction may be applied to the deviator stress ($\sigma_1' - \sigma_3'$) to account for the work done against friction on the belt plattens by the deviator stress ($\sigma_1' - \sigma_3'$). A similar correction may be applied to the intermediate stress ($\sigma_2' - \sigma_3'$) with respect to the axial plattens. No correction is applied to the stress in the cell direction since it is assumed in the theory that the corrections are only applied to stresses in excess of the cell pressure.

It is believed that a platten friction correction is only applicable where the stress to be corrected is applied across a rigid boundary, e.g. σ_2' in the ISC test. In which case, the load lost due to platten friction divided by the sample cross-sectional area is subtracted from the applied stress. Where the stress is applied across a flexible boundary, e.g. $\sigma_2' = \sigma_3'$ in a triaxial compression test, it is reasonable to assume that only that portion of the sample immediately adjacent to the rigid frictional boundary is affected by its presence. Therefore no correction should be applied in a conventional triaxial compression or extension test to σ_3' or σ_1' , respectively.

The derivation of the equations used for the platten friction correction is given in Fig A6.2. It is noted that Wade (1963) has what appears to be a typographical error in equation (3) and in addition does not make it clear that W_e is for the two ends of the specimen and not for $\frac{1}{4}$ of the end area of one platten as denoted by Wood, see Wade, pp 138-140. However Wade's final equation, A2-4, appears to be correct.

The platten friction corrections for selected ISC tests were calculated using equations (3) & (4) and are shown together with sample sheath strength corrections in Fig A6.3.

The sample sheath strength corrections are, by themselves, insignificant and could be neglected. The platten friction corrections are small and insignificant for plane strain tests and for tests with the ISC belt opening where the intermediate principal stress is low. They become just significant as the intermediate principal stress increases, i.e. as the ratio $b = (\sigma_2' - \sigma_3')/(\sigma_1' - \sigma_3')$ increases from 0.3 to 1.0. For b values close to 1.0 the combined sample sheath strength correction and platten friction correction reduces the measured value of ϕ' by 0.2 degrees. In relation to the scatter of the measured values this is small but is



Following Wood's notation, consider an element $(dx.dy)$ on the belt face,
For an undrained plane strain test, strain, $\varepsilon_y = -\varepsilon_x$

Work done on element by friction force $= \varepsilon_y.(x^2+y^2)^{1/2}.\sigma.\mu.dx.dy$

where μ = equivalent coefficient of friction of the lubricated platten

σ = normal stress

Total work done on two ends of specimen $= 8\int_0^h\int_0^b \varepsilon_y(x^2+y^2)^{1/2}.\sigma.\mu.dx.dy$

$$= \frac{4}{3}.\sigma.\mu.h^3.\varepsilon_y\left[\frac{b^3}{h^3}\sinh^{-1}\frac{h}{b} + \sinh^{-1}\frac{b}{h} + \frac{2b}{h}\left(1+\frac{b^2}{h^2}\right)^{1/2}\right] \quad \ldots (2)$$

For a drained plane strain test, $\varepsilon_y \neq \varepsilon_x$, and Wade extended the above theory to account for this. Clearly Wade's extension also applies to the ISC test in which the strain in the belt direction also varies.
For the ISC test, following Wade's extended theory,

Work done on element by friction force $= (x^2\varepsilon_x^2 + y^2\varepsilon_y^2)^{1/2}.\sigma.\mu.dx.dy$

Total work done on two ends of specimen, W_e $= 8\int_0^h\int_0^b (x^2\varepsilon_x + y^2\varepsilon_y)^{1/2}.\sigma.\mu.dx.dy$

$$= \frac{4}{3}.\sigma.\mu.\frac{h^3.\varepsilon_y^2}{\varepsilon_x}\left[\frac{b^3.\varepsilon_x^3}{h^3.\varepsilon_y^3}.\sinh^{-1}\frac{h.\varepsilon_y}{b.\varepsilon_x} + \sinh^{-1}\frac{b.\varepsilon_x}{h.\varepsilon_y} + \frac{2.b.\varepsilon_x}{h.\varepsilon_y}\left(1-\frac{b^2.\varepsilon_x^2}{h^2.\varepsilon_y^2}\right)^{1/2}\right] \quad \ldots (3)$$

Equating the total work done on the two ends of the specimen, W_e, to the work done by the deviator stress $(\sigma_1-\sigma_3)$ in deforming the sample,

Correction to be applied to $(\sigma_1-\sigma_3)$ $= \dfrac{W_e}{\varepsilon_y.H.B.C}$ $\quad \ldots (4)$

PLATTEN FRICTION CORRECTION

FIG. A6.2

Test number	Independent stress control				
	ISC13	ISC17	ISC110	ISC113	ISC120
Porosity, n_i %	All data adjusted to correspond to 39.0%				
Density	dense				
σ_3', lbs/sq. ins.	30.0				
$(\sigma_1' - \sigma_3')$, lbs/sq. ins	137.1	121.9	139.1	135.0	124.3
Sheath correction, lbs/sq. ins.	0.1	0.3	0.1	0.1	0.2
Platten friction correction, lbs/sq.ins.	0.2	0.1	1.2	1.3	0.3
Corrected $(\sigma_1' - \sigma_3')$, lbs/sq. ins.	136.8	121.5	137.8	133.6	123.8
Measured ϕ', degrees	44.1	42.0	44.3	43.7	42.4
Corrected ϕ', degrees	44.1	42.0	44.1	43.6	42.3
Change in $(\sigma_1' - \sigma_3')$ required for a change in ϕ' of 0.1° lbs/sq.ins.	0.8	0.7	0.8	0.8	0.7
$(\sigma_2' - \sigma_3')$, lbs/sq.ins.	38.2	10.8	120.2	134.0	39.0
Sheath correction lbs/sq.ins.	0	0.2	0.1	0.1	0
Platten friction correction, lbs/sq.ins.	0	0.9	1.2	1.4	0
Corrected $(\sigma_2' - \sigma_3')$ lbs/sq. ins.	38.2	9.7	118.9	132.5	39.0

INDEPENDENT STRESS CONTROL TESTS

TYPICAL CORRECTIONS TO MEASURED $(\sigma_1' - \sigma_3')$, $(\sigma_2' - \sigma_3')$ AND ϕ' FOR SAMPLE SHEATH STRENGTH AND PLATTEN FRICTION

FIG. A6.3

included in the general comparison of the results. Furthermore, comparing the ISC test results as b approaches 1.0 with the cuboidal extension tests the measured ϕ' is in both cases reduced by a similar amount, 0.2 degrees. It does not appear possible to significantly vary the difference in measured strengths at b = 1.0 by invoking sample sheath strength and platten friction corrections, unless the foregoing analysis is in serious error. This does not seem likely. Attempts at a more rigorous analysis of the sample sheath strength and platten friction were made, but are not reported as they were not altogether satisfactory. However they did not result in corrections significantly different from those computed from equations (1), (3) and (4), and given in Fig A6.3. Hence the Henkel & Gilbert, Wood, Cornforth and Wade type of analysis is considered satisfactory for the present problem.

Appendix A7

Typical test computations

A7.1 Cylindrical triaxial compression

Test A/6 — Date: 2/5/64

Sample: 4 ins diameter, 4 ins high

Ends: lubricated, 1/0.009 ins thick membrane.

Sample sheath 0.020 ins thick.

Type: compression, drained to atmosphere.

Material: Saturated Ham River sand, Batch 1.

Sample built in two halves, vibrated.

G = 2.674

Weight of sand

Wt.of tin & dry sand before building sample	=	4398.9 gm
Wt.of tin & dry sand after building sample	=	3058.4 gm
Wt.of dry sand used in sample	=	1340.5 gm
Wt.of tin & dry sand recovered after test	=	3979.7 gm
Wt. of tin	=	1643.0 gm
Wt.of dry sand recovered after test	=	1336.7 gm
Average weight of sand in sample	=	1338.6 gm

Sample dimensions measured under a suction of 2 ft of water.

	Diameter (ins)		Height (ins)
Top	3.963	3.968	4.065
Centre	3.971	3.974	4.054
Bottom	3.971	3.969	4.053
	Mean = 3.969		4.058
			Mean = 4.058
	Subtract twice sample sheath thickness		Add twice sample sheath thickness
			0.040
	D_i = 3.929 ins		H_i = 4.098

Initial state

Initial cross-sectional area, $A_i = \frac{\pi}{4} 3.929^2 = 12.13 \text{ ins}^2$

Porous disc volume correction = 0.03 ins^3

Initial volume of sample, V_i = 12.13 x 4.098 - 0.03

= 49.64 ins^3

= 813.7 cc

Initial porosity of sample, $n_i = 1 - \frac{1338.6}{2.674 \times 813.7}$

= 38.5%

End of consolidation state

Change in volume on applying cell pressure, ΔV = 6.5 cc

Reduction in height, $\Delta H = \frac{6.5 \times 4.098}{3 \times 813.7}$

= 0.011 ins

Height, H_c = 4.087 ins

Volume, V_c = 807.2 cc

Area, $A_c = \frac{807.2}{4.087 \times 16.39} = 12.05 \text{ ins}^2$

Porosity, $n_c = 1 - \frac{1338.6}{2.674 \times 807.2} = 38.1\%$

Test details

Axial proving ring: Scale factor 90/000

Axial strain rate: Gear 2/17, 0.007 ins/min.

Initial air reading - 00247 (20.4°C)

Initial water reading - 00228

Drainage at both ends of sample.

Shear test: see Figs A7.1 & A8.13. Cell pressure, $\sigma_3' = 40.0$ psi

Failure state

Axial strain, $\Delta H/H_c$ = + 7.2%

Volumetric strain, $\Delta V/V_c$ = - 3.9%

Average lateral strain, $\Delta D/D_c$ = - 6.4%

Volumetric strain rate, $\frac{d(\Delta V/V_c)}{d(\Delta H/H_c)} = - 0.72$

Max. angle of shearing resistance, $\phi' = \sin^{-1} \frac{162.3}{242.3} = 42.1°$

Porosity, $n_f = 1 - \frac{1338.6}{2.674 \times 838.7} = 40.4\%$

Time	Cell pressure σ_3' lbs/sq.ins	Cbl meter decade reading	Change in decade reading	Axial dial gauge reading ins $\times 10^{-3}$	Corrected axial deformation ins $\times 10^{-3}$	Burette reading cc	ΔV cc	$\frac{\Delta H}{H_c}$ %	$\frac{\Delta V}{V_c}$ %	Area A_s ins^2	$\sigma_1' - \sigma_3'$ lbs/sq.ins	σ_1' lbs/sq.ins				
						20·9	initial burette reading									
						20·7	after lowering 2ft									
						20·6	remove mould									
						20·1	after measuring up									
	0					19·6	cell filled									
	2·0					17·8										
						18·3	raise burette									
	3·0					18·2										
	4·0					17·8										
	5·0					17·5										
	10·0					16·5										
	15·0					15·8										
	20·0					15·2										
	25·0					14·6										
	30·0					14·2										
	35·0					13·8										
	40·0					13·4										
	40·0	-00224	0	6	0	16·5	0	0	0	12·05	0·3	40·3				
		00000	224	7	0	16·4	+ 0·1	0	+ 0·01	12·05	2·5	42·5				
		+ 01000	1224	10	1	16·2	+ 0·3	+ 0·02	+ 0·04	12·06	13·4	50·4				
		02000	2224	13	2	16·0	0·5	0·05	0·06	12·06	23·7	63·7				
		03000	3224	16	4	15·8	0·7	0·10	0·09	12·06	34·0	74·0				
		04000	4224	20	6	15·6	0·9	0·15	0·11	12·06	44·3	84·3				
		05300	5524	25	10	15·3	1·2	0·24	0·12	12·07	57·9	97·9				
		06000	6224	28	12	15·2	1·3	0·30	0·16	12·07	65·1	105·1				
		07000	7224	33	15	15·1	1·4	0·37	0·17	12·08	75·6	115·6				
		08000	8224	39	20	15·1	1·4	0·49	0·17	12·09	85·7	125·7				
		09000	9224	47	27	15·2	1·3	0·66	0·16	12·12	95·8	135·8				
		10000	10224	57	36	15·5	+ 1·0	0·88	+ 0·12	12·15	105·7	145·7				
		11000	11224	70	47	16·2	+ 0·3	1·15	+ 0·04	12·19	115·9	155·9				
		12000	12224	87	63	17·3	- 0·8	1·54	- 0·10	12·26	125·1	165·1				
		13100	13324	111	86	19·4	- 2·9	2·11	- 0·36	12·36	134·6	174·6				
		14100	14324	140	114	22·4	5·9	2·79	0·78	12·49	143·4	183·4				
		15000	15224	172	146	26·3	9·8	3·55	1·21	12·65	150·3	190·3				
		16000	16224	219	191	32·7	16·2	4·67	2·01	12·90	156·8	196·8				
		16600	16824	258	229	38·1	21·6	5·60	2·67	13·11	160·0	200·0				
		17000	17224	293	264	43·2	26·7	6·46	3·31	13·32	161·0	201·0				
		17460	17684	363	323	51·7	35·2	7·90	4·36	13·66	162·3	202·3				
		17720	17944	405	376	59·0	42·5	9·18	5·26	13·97	160·2	200·2				
		17840	18064	463	433	67·2	50·7	10·60	6·27	14·33	157·0	197·0				
		17840	18064	501	471	72·3	55·8	11·52	6·91	14·57	154·5	194·5				
Slip zone is first observed		17710	17934	551	521	78·4	61·9	12·75	7·67	14·88	150·3	190·3				
		17100	17324	616	587	85·2	68·7	14·36	8·50	15·28	141·3	181·3				
		16100	16324	681	652	90·8	74·3	15·95	9·20	15·67	130·1	170·1				
		15270	15494	738	711	94·0	77·5	17·40	9·59	16·00	120·9	160·9				
		15310	15534	809	782	96·3	79·8	19·14	9·88	16·38	118·5	158·5				
		15440	15664	876	847	98·2	81·7	20·73	10·11	16·75	116·7	156·7				
		16000	16224	949	921	99·8	83·3	22·54	10·31	17·17	118·3	158·3				
		16290	16514	1020	991	101·1	84·6	24·25	10·48	17·59	117·4	157·4				
		16730	16964	1081	1052	102·0	85·5	25·74	10·59	17·96	117·9	157·9				
		17360	17584	1149	1119	103·0	86·5	27·38	10·71	18·38	119·4	159·4				
		18010	18234	1206	1176	104·0	- 87·5	+ 28·78	- 10·83	18·76	121·3	161·3				
	40·0	18400	18624	1240	1209	104·6	- 88·1	+ 29·95	- 10·90	19·06	122·0	162·0				
Stop Test &	Reverse															
	40·0	- 00210	14	clear	—	96·1		—								

TEST A16. CYLINDRICAL TRIAXIAL COMPRESSION. TEST DATA

FIG. A7.1

A7.2 Cuboidal triaxial extension

Test ICE/4

Date:26/5/66

Sample: H = 3.3 ins
B = 3.2 ins
C = 2.1 ins

Type: extension, drained to atmosphere.

Material: saturated Han River sand Batch 2, Bags 1 & 2 (mixed), Sample built in normal way.

Ends: lubricated, 3/0.010 ins thick membranes.

Sample sheath 0.012 ins thick.

G = 2.664

Weight of sand

Wt. of tin & dry sand before building sample	= 1563.2 gm
Wt. of tin & dry sand after building sample	= 969.1 gm
Wt. of dry sand used in sample	= 594.1 gm
Wt. of tin & dry sand recovered after test	= 3608.5 gm
Wt.of tin	= 3015.0 gm
Wt.of dry sand recovered after test	= 593.5 gm
Average weight of sand in sample	= 593.8 gm

Sample dimensions measured under a suction of 2 ft of water.

Height (ins)	Belt width (ins)	Cell width (ins)
3.280	3.248	2.122
3.277	3.250	2.116
3.282	3.248	2.130
3.273	3.249	2.122
Mean = 3.278	Mean = 3.249	Mean = 2.122
Add twice sample sheath thickness	Subtract twice sample sheath thickness	Subtract twice sample sheath thickness
0.024	0.024	0.024
H_i = 3.302 ins	B_i = 3.225 ins	C_i = 2.098ins

Initial state

Initial cross-sectional area, A_i = 3.225 x 2.098 = 6.766 ins^2

Porous disc volume correction = 0.03 ins^3

Initial volume of sample, V_i = 3.302 x 6.766 - 0.03

= 22.30 ins^3

= 365.5 cc

Initial porosity of sample, n_i = $1 - \frac{593.8}{2.664 \times 365.5}$

= 39.1%

End of consolidation state

Change in volume on applying cell pressure, ΔV = 5.5 cc

Reduction in height, ΔH = $\frac{5.5 \times 3.302}{3 \times 365.5}$

= 0.017 ins

Height, H_c = 3.285 ins

Volume, V_c = 360.0 cc

Area, A_c = $\frac{360.0}{3.285 \times 16.39}$ = 6.685 ins^2

Porosity, n_c = $1 - \frac{593.5}{2.664 \times 360.0}$ = 38.1%

Test details

Axial proving ring:
Scale factor 90/000
Initial air reading - 00560
Initial water reading - 00552
Shear test: see Figs A7.2 & A10.21.

Axial strain rate: Gear 2/10, 0.0035 ins/min

Cell pressure, σ_1' = 140.0 psi

Failure state

Axial strain, $\Delta H/H_c$ = - 4.8%

Volumetric strain, $\Delta V/V_c$ = - 0.8%

Average lateral strain, $\Delta B/B_c$ = $\Delta C/C_c$ = + 1.9%

Volumetric strain rate, $\frac{d(\Delta V/V_c)}{d(\Delta H/H_c)}$ = + 0.30

$\frac{d(\Delta V/V_c)}{d(\Delta B/B_c)}$ = $\frac{d(\Delta V/V_c)}{d(\Delta C/C_c)}$ = - 0.97

Max. angle of shearing resistance, ϕ' = $\sin^{-1} \frac{113.0}{167.0}$ = 42.5°

Porosity, n_f = $1 - \frac{593.8}{2.664 \times 362.9}$ = 38.6%

Time	Cell pressure σ_1' lbs/sqins	C61 meter decade reading	Change in decade reading	Axial dial gauge reading ins $\times 10^{-3}$	Corrected axial deformation ins $\times 10^{-3}$	Burette reading cc	ΔV cc	$\frac{\Delta H}{Hc}$ %	$\frac{\Delta V}{Vc}$ %	Area A_s ins^2	$\sigma_1' - \sigma_3'$ lbs/sqins	σ_3' lbs/sqins				
						80.0	initial burette reading									
						70.2	after lowering 2ft									
						70.4	remove mould									
						70.3	after measuring up									
	0					70.0	cell filled									
	2.0					69.7										
						70.4	raise burette									
	3.0					70.2										
	4.0					70.0										
	5.0					69.8										
	10.0					69.1										
	15.0					68.7										
	20.0					68.4										
	25.0					68.1										
	30.0					67.9 / 68.4	24 hours interval									
	40.0					68.2										
	50.0					67.8										
	60.0					67.5										
	70.0					67.3										
	80.0					67.1										
	90.0					66.8										
	100.0					66.6										
	110.0					66.5										
	120.0					66.3										
	130.0					66.1										
	140.0					66.0										
	140.0	- 00545	0	600	0	65.9	0	0	0	6.69	0	140.4				
		- 01000	455	595	0	65.9	0	0	0	6.69	8.6	131.8				
		- 02000	1455	588	3	65.9	0	- 0.09	0	6.68	27.5	112.9				
		- 03000	2455	579	9	65.9	0	- 0.27	0	6.67	46.3	94.1				
		04100	3555	571	14	65.8	+ 0.1	0.43	+ 0.03	6.66	66.9	73.5				
		04900	4355	661	23	65.6	+ 0.3	0.70	+ 0.08	6.64	82.2	58.1				
		05400	4855	551	31	65.6	+ 0.3	0.94	+ 0.08	6.62	91.7	48.7				
		05760	5206	538	44	65.7	+ 0.2	1.34	+ 0.06	6.60	98.6	41.8				
		05940	5396	626	55	65.9	0	1.68	0	6.59	102.2	38.2				
		06020	5476	519	62	66.1	- 0.2	1.89	- 0.06	6.57	104.1	36.3				
		06130	5585	507	74	66.3	- 0.4	2.25	- 0.11	6.55	106.7	33.7				
		06200	5655	497	83	66.6	0.7	2.53	0.19	6.54	108.0	32.4				
		06310	5765	472	108	67.2	1.3	3.28	0.36	6.50	110.9	29.5				
		06330	5785	466	114	67.4	1.5	3.47	0.42	6.49	111.3	29.1				
		06350	5805	455	125	67.7	1.8	3.80	0.50	6.48	112.1	28.3				
		06370	5825	442	138	68.2	2.3	4.20	0.64	6.46	113.1	27.3				
		06380	5835	433	147	68.4	2.5	4.47	0.69	6.44	113.4	27.0				
		06370	5825	418	162	69.0	3.1	4.93	0.86	6.43	113.4	27.0				
		06350	5805	412	168	69.2	3.3	5.11	0.91	6.42	113.2	27.2				
		06300	5755	403	177	69.4	- 3.5	- 5.39	- 0.97	6.41	112.5	27.9				
	140.0	06260	5715	398	182	69.6	- 3.7	- 5.54	- 1.03	6.40	111.9	28.5				
	Stop Test & Reverse															
	140.0	- 00620	75	clear	—											

TEST ICE14. CUBOIDAL TRIAXIAL EXTENSION. TEST DATA.

FIG. A7.2

A7.3 Independent stress control

Test ISC/7 Date: 2/10/66

Sample: H = 3.3 ins
B = 3.3 ins
C = 2.1 ins

Type: belt opening, drained to atmosphere.

Ends: axial, 2/0.010 ins thick membranes.
belt, 1/0.010 thick membrane & sample sheath.

Material: saturated Ham River sand, Batch 2, Bags 1 & 2 (mixed).

Sample built in normal way.

Sample sheath 0.013 ins thick.

G = 2.664

Weight of sand

Wt. of tin & dry sand before building sample	=	1528.8 gm
Wt.of tin & dry sand after building sample	=	933.1 gm
Wt. of dry sand used in sample	=	595.7 gm
Wt. of tin & dry sand recovered after test	=	1423.4 gm
Wt of tin	=	828.3 gm
Wt.of dry sand recovered after test	=	595.1 gm
Average weight of sand in sample	=	595.4 gm

Sample dimensions measured under a suction of 2 ft of water.

Height (ins)	Belt width (ins)	Cell width (ins)
3.231	3.280	2.098
3.284	3.277	2.101
3.231	3.272	2.100
3.283	3.278	2.099
Mean = 3.282	Mean = 3.277	Mean = 2.100
Add twice sample sheath thickness	Subtract twice sample sheath thickness	Subtract twice sample sheath thickness
0.026	0.026	0.026
H_i = 3.308 ins	B_i = 3.251 ins	C_i = 2.074 ins

Initial state

Initial axial cross-sectional area, A_i = 3.251 x 2.074 = 6.743 ins^2

Porous disc volume correction = 0.03 ins^3

Initial volume of sample, V_i = 3.308 x 6.743 - 0.03

= 22.78 ins^3

=365.1 cc

Initial porosity of sample, n_i = $1 - \frac{595.4}{2.664 \times 365.1}$

= 38.8%

End of consolidation state

Change in volume on applying cell pressure, ΔV = 3.4 cc

Reduction in height, ΔH = $\frac{3.4 \times 3.308}{3 \times 365.1}$

= 0.010 ins

Height, H_c = 3.298 ins

Volume, V_c = 361.7 cc

Area, A_c = $\frac{361.7}{3.298 \times 16.39}$ = 6.691 ins^2

Porosity, n_c = $1 - \frac{595.4}{2.664 \times 361.7}$ = 38.2%

Cell width, C_c = $2.074 - \frac{3.4 \times 2.074}{3 \times 365.1}$ = 2.067 ins

Belt width, B_c = $3.251 - \frac{3.4 \times 3.251}{3 \times 365.1}$ = 3.241 ins

Area, A_c* = 3.298 x 2.067 = 6.817 ins^2

Test details

Axial proving ring:

Scale factor 90/000

Initial air reading - 00402

Initial water reading - 00387

Belt proving ring:

Scale factor: 90/000

Initial water reading + 01270

Axial strain rate, Gear 2/5, 0.002 ins/min

Belt strain rate, 0.001 ins/min, opening.

Cell pressure, σ_3' = 30.0 psi

Shear test: see Figs A7.3 & A11.7.

Time	Cell pressure σ_3' lbs/sq.ins	Axial direction: Cell meter decade reading	Change in decade reading	Dial gauge reading ins x 10^{-3}	Corrected deformation ins x 10^{-3}	$\frac{\Delta H}{H_c}$ %	Area A_s ins^2	$\sigma_1' - \sigma_3'$ lbs/sq.ins	σ_1' lbs/sq.ins	Burette reading cc	ΔV cc	$\frac{\Delta V}{V_c}$ %	ISC belt direction: Cell meter Mk. II decade reading	Change in decade reading	Dial gauge #1 reading ins x 10^{-3}	Dial gauge #2 reading ins x 10^{-3}	Deformation #1 ins x 10^{-3}	Deformation #2 ins x 10^{-3}	Average deformation ins x 10^{-3}	$\frac{\Delta B}{B_c}$ %	$\frac{\Delta V}{B_c} + A_c^*$ ins^2	Area A_s^* ins^2	$\sigma_2' - \sigma_3'$ lbs/sq.ins	σ_2' lbs/sq.ins
										99·1	initial burette reading													
										67·9	after lowering													
										68·1	remove mould													
										67·9	after measuring up													
										66·5	cell filled													
										66·1														
										66·4	raise burette													
										66·3														
										66·0														
										65·8														
										65·0														
										64·6														
										64·2														
										63·9														
										63·6														
										63·0			01270	0	belt clear of sample									
										63·0			01320	50	260·9	192·0								
										63·0			01400	130	264·2	196·9								
										63·0			01430	160	266·2	198·1								
										63·0			01460	190	266·7	199·2								
0										63·0	0	0	01460	190	266·2	199·5	0	0	0	0	6·82	6·82	3·0	33·0
2·0										62·9	+ 0·1	+ 0·03	01410	140	264·2	198·9	0	0·6	0·3	- 0·01	6·82	6·81	2·2	32·2
3·0										62·7	+ 0·3	+ 0·09	01360	90	266·4	196·9	0·8	2·6	1·7	- 0·05	6·81	6·80	1·4	31·4
4·0										62·6	0·4	0·11	01340	70	266·9	196·1	2·3	4·4	3·3	0·10	6·81	6·80	1·2	31·2
5·0										62·5	0·5	0·14	01320	50	263·2	193·4	4·0	6·1	5·0	0·15	6·81	6·79	0·8	30·8
10·0										62·3	0·7	0·19	01310	40	261·6	191·5	5·6	8·0	6·8	0·21	6·80	6·79	0·6	30·6
15·0										62·3	0·7	0·19	01310	40	259·0	188·9	8·2	10·6	9·4	0·29	6·80	6·78	0·6	30·6
20·0										62·4	+ 0·6	+ 0·17	01310	40	256·1	184·5	12·1	15·0	13·6	0·42	6·81	6·78	0·6	30·6
25·0										62·6	+ 0·4	+ 0·11	01310	40	249·6	179·0	17·6	20·5	19·0	0·59	6·81	6·77	0·6	30·6
30·0										63·3	- 0·3	- 0·08	01320	50	240·8	170·1	26·4	29·4	27·9	0·86	6·82	6·77	0·8	30·8
										63·7	- 0·7	- 0·19	01330	60	236·6	164·6	31·7	34·9	33·3	1·03	6·83	6·76	1·0	31·0
										64·5	1·5	0·41	01360	90	227·9	157·2	39·3	42·3	40·8	1·26	6·84	6·76	1·4	31·4
										65·2	2·2	0·61	01410	140	220·0	150·4	47·2	49·1	48·2	1·48	6·86	6·77	2·2	32·2
										66·1	3·1	0·86	01460	190	210·8	142·9	56·4	56·6	56·5	1·74	6·88	6·77	3·0	33·0
										67·0	4·0	1·11	01520	250	201·4	135·3	65·8	64·2	65·0	2·00	6·89	6·76	4·0	34·0
										67·8	4·8	1·33	01570	300	193·9	127·5	73·3	72·0	72·6	2·24	6·91	6·75	4·8	34·8
										68·7	5·7	1·58	01620	350	185·2	119·2	82·0	80·3	81·1	2·50	6·92	6·75	5·6	35·6
										69·7	6·7	1·85	01680	410	175·8	110·2	91·4	89·3	90·3	2·78	6·94	6·75	6·5	36·5
										70·7	7·7	2·13	01760	490	165·2	101·3	102·0	98·2	100·1	3·09	6·96	6·75	7·8	37·8
										71·8	8·8	2·43	01820	550	154·1	91·9	113·1	107·6	110·3	3·40	6·98	6·75	8·7	38·7
										72·7	9·7	2·68	01870	600	145·0	84·3	122·2	115·2	118·7	3·66	7·00	6·75	9·6	39·6
										73·6	10·6	2·93	01930	660	136·9	77·9	130·3	121·6	125·9	3·88	7·02	6·76	10·5	40·5
										74·3	11·3	3·12	01970	700	130·2	72·9	137·0	126·6	131·8	4·06	7·03	6·76	11·1	41·1
										75·3	12·3	3·40	02010	740	122·5	66·4	144·7	135·0	139·8	4·28	7·05	6·76	11·9	41·9
										76·0	13·0	3·59	02040	770	116·9	59·3	150·3	140·2	145·2	4·47	7·06	6·76	12·3	42·3
										76·6	13·6	3·76	02030	760	111·9	55·8	155·3	143·7	149·5	4·61	7·07	6·77	12·1	42·1
										77·5	14·5	4·01	02050	780	105·5	49·5	161·7	150·0	155·8	4·80	7·09	6·77	12·4	42·4
										78·1	15·1	4·17	02040	770	101·0	45·5	166·2	154·0	160·1	4·93	7·10	6·77	12·2	42·2
										78·7	15·7	4·34	02000	730	97·1	40·3	170·1	159·3	164·7	5·07	7·11	6·77	11·6	41·6
										79·2	- 16·2	- 4·48	01980	710	94·9	37·0	172·3	162·5	167·6	- 5·17	7·12	6·77	11·3	41·3
										79·7	- 16·7	- 4·61	01920	650	90·8	32·9	176·4	166·6	171·7	- 5·30	7·13	6·78	10·3	40·3
30·0		06660	7090	362	334	+ 10·11	7·77	114·9	145·3															
Stop Test & Reverse																								
		- 00408	22	clear	—								01326	58	clear	—								

TEST ISC17. INDEPENDENT STRESS CONTROL. TEST DATA.

FIG. A7.3

Failure state

Axial strain, $\Delta H/H_c = + 8.4\ \%$

Belt strain, $\Delta B/B_c = - 4.5\ \%$

Volumetric strain, $\Delta V/V_c = - 3.6\ \%$

Average cell strain, $\Delta C/C_c = - 8.2\ \%$

Volumetric strain rate, $\dfrac{d(\Delta V/V_c)}{d(\Delta H/H_c)} = - 0.62$

Max. angle of shearing resistance, $\phi' = \sin^{-1} \dfrac{123.1}{183.1} = 42.2^{\circ}$

Porosity, $n_f = 1 - \dfrac{595.4}{2.664 \times 374.7} = 40.4\%$

Appendix A 8

Graphical presentation of cylindrical triaxial compression test results.

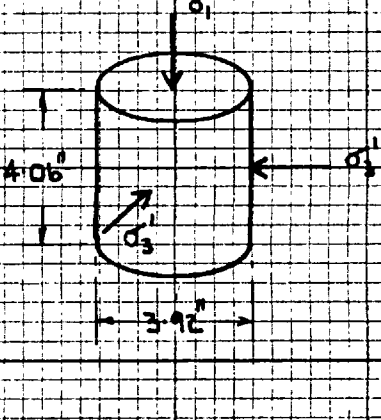
Slip planes first observed

Axial stress, σ_1'

End of test

$\Delta V/V_c$

Cell pressure, σ_3'



Stress, lbs. / sq. in.

Volumetric Strain, $\Delta V/V_c$ %

Axial strain, $\Delta H/H_c$ %

TEST X/1. CYLINDRICAL TRIAXIAL COMPRESSION.

Ham River Sand, Batch #1. Date: 9/2/64

n_i = 39.9%

1/0.009" thick lubricated membrane used at each end of sample.

Sample sheath 0.020" thick.

FIG. A8.1

Stresses, lbs / sq ins

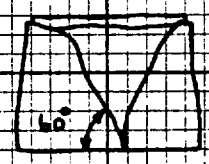
Axial stress, σ_1'

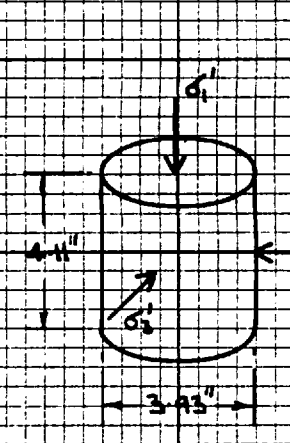
Cell pressure, σ_3'

$\Delta V/V_c$

Volumetric strain $\Delta V/V_c$ %

Axial strain, $\Delta H/H_c$ %





TEST X/3. CYLINDRICAL TRIAXIAL COMPRESSION.

Ham River Sand, Batch*1. Date: 15/2/64

n_i = 38·3%

1/0·009" thick lubricated membrane used at each end of sample.

Sample sheath 0·020" thick.

FIG. A8.2.

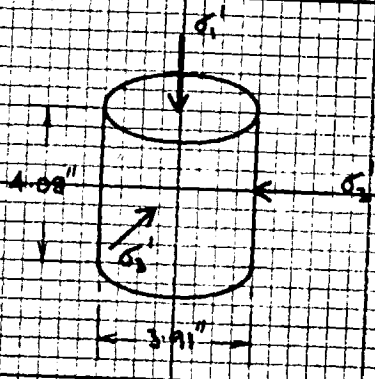
Stresses, lbs / sq. ins

160
140
120
100
80
60
40
20
0

Axial stress, σ_1'

End of Test

Cell pressure, σ_3'



$\Delta V / V_c$

Volumetric strain, $\Delta V / V_c$ %

-2.0
-1.0
0
+1.0

0 2 4 6 8 10 12 14 16
16 18 20 22 24 26

Axial strain, $\Delta H / H_c$ %

TEST X14. CYLINDRICAL TRIAXIAL COMPRESSION.

Ham River Sand, Batch #1 Date 19/2/64

n_i = 45.4%

Two 0.008" thick lubricated membrane used at each end of sample

Sample sheath 0.020" thick

FIG. A9.3

Axial stress, σ_1

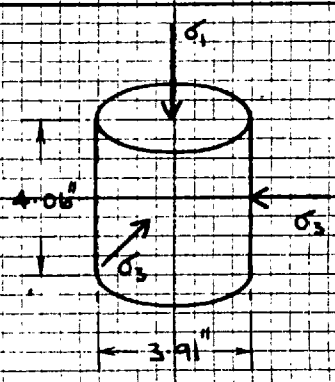
Axial stress, σ_1'

End of test

Cell pressure, σ_3

Pore water pressure, $u = 40$ lbs/sq.ins.

σ_3'



$\Delta V/V_c$

Stresses, lbs/sq.ins.

Volumetric strain, $\Delta V/V_c$ %

Axial strain, $\Delta H/H_c$ %

TEST X/5. CYLINDRICAL TRIAXIAL COMPRESSION.

Ham River Sand, Batch #1. Date: 22/2/64

$n_c = 44.8$ %

1/10·009" thick lubricated membrane used at each end of sample.

Sample sheath 0·020" thick.

FIG. A8.4

Axial stress, σ_1'

End of test

Cell pressure, σ_3'

$\Delta V/V_c$

σ_1'

4·12"

σ_3'

σ_3'

3·92"

Stresses, lbs / sq. ins.

Volumetric strain, $\Delta V/V_c$ %

Axial strain, $\Delta H/H_c$ %

TEST X/b. CYLINDRICAL TRIAXIAL COMPRESSION.

Ham River Sand, Batch #1. Date: 28/2/64

n_i = 43·4 %

0·009" thick lubricated membrane used at each end of sample.

Sample sheath 0·020" thick.

FIG. A8.5

Stresses, lbs/sq. ins.

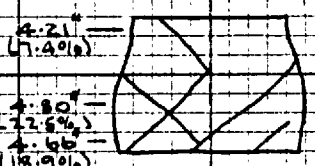
Axial stress, σ_1'

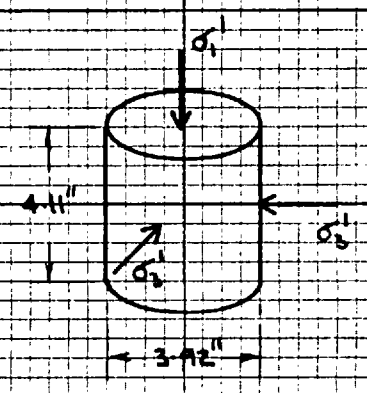
Cell pressure σ_3'

$\Delta V/V_c$

Volumetric strain, $\Delta V/V_c$ %

Axial strain, $\Delta H/H_c$ %





TEST XII. CYLINDRICAL TRIAXIAL COMPRESSION.

Ham River Sand, Batch #1. Date: 1/3/64

n_i = 41.9 %

Two 0.009" thick lubricated membrane used at each end of sample.

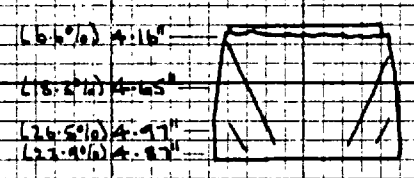
Sample sheath 0.020" thick.

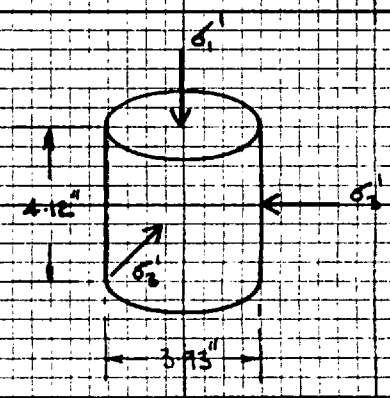
FIG. A8.6

Axial stress, σ_1'

Cell pressure, σ_3'

$\Delta V/V_c$





Stresses, lbs/sq. ins.

180 160 140 120 100 80 60 40 20 0

-80 -70 -60 -50 -40 -30 -20 -10 0 +10

0 2 4 6 8 10 12 14 16

16 18 20 22 24 26

Axial strain, $\Delta H/H_c$ %

TEST X18. CYLINDRICAL TRIAXIAL COMPRESSION.

Ham River Sand, Batch #1. Date: 15/10/64

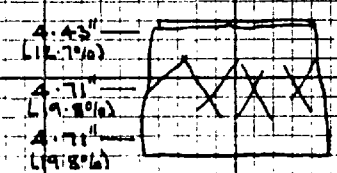
n_i = 40.9 %

0.009" thick lubricated membrane used at each end of sample.

Sample sheath 0.020" thick.

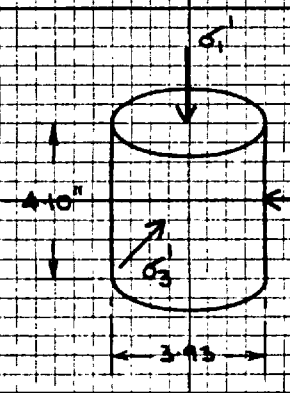
FIG A8.7

Axial stress, σ_1'



Cell pressure σ_3'

$\Delta V/V_c$



Stresses - lbs / sq. ins.

Volumetric strain, $\Delta V/V_c$ %

Axial strain, $\Delta H/H_c$ %

TEST X19. CYLINDRICAL TRIAXIAL COMPRESSION.

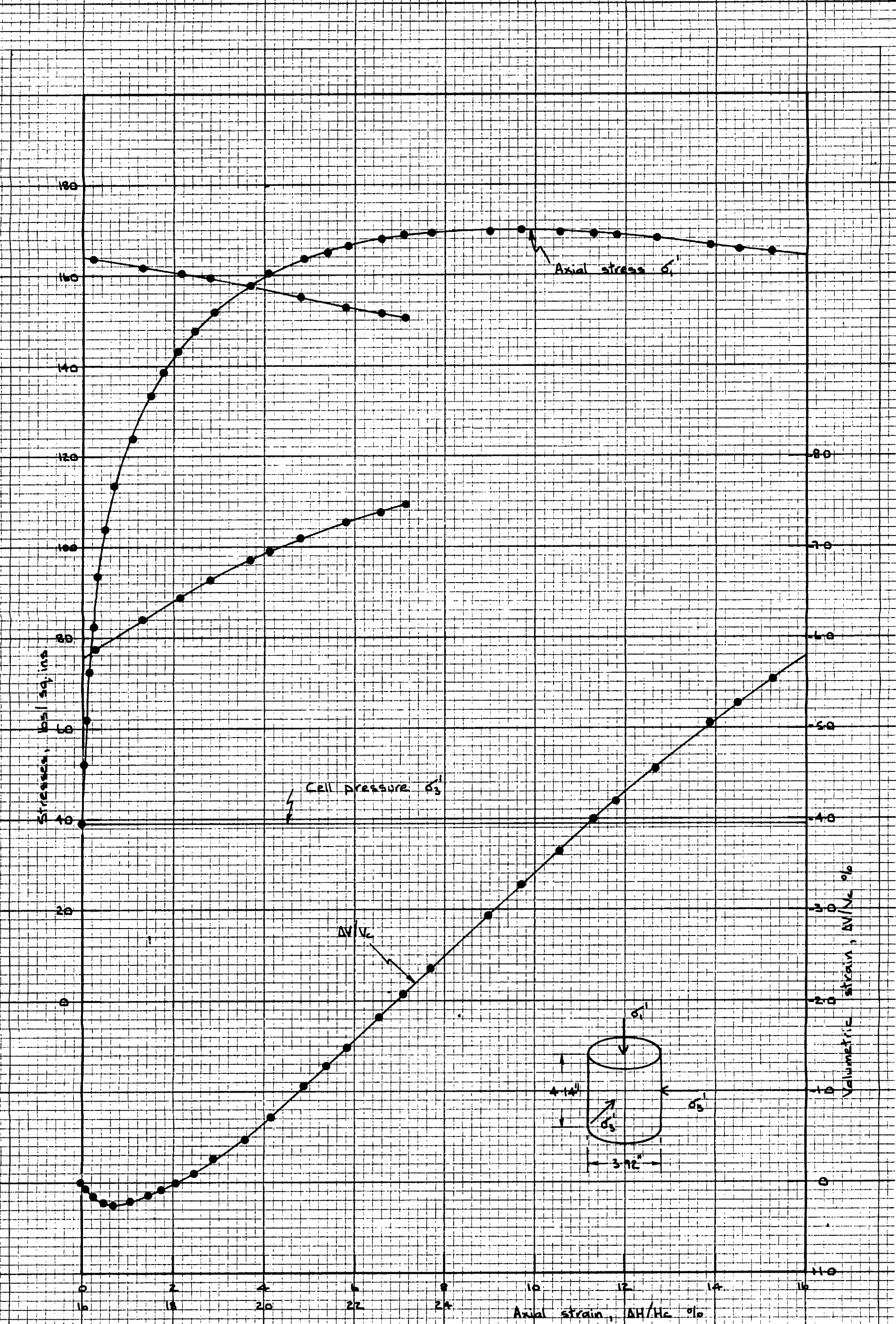
Ham River Sand, Batch #1, Reused. Date: 22/10/64

n_i = 40·2 %

0·009" thick lubricated membrane used at each end of sample.

Sample sheath 0·020" thick.

FIG. A8.8



TEST X110. CYLINDRICAL TRIAXIAL COMPRESSION.

Ham River Sand, Batch *1, Reused. Date: 23/11/64

n_i = 41·1%

110·009" thick lubricated membrane used at each end of sample.

Sample sheath 0·020" thick.

FIG. A8.9

Axial stress σ_1'

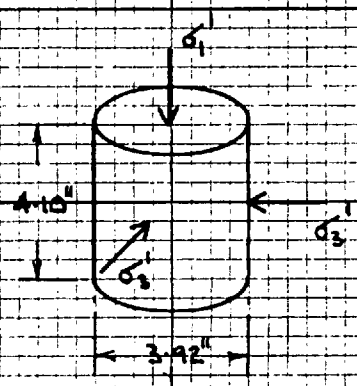
Cell pressure σ_3'

$\Delta V/V_c$

Stresses, lbs/sq.ins.

Volumetric strain, $\Delta V/V_c$

Axial strain, $\Delta H/H_c$ %



TEST XIII. CYLINDRICAL TRIAXIAL COMPRESSION.

Ham River Sand, Batch*1, Reused. Date: 1/12/64

n_i = 40·8%

0·009" thick lubricated membrane used at each end of sample.

Sample sheath 0·020" thick.

FIG. A8.10

Axial stress σ_1'

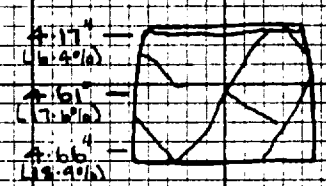
Cell pressure, σ_3'

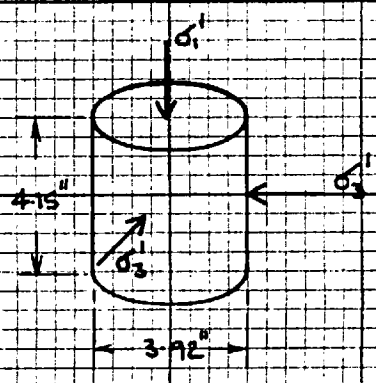
$\Delta V/V_c$

Stresses - lbs / sq. in.

Volumetric strain, $\Delta V/V_c$ %

Axial strain, $\Delta H/H_c$ %





TEST X12. CYLINDRICAL TRIAXIAL COMPRESSION.

Ham River Sand, Batch #1, Reused. Date: 5/12/64

n_i = 41.0 %

1/0.004" thick lubricated membrane used at each end of sample.

Sample sheath 0.020" thick

FIG. A8.11

Axial stress σ_1'

Cell pressure, σ_3'

$\Delta V/V_c$

4.30" (9.1%)
4.68" (19.4%)
4.13" (20.7%)
End of test

σ_1'
4.12"
σ_3'
σ_3'
3.92"

Stresses, lbs / sq. ins.

Volumetric strain, $\Delta V/V_c$ %

Axial strain, $\Delta H/H_c$ %

TEST X/13. CYLINDRICAL TRIAXIAL COMPRESSION.

Ham River Sand, Batch #1, Reused. Date 21/12/64

h_i = 41.1%

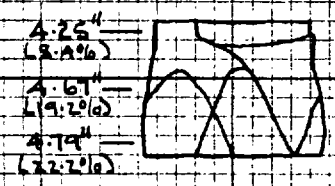
0.009" thick lubricated membrane used at each end of sample.

Sample sheath 0.020" thick.

FIG A8.12.

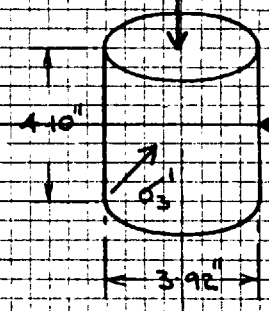
Axial stress, σ_1'

Cell pressure, σ_3'



End of test

$\Delta V/V_c$



Stresses, lbs/sq. ins.

Volumetric strain, $\Delta V/V_c$ %

Axial strain, $\Delta H/H_c$ %

TEST A11. CYLINDRICAL TRIAXIAL COMPRESSION.

Ham River Sand, Batch #1. Date: 15/4/64

n_i = 39·8%, Sample made in 'two halves'

Two 0·009" thick lubricated membrane used at each end of sample.

Sample sheath 0·020" thick

FIG. A8.13

Axial stress, σ_1'

Cell pressure, σ_3'

$\Delta V/V_c$

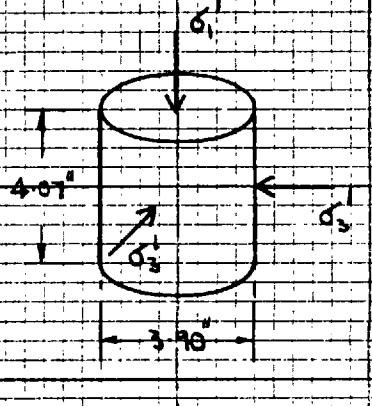
Stresses, lbs/sq.ins.

Volumetric strain, $\Delta V/V_c$ %

Axial strain, $\Delta H/H_c$ %

(9.7%) 4.28" —
(24.9%) 4.97" —
(15.1%) 4.49" —

End of test



TEST A12. CYLINDRICAL TRIAXIAL COMPRESSION.

Ham River Sand, Batch #1. Date: 17/4/64

n_i = 44.7%, Sample made in 'two halves'.

1/0.009" thick lubricated membrane used at each end of sample.

Sample sheath 0.020" thick.

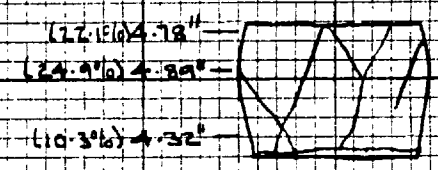
FIG. A8.14

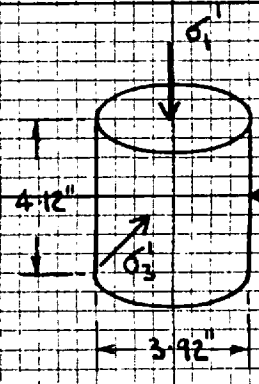
Slip planes first observed

Axial stress, σ_1'

Cell pressure, σ_3'

$\Delta V/V_c$





Stresses, lbs/sq.ins.

Volumetric strain, $\Delta V/V_c$ %

Axial strain, $\Delta H/H_c$ %

TEST A13. CYLINDRICAL TRIAXIAL COMPRESSION.

Ham River Sand, Batch #1. Date 22/4/64

n_i = 40.9%. Sample made in 'two halves'

1/0.009" thick lubricated membrane used at each end of sample.

Sample sheath 0.020" thick.

FIG. A8.15

Stresses, lbs/sq.ins.

Axial stress, σ_1'

Cell pressure, σ_3'

$\Delta V/V_c$

4·08" (4·1⅛)
5·02" (5·1⅛)
4·87" (4·⅞)
End of test

σ_1'
σ_3'
σ_3'
4·08"
3·92"

Volumetric strain, $\Delta V/V_c$ %

Axial strain, $\Delta H/H_c$ %

TEST A14. CYLINDRICAL TRIAXIAL COMPRESSION.

Ham River Sand, Batch #1. Date: 25/4/64
n_i = 42·5%. Sample made in 'two halves'
1/0·009" thick lubricated membrane used at each end of sample.
Sample sheath 0·012" thick.

FIG. A8.16

Slip planes first observed

Axial stress, σ_1'

Stresses, lbs/sq.ins.

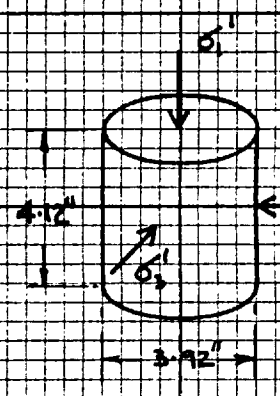
Cell pressure, σ_3'

$\Delta V/V_c$

Volumetric strain, $\Delta V/V_c$ %

(24.3°/o) 4.87" —
(27.8°/o) 5.01" —
(9.9°/o) 4.31" —

End of test



Axial strain, $\Delta H/H_c$ %

TEST A/S. CYLINDRICAL TRIAXIAL COMPRESSION.

Ham River Sand, Batch #1. Date: 28/4/64
n_i: 39.4 °/o Sample made in 'two halves'
1/o.009" thick lubricated membrane used at each end of sample.
Sample sheath 0.020" thick

FIG. AR.17

Slip planes first observed

Axial stress, σ_1'

Stress, lbs / sq. ins.

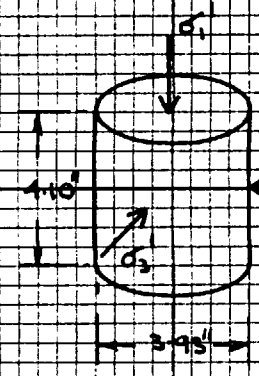
200
180
160
140
120
100
80
60
40
20
0

$\Delta V/V_c$

Cell pressure, σ_3'

-11·0
-10·0
-9·0
-8·0
-7·0
-6·0
-5·0
-4·0
-3·0
-2·0
-1·0
0
+1·0

Volumetric strain, $\Delta V/V_c$ %



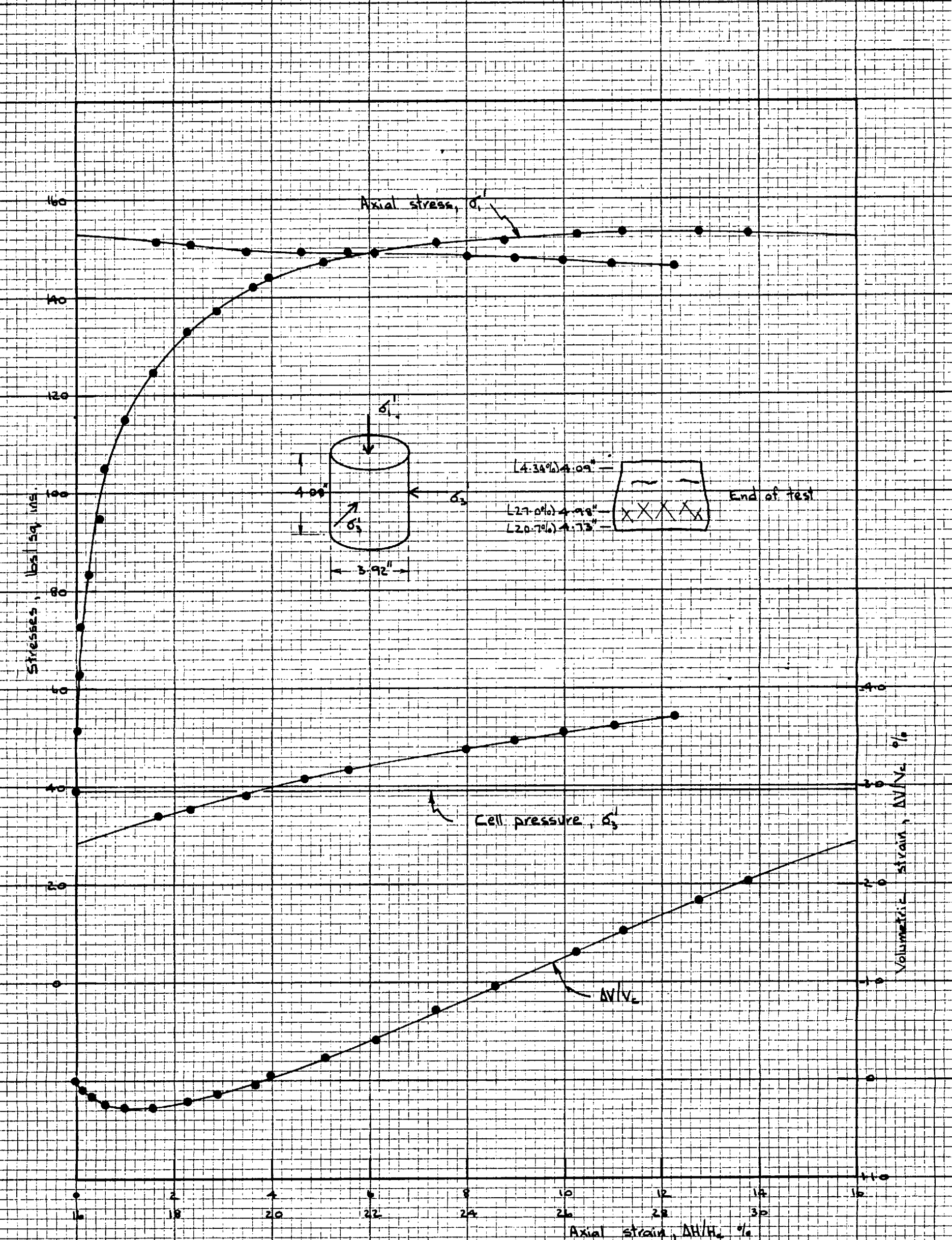
0 2 4 6 8 10 12 14 16
16 18 20 22 24 26 28 30

Axial strain, $\Delta H/H_c$ %

TEST A/6. CYLINDRICAL TRIAXIAL COMPRESSION.

Ham River Sand, Batch #1. Date: 2/5/64
n_i = 38·5 %. Sample made in 'two halves'.
0·004" thick lubricated membrane used at each end of sample.
Sample sheath 0·020" thick.

FIG. A8.19



TEST A11. CYLINDRICAL TRIAXIAL COMPRESSION.

Ham River Sand. Batch #1. Date: 4/9/64

n_i = 40.0%, Sample made in two halves.

0.009" thick lubricated membrane used at each end of sample.

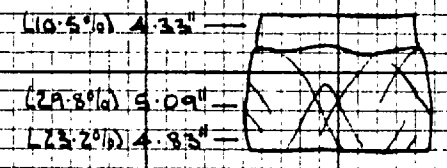
Sample sheath 0.020" thick.

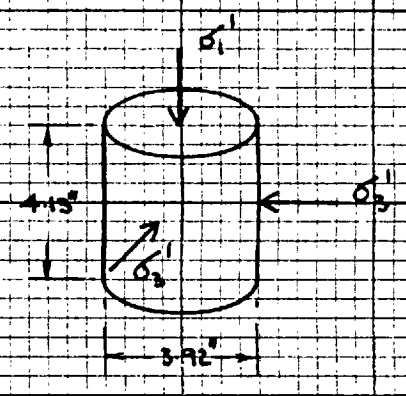
FIG. A8.19

Axial stress, σ_1'

Cell pressure, σ_3'

$\Delta V/V_c$





Stresses, lbs/sq.ins.

Volumetric strain, $\Delta V/V_c$ %

Axial strain, $\Delta H/H_c$ %

TEST A18. CYLINDRICAL TRIAXIAL COMPRESSION.

Ham River Sand, Batch * 1. Date: 19/3/64

n_i = 40·8 %, Sample made in 'two halves'

0·009" thick lubricated membrane used at each end of sample.

Sample sheath 0·020" thick.

FIG. A8.20

Axial stress, σ_1'

$\Delta V/V_c$

Cell pressure, σ_3'

End of test

4·76" (12·4%)
4·68" (19·4%)
4·36" (11·2%)

4·09"

3·72"

Stresses, lbs/sq. ins.

Volumetric strain $\Delta V/V_c$ %

Axial strain, $\Delta H/H_c$ %

TEST A/9. CYLINDRICAL TRIAXIAL COMPRESSION.

Ham River Sand, Batch #1. Date: 13/9/64
n_i = 41·0%, Sample made in "two halves"
3/0·024" thick lubricated membranes used
at each end of sample.
Sample sheath 0·020" thick.

FIG. A8.21

Axial stress, σ_1'

$\Delta V/V_c$

Cell pressure, σ_3'

4.06" (3.69%)
4.66" (13.91%)
4.76" (21.15%)
End of test

σ_1'
4.08"
σ_3'
σ_3'
3.92"

Stresses, lbs/sq.ins.

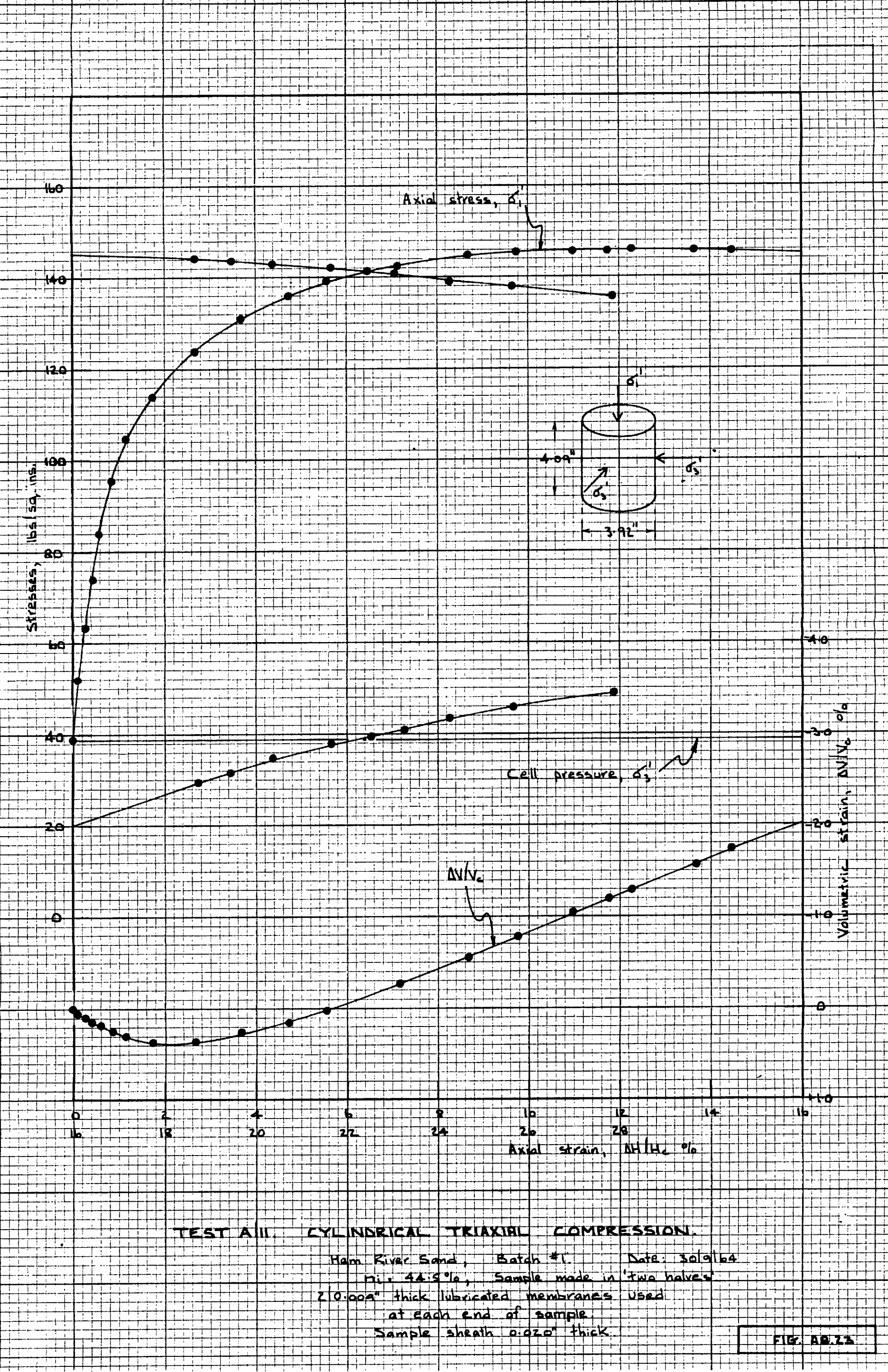
Volumetric strain, $\Delta V/V_c$ %

Axial strain, $\Delta H/H_c$ %

TEST A/10. CYLINDRICAL TRIAXIAL COMPRESSION.

Ham River Sand, Batch #1. Date: 20/9/64
n_i: 40.8%, Sample made in 'two halves'
s/o.024" thick lubricated membranes used
at each end of sample.
Sample sheath 0.020" thick.

FIG. AB.22



TEST A11. CYLINDRICAL TRIAXIAL COMPRESSION.

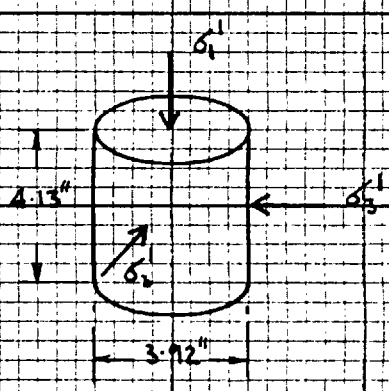
Ham River Sand, Batch #1. Date: 30/9/64
n_i = 44·5%, Sample made in 'two halves'
2 @ 0·009" thick lubricated membranes used at each end of sample.
Sample sheath 0·020" thick.

FIG. A8.23

Axial stress, σ_1'

Cell pressure, σ_3'

$\Delta V/V_c$



Stresses, lbs/sq.in.

Volumetric strain, $\Delta V/V_c$ %

Axial strain, $\Delta H/H_c$ %

TEST A12. CYLINDRICAL TRIAXIAL COMPRESSION.

Ham River Sand, Batch #1. Date: 4/10/64.
n_i = 38.3 %, Sample made in 'two halves'.
2 | 0.008" thick lubricated membranes used at each end of sample.
Sample sheath 0.020" thick.

FIG. A8.24

Axial stress, σ_1'

End of test

4.28" (9.2%)
4.76" (2.4%)
4.37" (1.5%)

Cell pressure, σ_3'

$\Delta V/V_c$

ΔV

σ_1'

4.13"

σ_3'

σ_2'

3.92"

Stresses, lbs/sq. ins.

Volumetric strain $\Delta V/V_c$ %

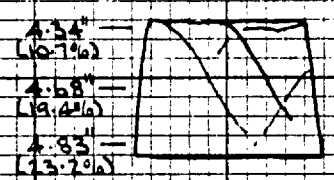
Axial strain, $\Delta H/H_c$ %

TEST A13. CYLINDRICAL TRIAXIAL COMPRESSION.

Ham River Sand, Batch #1. Date: 11/10/64
n_i = 42.9 %, Sample made in 'two halves'.
10.009" thick lubricated membrane used at each end of sample.
Sample sheath 0.020" thick.

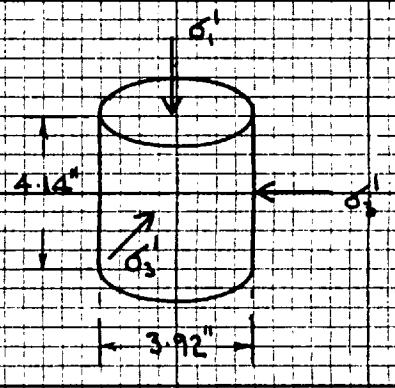
FIG. A8.25

Axial stress, σ_1'



Cell pressure σ_3'

$\Delta V/V_c$



Stresses, lbs/sq.ins.

Volumetric strain, $\Delta V/V_c$ %

Axial strain, $\Delta V/V_c$ %

TEST A/14. CYLINDRICAL TRIAXIAL COMPRESSION.

Ham River Sand, Batch #1. Date: 18/10/64
n_i = 40·4 %, Sample made in 'two halves'.
2/0·009" thick lubricated membranes used at each end of sample.
Sample sheath 0·020" thick.

FIG. A8.26

Axial stress, σ_1'

Cell pressure σ_3'

$\Delta V/V_c$

4.26" (9.4%)
4.74" (20.1%)
4.67" (8.9%)
End of test.

σ_1'
4.13"
σ_3'
σ_3'
3.93"

Stresses, lbs/sq. ins.

Volumetric strain, $\Delta V/V_c$ %

Axial strain, $\Delta H/H_c$ %

TEST A/15. CYLINDRICAL TRIAXIAL COMPRESSION.

Ham River Sand, Batch #1. Date: 28/11/64

n_i = 40.7%, Sample built in 'two halves'
1/0.009" thick lubricated membrane used at each end of sample.
Sample sheath 0.020" thick.

FIG. A8.27

Axial stress, σ_1'

Cell pressure, σ_3'

4·19" (6·4%)
4·65" (18·3%)
4·60" (17·9%)
End of test

$\Delta V/V_c$

σ_1'
4·12"
σ_3'
σ_3'
3·93"

Stresses, lbs/sq.ins.

Volumetric strain, $\Delta V/V_c$ %

Axial strain, $\Delta H/H_c$ %

TEST A/16. CYLINDRICAL TRIAXIAL COMPRESSION.

Ham River Sand Batch # 1 Date: 30/11/64
n_i = 41·1%, Sample made in 'two halves'
1/10·009" thick lubricated membrane used at each end of sample.
Sample sheath 0·020" thick.

FIG. A8.28

Axial stress, σ_1'

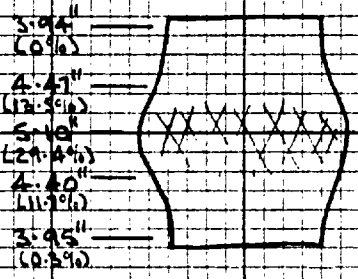
Cell pressure, σ_3'

$\Delta V/V_c$

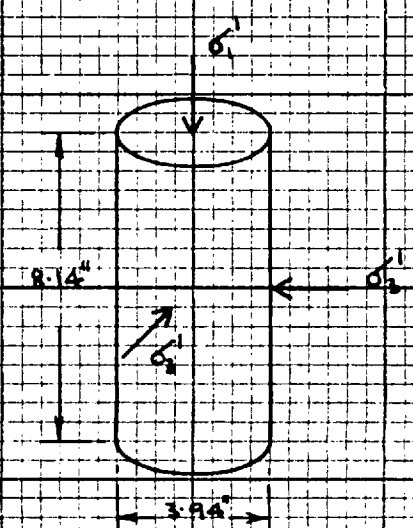
Volumetric strain, $\Delta V/V_c$ %

Axial strain, $\Delta H/H_c$ %

Stress, lbs/sq.ins.



End of test.



TEST B11. CYLINDRICAL TRIAXIAL COMPRESSION.

Ham River Sand, Batch # 1. Date: 22/5/64.

n_i = 45.1%, Sample made in 'two halves'.

Direct contact between sample and platens.

Sample sheath 0.020" thick.

FIG. A8.29

Slip planes first observed

Axial stress, σ_1'

$\Delta V/V_c$

Cell pressure, σ_3'

4·05" (25%)
4·47" (13·2%)
5·11" (29·1%)
4·66" (18·0%)
4·30" (8·9%)

End of test

σ_1'
8·13"
σ_3'
3·98"

Stresses, lbs / sq. ins.

Volumetric strain, $\Delta V/V_c$ %

Axial strain, $\Delta H/H_c$ %

TEST B/2. CYLINDRICAL TRIAXIAL COMPRESSION.

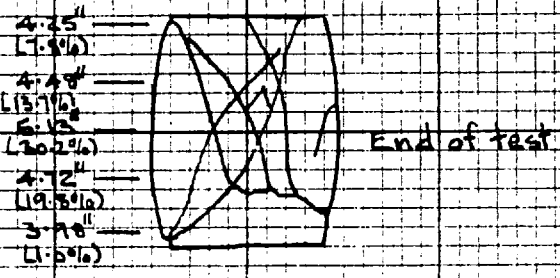
Ham River Sand, Batch *1. Date: 1/6/64
n_c = 39·7%, Sample made in 'two halves'.
Direct contact between sample and platens.
Sample sheath 0·020" thick.

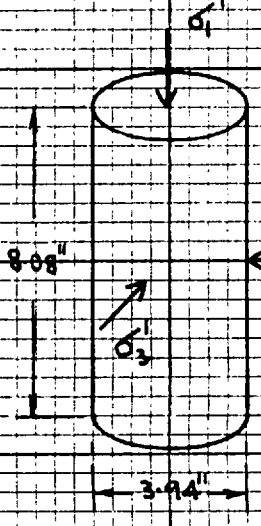
FIG. A8.30

Axial stress, σ_1'

Cell pressure, σ_3'

$\Delta V/V_c$





Stress, lbs/sq. ins.

Volumetric strain, $\Delta V/V_c$ %

Axial strain, $\Delta H/H_c$ %

TEST B15. CYLINDRICAL TRIAXIAL COMPRESSION.

Ham River Sand, Batch #1 Date: 9/6/64.
n_i = 42·1%, Sample made in 'two halves'.
Direct contact between sample and platens.
Sample sheath 0·020" thick.

FIG. A8.51

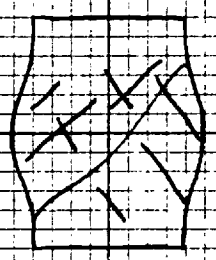
Stresses, lbs./sq. ins.

180
160
140
120
100
80
60
40
20
0

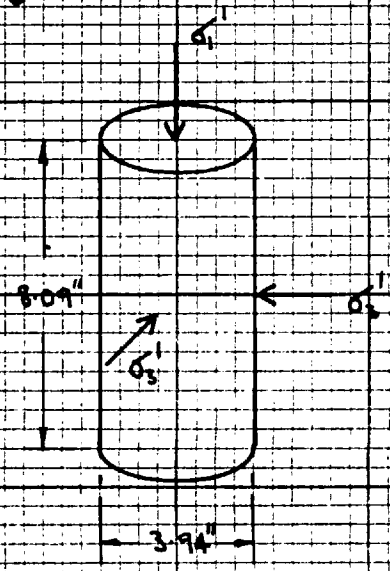
Axial stress, σ_1'

Cell pressure, σ_3'

$\Delta V/V_c$



End of test



-4.0
-3.0
-2.0
-1.0
0
+1.0

Volumetric strain, $\Delta V/V_c$ %

0 2 4 6 8 10 12 14 16
16 18 20 22 24 26 28

Axial strain, $\Delta H/H_c$ %

TEST B14. CYLINDRICAL TRIAXIAL COMPRESSION.

Ham River Sand, Batch #1. Date: 11/6/64.
n_i = 43.1 %, Sample made in 'two halves'.
Direct contact between sample and platens.
Sample sheath 0.020" thick.

FIG. A8.32

Axial stress, σ_1'

Cell pressure, σ_3'

$\Delta V/V_c$

σ_1'

8·10"

σ_3'

3·96"

Stresses, lbs/sq.ins.

Volumetric strain, $\Delta V/V_c$ %

Axial strain, $\Delta H/H_c$ %

TEST B/S. CYLINDRICAL TRIAXIAL COMPRESSION.

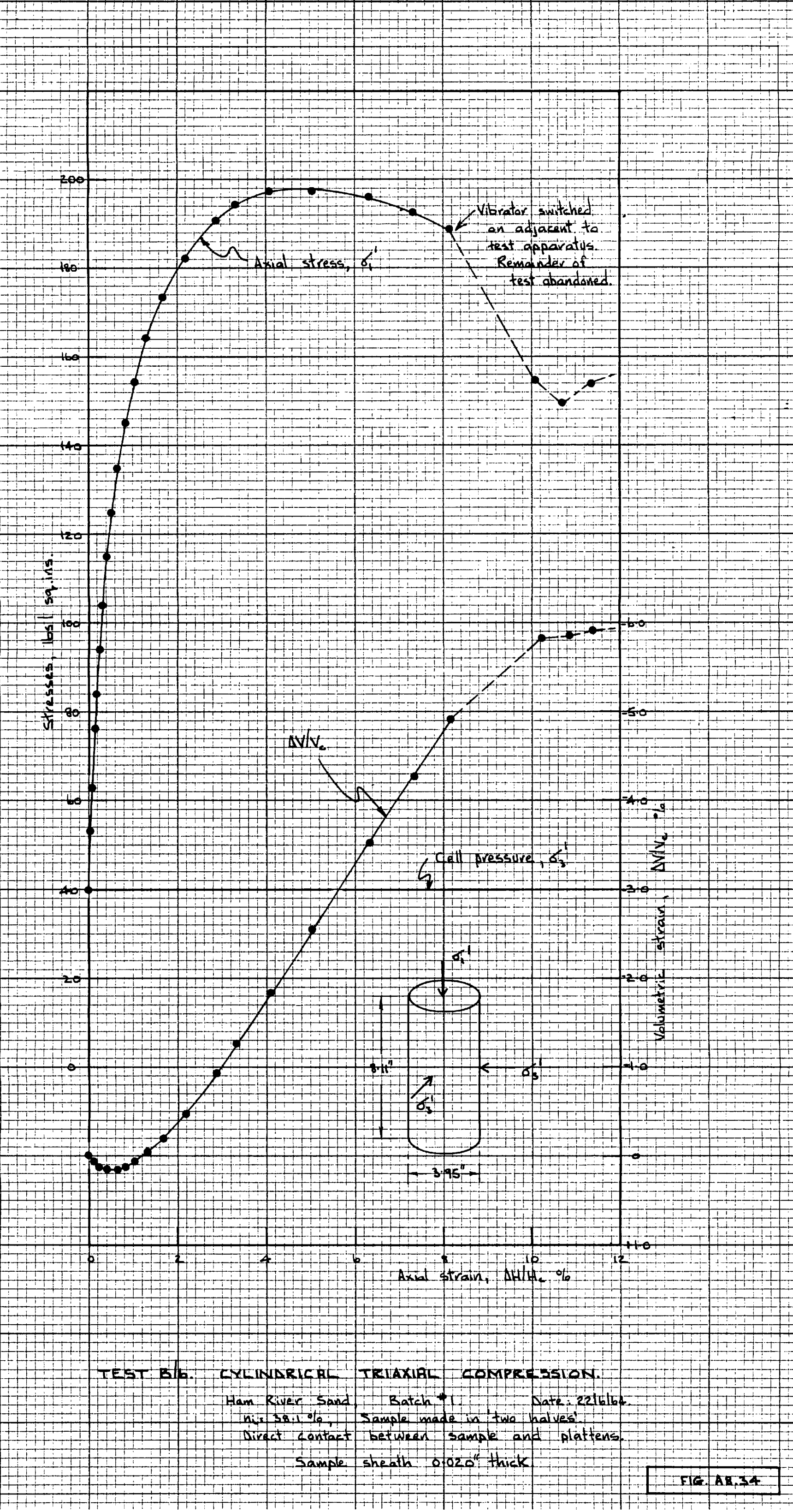
Ham River Sand, Batch #1. Date: 17/6/64.

n_i 40·2 %, Sample made in 'two halves'

Direct contact between sample and platters.

Sample sheath 0·020" thick.

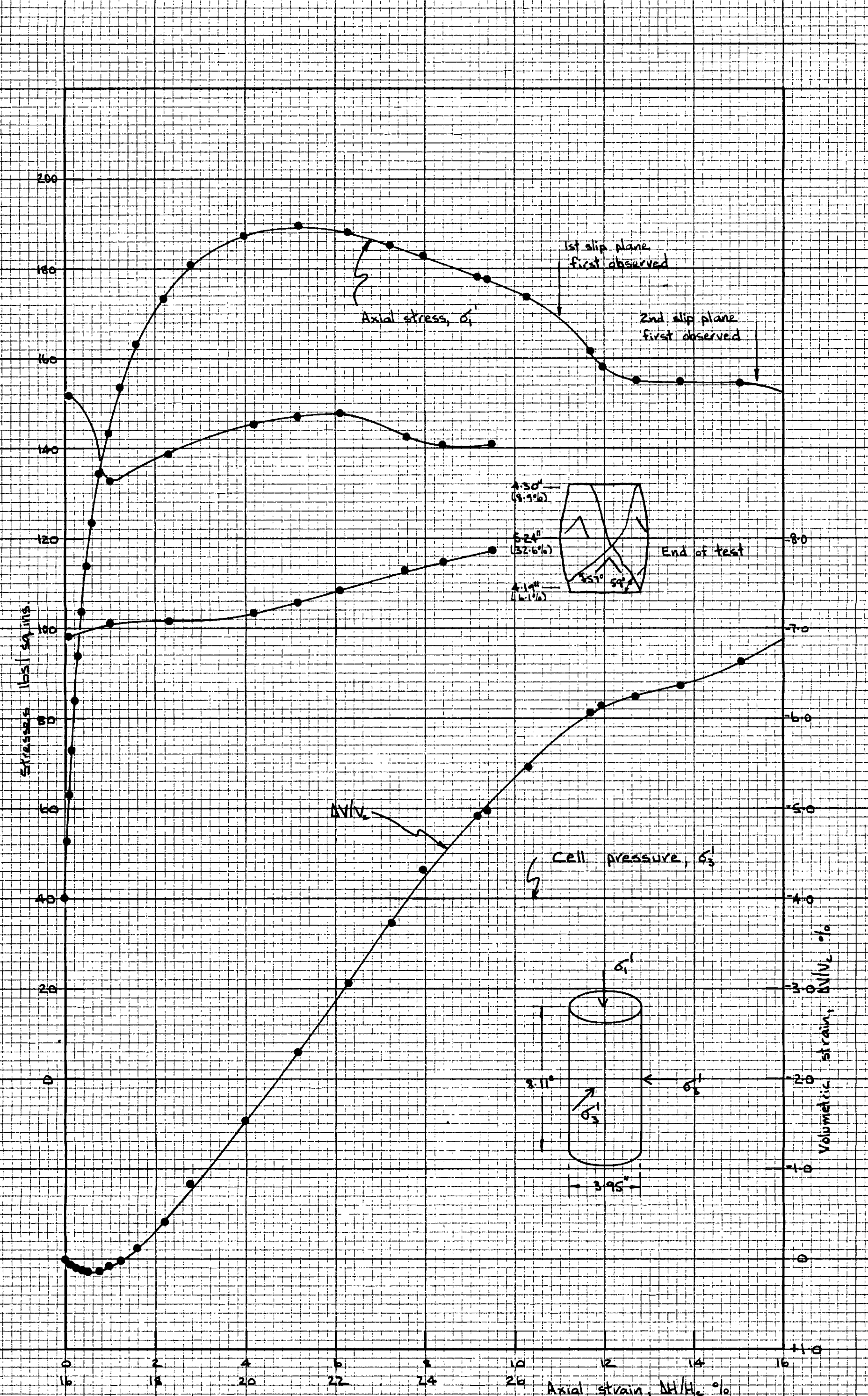
FIG. A8.33



TEST B/6. CYLINDRICAL TRIAXIAL COMPRESSION.

Ham River Sand, Batch #1. Date: 22/6/64.
n_i = 38·1 %, Sample made in 'two halves'.
Direct contact between sample and plattens.
Sample sheath 0·020" thick.

FIG. A8.34



TEST B/7. CYLINDRICAL TRIAXIAL COMPRESSION.

Ham River Sand, Batch #1. Date: 23/6/64.
n_i : 38·7%, Sample made in 'two halves'
Direct contact between sample and platterns.
Sample sheath 0·020" thick.

FIG A8.35

Stresses, lbs sq. ins.

160
140
120
100
80
60
40
20
0

Axial stress, σ_1'

σ_1'

σ_3'

8.09"

3.94"

3.96" (0.6%)

3.96" (30.9%)

3.96" (0.6%)

57°

65°

End of test

Cell pressure, σ_3'

$\Delta V/V_c$

Volumetric strain, $\Delta V/V_c$ %

-20
-10
0
+10

0 2 4 6 8 10 12 14 16
18 20 22 24 26

Axial strain, $\Delta H/H_c$ %

TEST B/8. CYLINDRICAL TRIAXIAL COMPRESSION.

Ham River Sand, Batch #1. Date: 25/6/64.
n_i = 44.4%, Sample made in 'two halves'
Direct contact between sample and platens.
Sample sheath 0.020" thick.

FIG. A8.36

Axial stress, σ_1

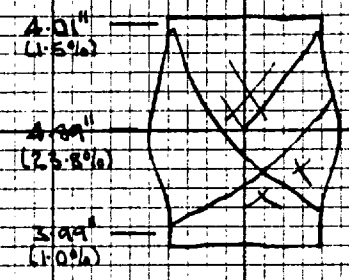
Cell pressure, σ_3'

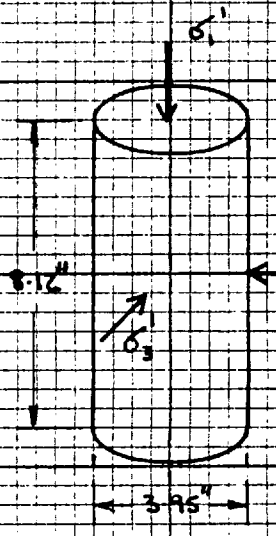
$\Delta V/V_c$

Stresses, lbs/sq.ins.

Volumetric strain, $\Delta V/V_c$ %

Axial strain, $\Delta H/H_c$ %





TEST B/9. CYLINDRICAL TRIAXIAL COMPRESSION.

Ham River Sand, Batch #1, Reused. Date: 27/10/64.
n_i = 39.4%, Sample made in 'two halves'.
Direct contact between sample and plattens.
Sample sheath 0.020" thick.

FIG BB.37

Stresses, tons / sq. ins.

160
140
120
100
80
60
40
20
0

Axial stress, σ_1'

σ_1'

3·94" (0%)
4·37" (10·9%)
5·03" (27·6%)
4·55" (16·5%)
3·96" (5·1%)

End of test

8·04"

σ_2'

σ_3'

3·94"

Cell pressure, σ_3'

Volumetric strain, $\Delta V/V_o$ %

+1·0
0
-1·0

$\Delta V/V_o$

0 2 4 6 8 10 12 14 16
16 18 20 22 24 26

Axial strain, $\Delta H/H_o$ %

TEST C/1. CYLINDRICAL TRIAXIAL COMPRESSION.

Ham River Sand, Batch #1. Date: 25/5/64.
n_i = 45·5%, Sample made in 'two halves'.
110·009" thick lubricated membrane used at each end of sample.
Sample sheath 0·020" thick.

FIG. A5.39

Axial stress, σ_1'

Cell pressure, σ_3'

$\Delta V/V_i$

4·34" (9·9%)
4·81" (21·8%)
5·08" (29·5%)
4·32" (9·4%)
4·19" (4·8%)

End of test

σ_1'

8·14"

σ_3'

3·95"

Stresses, lbs/sq. ins.

Volumetric strain, $\Delta V/V_i$ %

Axial strain, $\Delta H/H_i$ %

TEST C/2. CYLINDRICAL TRIAXIAL COMPRESSION.

Ham River Sand, Batch #1. Date 28/5/64.
n_i = 39·4%, Sample made in two halves.
Two 0·009" thick lubricated membrane used at each end of sample.
Sample sheath 0·020" thick.

FIG. A8.39

Slip planes first observed

Axial stress, σ_1'

Cell pressure, σ_3'

$\Delta V/V_c$

End of test

4.15" (5.3%)
4.64" (17.5%)
5.16" (30.6%)
4.94" (25.1%)
4.24" (7.3%)

σ_1'

8.09"

σ_3'

3.94"

Stresses, lbs / sq. ins.

Volumetric strain, $\Delta V/V_c$ %

Axial strain, $\Delta H/H_c$ %

TEST C/3. CYLINDRICAL TRIAXIAL COMPRESSION.

Ham River Sand, Batch #1. Date: 4/6/64.
n_i = 42.0 %, Sample made in 'two halves'.
2/0.009" thick lubricated membranes used at each end of sample.
Sample sheath 0.020" thick.

FIG. A3.40

Axial stress, σ_1'

End of test

$\Delta V/V_c$

Cell pressure, σ_3'

σ_1'

σ_3'

3.09"

3.94"

Stresses, lbs/sq.ins

Volumetric strain, $\Delta V/V_c$ %

Axial strain, $\Delta H/H_c$ %

TEST C14. CYLINDRICAL TRIAXIAL COMPRESSION.

Ham River Sand, Batch #1. Date: 23/6/64.
n_i = 42.9 %. Sample made in two halves.
3 @ 0.024" thick lubricated membranes used at each end of sample.
Sample sheath 0.020" thick.

FIG. A5.41

Axial stress, σ_1'

Cell pressure, σ_3'

$\Delta V/V_c$

4·09" (3·5%)

5·04" (27·6%)

4·73" (7·1%)

End of test

8·11"

3·96"

Stress, lbs/sq.ins.

Volumetric strain, $\Delta V/V_c$ %

Axial strain, $\Delta H/H_c$ %

TEST C/5. CYLINDRICAL TRIAXIAL COMPRESSION.

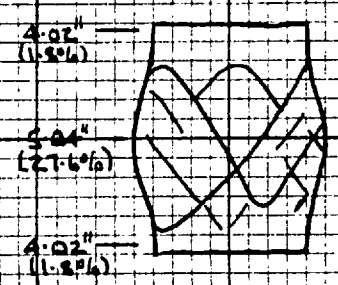
Ham River Sand, Batch #1. Date: 10/1/64.
n_i = 38·6%, Sample made in 'two halves'.
Two 0·009" thick lubricated membrane used at each end of sample.
Sample sheath 0·020" thick.

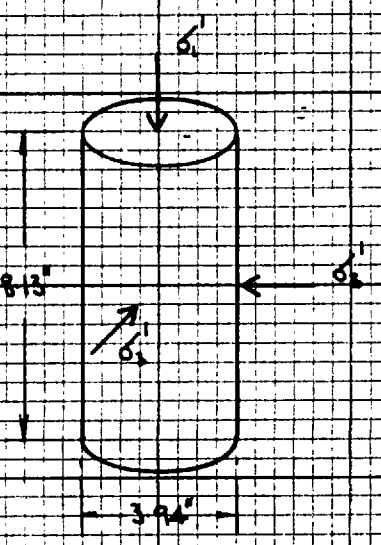
FIG. A8.42

Stresses, lbs / sq.ins.

160
140
120
100
80
60
40

Axial stress, σ_1'





Cell pressure, σ_3'

-3·0
-2·0
-1·0
0
+1·0

Volumetric strain, $\Delta V/V_c$ %

$\Delta V/V_c$

40
20
0

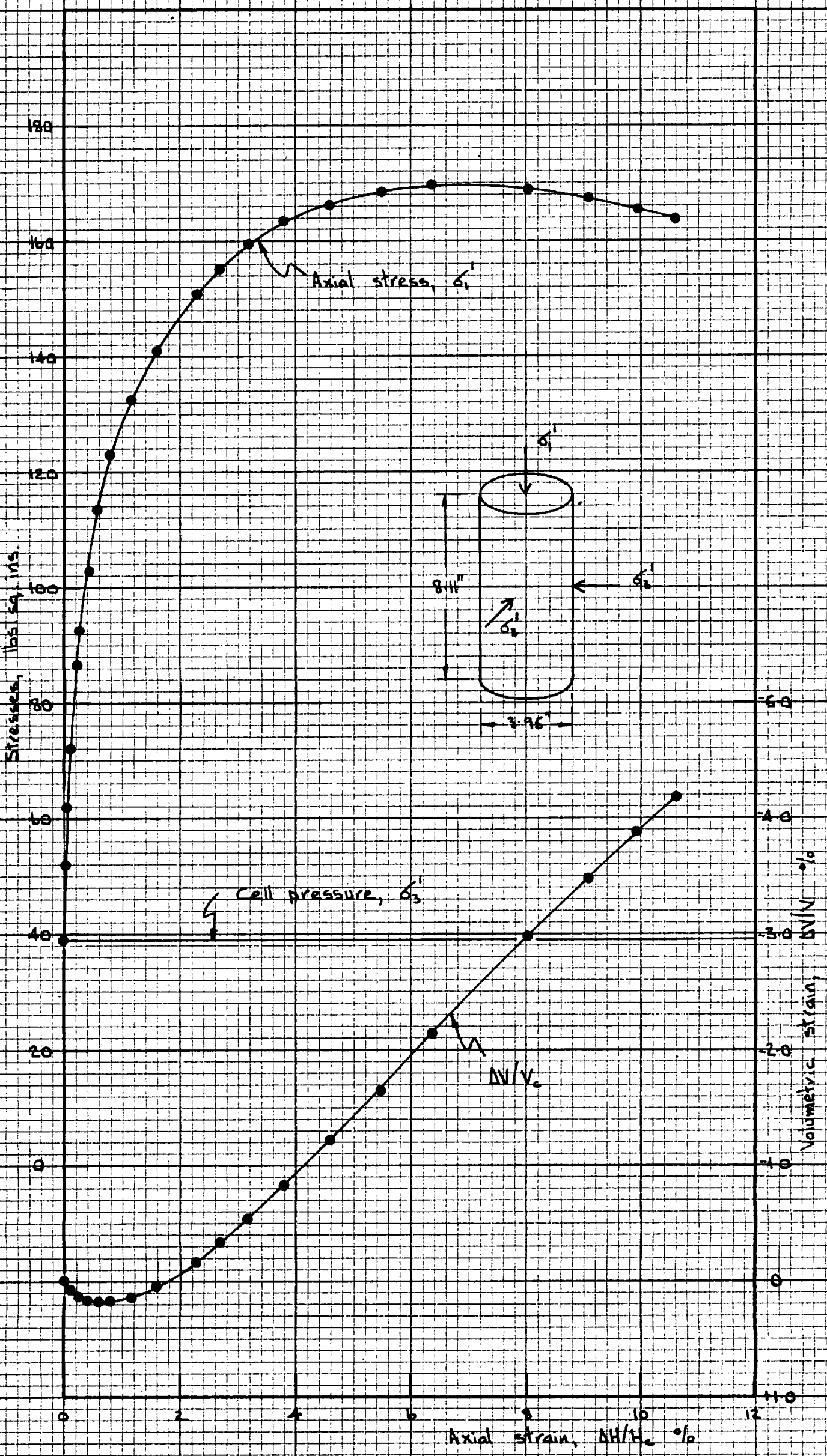
0 2 4 6 8 10 12 14 16
16 18 20 22 24 26

Axial strain, $\Delta H/H_c$ %

TEST C/16. CYLINDRICAL TRIAXIAL COMPRESSION.

Ham River Sand, Batch #1. Date: 10/8/64.
n_i = 44·2%, Sample made in 'two halves'
1/10·009" thick lubricated membrane used
at each end of sample.
Sample sheath 0·020" thick.

FIG. A8·3



TEST C/7. CYLINDRICAL TRIAXIAL COMPRESSION.

Ham River Sand, Batch # 1. Date: 11/9/64.
n_i = 40.6 %, Sample made in 'two halves'
w/0.009" thick lubricated membrane used
at each end of sample.
Sample sheath 0.020" thick.

FIG. A8.44

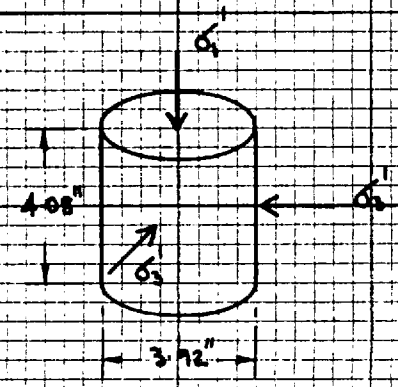
Axial stress, σ_1'

Cell pressure, σ_3'

$\Delta V/V_c$

4.74" (22.2%)

End of test.



Stresses, lbs / sq. ins.

Volumetric strain, $\Delta V/V_c$ %

Axial strain, $\Delta H/H_c$ %

TEST D/1. CYLINDRICAL TRIAXIAL COMPRESSION.

Ham River Sand, Batch #1. Date: 8/9/64.
n_i = 44.5%, Sample made in 'two halves'.
Direct contact between sample and plattens.
Sample sheath 0.020" thick.

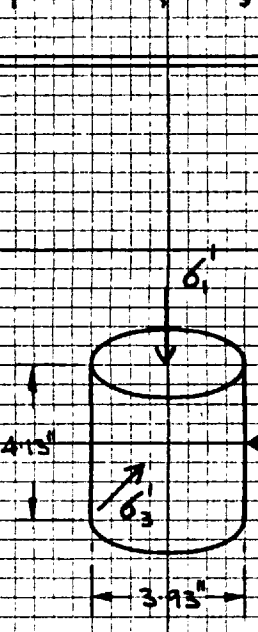
FIG. A8.45

Axial stress, σ_1'

$\Delta V/V_c$

Cell pressure, σ_3'





Stresses, lbs / sq. ins.

Volumetric strain, $\Delta V/V_c$ %

Axial strain, $\Delta H/H_c$ %

TEST D/2. CYLINDRICAL TRIAXIAL COMPRESSION.

Ham River Sand, Batch #1, Date: 11/9/64.
H_c 3·9·1"o, Sample made in two halves.
Direct contact between sample and platteens.
Sample sheath 0·020" thick.

FIG. AR.46

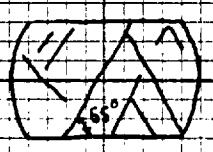
Stresses, lbsf sq. ins.

220
200
180
160
140
120
100
80
60
40
20
0

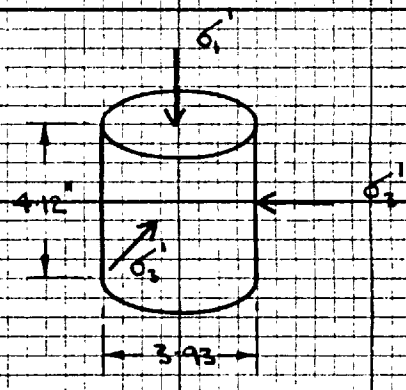
Axial stress, σ_1'

Cell pressure, σ_3'

$\Delta V/V_c$



End of test



Volumetric strain, $\Delta V/V$

6·0
5·0
4·0
3·0
2·0
1·0
0
1·0

0 2 4 6 8 10 12 14 16
16 18 20 22 24 26

Axial strain, $\Delta H/H_c$ %

TEST D/3. CYLINDRICAL TRIAXIAL COMPRESSION.

Ham River Sand, Batch #1. Date: 17/9/64
n_i = 41·0%, Sample made in 'two halves'
Direct contact between sample and plattens.
Sample sheath 0·020" thick.

FIG. A8.47

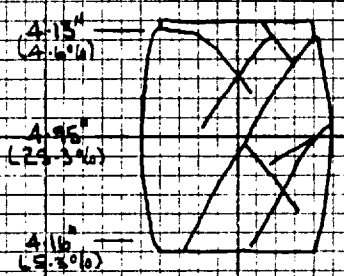
Stresses, lbs/sq.ins.

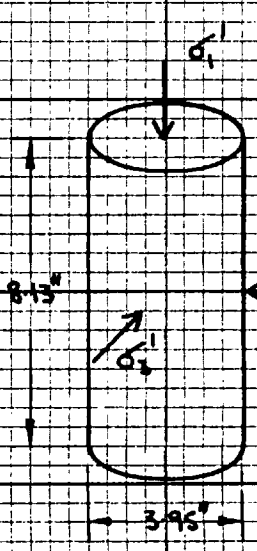
120
100
80
60
40
20
0

Axial stress, σ_1'

Cell pressure, σ_3'

$\Delta V/V_c$





6.0
5.0
4.0
3.0
2.0
1.0
0

Volumetric strain, $\Delta V/V_c$ %

0 2 4 6 8 10 12 14 16
16 18 20 22 24

Axial strain, $\Delta H/H_c$ %

TEST B1/1. CYLINDRICAL TRIAXIAL COMPRESSION

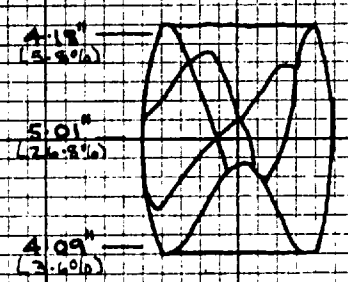
Ham River Sand, Batch #2, Bag #5. Date: 2/11/64.
n_i = 40·3%, Sample made in 'two halves'
Direct contact between sample and platterns.
Sample sheath 0·020" thick.

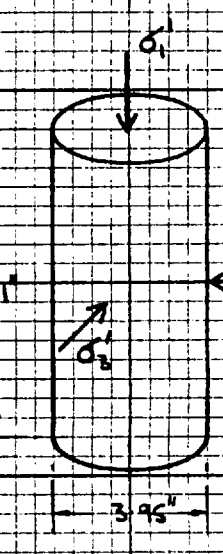
FIG. A8.42

Axial stress, σ_1'

Cell preessure, σ_3'

$\Delta V/V_c$





Stresses, lbs/sq.ins.

Volumetric strain, $\Delta V/V_c$ %

Axial strain, $\Delta H/H_c$ %

TEST B12. CYLINDRICAL TRIAXIAL COMPRESSION.

Ham River Sand, Batch #2, Bag #5. Date: 7/11/64.
n_i = 40.2%, Sample made in 'two halves'.
Direct contact between sample and platters.
Sample sheath 0.020" thick.

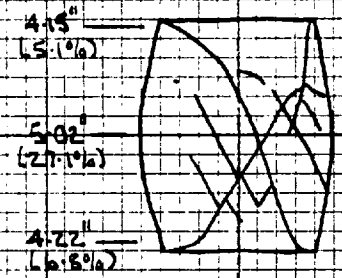
FIG. A8.49

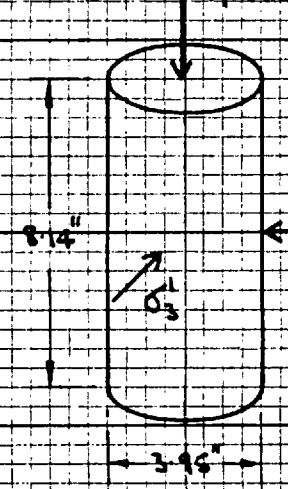
Stresses, lbs / sq.ins.

Axial stress, σ_1'

Cell pressure, σ_3'

$\Delta V/V_c$





Volumetric strain, $\Delta V/V_c$ %

Axial strain, $\Delta H/H_c$ %

TEST B15. CYLINDRICAL TRIAXIAL COMPRESSION.

Ham River Sand, Batch #2, Bag #5, Reused once. Date: 16/11/64
n_i: 40.7%, Sample made in 'two halves'
Direct contact between sample and plattens.
Sample sheath 0.020" thick.

FIG. A8.50

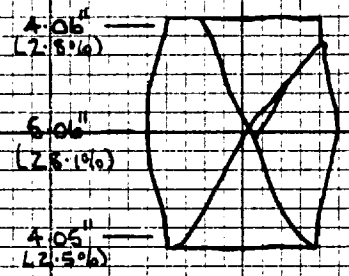
Stresses, lbs/sq.ins.

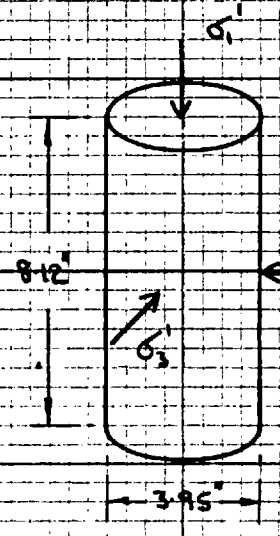
160
140
120
100
80
60
40
20
0

Axial stress, σ_1'

Cell pressure, σ_3'

$\Delta V/V_c$





-6·0
-5·0
-4·0
-3·0
-2·0
-1·0
0
+1·0

Volumetric strain, $\Delta V/V_c$ %

0 2 4 6 8 10 12 14 16
16 18 20 22 24

Axial strain, $\Delta H/H_c$ %

TEST B1/4. CYLINDRICAL TRIAXIAL COMPRESSION.

Ham River Sand, Batch #2, Bag# 5, Reused twice. Date: 19/11/64.
n_i = 40·1%, Sample made in 'two halves'.
Direct contact between sample and flattens.
Sample sheath 0·020" thick.

FIG. A8.51

Axial stress, σ_1'

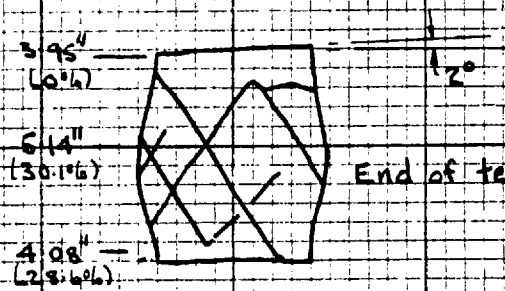
Cell pressure σ_3'

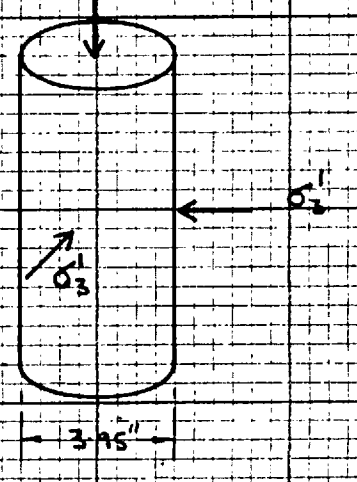
$\Delta V/V_c$

Stresses, lbs/sq. ins.

Volumetric strain, $\Delta V/V_c$ %

Axial strain, $\Delta H/H_c$ %





TEST E11. CYLINDRICAL TRIAXIAL COMPRESSION.

Ham River Sand, Batch #1, Reused once. Date: 2/11/65.

n_i = 42.1 %

1/4" thick porous disc used at each end of sample.

3/4" diam. half-ball between top platten and load cell.

Sample sheath 0.020" thick.

FIG. A8.52

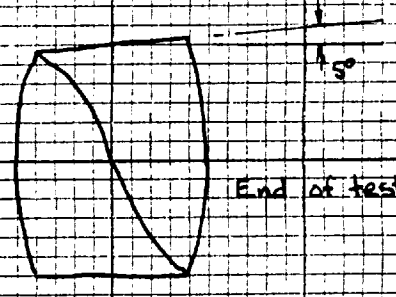
Rotation of top platten first observed.

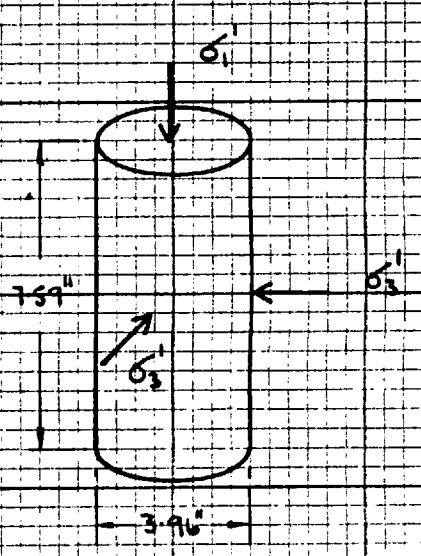
Axial stress, σ_1'

Cell pressure, σ_3'

$\Delta V/V_c$

End of test.





Stresses, lbs/sq ins.

Volumetric strain, $\Delta V/V_c$ %

Axial strain, $\Delta H/H_c$ %

TEST E/2. CYLINDRICAL TRIAXIAL COMPRESSION.

Ham River Sand, Batch #1, Reused once. Date: 5/1/65.
n_i: 39.2%.
1/4" thick porous disc used at each end of sample.
3/4" diam. half-ball between top platten and load cell.
Sample sheath 0.020" thick.

FIG. A8.53

Rotation of top platten first observed.

Axial stress, σ_1'

σ_1'

σ_3'

σ_3'

3.96" (10.3%)

4.64" (17.5%)

4.28" (8.4%)

10°

End of test.

7.57"

3.95"

Cell pressure, σ_3'

$\Delta V/V_c$

Stresses, lbs/sq. ins.

Volumetric strain, $\Delta V/V_c$ %

Axial strain, $\Delta H/H_c$ %

TEST E13. CYLINDRICAL TRIAXIAL COMPRESSION.

Ham River Sand; Batch #1, Reused once. Date: 7/11/65.

n_i: 45.3 %

1/4" thick porous disc used at each end of sample.

3/4" diam. half-ball between top platten and load cell.

Sample sheath 0.020" thick.

FIG. A8.54

1st slip plane first observed.

2nd slip plane first observed.

Axial stress σ_1'

4.08" [3.3%]

4.84" [22.5%]

4.26" [7.8%]

End of test

Cell pressure, σ_3'

$\Delta V/V_c$

σ_1'

7.59"

σ_3'

3.95"

Stress, lbs / sq. ins

Volumetric strain, $\Delta V/V_c$ %

Axial strain, $\Delta H/H_c$ %

TEST E14. CYLINDRICAL TRIAXIAL COMPRESSION.

Ham River Sand, Batch #1, Reused once. Date: 10/1/65.

w_i = 39.8%

1/4" thick porous disc used at each end of sample.

Sample sheath 0.020" thick.

FIG. A8.55

Stresses, lbs/sq.ins.

Volumetric strain, $\Delta V/V_c$ %

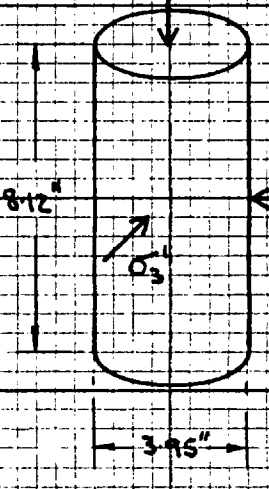
Axial strain, $\Delta H/H_c$ %

σ_1' Axial stress

σ_3' Cell pressure

$\Delta V/V_c$

End of test.



TEST SAII. CYLINDRICAL TRIAXIAL COMPRESSION.

Ham River Sand, Batch #2, Bag #3. Date: 18/1/65.
n_i 41·5%, Sample made in 'two halves'.
Direct contact between sample and platens.
Sample sheath 0·020" thick.

FIG. A8.56

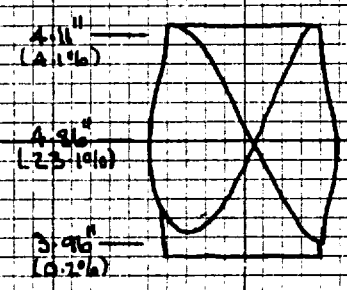
Stresses, lbs/sq.ins.

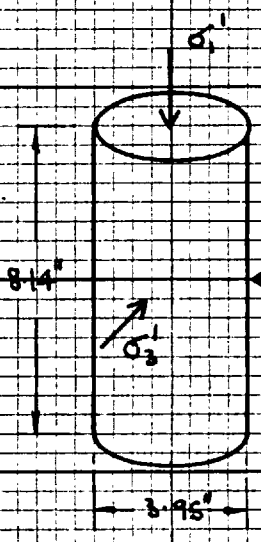
180
160
140
120
100
80
60
40
20
0

Axial stress, σ_1'

Cell pressure, σ_3'

$\Delta V/V_c$





Volumetric strain, $\Delta V/V_c$ %

-5·0
-4·0
-3·0
-2·0
-1·0
0
+1·0

0 2 4 6 8 10 12 14 16
16 18 20 22

Axial strain, $\Delta H/H_c$ %

TEST 5A/2. CYLINDRICAL TRIAXIAL COMPRESSION.

Haw River Sand, Batch #2, Bag #3. Date: 28/11/65
n_i = 41·6 % Sample made in 'two halves'
Direct contact between sample and platens.
Sample sheath 0·020" thick.

FIG. A8.57

Axial stress, σ_1'

End of test

Cell pressure, σ_3'

$\Delta V/V_c$

σ_1'

8·15"

σ_3'

σ_3'

3·96"

Stresses, lbs/sq.ins

Volumetric strain, $\Delta V/V_c$ %

Axial strain, $\Delta H/H_c$ %

TEST SA15. CYLINDRICAL TRIAXIAL COMPRESSION.

Ham River Sand, Batch*2, Bag*3. Date: 6/2/65

n_i = 41·6%, Sample made in 'two halves'

Direct contact between sample and platters.

Sample sheath 0·020" thick.

FIG. A8.58

Stresses, lbs/sq. ins.

180
160
140
120
100
80
60
40
20
0

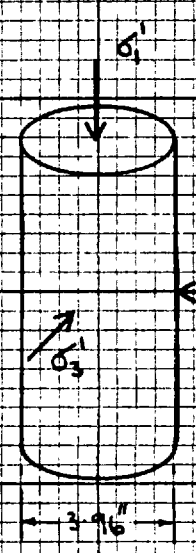
Axial stress, σ_1'

Cell pressure, σ_3'

$\Delta V/V_c$

-6.0
-5.0
-4.0
-3.0
-2.0
-1.0
0
+1.0

Volumetric strain, $\Delta V/V_c$ %



0 2 4 6 8 10 12 14 16
16 18 20 22 24

Axial strain, $\Delta H/H_c$ %

TEST SA14. CYLINDRICAL TRIAXIAL COMPRESSION.

Ham River Sand, Batch #2, Bag #3. Date: 10/2/65.
n_i = 41.1%, Sample made in 'two halves'.
Direct contact between sample and plattens.
Sample sheath 0.020" thick.

FIG. A8.59

Axial stress, σ_1'

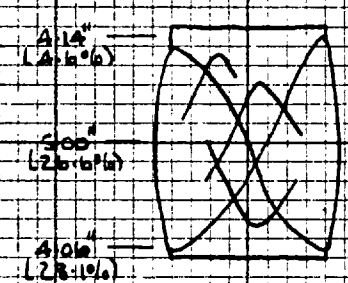
Cell pressure, σ_3'

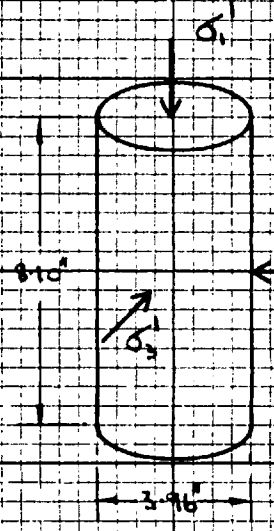
$\Delta V/V_c$

Volumetric strain, $\Delta V/V_c$ %

Stresses, lbs / sq. in.

Axial strain, $\Delta H/H_c$ %





TEST SB11. CYLINDRICAL TRIAXIAL COMPRESSION.

Ham River Sand, Batch #2, Bag #3. Date: 19/11/65.
n_i = 41.4 %, Sample made in two halves.
0.009" thick lubricated membrane used at each end of sample.
Sample sheath 0.020" thick.

FIG. A8.60

Stresses, lbs/sq. ins.

Axial stress, σ_1'

Cell pressure σ_3'

$\Delta V/V_c$

Volumetric strain, $\Delta V/V_c$ %

Axial strain, $\Delta H/H_c$ %

(2.8°)24·04"
(5.8°)24·18"
(8.90)4·30"
(9.44)3·32"
(6.8°)24·22"
(2.34)24·04"

End of test

σ_1'

8·09"

σ_3'

σ_3'

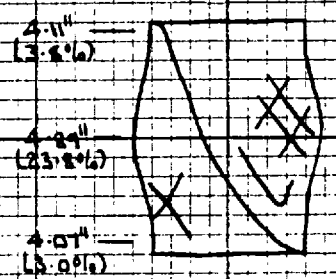
3·95"

TEST SB12. CYLINDRICAL TRIAXIAL COMPRESSION.

Ham River Sand, Batch #2, Bag #3. Date: 29/1/65.
n_i = 41·6%, Sample made in 'two halves'
0·009" thick lubricated membrane used
at each end of sample.
Sample sheath 0·020" thick.

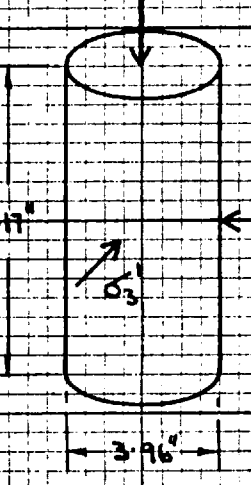
FIG. A8.61

Axial stress, σ_1'



Cell pressure, σ_3'

$\Delta V/V_c$



Stresses, lbs / sq. ins.

Volumetric strain, $\Delta V/V_c$ %

Axial strain, $\Delta H/H_c$ %

TEST SB13. CYLINDRICAL TRIAXIAL COMPRESSION.

Ham River Sand, Batch #2, Bag #3. Date: 4/2/65.
n_i = 42.0%, Sample made in two halves
lio·009" thick lubricated membrane used
at each end of sample.
Sample sheath 0·020" thick.

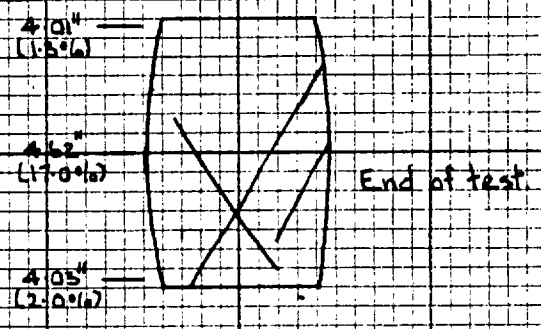
FIG. A8.62.

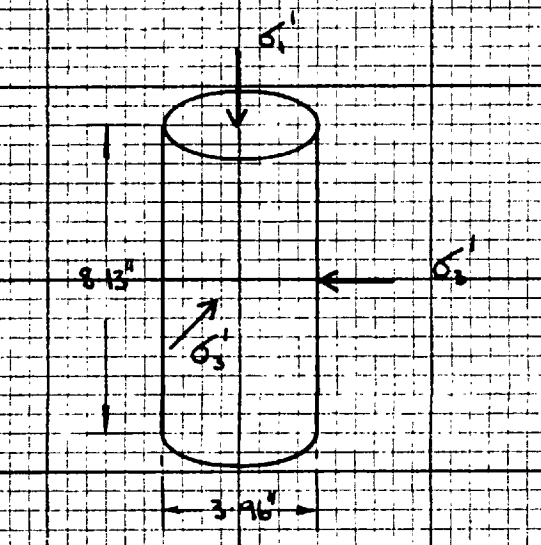
Stresses, lbs/sq.ins.

Axial stress, σ_1'

Cell pressure, σ_3'

$\Delta V/V_c$





Volumetric strain, $\Delta V/V_c$ %

Axial strain, $\Delta H/H_c$ %

TEST SB/4. CYLINDRICAL TRIAXIAL COMPRESSION.

Ham River Sand, Batch#2, Bag#3. Date: 7/2/65.
n_c = 41.4 %, Sample made in 'two halves'
110.009" thick lubricated membrane used at each end of sample.
Sample sheath 0.020" thick.

FIG. AB.63

Stresses, tsf sq. ins.

160
140
120
100
80
60
40
20
0

Axial stress, σ_1'

4.01" (1.5%)
4.16" (2.0%)
4.04" (2.0%)
End of test.

Cell pressure, σ_3'

$\Delta V/V_c$

σ_1'
8.13"
σ_3'
σ_3'
3.96"

-5.0
-4.0
-3.0
-2.0
-1.0
0
+1.0

Volumetric strain, $\Delta V/V_c$ %

0 2 4 6 8 10 12 14 16

Axial strain, $\Delta H/H_c$ %

TEST SB15. CYLINDRICAL TRIAXIAL COMPRESSION.

Ham River Sand, Batch*2, Bag*4 Date: 11/2/65.
n_i = 41.2 %, Sample made in 'two halves'.
Two .009" thick lubricated membrane used at each end of sample.
Sample sheath 0.020" thick.

FIG. A8.64

Axial stress, σ_1'

Cell pressure, σ_3'

$\Delta V/V_c$

$(8.4\%)4.26"$

$(18.6\%)4.66"$

$(9.7\%)4.31"$

End of test.

σ_1'

4.09"

σ_3'

σ_3'

3.93"

Axial stress, lbs/sq.in.

Volumetric strain, $\Delta V/V_c$ %

Axial strain, $\Delta H/H_c$ %

TEST SC/1 CYLINDRICAL TRIAXIAL COMPRESSION.

Ham River Sand, Batch #2, Bag #3. Date: 20/11/65.
W_c = 40.8%, Sample made in 'two halves'.
Direct contact between sample and platterns.
Sample sheath 0.020" thick.

FIG A2.65

Axial stress, σ_1'

5.6"Dia 1.5" —
4.8"Dia 5.4" —
4.9"Dia 2.0" —

End of test

Stresses, lbs/sq.ins

Cell pressure, σ_3'

$\Delta V/V_c$

σ_1'

4.13"

σ_3'

3.93"

Volumetric strain, $\Delta V/V_c$ %

Axial strain, $\Delta H/H_c$ %

TEST SC12. CYLINDRICAL TRIAXIAL COMPRESSION.

Ham River Sand, Batch#2, Bag#3. Date: 11/2/65.
n_c = 41.6 %, Sample made in 'two halves'
Direct contact between sample and platens.
Sample sheath 0.020" thick.

FIG. A8.66

Stresses, lbs/sq.ins.

Axial stress, σ_1'

Cell pressure, σ_3'

$\Delta V/V_c$

Volumetric strain, $\Delta V/V_c$ %

Axial strain, $\Delta H/H_c$ %

(2.5%) 4.03"

(4.8%) 4.51"
(17.3%) 4.61"
(4.9%) 4.51"

End of test.

4.11"

σ_1'

σ_3'

σ_3'

3.93"

TEST SOIL. CYLINDRICAL TRIAXIAL COMPRESSION.

Ham River Sand, Batch #2, Bag #3. Date: 21/11/65.
n_i = 41.2 %, Sample made in 'two halves'
Two 0.009" thick lubricated membrane used at each end of sample.
Sample sheath 0.020" thick.

FIG. A8.67

Axial stress, σ_1'

Cell pressure, σ_3'

$\Delta V/V_c$

(9.7%) 4.31" —
(9.4%) 4.69" —
(6.3%) 4.57" —

End of test

σ_1'

4.12"

σ_3'

σ_3'

3.73"

Stresses, lbs/sq.ins.

Volumetric strain, $\Delta V/V_c$ %

Axial strain, $\Delta H/H_c$ %

TEST SD12 : CYLINDRICAL TRIAXIAL COMPRESSION.

Ham River Sand, Batch #2, Bag #3. Date: 30/11/65.
n_i = 41.6%, Sample made in two halves.
11/0.004" thick lubricated membrane used at each end of sample.
Sample sheath 0.020" thick.

FIG. A8.62

Axial stress, σ_1'

(6.6%) 4.12" —
(7.4%) 4.09" —
(21.4%) 4.76" —
(20.9%) 4.74" —

End of test

$\Delta V/V_c$

Cell pressure, σ_3'

σ_1'

4.13"

σ_3'

σ_3'

3.92"

Stresses, lbs/sq.ins.

Volumetric strain, $\Delta V/V_c$ %

Axial strain, $\Delta H/H_c$ %

TEST SD11. CYLINDRICAL TRIAXIAL COMPRESSION.

Ham River Sand, Batch #2, Bag #3. Date: 26/1/65.
n_i = 41.3%. Sample made in 'two halves'
2 to 0.009" thick lubricated membranes used
at each end of sample.
Sample sheath 0.020" thick.

FIG. A8.69

Stresses, lbs/sq. ins.

Axial stress, σ_1'

Cell pressure, σ_3'

$\Delta V/V_c$

Volumetric strain, $\Delta V/V_c$ %

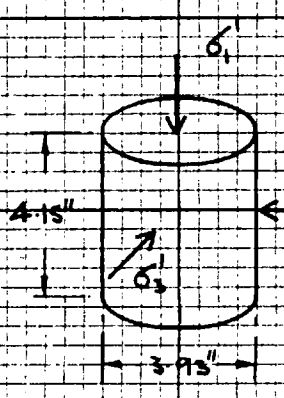
(6·9%) 4·20" —

(17·4%) 4·60" —

(18·6%) 4·66" —

(17·10%) 4·61" —

End of test.



Axial strain, $\Delta H/H_c$ %

TEST SD1/2. CYLINDRICAL TRIAXIAL COMPRESSION.

Ham River Sand, Batch #2, Bag #3. Date: 2/2/65.
n_L = 41·4 %, Sample made in 'two halves'.
2 lo·009" thick lubricated membranes used at each end of sample.
Sample sheath 0·020" thick.

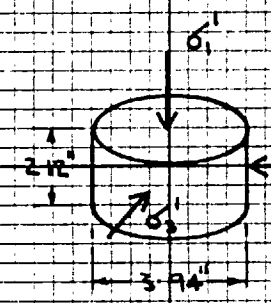
FIG. A9.70

Axial stress, σ_1'

Cell pressure, σ_3'

(11.9%) 4.41" —
(15.8%) 4.56" —
(16.3%) 4.59" —
End of test

$\Delta V/V_c$



Stresses, lbs/sq. ins.

Volumetric strain, $\Delta V/V_c$ %

Axial strain, $\Delta H/H_c$ %

TEST SE/L CYLINDRICAL TRIAXIAL COMPRESSION

Ham River Sand, Batch #2, Bag #3. Date: 23/11/65.
n_i = 41.6%
/10.009" thick lubricated membrane used at each end of sample.
Sample sheath 0.020" thick.

FIG A8.71

Axial stress, σ_1'

(8.6%)4.28" — (12.7%)4.44" — End of test.

Cell pressure, σ_3'

$\Delta V/V_c$

σ_1'

2.16"

σ_3'

σ_3'

3.74"

Stresses, lbs / sq. ins.

Volumetric strain, $\Delta V/V_c$ %

Axial strain, $\Delta H/H_c$ %

TEST SE12. CYLINDRICAL TRIAXIAL COMPRESSION.

Ham River Sand, Batch #2, Bag #3. Date: 3/2/65.

n_i = 42.2 %

Two 0.009" thick lubricated membrane used at each end of sample.

Sample sheath 0.020" thick.

FIG. A8.12

Axial stress, σ_1'

Cell pressure, σ_3'

$\Delta V/V_c$

4.08" (4.19%)
4.61" (15.1%)
4.63" (15.4%)

End of test.

σ_1'

4.11"

σ_3'

σ_3'

3.92"

Stress, lbs/sq.ins.

Volumetric strain, $\Delta V/V_c$ %

Axial strain, $\Delta H/H_c$ %

TEST SF11. CYLINDRICAL TRIAXIAL COMPRESSION.

Ham River Sand, Batch #2, Bag #3. Date: 27/11/65.

n_i = 41.8%

No.008" thick lubricated membrane used at each end of sample.

Sample sheath 0.020" thick.

FIG A9.73

Stresses, lbs/sq.ins.

Axial stress, σ_1'

Cell pressure, σ_3'

$\Delta V/V_c$

Volumetric strain, $\Delta V/V_c$ %

Axial strain, $\Delta H/H_c$ %

(2.3%) 4.02"
(10.4%) 4.34"
(12.7%) 4.43"
(12.2%) 4.41"
End of test

4.14"

3.93"

TEST SF12. CYLINDRICAL TRIAXIAL COMPRESSION.

Ham River Sand, Batch*2, Bag*3. Date: 8/2/65.

n_i = 41.4 %

11b:009" thick lubricated membrane used at each end of sample.

Sample sheath 0.020" thick.

FIG. A8.74

Appendix A 9

Graphical presentation of cylindrical triaxial compression and extension test results.

Stresses, lbs/sq. ins.

Axial stress, σ_1'

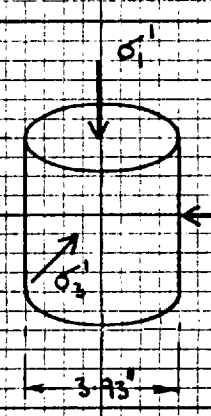
Cell pressure, σ_3'

$\Delta V/V_c$

Volumetric strain, $\Delta V/V_c$ %

Axial strain, $\Delta H/H_c$ %

(9.2%)4.29" —
(16.5%)4.58" —
(20.4%)4.73" —
(19.3%)4.69" —
End of test.



TEST H/1. CYLINDRICAL TRIAXIAL COMPRESSION.

Ham River Sand, Batch #2, Bag #4. Date: 2/16/65.
n_i = 41.3%, Sample made in 'two halves'.
2/0.010" thick lubricated membranes used at each end of sample.
Sample sheath 0.020" thick.

FIG. A9.1

Axial stress, σ_1'

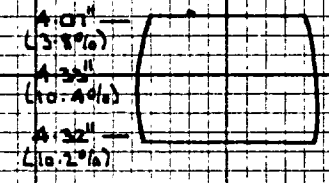
Cell pressure, σ_3'

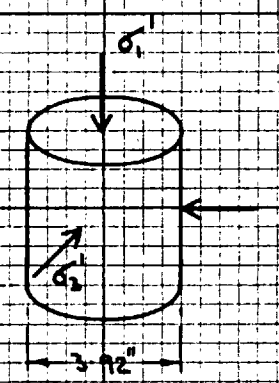
$\Delta V/V_c$

Stresses, lbs/sq.ins.

Volumetric strain, $\Delta V/V_c$ %

Axial strain, $\Delta H/H_c$ %





TEST H/2. CYLINDRICAL TRIAXIAL COMPRESSION.

Ham River Sand, Batch #2, Bag #4. Date: 7/7/65
n_i = 41·9 %, Sample made in 'two halves'.
2/0·010" thick lubricated membranes used at each end of sample.
Sample sheath 0·020" thick.

FIG. A9.2

Axial stress, σ_1'

Cell pressure, σ_3'

$\Delta V/V_i$

4·30" (9·4%)
4·51" (4·8%)
4·38" (11·6%)

End of test

4·17"

σ_1'

σ_3'

3·93"

Stresses, lbs/sq. ins.

Volumetric strain, $\Delta V/V_i$ %

Axial strain, $\Delta H/H_i$ %

TEST H/3. CYLINDRICAL TRIAXIAL COMPRESSION.

Ham River Sand, Batch #2, Bag #4. Date: 11/7/65.
n_i = 40·4 %, Sample made in two halves'
2 lo·010" thick lubricated membranes used
at each end of sample.
Sample sheath 0·020" thick.

FIG. A9.3

Axial stress, σ_1'

Cell pressure, σ_3'

$\Delta V/V_c$

End of test

4·07" (4·1%)
4·44" (13·6%)
4·47" (14·2%)

4·10"

3·91"

Stresses, lbs/sq.ins.

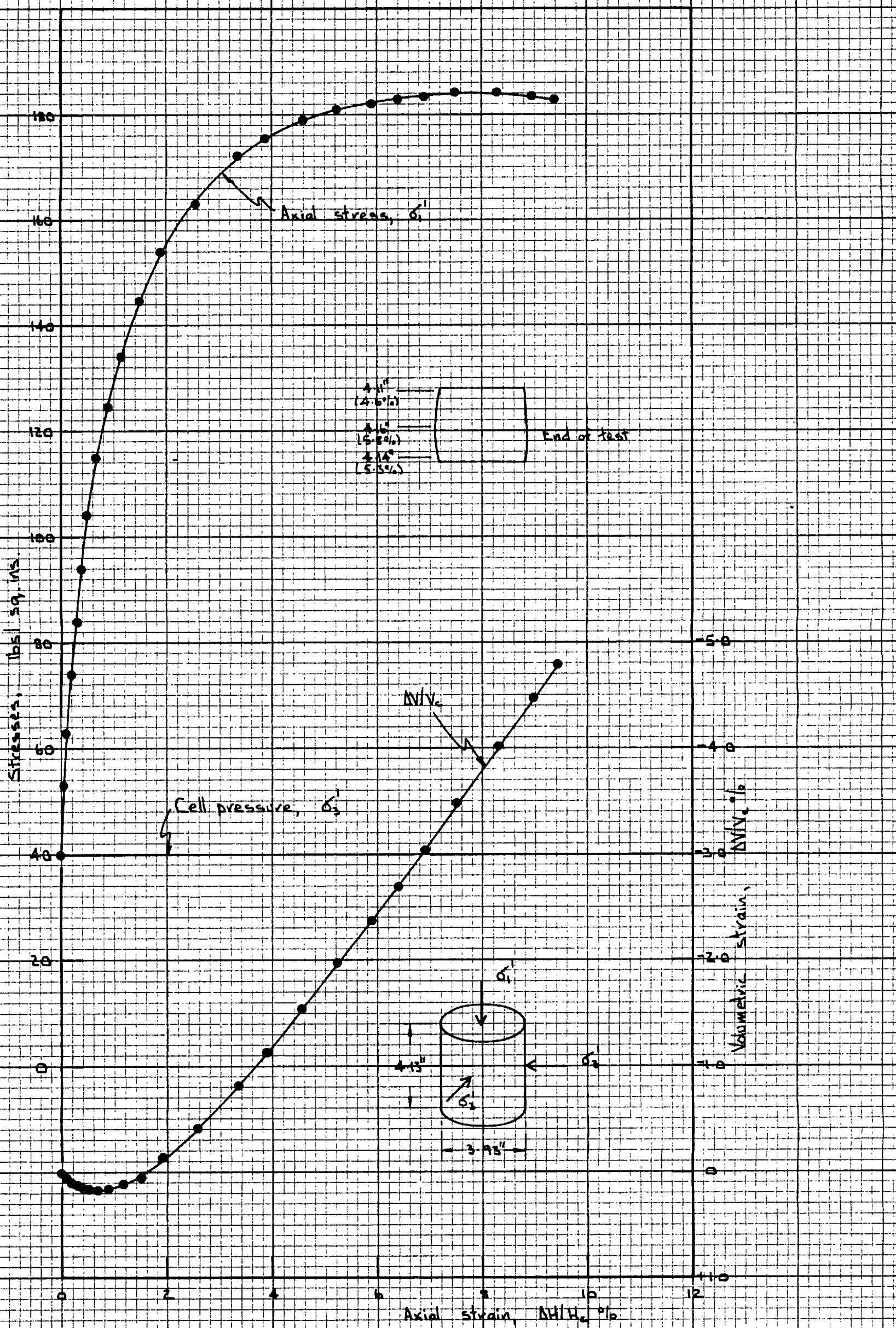
Volumetric strain, $\Delta V/V_c$ %

Axial strain, $\Delta H/H_c$ %

TEST H/4. CYLINDRICAL TRIAXIAL COMPRESSION.

Ham River Sand, Batch #2, Bag #4. Date: 29/8/65.
n_c = 44·4%, Sample made in two halves
2 lo·olo" thick lubricated membranes used
at each end of sample.
Sample sheath 0·020" thick.

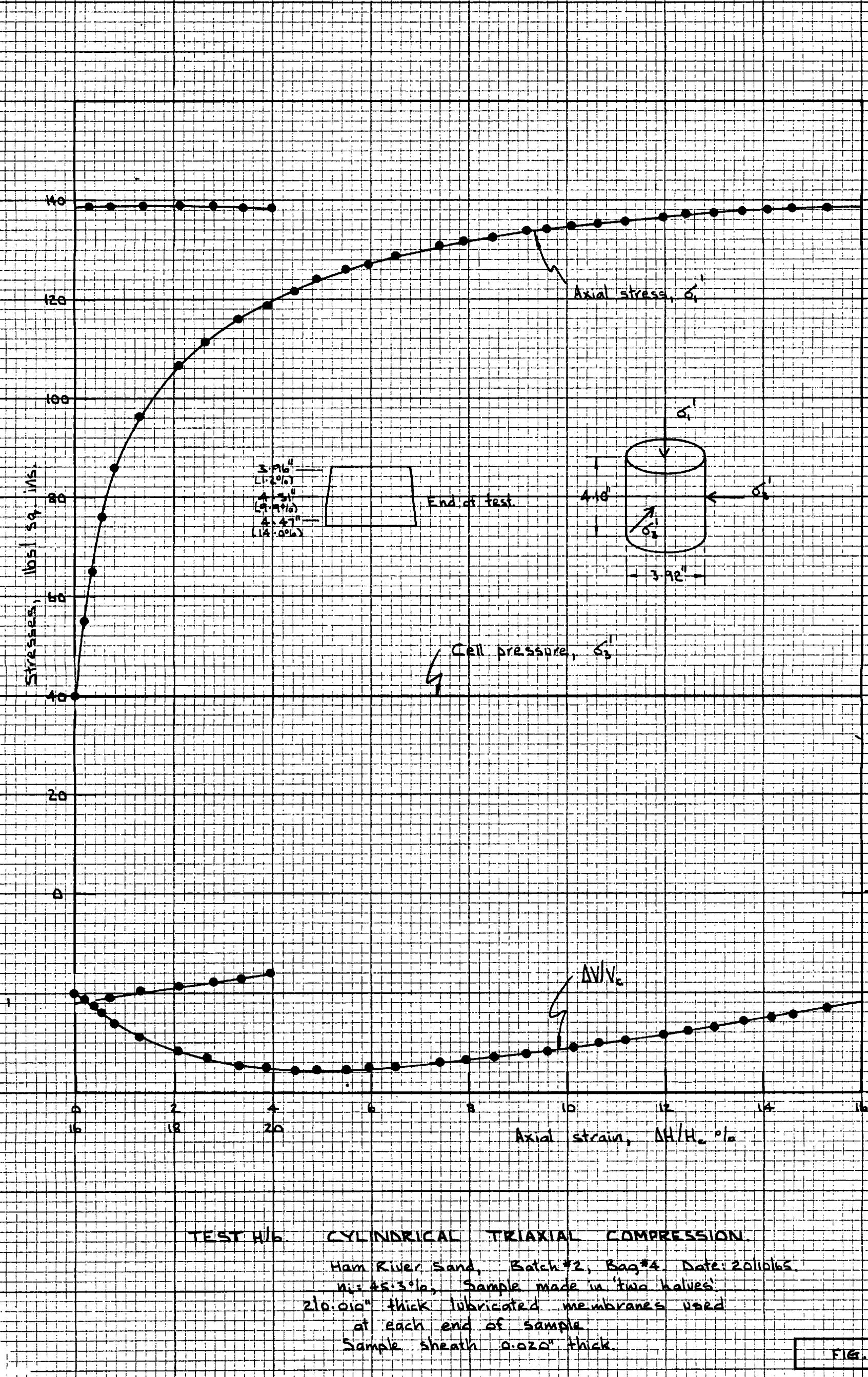
FIG. A9.4



TEST H/5. CYLINDRICAL TRIAXIAL COMPRESSION.

Ham River Sand, Batch #2, Bag #4. Date: 31/8/65.
n_c = 38·6%, Sample made in 'two halves'
2 to 0·010" thick lubricated membranes used at each end of sample.
Sample sheath 0·020" thick.

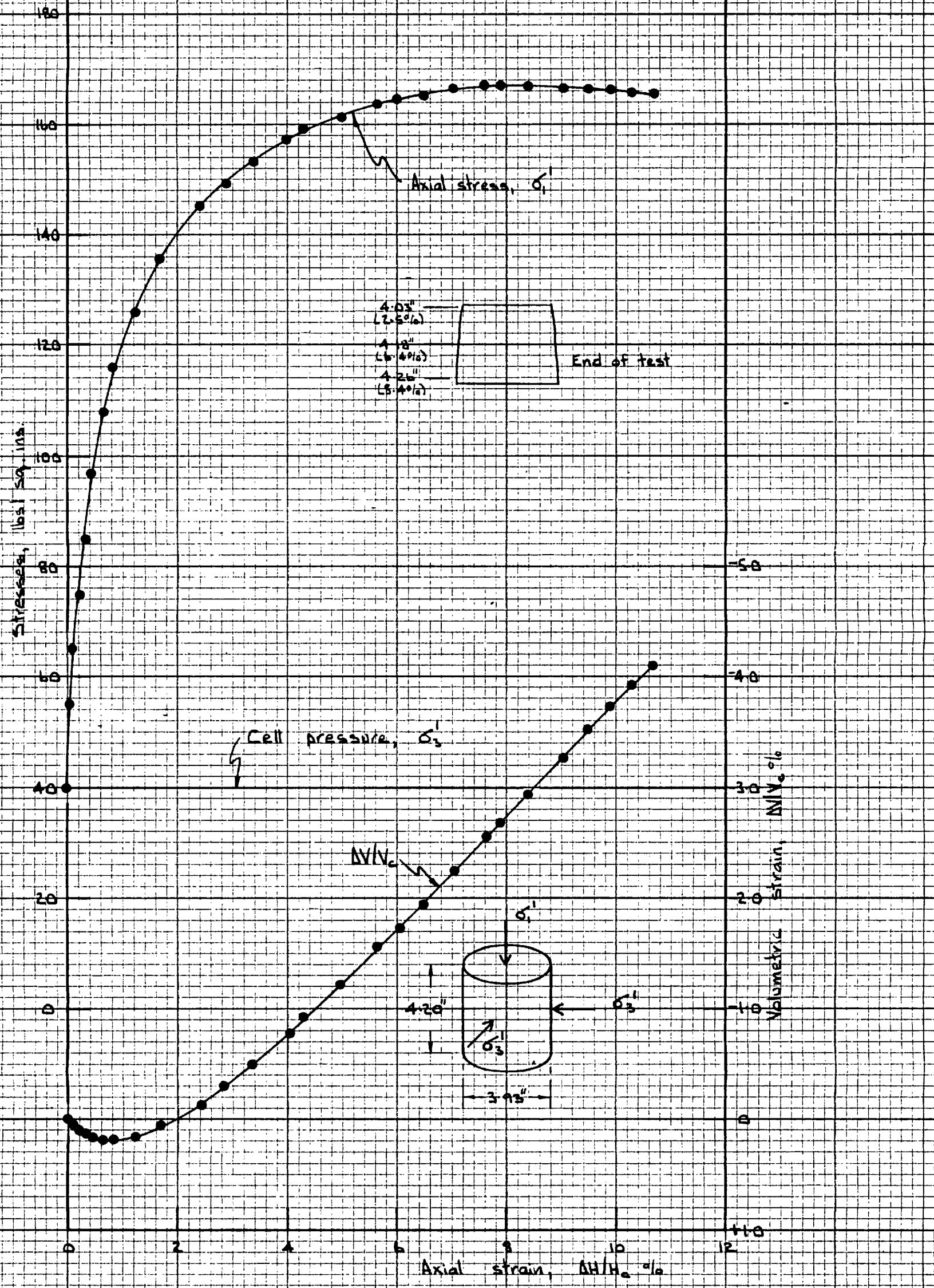
FIG. A9.5



TEST H/6. CYLINDRICAL TRIAXIAL COMPRESSION.

Ham River Sand, Batch #2, Bag #4. Date: 20/10/65.
n_i: 45.3%, Sample made in 'two halves'
2 lo.010" thick lubricated membranes used
at each end of sample.
Sample sheath 0.020" thick.

FIG. A9.6



TEST H/7. CYLINDRICAL TRIAXIAL COMPRESSION.

Ham River Sand, Batch #2, Bag #4. Date: 22/10/65.
n_i = 40.1 %. Sample made in 'two halves'
2 10·010" thick lubricated membrane used
at each end of sample.
Sample sheath 0·020" thick.

FIG. A9.7

Stresses, lbs/sq.ins.

180
160
140
120
100
80
60
40
20
0

Axial stress, σ_1'

$(\sigma_1' - \sigma_3')$

4·14" (5·3%)
4·32" (9·8%)
4·28" (8·9%)

End of test

Transfer to self-compensating mercury control

σ_3'

$\Delta V/V_c$

Cell pressure, σ_3'

σ_1'

4·11"

σ_3'

σ_3'

3·93"

Volumetric strain, $\Delta V/V_c$ %

-3·0
-2·0
-1·0
0
+1·0

0 2 4 6 8 10 12 14 16

Axial strain, $\Delta H/H_c$ %

TEST HA11. CYLINDRICAL TRIAXIAL COMPRESSION.

Ham River Sand, Batch #2, Bag #4. Date: 11/1/65.
n_i = 40·4%, Sample made in 'two halves'
2 lo·010" thick lubricated membranes used at each end of sample.
Sample sheath 0·020" thick.

FIG. A9.8

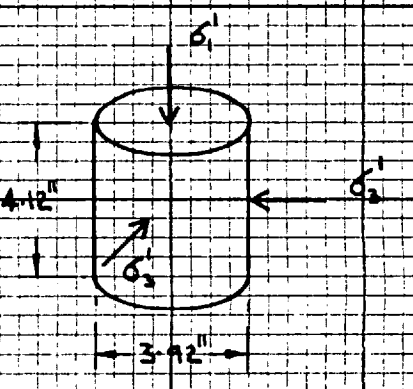
Axial stress, σ_1'

$(\sigma_1' - \sigma_3')$

$\Delta V/V_c$

Transfer to self-compensating mercury control.

Cell pressure, σ_3'



Stresses, lbs/sq ins.

Volumetric strain, $\Delta V/V_c$ %

Axial strain, $\Delta H/H_c$ %

TEST HA/2. CYLINDRICAL TRIAXIAL COMPRESSION.

Ham River Sand. Batch*2, Bag*4. Date: 13/7/65.
n_i = 40·4%, Sample made in 'two halves'
2 lo·olo" thick lubricated membranes used at each end of sample.
Sample sheath 0·020" thick.

FIG. A9.9

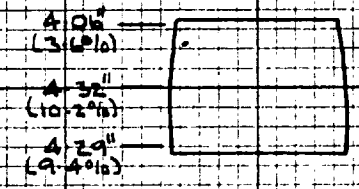
Axial stress, σ_1'

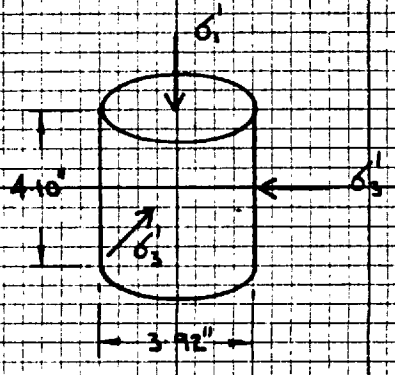
$(\sigma_1' - \sigma_3')$

Cell pressure, σ_3'

Transfer to self-compensating mercury control.

End of test.





$\Delta V/V_c$

Stresses, lbs / sq. ins.

Volumetric strain, $\Delta V/V_c$ %

Axial strain, $\Delta H/H_c$ %

TEST HA/3. CYLINDRICAL TRIAXIAL COMPRESSION.

Ham River Sand, Batch #2, Bag #4. Date: 15/3/65.
n_i = 45·2 %, Sample made in 'two halves'
2 lo-gio" thick lubricated membranes used at each end of sample.
Sample sheath 0·026" thick.

FIG. A9.10

Stresses, lbs/sq. ins.

160
140
120
100
80
60
40
20
0

Axial stress, σ_1'

$(\sigma_1' - \sigma_3')$

4·02" (2·8%)
4·39" (12·3%)
4·44" (13·5%)

End of test

Cell pressure, σ_3'

Transfer to self-compensating mercury control

$\Delta V/V_c$

σ_1'

4·12"

σ_3'

σ_3'

3·91"

Volumetric strain, $\Delta V/V_c$ %

+2·0
+1·0
0
+1·0

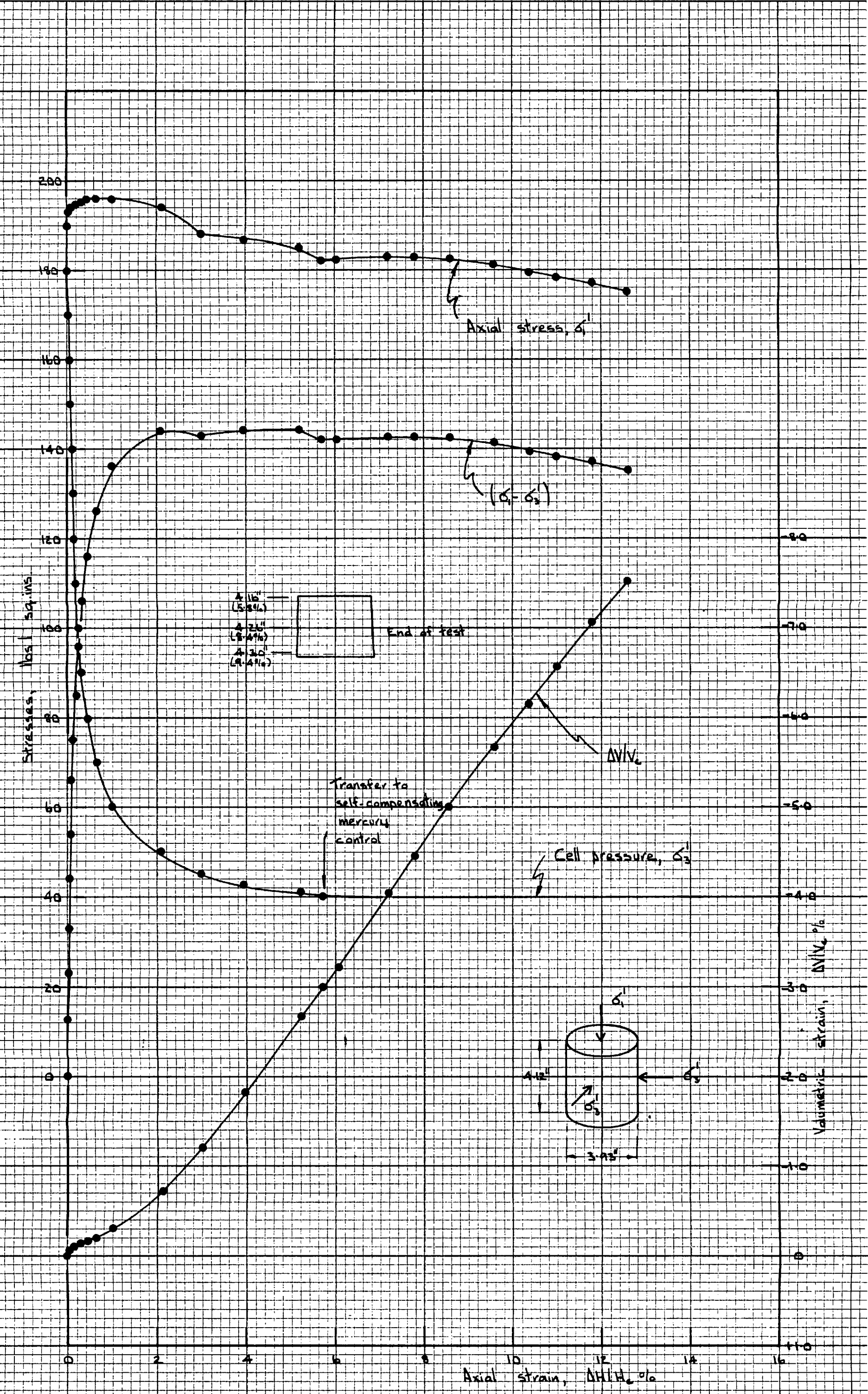
0 2 4 6 8 10 12 14 16

Axial strain, $\Delta H/H_c$ %

TEST HA14. CYLINDRICAL TRIAXIAL COMPRESSION.

Ham River Sand, Batch #2, Bag #4. Date: 23/7/65.
n_i = 44·0%, Sample made in 'two halves'.
2 10·010" thick lubricated membranes used at each end of sample.
Sample sheath 0·020" thick.

FIG. A9.11



TEST HA15. CYLINDRICAL TRIAXIAL COMPRESSION.

Ham River Sand, Batch #2, Bag #4. Date: 2/9/65.
n_i = 39·6 %, Sample made in 'two halves'
2 lo·olo" thick lubricated membranes used at each end of sample.
Sample sheath o·o2o" thick.

FIG. A9.12

Axial stress, σ_1'

$(\sigma_1' - \sigma_3')$

Cell pressure, σ_3'

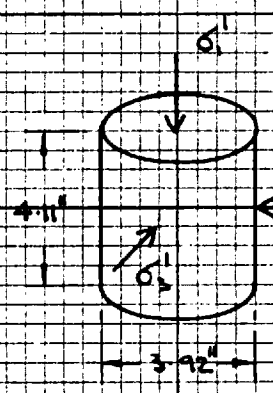
Transfer to self-compensating mercury control.

$\Delta V/V_c$

Stresses, tsf sq. ins.

Volumetric strain, %

Axial strain, $\Delta H/H_c$ %



TEST HA16 CYLINDRICAL TRIAXIAL COMPRESSION.

Ham River Sand, Batch #2, Bag #4 Date: 6/9/65
n_i = 42.4 %, Sample made in two halves
2 @ 0.010" thick lubricated membranes used at each end of sample.
Sample sheath 0.020" thick.

FIG. A9.13

Cell pressure σ_3'

$(\sigma_1' - \sigma_3')$

Axial stress, σ_1'

Stresses, lbs/sq.ins.

160
140
120
100
80
60
40
20
0

(2.1%) 3.85"
(2.8%) 3.82"
(5.4%) 3.71"
(9.7%) 3.55"
End of test

σ_3'
4.13"
σ_1'
σ_1'
3.93"

Volumetric strain, $\Delta V/V_c$ %

+10
0
-10

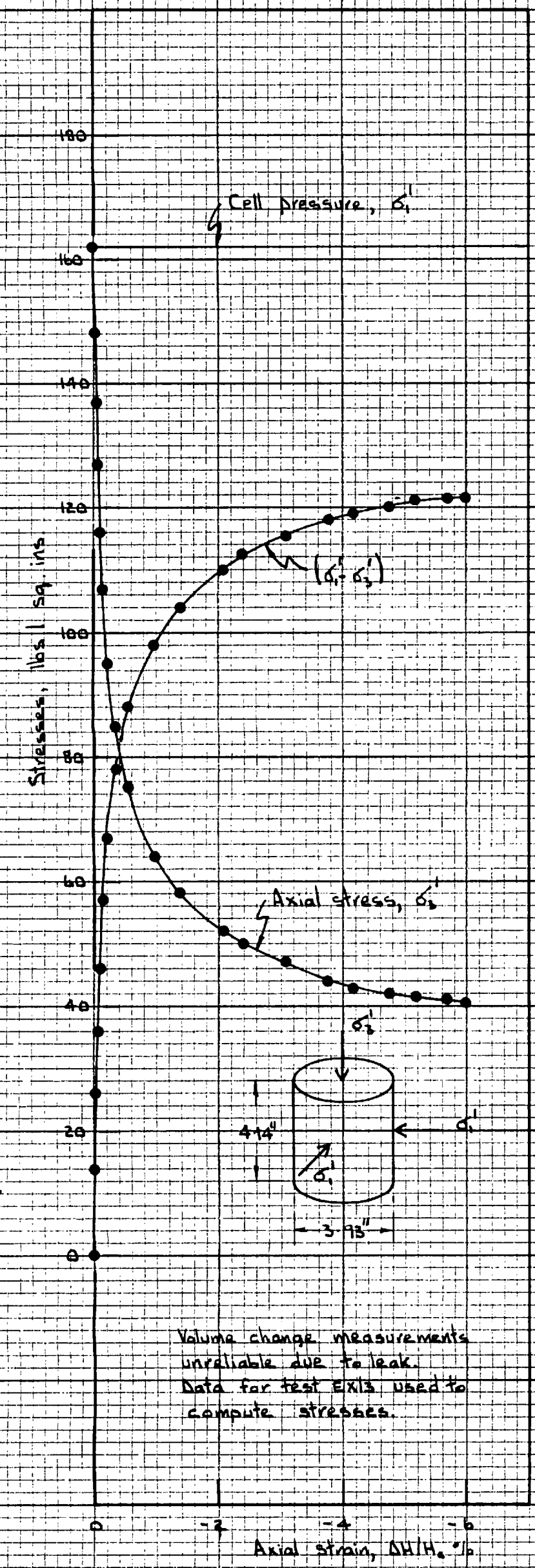
0 -2 -4 -6 -8 -10 -12

Axial strain $\Delta H/H_c$ %

TEST EX11. CYLINDRICAL TRIAXIAL EXTENSION.

Ham River Sand, Batch #2, Bag #4. Date: 11/9/65.
n_s 41.4%
2 0.010" thick lubricated membranes used at each end of sample.
Sample sheath 0.020" thick.

FIG. A9.14



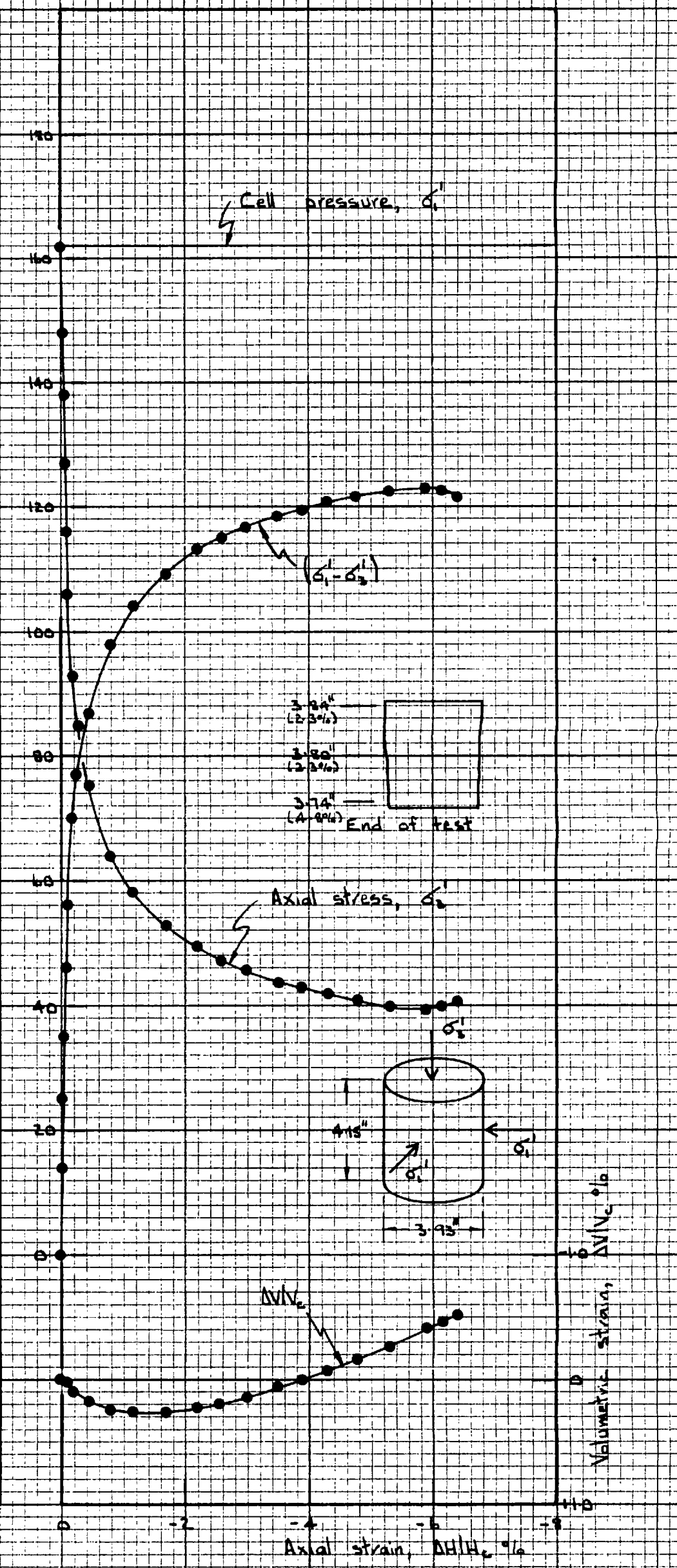
Volume change measurements unreliable due to leak. Data for test EX13 used to compute stresses.

TEST EX12

CYLINDRICAL TRIAXIAL EXTENSION.

Ham River Sand, Batch #2, Bag #4.
n_i = 41·5%, Date: 4/9/65.

2 lo·olo" thick lubricated membranes used at each end of sample.
Sample sheath 0·020" thick.



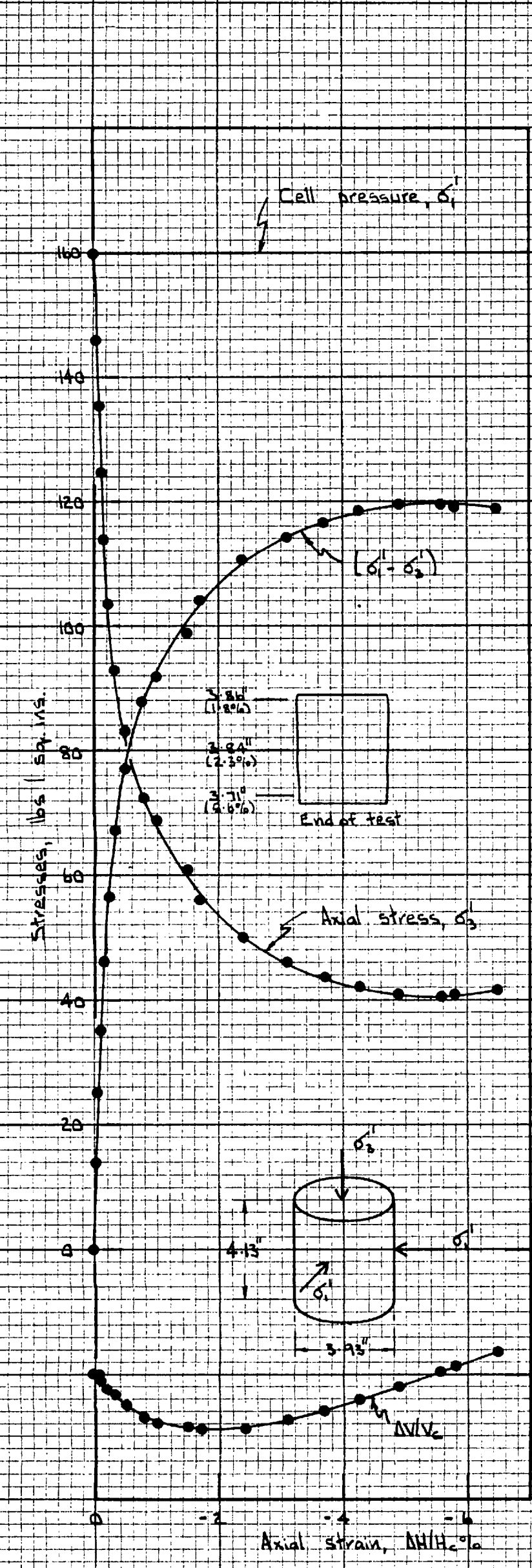
TEST EX13.

CYLINDRICAL TRIAXIAL EXTENSION.

Ham River Sand, Batch #2, Bag #4
n_i = 41·4%, Date: 16/9/65.

2 lo·olo" thick lubricated membranes used at each end of sample.
Sample sheath 0·020" thick.

FIG. A9.15

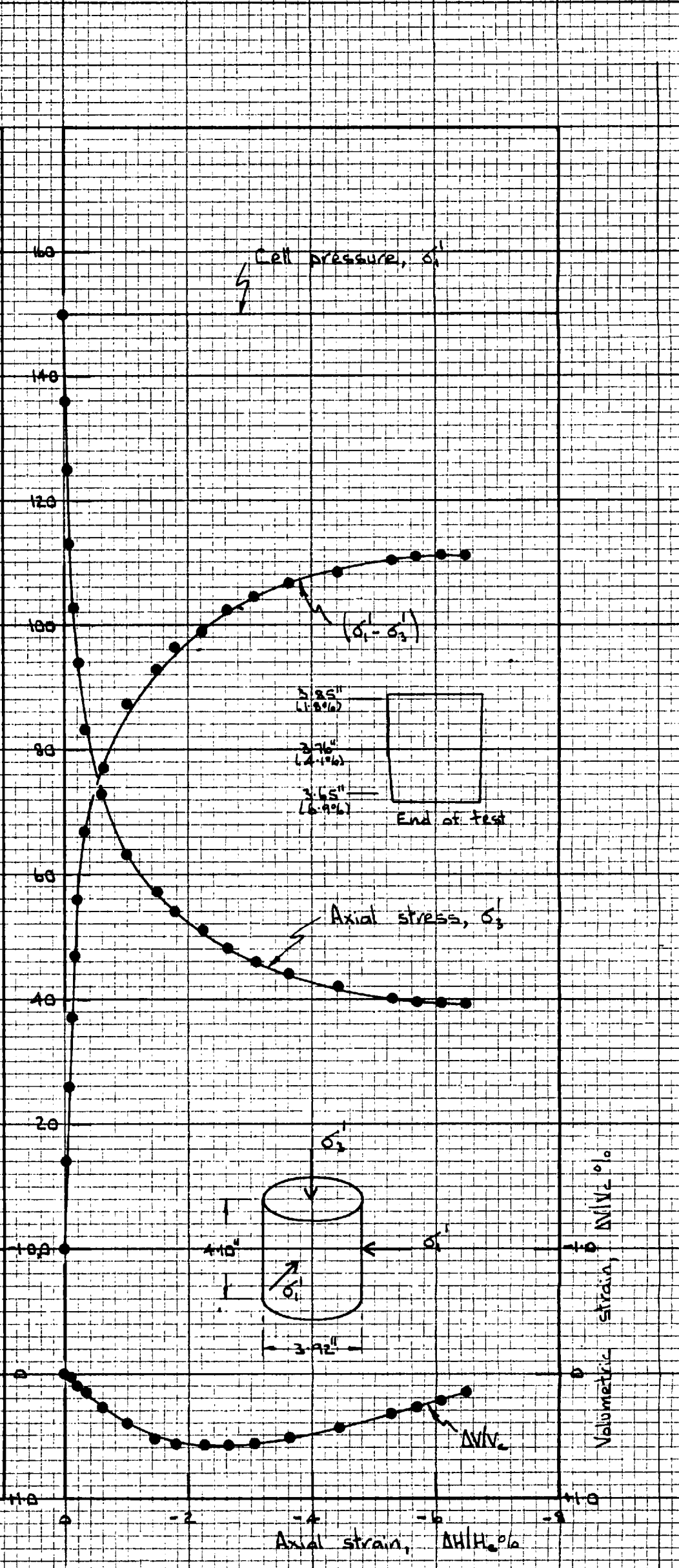


TEST EX14

CYLINDRICAL TRIAXIAL EXTENSION.

Ham River Sand, Batch #2, Bag #4.
n_i = 41·4%, Date: 18/9/65.

2 to 0·010" thick lubricated membranes used at each end of sample.
Sample sheath 0·020" thick.



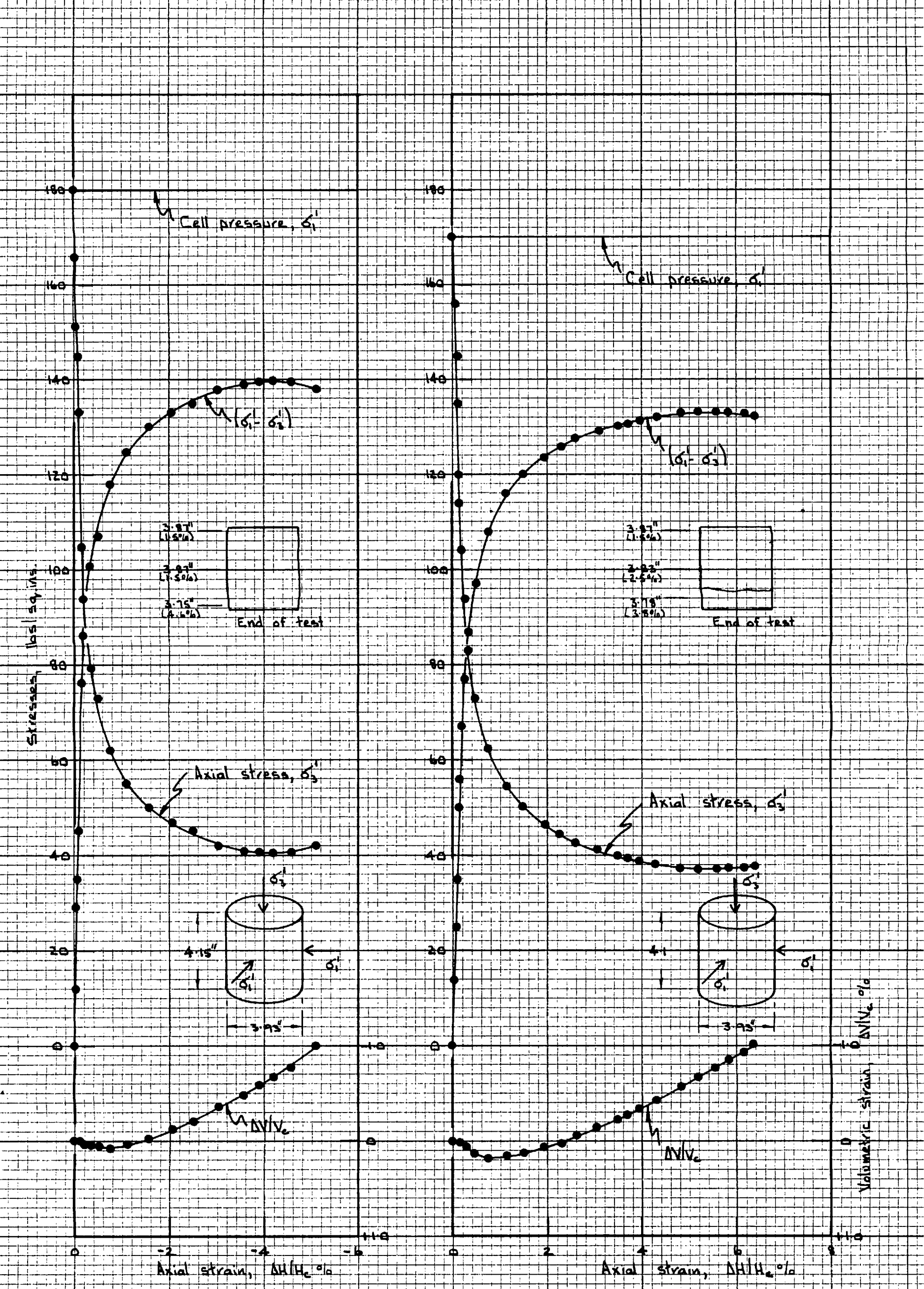
TEST EX15.

CYLINDRICAL TRIAXIAL EXTENSION.

Ham River Sand, Batch #2, Bag #4.
n_i = 42·5%, Date: 20/9/65.

2 to 0·010" thick lubricated membranes used at each end of sample.
Sample sheath 0·020" thick.

FIG. A9.16



TEST EX16.

CYLINDRICAL TRIAXIAL EXTENSION.

Ham River Sand, Batch*2, Bag*4.
n_i = 39·1%, Date: 23/9/65.

2 to 0·010" thick lubricated membranes used at each end of sample.
Sample sheath 0·020" thick.

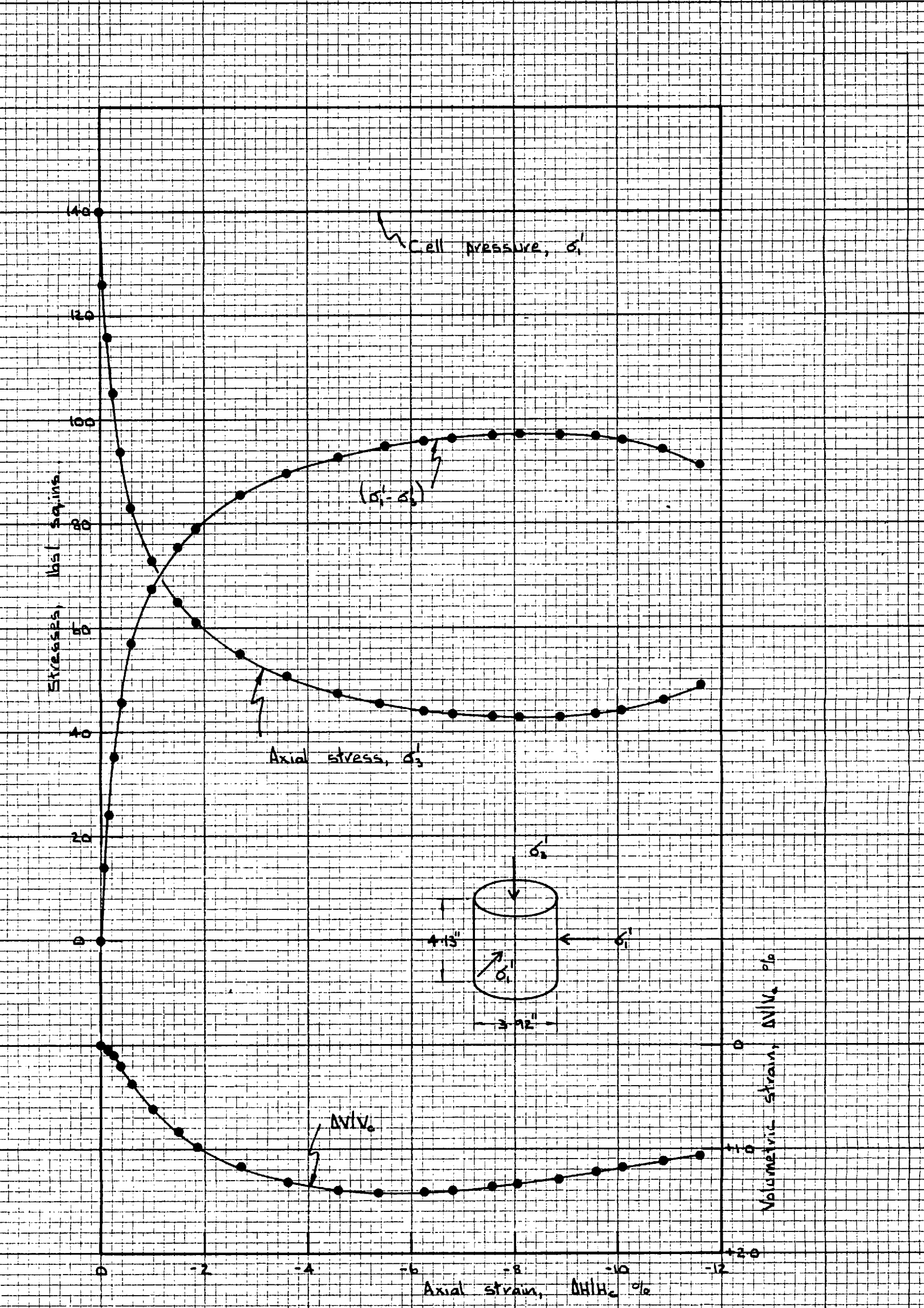
TEST EX12.

CYLINDRICAL TRIAXIAL EXTENSION.

Ham River Sand, Batch*2, Bag*4, Reused once.
n_i = 39·6%, Date: 16/10/65.

2 to 0·010" thick lubricated membranes used at each end of sample.
Sample sheath 0·020" thick.

FIG. A9.17



TEST EXIT. CYLINDRICAL TRIAXIAL EXTENSION.

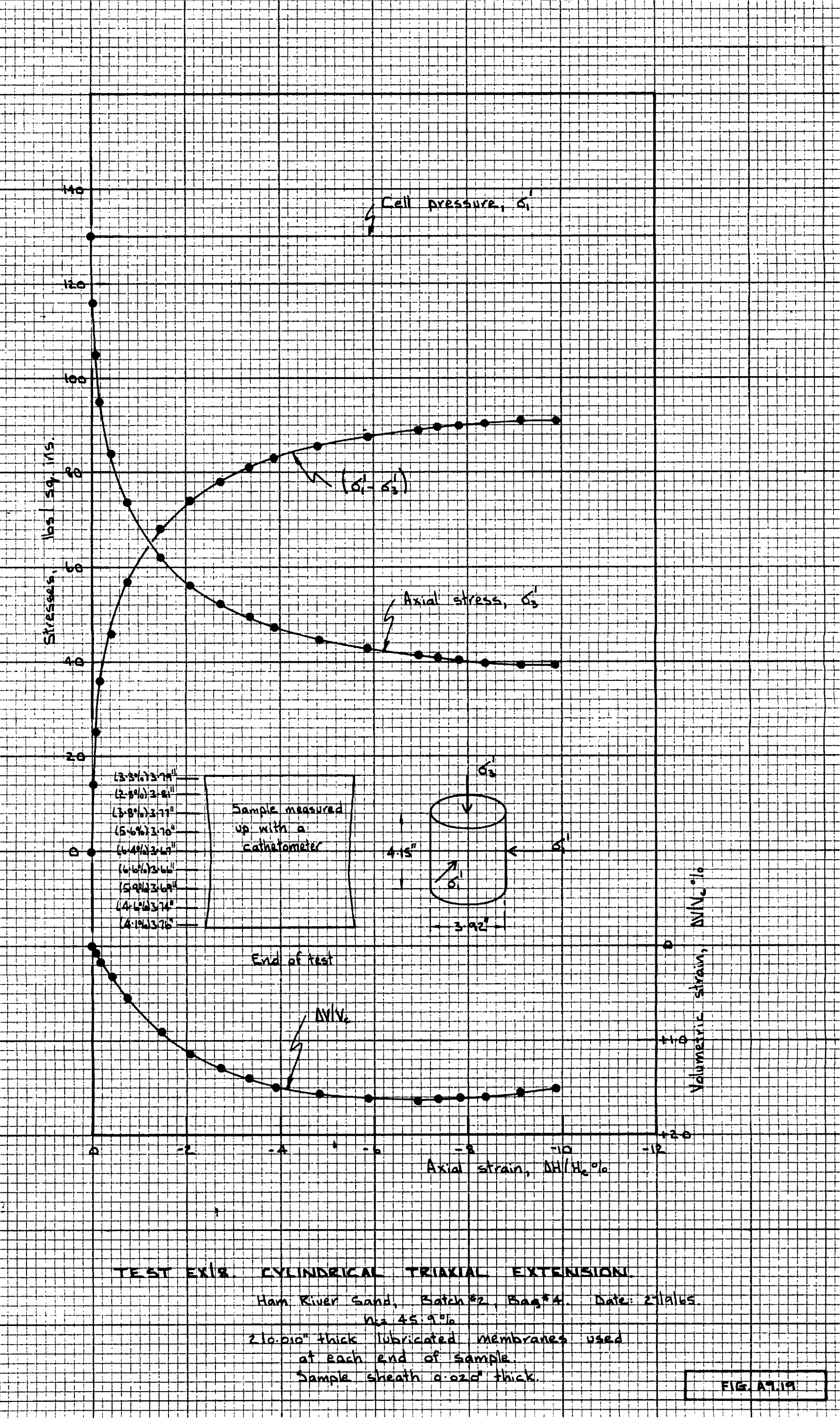
Ham River Sand, Batch#2, Bag#4. Date: 2/5/1965

n_i = 45.5%

2 @ 0.010" thick lubricated membranes used at each end of sample.

Sample sheath 0.020" thick.

FIG. A9.18



TEST EX18. CYLINDRICAL TRIAXIAL EXTENSION.

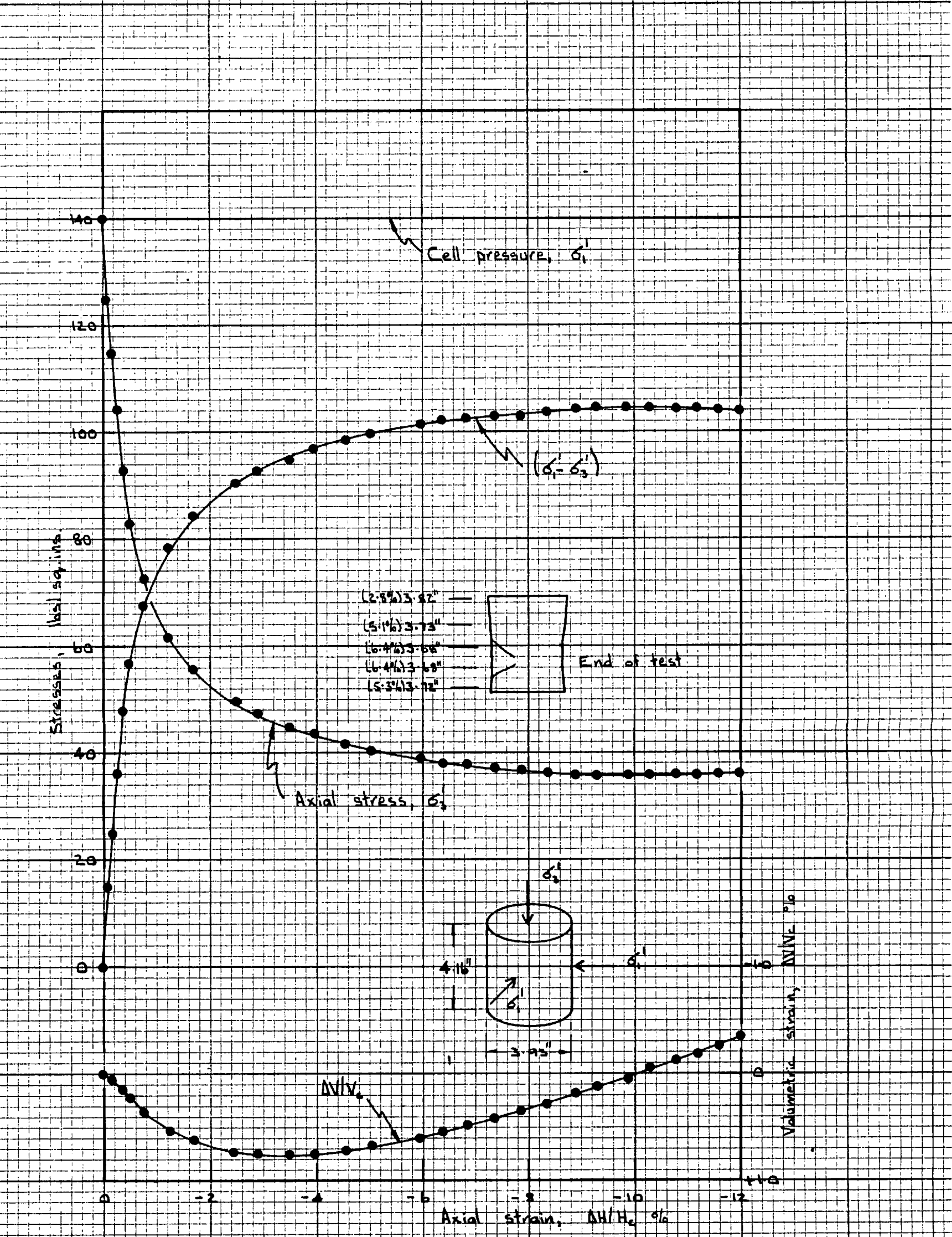
Ham River Sand, Batch #2, Bag #4. Date: 2/19/65.

n_i = 45·9%

2 10·010" thick lubricated membranes used at each end of sample.

Sample sheath 0·020" thick.

FIG. A9.19



TEST EX19. CYLINDRICAL TRIAXIAL EXTENSION.

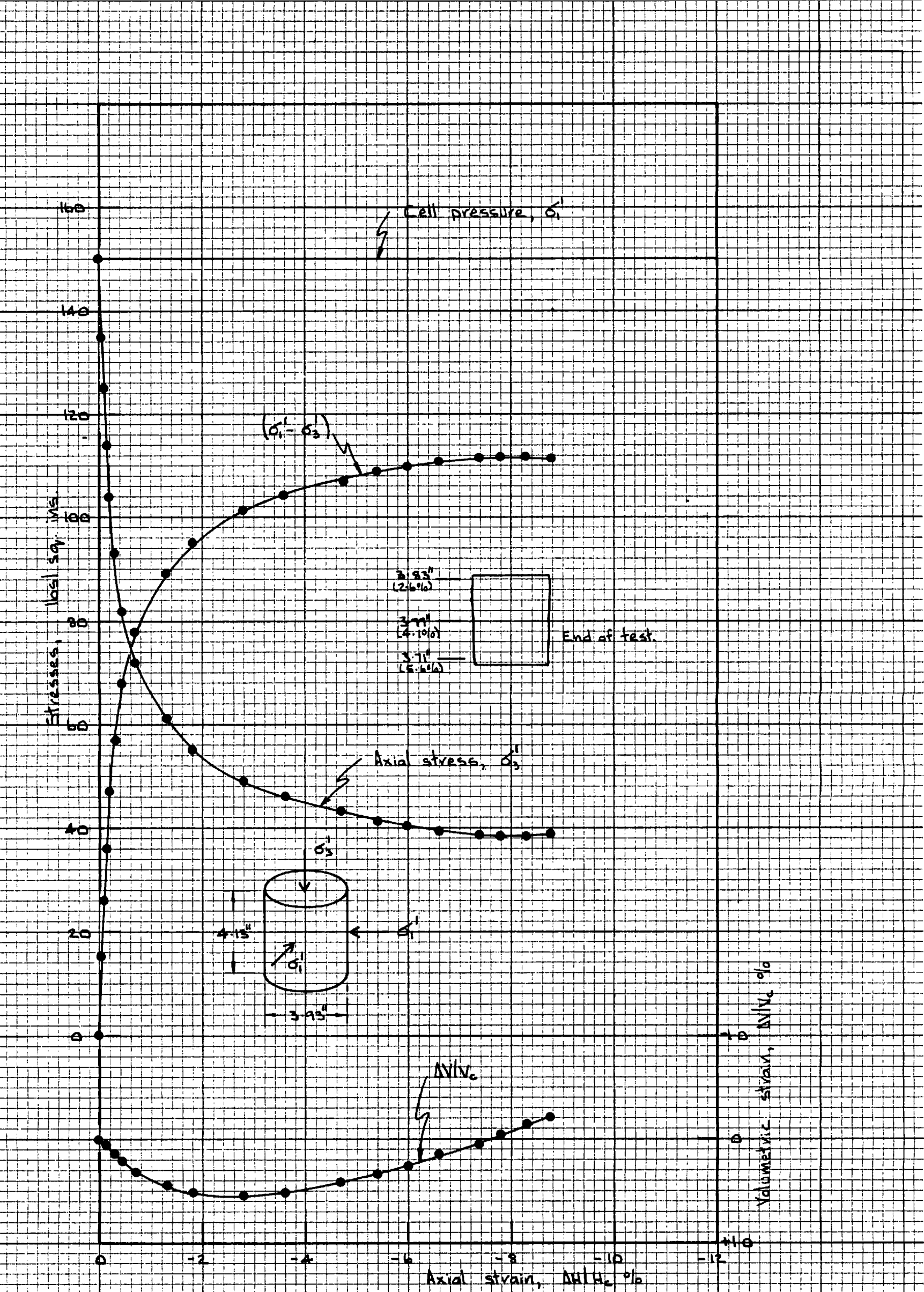
Ham River Sand, Batch #2, Bag #4. Date: 31/10/65.

n_i = 43·8 %

2 | 0·010" thick lubricated membranes used at each end of sample.

Sample sheath 0·020" thick.

FIG. A9.20



TEST EX110. · CYLINDRICAL TRIAXIAL EXTENSION.

Ham River Sand, Batch #2, Bag #4, Reused once.
n_i = 42.5 %, Date: 5/10/65
2 | 0.010" thick lubricated membranes used at each end of sample.
Sample sheath 0.020" thick.

FIG. A9.21

Cell pressure, σ_3'

$(\sigma_1' - \sigma_3')$

Axial stress, σ_1'

$\Delta V/V_c$

Stresses, lbs / sq. ins.

160
140
120
100
80
60
40
20
0

3·82"
(2·6%)
3·80"
(3·0%)
3·59"
(8·4%)
End of test

σ_3'
4·14"
σ_1'
σ_1'
3·92"

1·0
0
-1·0

Volumetric strain, $\Delta V/V_c$ %

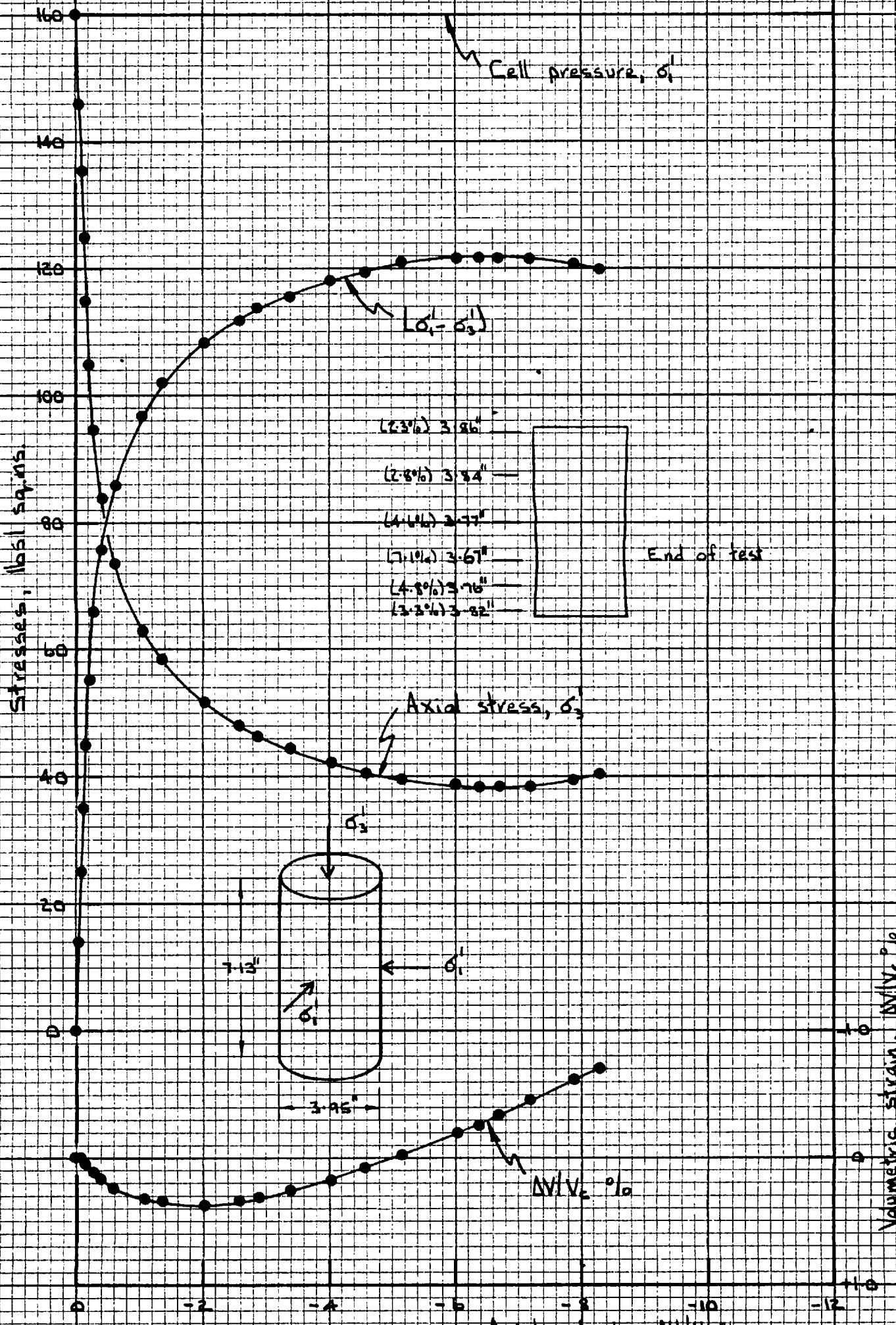
0 -2 -4 -6 -8 -10 -12

Axial strain, $\Delta H/H_c$ %

TEST EXIII. CYLINDRICAL TRIAXIAL EXTENSION.

Hawk River Sand, Batch #2, Bag #4, Reused once.
n_i = 42·5%, Date: 11/10/65.
2 to 0·10" thick lubricated membranes used at each end of sample.
Sample sheath 0·020" thick.

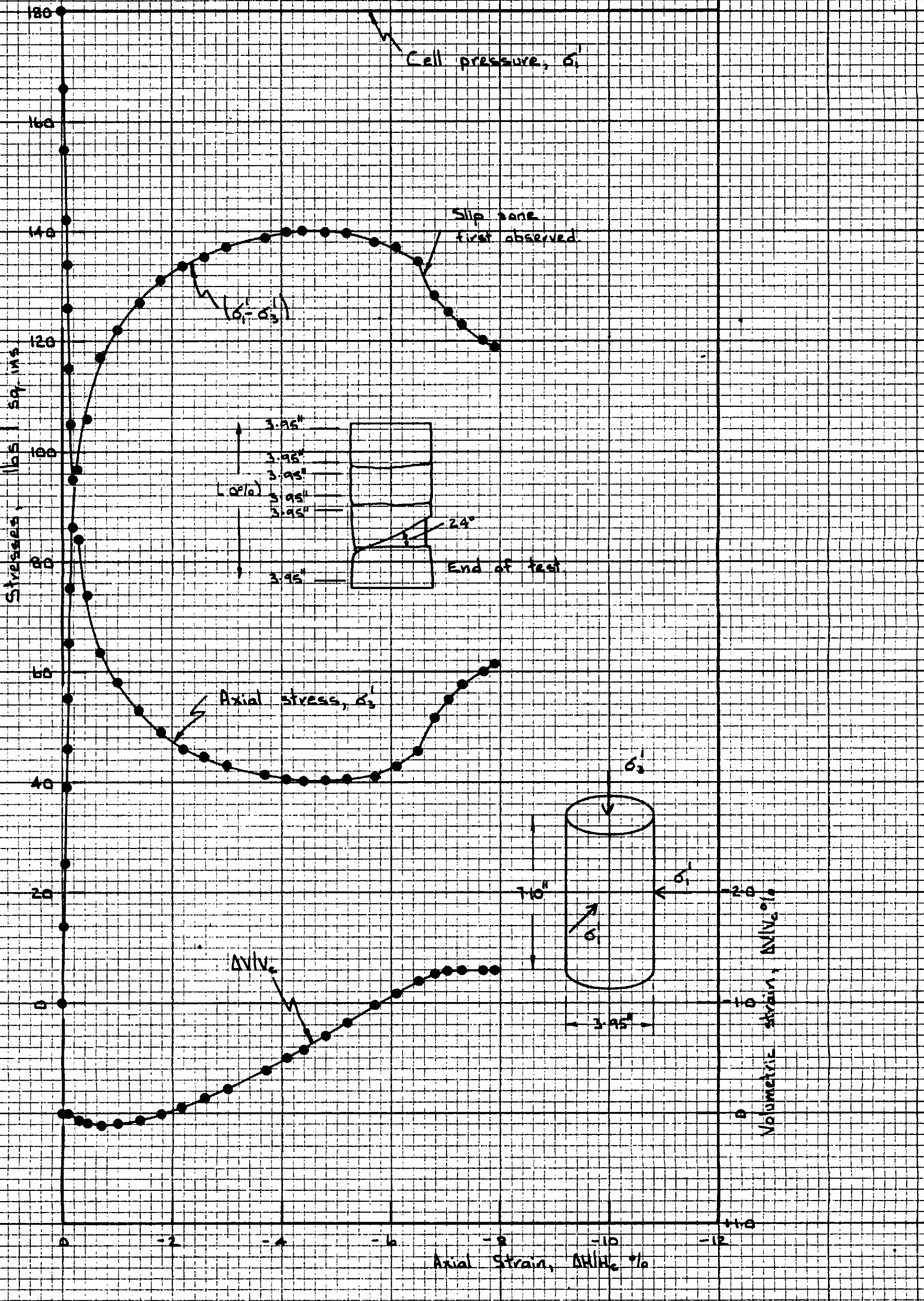
FIG. A9.22



TEST E111. CYLINDRICAL TRIAXIAL EXTENSION.

Ham River Sand, Batch*2, Bag*4, Reused once.
n_i = 41.0%, Date: 2/11/65.
2 lo.010" thick lubricated membranes used at each end of sample.
Sample sheath 0.020" thick.

FIG. A9.23



TEST E1/2 CYLINDRICAL TRIAXIAL EXTENSION

Ham River Sand, Batch #2, Bag #4. Reused once.
n_i = 38.8 %, Date: 6/11/65.
2 lo.010" thick lubricated membranes used at each end of sample.
Sample sheath 0.020" thick.

FIG. A9.24

Cell pressure, σ_3'

$(\sigma_1' - \sigma_3')$

Axial stress σ_1'

Stresses, lbs/sq.ins.

140
120
100
80
60
40
20
0

σ_3'

7·10"

σ_1'

σ_1'

3·94"

(2·3%) 3·65"
(3·6%) 3·60"
(5·8%) 3·71"
(7·6%) 3·64"
(10·1%) 3·54"
(11·4%) 3·49"
(13·9%) 3·51"
(7·1%) 3·66"
(5·3%) 3·73"

End of test.

$\Delta V/V_c$

Volumetric strain, $\Delta V/V_c$ %

0
+1·0
+2·0

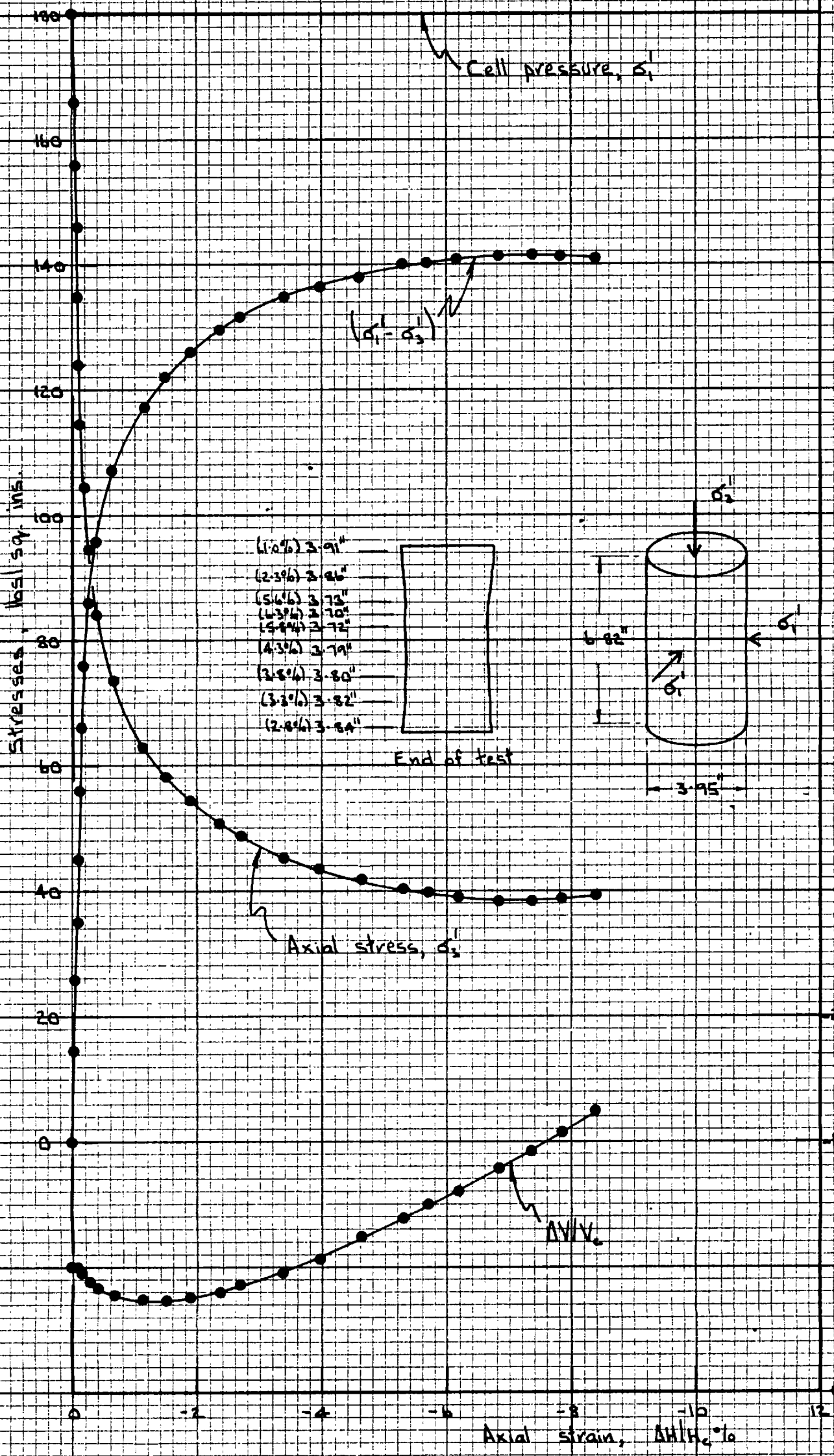
0 -2 -4 -6 -8 -10 -12

Axial strain, $\Delta H/H$, %

TEST EL 13. CYLINDRICAL TRIAXIAL EXTENSION.

Ham River Sand, Batch* 7, Bag* 4. Reused once.
n_c = 45·3 %, Date: 11/11/65.
2 10·010" thick lubricated membranes used at each end of sample.
Sample sheath 0·020" thick.

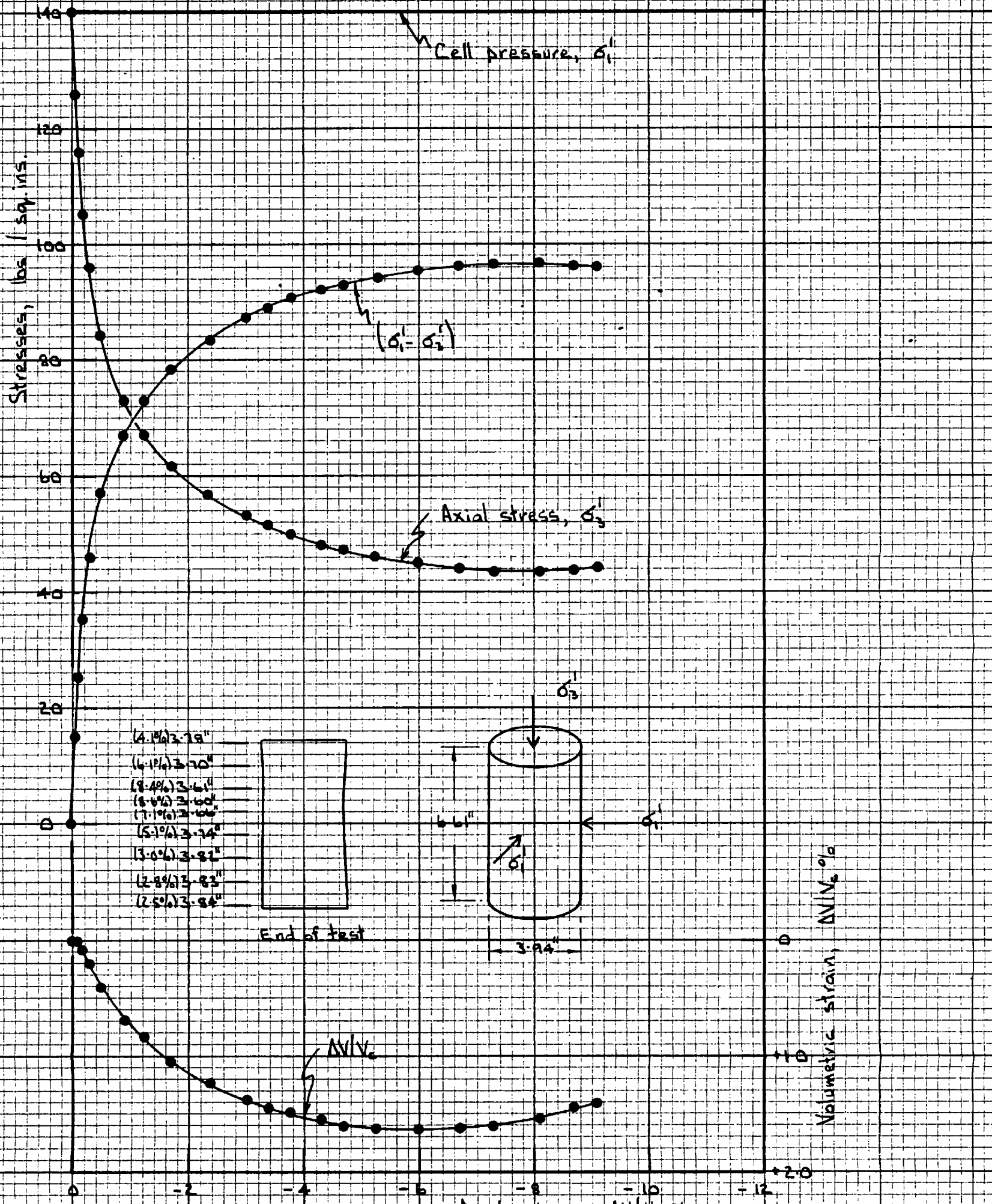
FIG. A9.25



TEST ELA11. CYLINDRICAL TRIAXIAL EXTENSION.

Ham River Sand, Batch #2, Bag #4, Reused once.
n_c = 39.4 %, Date: 15/11/65
1/4" thick porous disc used at each end of sample.
Sample sheath 0.020" thick.

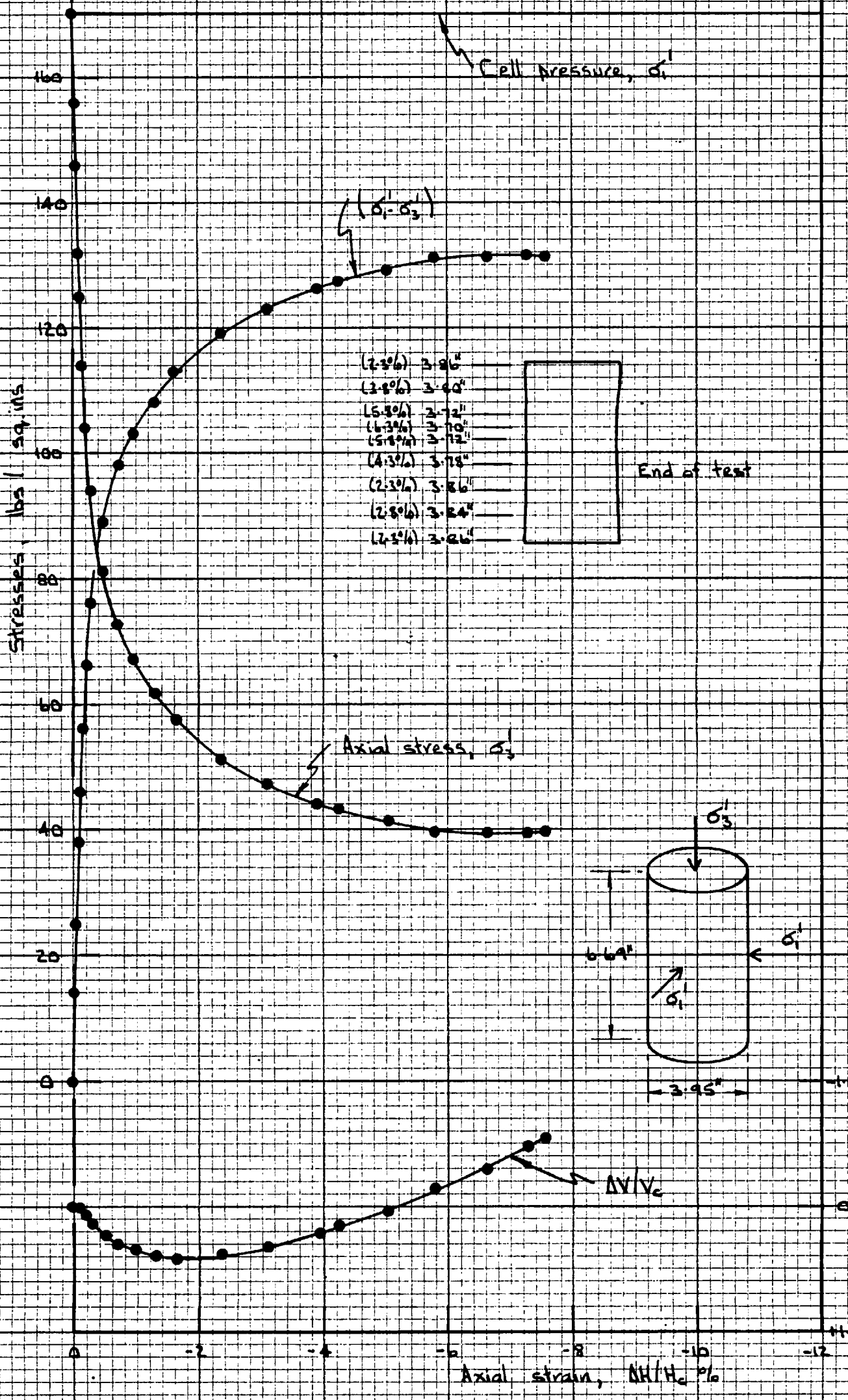
FIG. A9.26



TEST ELAIL. CYLINDRICAL TRIAXIAL EXTENSION.

Ham River Sand, Batch*2, Bag*4, Reused once.
n_i = 45·2 %, Date: 18/11/65.
1/4" thick porous disc used at each end of sample.
Sample sheath 0·020" thick.

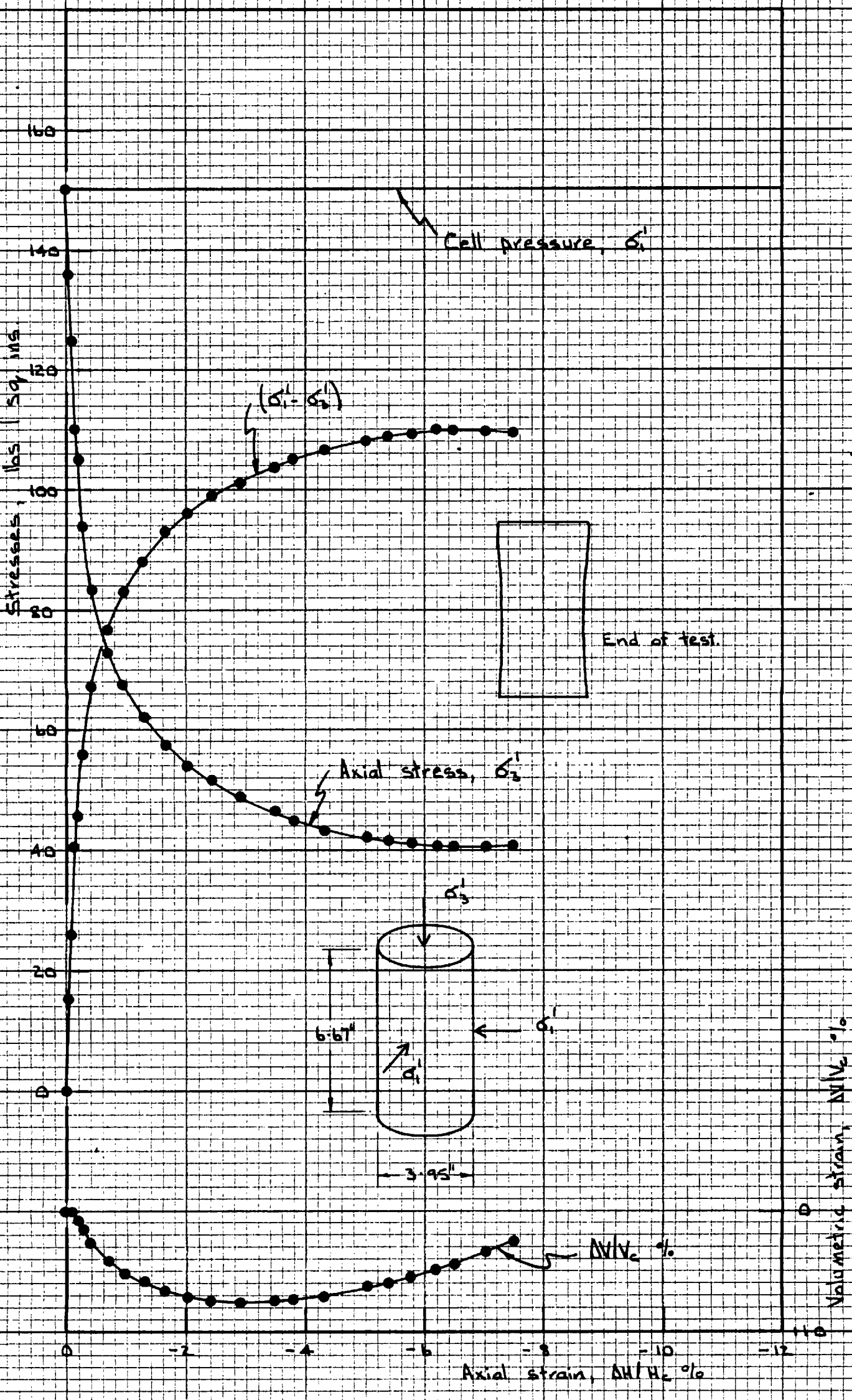
FIG. A9.27



TEST EL A13. CYLINDRICAL TRIAXIAL EXTENSION

Ham River Sand, Batch #2, Bag #4; Reused once.
n_i = 40·4 %, Date: 22/11/65.
1/4" thick porous disc used at each end of sample.
Sample sheath 0·020" thick.

FIG A9.28



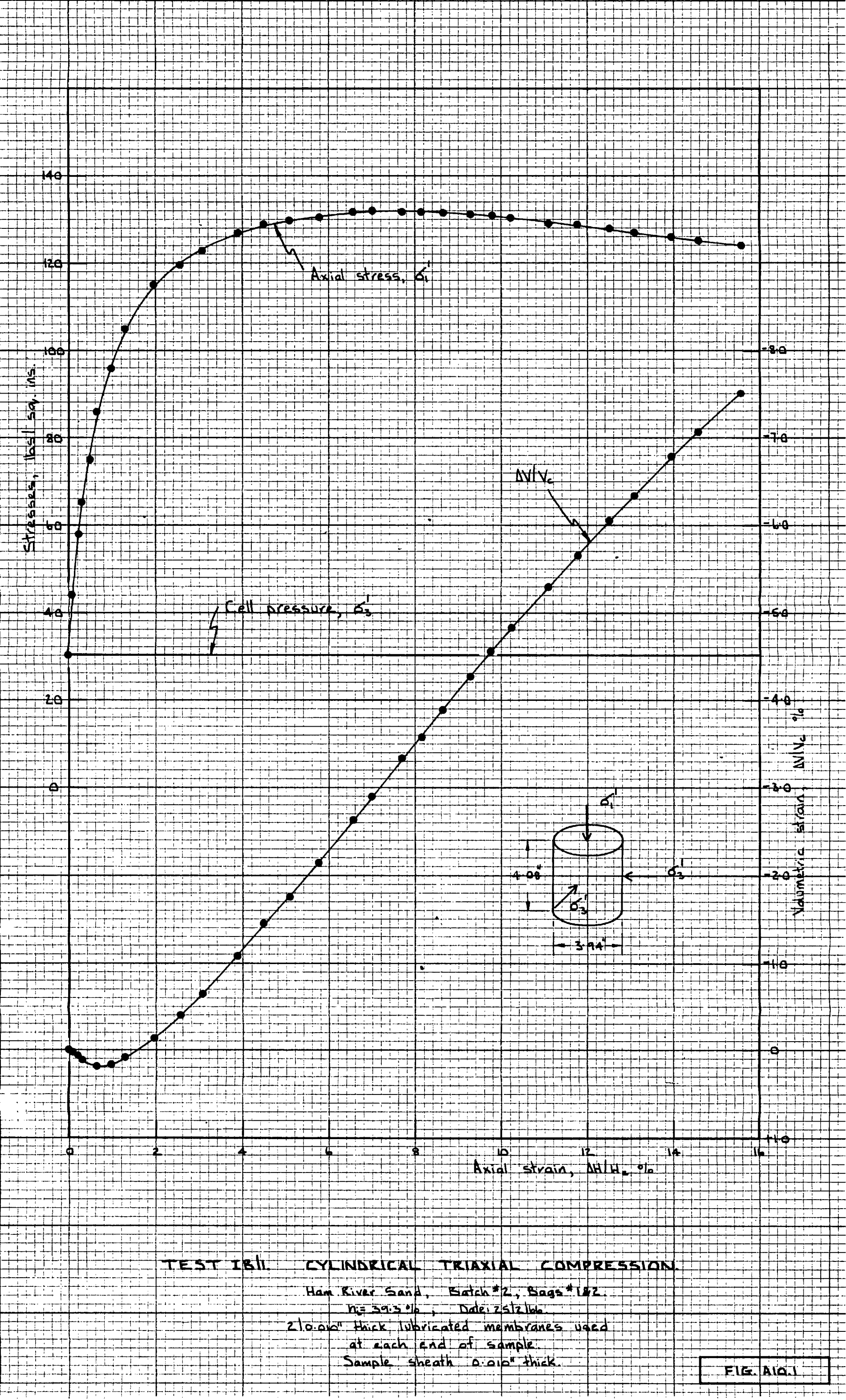
TEST EL A/4. CYLINDRICAL TRIAXIAL EXTENSION.

Ham River Sand, Batch #2, Bag #4, Reused once.
n_i = 42·3 %, Date: 26/11/65.
1/4" thick porous disc used at each end of sample.
Sample sheath 0·020" thick.

FIG. A9.29

Appendix A 10

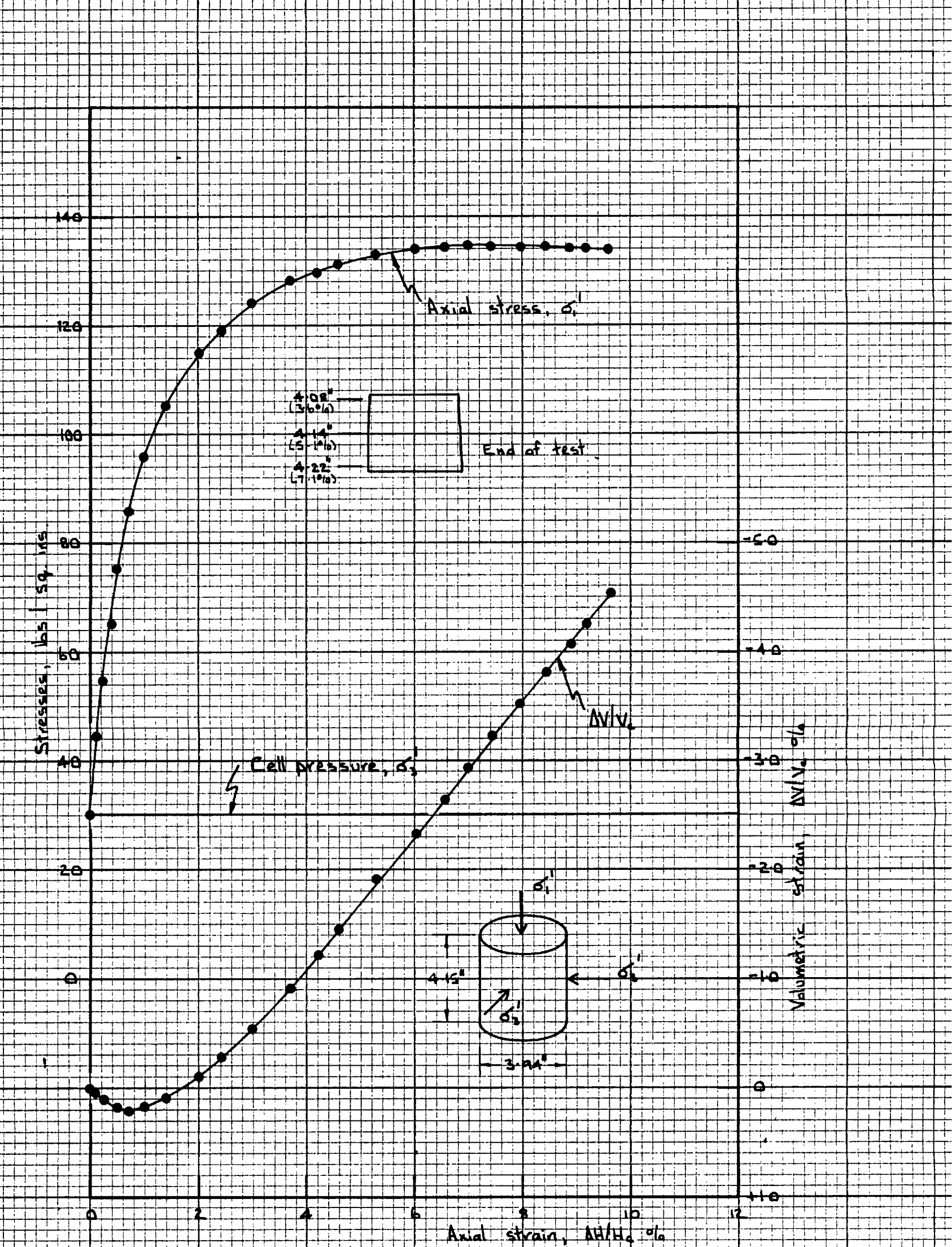
Graphical presentation of cuboidal triaxial compression and extension test results.



TEST IB11. CYLINDRICAL TRIAXIAL COMPRESSION.

Ham River Sand, Batch #2, Bags #1&2.
n_i = 39.3 %, Date: 25/2/66.
2/0.010" thick lubricated membranes used at each end of sample.
Sample sheath 0.010" thick.

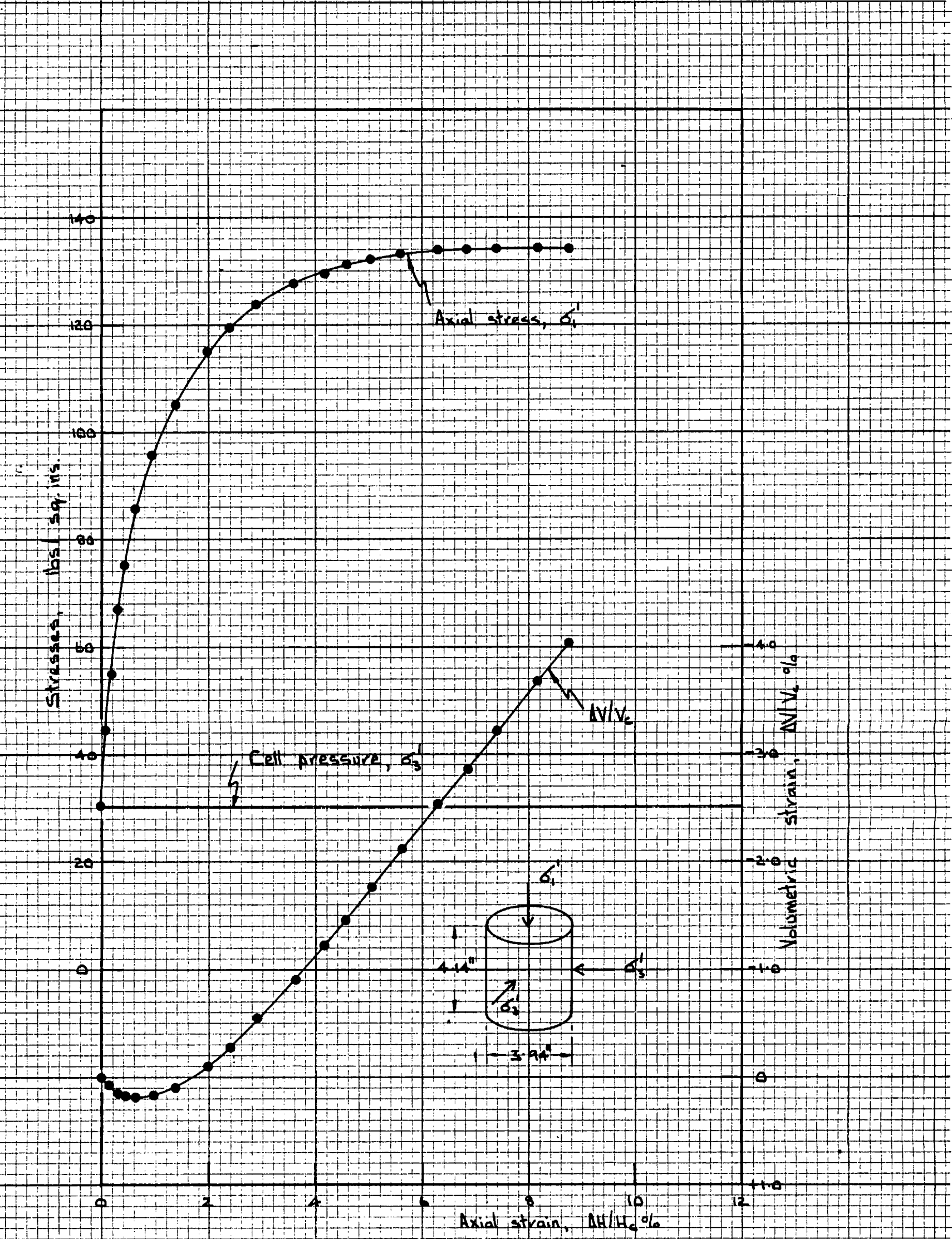
FIG. A10.1



TEST IB12. CYLINDRICAL TRIAXIAL COMPRESSION.

Ham River Sand, Batch #2, Bags #1&2.
n_d 39·0%, Date: 26/2/66.
2 to 0·010" thick lubricated membranes used at each end of sample.
Sample sheath 0·010" thick.

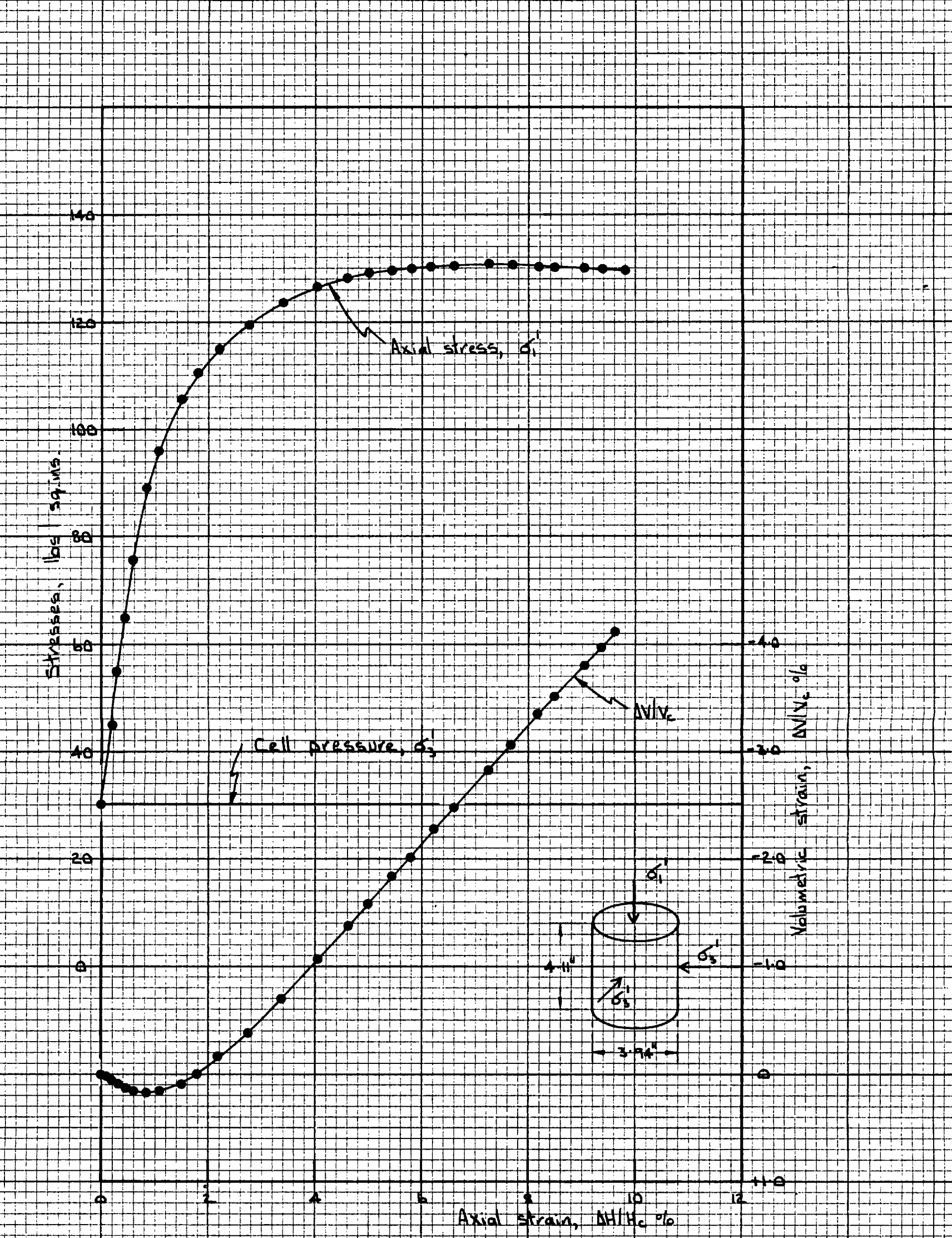
FIG. A10.2



TEST IB/3. CYLINDRICAL TRIAXIAL COMPRESSION.

Ham River Sand, Batch #2, Bags #1 & 2.
n_i = 39·2 %, Date: 11/3/66.
2/0·010" thick lubricated membranes used at each end of sample.
Sample sheath 0·010" thick.

FIG. A10.3



TEST IB/4. CYLINDRICAL TRIAXIAL COMPRESSION.

Ham River Sand, Batch #2, Bags #1&2.
n_i = 39.1%, Date: 23/4/66.
2 lo·010" thick lubricated membranes used at each end of sample.
Sample sheath 0·010" thick.

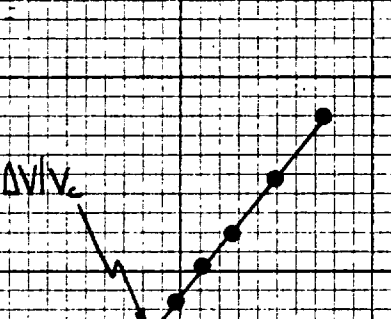
FIG. A10.4

Stresses, lbs / sq. ins.

Axial stress, σ_1'

$\Delta V/V_c$

Cell pressure, σ_3'



Volumetric strain, $\Delta V/V_c$ %

Axial strain, $\Delta H/H_c$ %

TEST IB/5. CYLINDRICAL TRIAXIAL COMPRESSION.

Ham River Sand, Batch #2, Bags #1 & 2.
n_i = 38.5 %, Date: 2/6/66.
2 to 0.010" thick lubricated membranes used at each end of sample.
Sample sheath 0.016" thick.

FIG. A10.5

Axial stress, σ_1'

$\Delta V/V_c$

Cell pressure, σ_3'

σ_1'

4·00

σ_3'

σ_3'

3·96"

Stresses, lbs/sq. ins.

140
120
100
80
60
40
20
0

Volumetric strain, $\Delta V/V_c$ %

4·0
3·0
2·0
1·0
0
1·0

0 2 4 6 8 10 12

Axial strain, $\Delta H/H_c$ %

TEST IB/b. CYLINDRICAL TRIAXIAL COMPRESSION.

Ham River Sand, Batch #2, Bags #1&2.
n_i = 38·9%, Date: 13/5/66.
2 | 0·010" thick lubricated membranes used at each end of sample.
Sample sheath 0·010" thick.

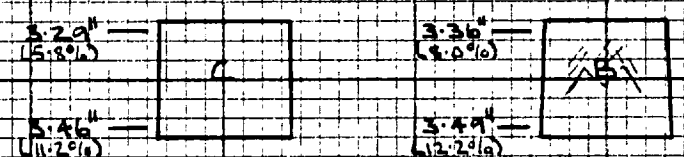
FIG. A10.b

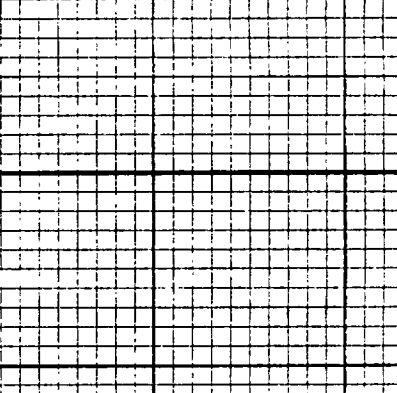
Axial stress, σ_1'

Cell pressure, σ_3'

$\Delta V/V_c$

End of test.





Stresses, lbs/sq. ins.

Volumetric strain, $\Delta V/V_c$ %

Axial strain, $\Delta H/H_c$ %

TEST IA11. CUBOIDAL TRIAXIAL COMPRESSION.

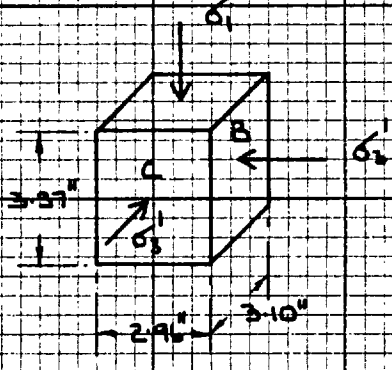
Ham River Sand, Batch *2, Bags* 1&2.
n_i = 39.7 %, Date: 14/2/66
2 lo·o10" thick lubricated membranes used at each end of sample.
Sample sheath 0·010" thick.

FIG. A10.7

Axial stress, σ_1'

$\Delta V/V_c$

Cell pressure, σ_3'



Stresses, lbs / sq. ins.

Volumetric strain, $\Delta V/V_c$ %

Axial strain, $\Delta H/H_c$ %

TEST IA/2. CUBOIDAL TRIAXIAL COMPRESSION.

Ham River Sand, Batch #2, Bags #1&2.
n_i = 39·0 %, Date: 17/2/66.
2 / 0·010" thick lubricated membranes used at each end of sample.
Sample sheath 0·010" thick.

FIG. A10.8

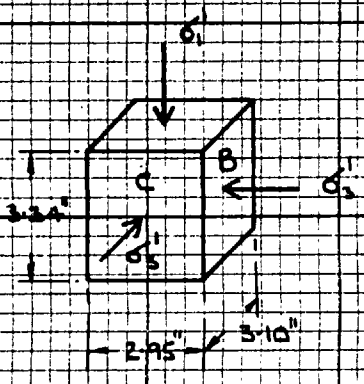
Stresses, lbs/sq. ins.

Axial stress, σ_1'

Cell pressure, σ_3'

$\Delta V/V_c$

Volumetric strain, $\Delta V/V_c$ %



Axial strain, $\Delta H/H_c$ %

TEST IA13. CUBOIDAL TRIAXIAL COMPRESSION.

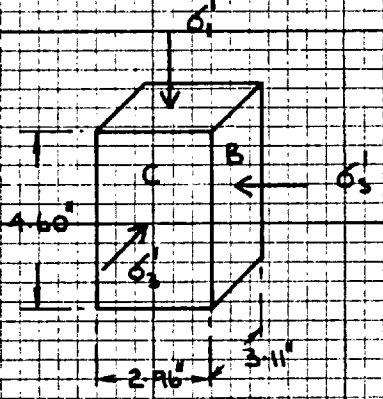
Ham River Sand, Batch #2, Bags #1&2.
n_i = 39.2 %, Date: 22/2/66.
3 lo.010" thick lubricated membranes used at each end of sample.
Sample sheath 0.010" thick.

FIG. A10.9

Axial stress, σ_1'

$\Delta V/V_c$

Cell pressure, σ_3'



Stresses, lbs / sq.ins.

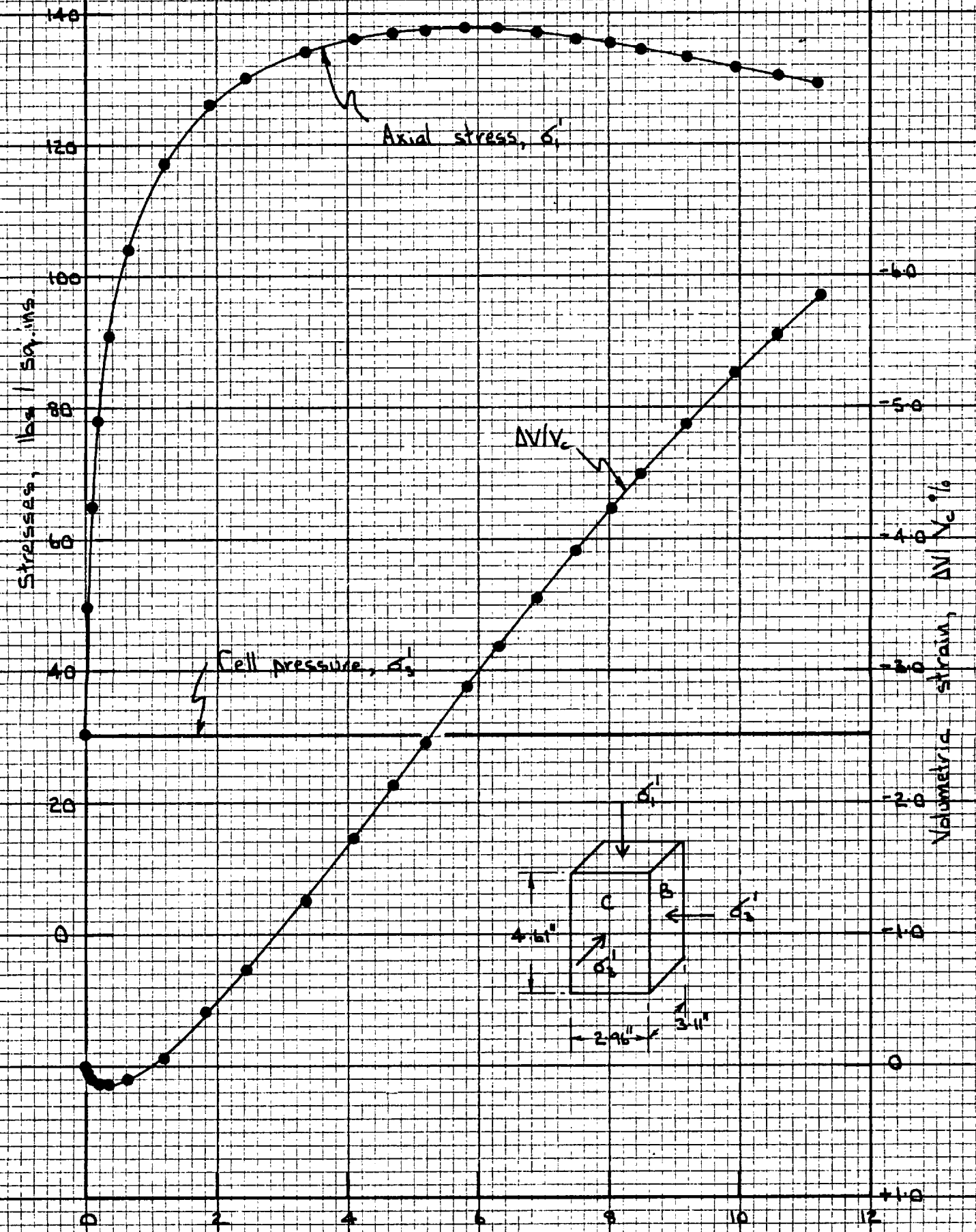
Volumetric strain, $\Delta V/V_c$ %

Axial strain, $\Delta H/H_c$ %

TEST IA4. CUBOIDAL TRIAXIAL COMPRESSION.

Ham River Sand, Batch #2, Bags #1&2.
n_i = 38.9 % Date: 7/3/66
2 @ 0.010" thick lubricated membranes used at each end of sample.
Sample sheath 0.010" thick.

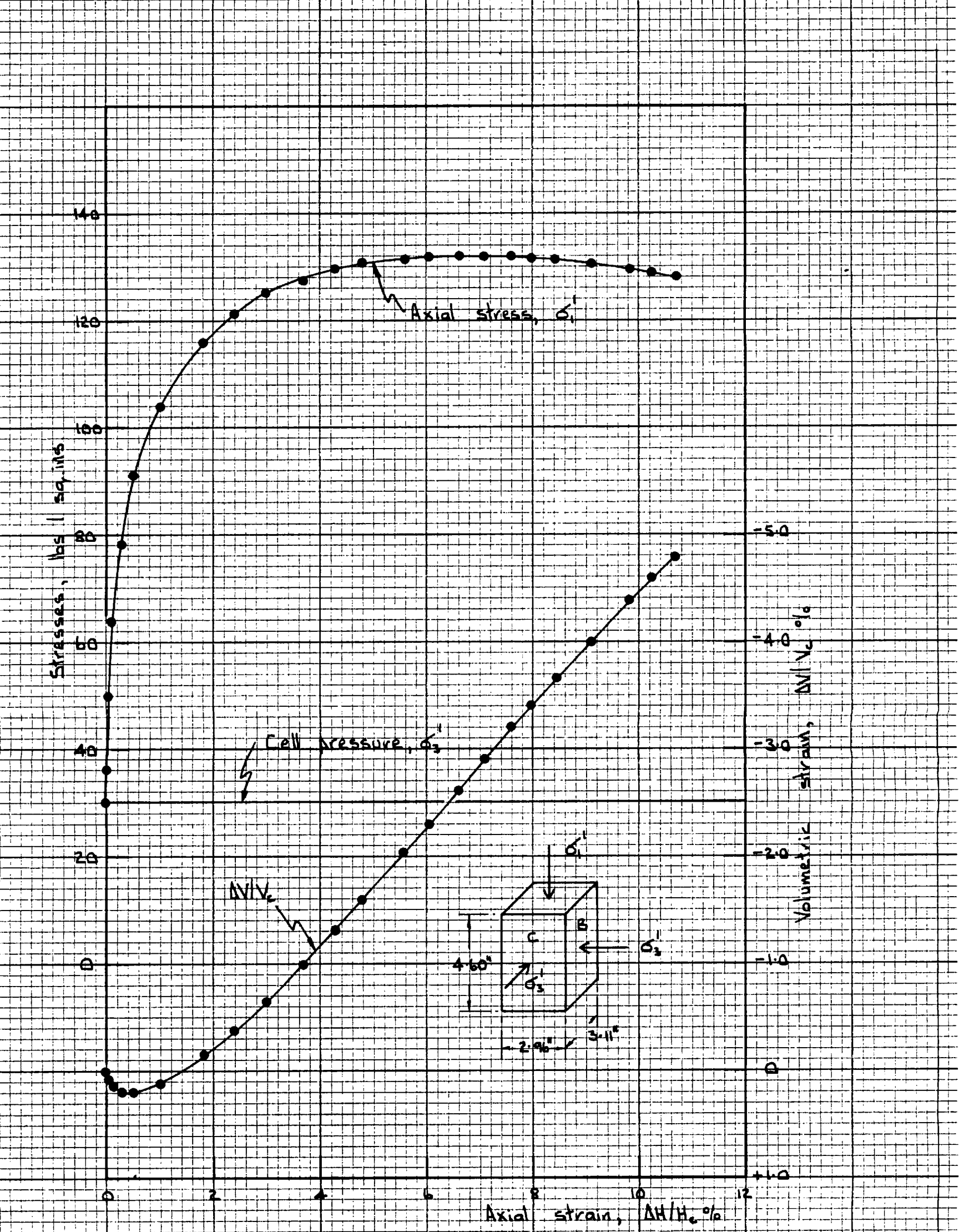
FIG. A10.10



TEST IA15. CUBOIDAL TRIAXIAL COMPRESSION.

Ham River Sand, Batch *2, Bags* 1&2.
n_i = 38.8%, Date: 9/3/66.
2/0.010" thick lubricated membranes used at each end of sample.
Sample sheath 0.010" thick.

FIG. A10.11



TEST IA/6. CUBOIDAL TRIAXIAL COMPRESSION.

Ham River Sand, Batch #2, Bags# 1&2.
n_i = 39·5%, Date: 13/3/66.
2 to 0·010" thick lubricated membranes used at each end of sample.
Sample sheath 0·010" thick.

FIG. A10.12.

Stresses, lbs / sq. ins.

140
120
100
80
60
40
20
0

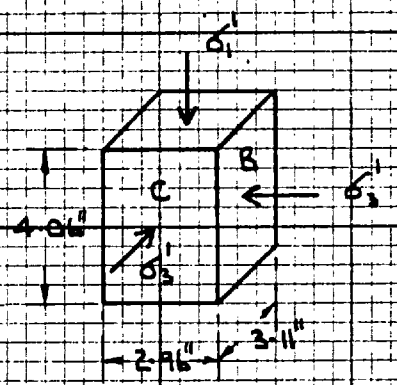
Axial stress, σ_1'

Cell pressure, σ_3'

$\Delta V/V_c$

-5.0
-4.0
-3.0
-2.0
-1.0
0
+1.0

Volumetric strain, $\Delta V/V_c$ %



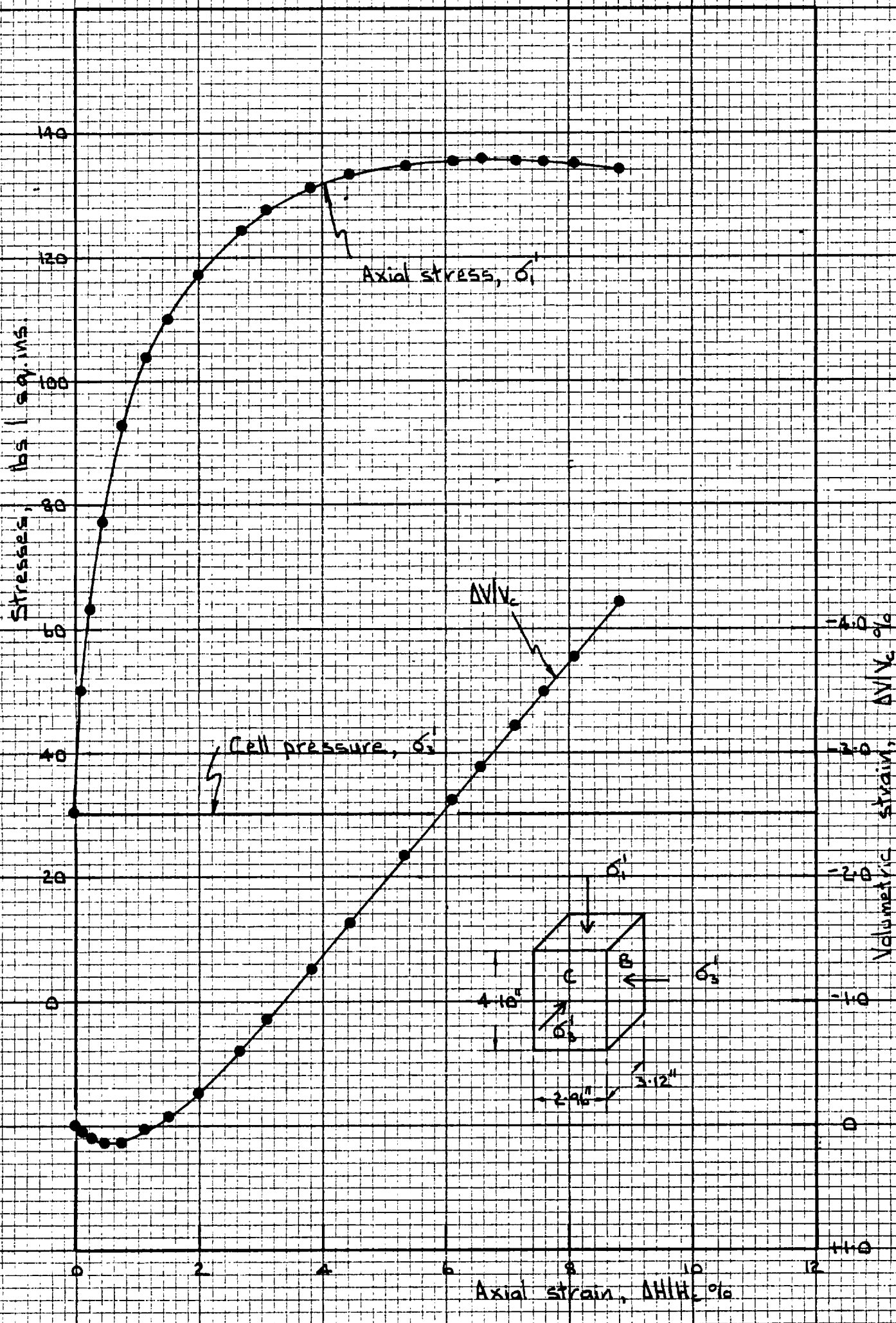
0 2 4 6 8 10 12

Axial strain, $\Delta H/H_c$ %

TEST IA/7. CUBOIDAL TRIAXIAL COMPRESSION.

Ham River Sand, Batch "2, Bags 1 & 2.
n_c = 39·6 %, Date: 15/3/66.
2/0·010" thick lubricated membranes used at each end of sample.
Sample sheath 0·010" thick.

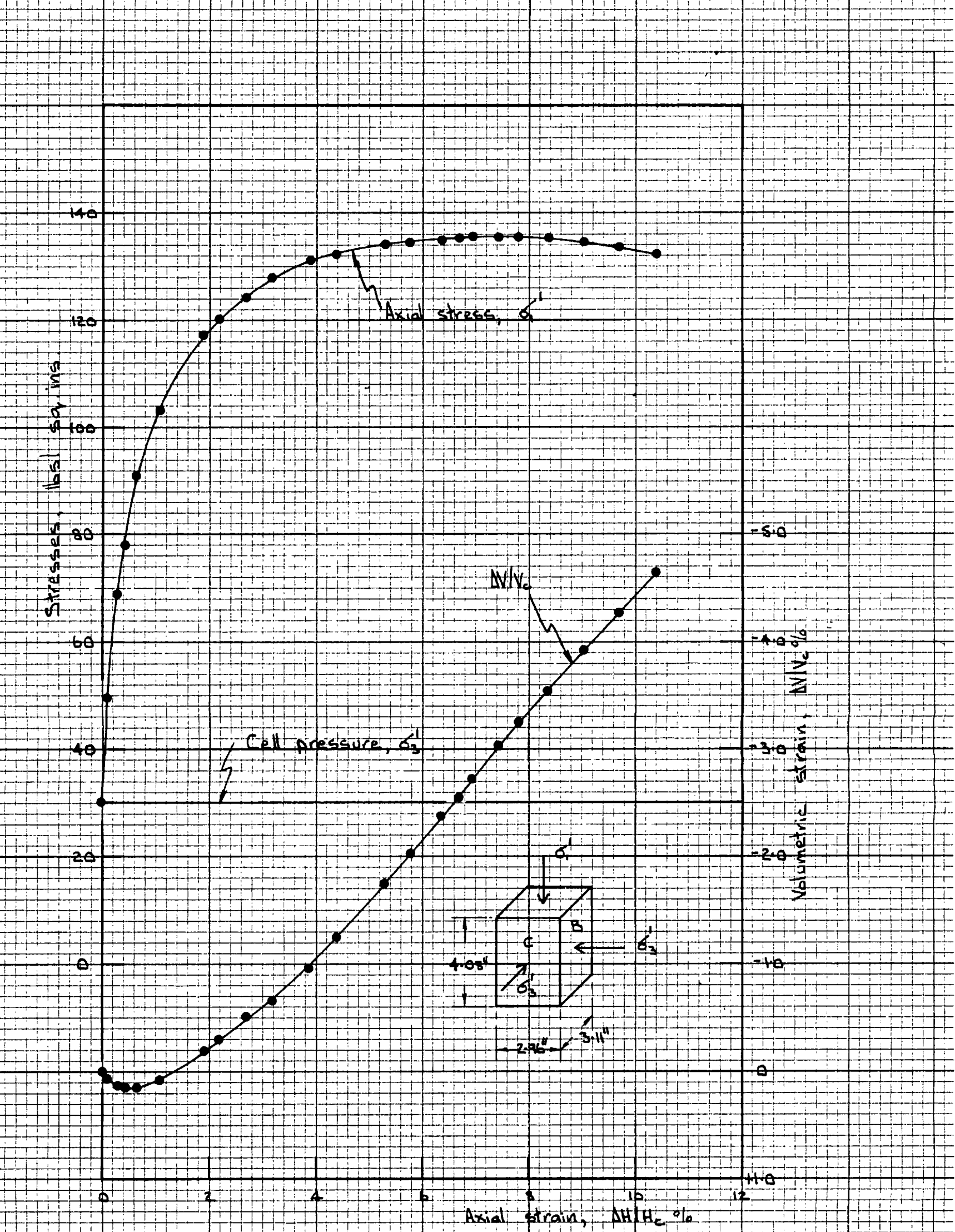
FIG. A10.13



TEST IA18. CUBOIDAL TRIAXIAL COMPRESSION.

Ham River Sand, Batch #2, Bags #1&2.
n_i = 38.7%, Date: 20/3/66.
2 to 0.010" thick lubricated membranes used at each end of sample.
Sample sheath 0.010" thick.

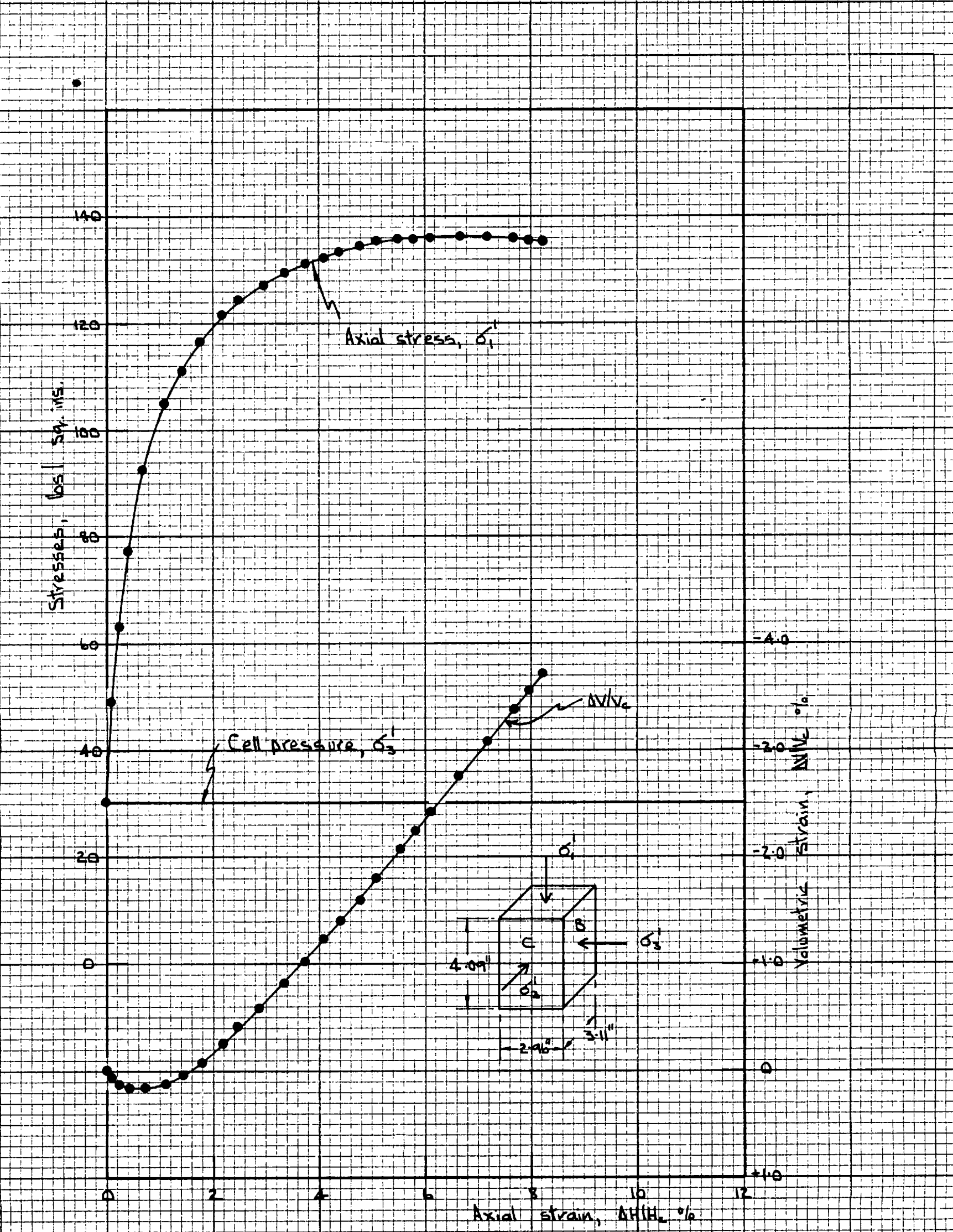
FIG. A10.14



TEST IA/9. CUBOIDAL TRIAXIAL COMPRESSION.

Ham River Sand, Batch*2, Bags*1&2.
n_i = 39.1%, Date: 22/3/66.
2 10·010" thick lubricated membranes used at each end of sample.
Sample sheath 0·010" thick.

FIG. A10.15



TEST IA/10. CUBOIDAL TRIAXIAL COMPRESSION.

Ham River Sand, Batch #2, Bags #1 & 2.
n_c = 39.3%, Date: 14/7/66.
2 lo·010" thick lubricated membranes used at each end of sample.
Sample sheath 0·012" thick.

FIG. A10.16

Axial stress, σ_1'

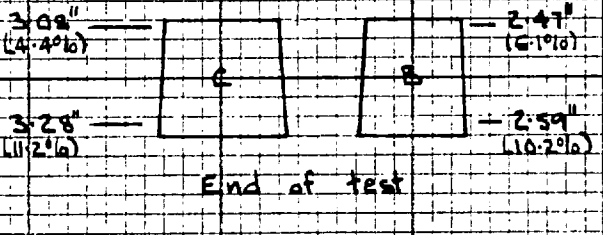
Cell pressure, σ_3'

$\Delta V/V_c$

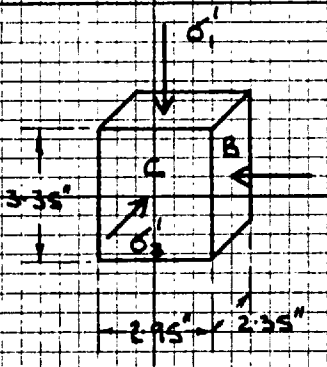
Stresses, lbs/sq. ins.

Volumetric strain, $\Delta V/V_c$ %

Axial strain, $\Delta H/H_c$ %



End of test



TEST IC11. CUBOIDAL TRIAXIAL COMPRESSION.

Ham River Sand, Batch #2, Bags #1&2.
n_i = 39·7%, Date: 29/4/66.
2 to 0·010" thick lubricated membranes used at each end of sample.
Sample sheath 0·010" thick.

FIG. A10.17

Axial stress, σ_1'

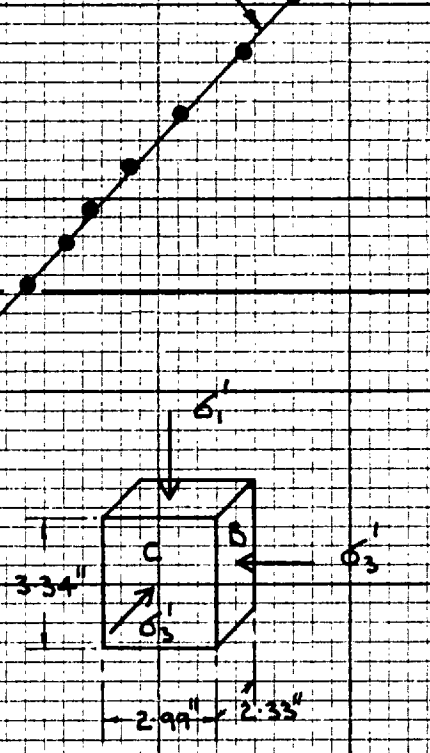
Cell pressure, σ_3'

$\Delta V/V_c$

Stresses, lbs/sq.ins.

Volumetric strain, $\Delta V/V_c$ %

Axial strain, $\Delta H/H_c$ %



TEST IC/2. CUBOIDAL TRIAXIAL COMPRESSION.

Haw River Sand, Batch #2, Bags #1&2.
n_i = 39·3%, Date: 6/5/66.
2/10·010" thick lubricated membranes used at each end of sample.
Sample sheath 0·010" thick.

FIG. A10.18

Axial stress, σ_1'

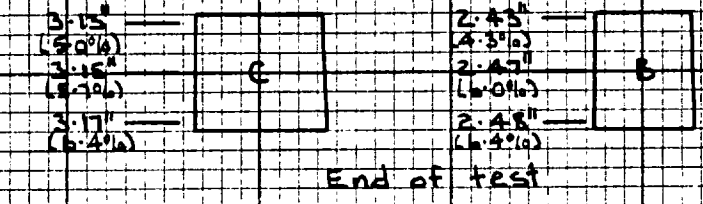
Cell pressure, σ_3'

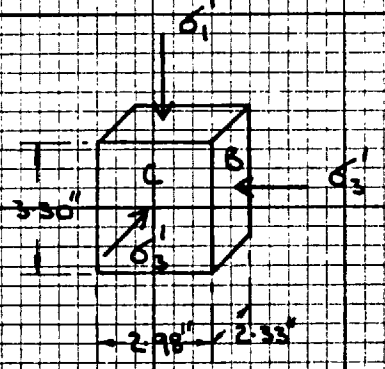
$\Delta V/V_c$

Stresses, lbs/sq.ins.

Volumetric strain, $\Delta V/V_c$ %

Axial strain, $\Delta H/H_c$ %

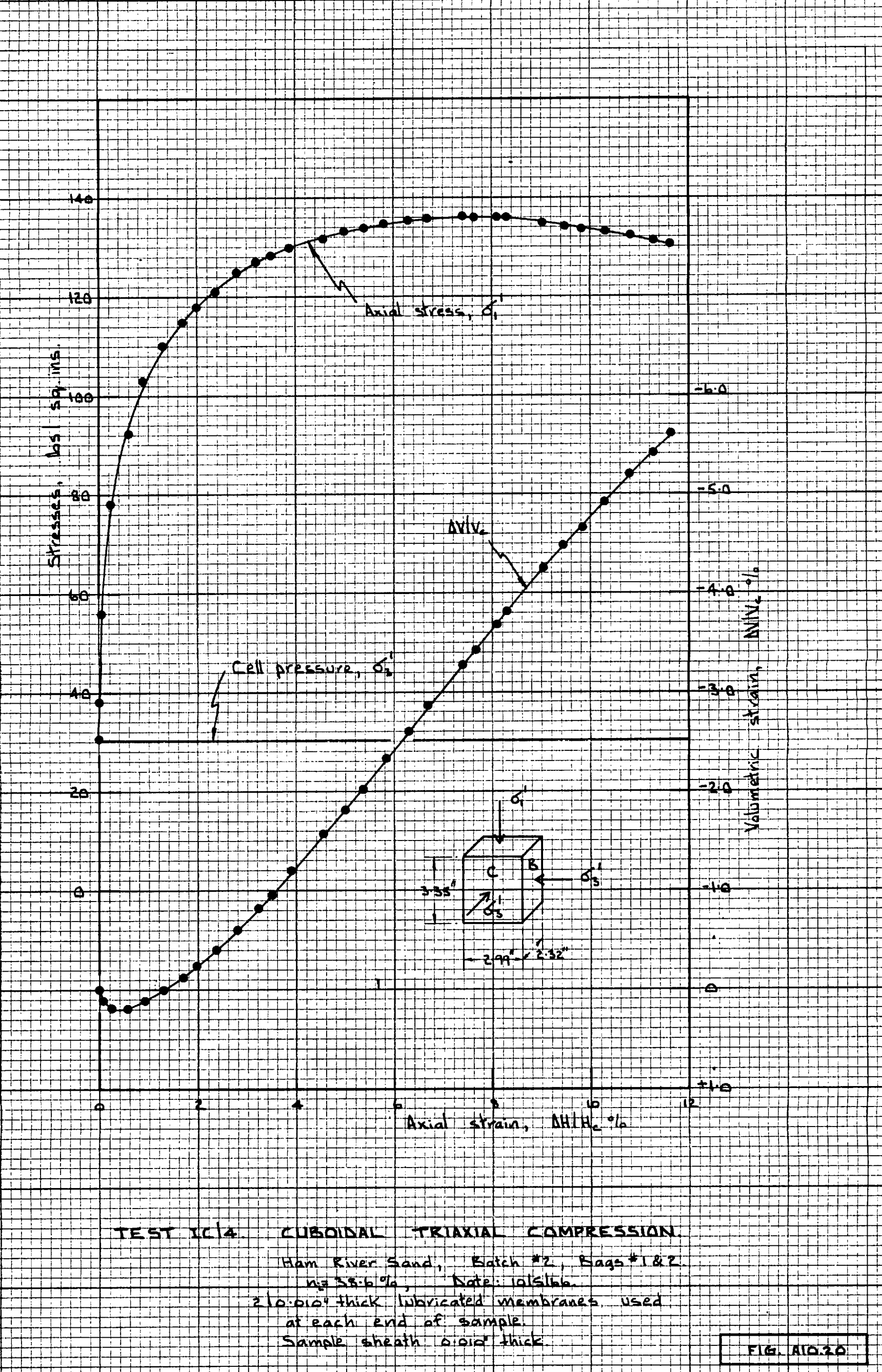




TEST IC/5. CUBOIDAL TRIAXIAL COMPRESSION.

Ham River Sand, Batch #2, Bags #1 & 2.
n_i = 38.9%, Date: 8/5/66.
2 to 0.010" thick lubricated membranes used at each end of sample.
Sample sheath 0.010" thick.

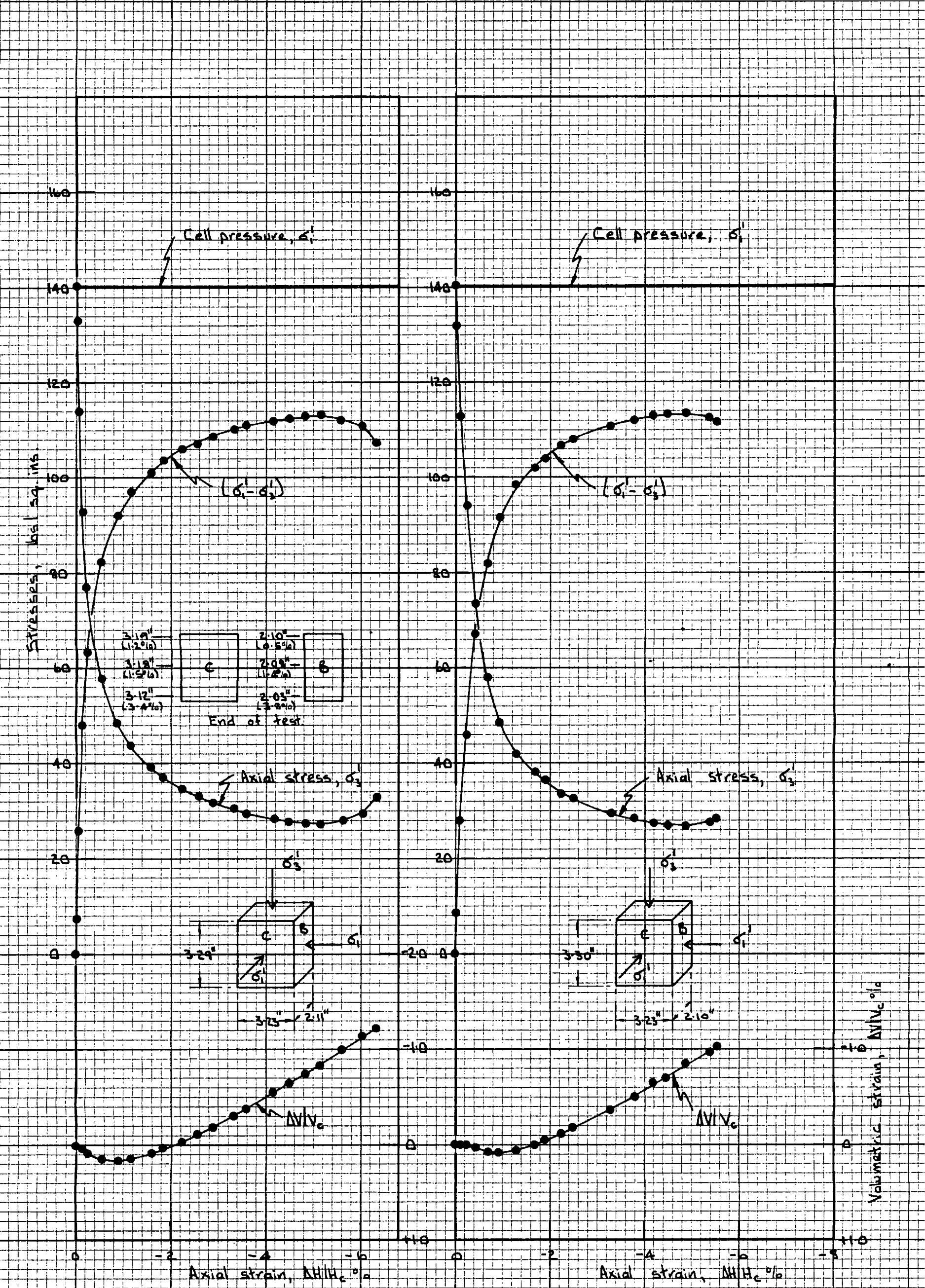
FIG. A10.19



TEST IC/4. CUBOIDAL TRIAXIAL COMPRESSION.

Ham River Sand, Batch #2, Bags #1 & 2.
n_i = 38.6 %, Date: 10/5/66.
2 10.010" thick lubricated membranes used at each end of sample.
Sample sheath 0.010" thick.

FIG. A10.20



TEST ICE 12.

CUBOIDAL TRIAXIAL EXTENSION.

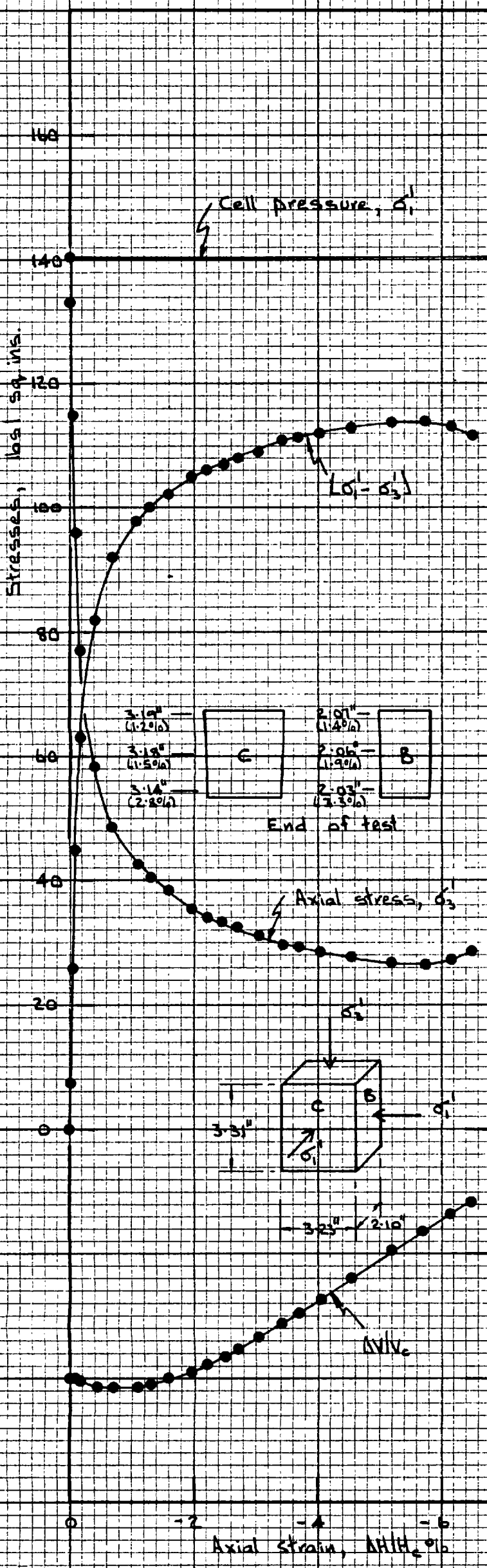
Ham River Sand, Batch*2, Bags*1&2.
n_i = 39·1%, Date: 22/5/66.
2 to 0·010" thick lubricated membranes used at each end of sample.
Sample sheath 0·010" thick.

TEST ICE 14.

CUBOIDAL TRIAXIAL EXTENSION.

Ham River Sand, Batch*2, Bags*1&2.
n_i = 39·1%, Date: 26/5/66.
3 to 0·010" thick lubricated membranes used at each end of sample.
Sample sheath 0·012" thick.

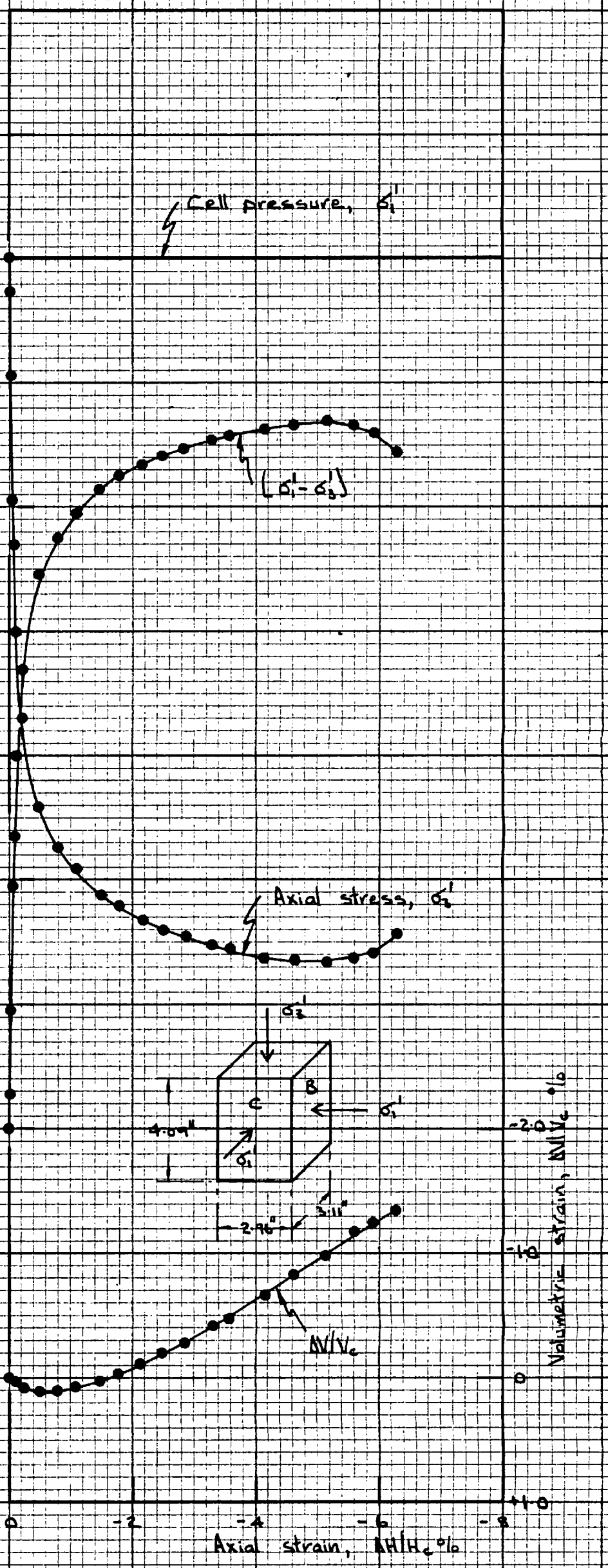
FIG. A10.21



TEST ICE15.

CUBOIDAL TRIAXIAL EXTENSION.

Ham River Sand, Batch #2, Bags #1&2.
n_i = 39·2 %, Date: 3/6/66.
2/0·010" thick lubricated membranes used at each end of sample.
Sample sheath 0·012" thick.

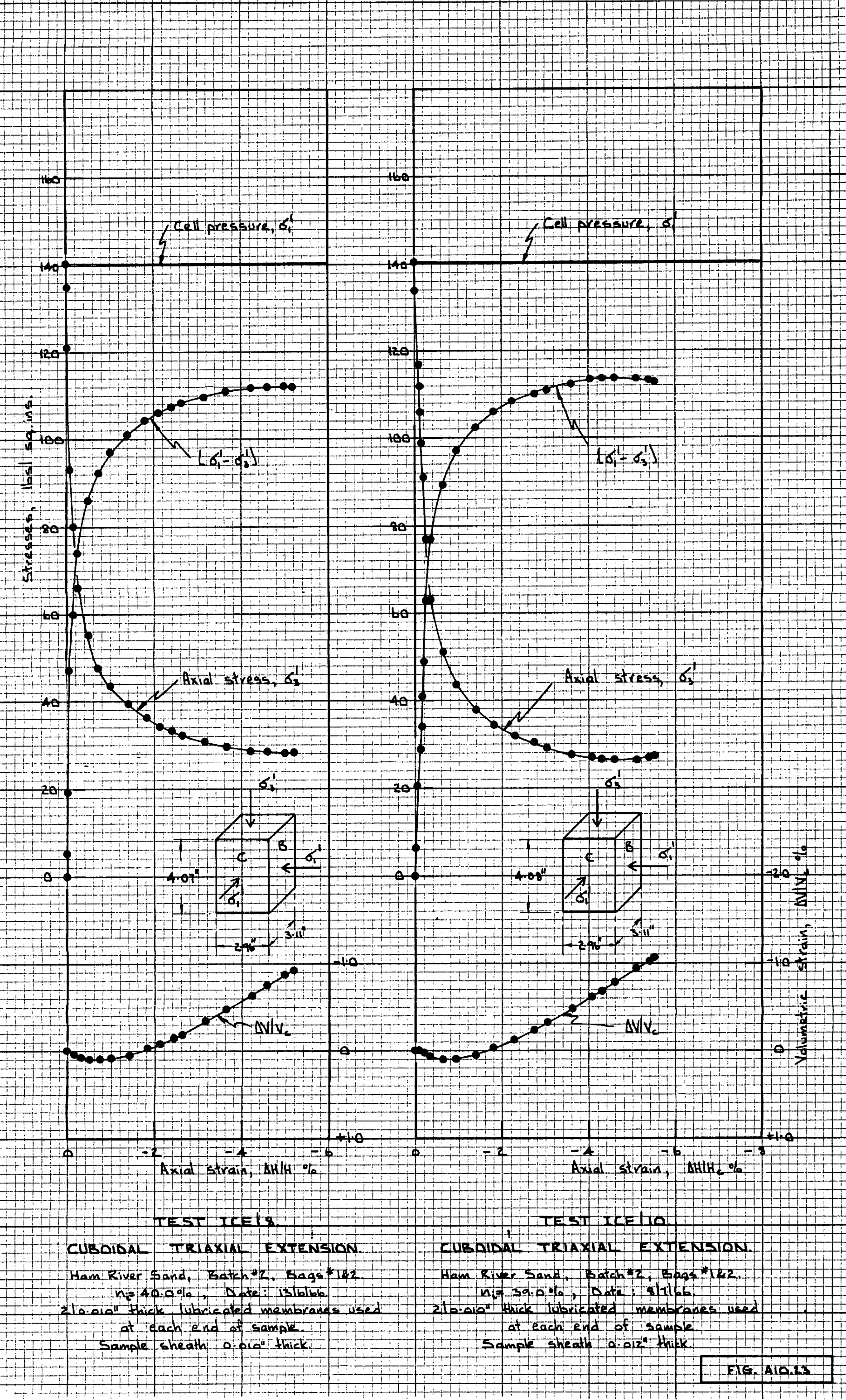


TEST ICE17.

CUBOIDAL TRIAXIAL EXTENSION.

Ham River Sand, Batch #2, Bags #1&2.
n_i = 39·2 %, Date: 3/6/66.
2/0·010" thick lubricated membranes used at each end of sample.
Sample sheath 0·010" thick.

FIG. A10.22



TEST ICE 18.

CUBOIDAL TRIAXIAL EXTENSION.

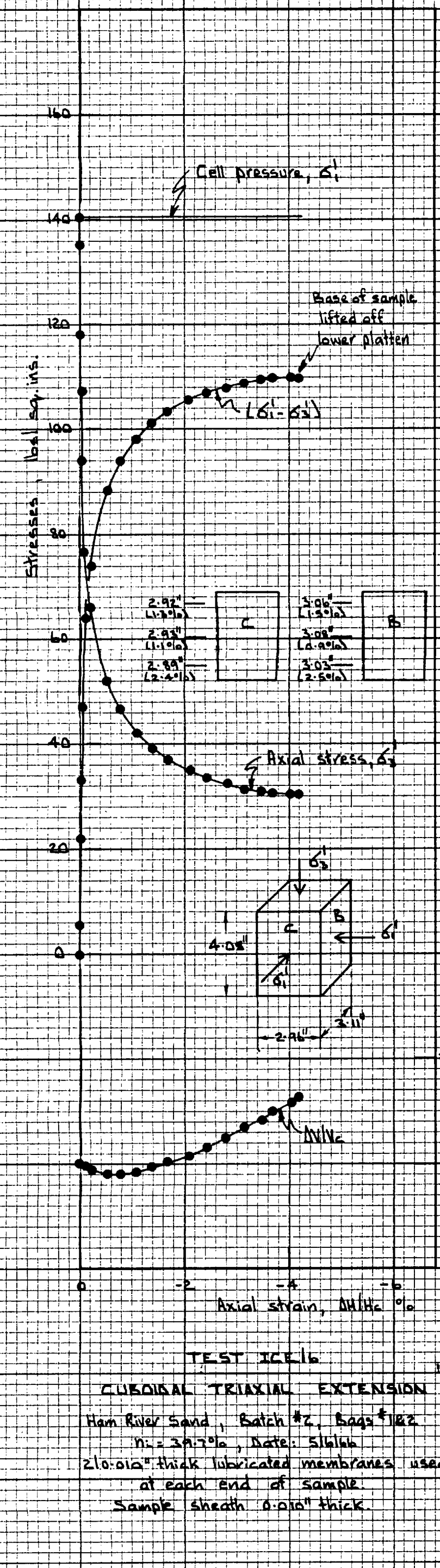
Ham River Sand, Batch #2, Bags #1&2.
n_i = 40.0%, Date: 13/6/66.
2 lo·010" thick lubricated membranes used at each end of sample.
Sample sheath 0·010" thick.

TEST ICE 10.

CUBOIDAL TRIAXIAL EXTENSION.

Ham River Sand, Batch #2, Bags #1&2.
n_i = 39.0%, Date: 9/7/66.
2 lo·010" thick lubricated membranes used at each end of sample.
Sample sheath 0·012" thick.

FIG. A10.13



TEST ICE16

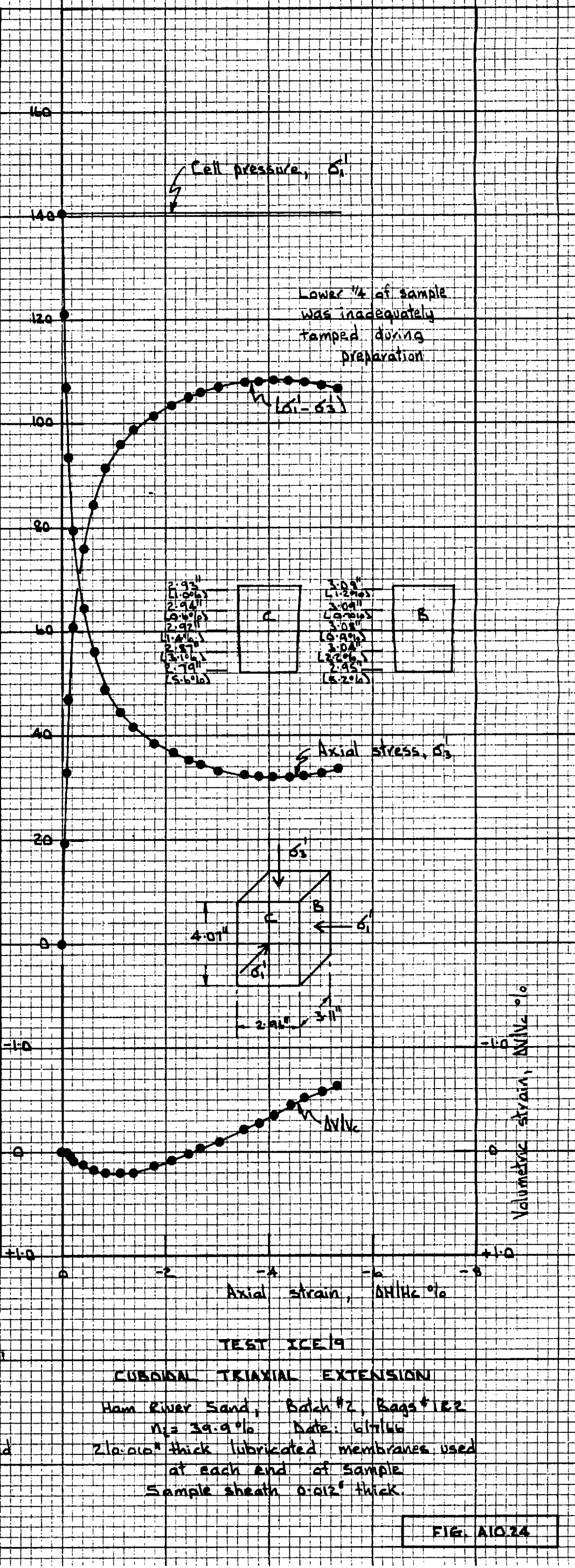
CUBOIDAL TRIAXIAL EXTENSION

Ham River Sand, Batch #2, Bags #1&2

n_i = 39.7%, Date: 5/16/66

2 lo·010" thick lubricated membranes used at each end of sample.

Sample sheath 0·010" thick.



TEST ICE19

CUBOIDAL TRIAXIAL EXTENSION

Ham River Sand, Batch #2, Bags #1&2

n_i = 39.9%, Date: 6/7/66

2 lo·010" thick lubricated membranes used at each end of sample.

Sample sheath 0·012" thick.

FIG. A10.24

Appendix A 11

Graphical presentation of independent stress control test results.

Axial stress, σ_1'

I.S.C. belt stress, σ_2'

Cell pressure, σ_3'

End of test

$\Delta V/V_c$

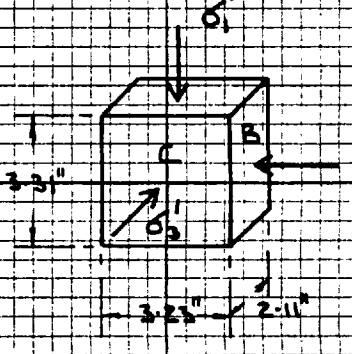
$\Delta B/B_c$

Stresses, lbs/sq.ins.

I.S.C. belt strain, $\Delta B/B_c$ %

Volumetric strain, $\Delta V/V_c$ %

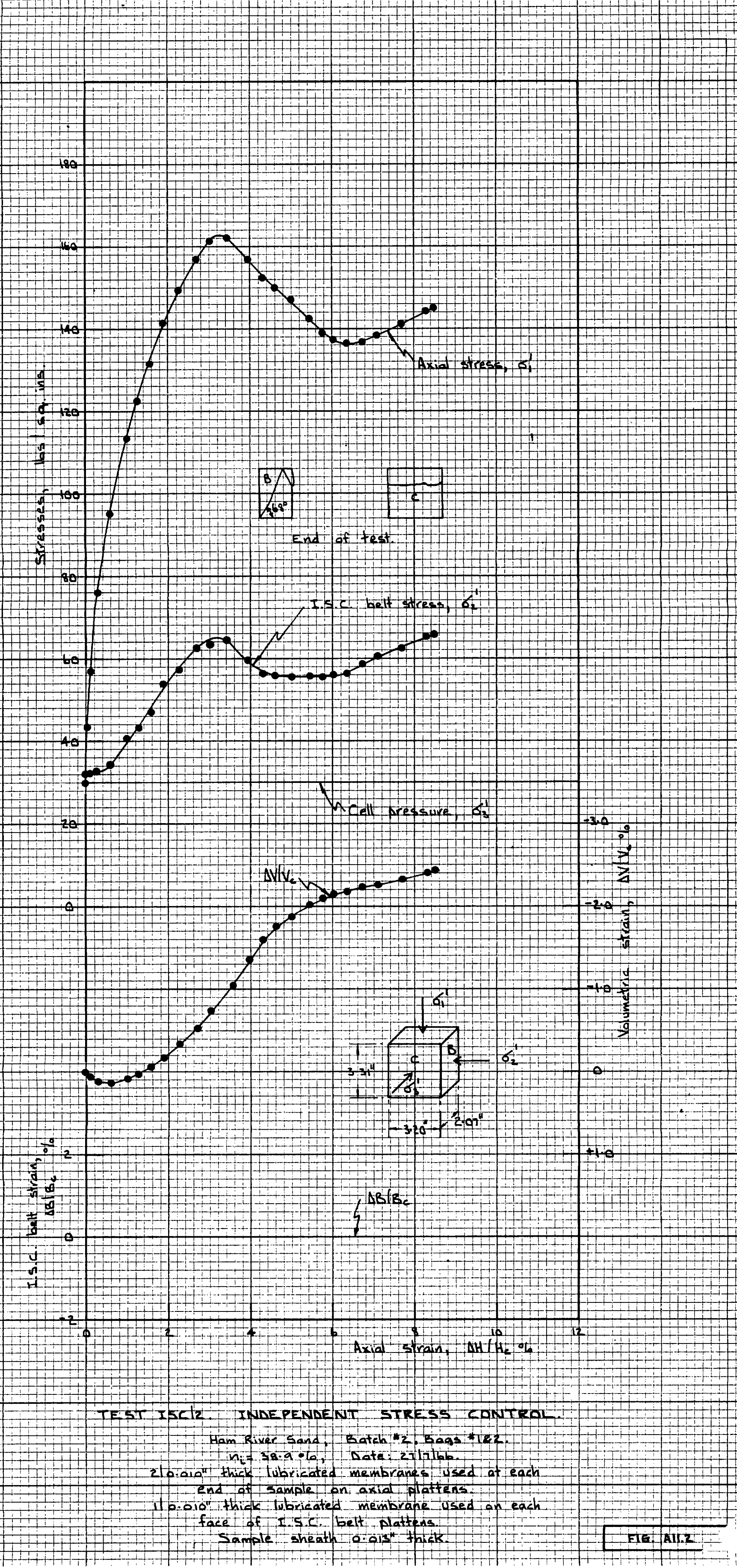
Axial strain, $\Delta H/H_c$ %



TEST ISC11 INDEPENDENT STRESS CONTROL.

Ham River Sand, Batch #2, Bags #1&2.
n_i = 39·0 %, Date: 18/7/66.
2 lo·olo" thick lubricated membranes used at each end of sample on axial platterns.
11 lo·olo" thick lubricated membrane used on each face of I.S.C. belt platterns.
Sample sheath o·o15" thick.

FIG. AII.1



TEST ISC12. INDEPENDENT STRESS CONTROL.

Ham River Sand, Batch #2, Bags #1&2.
n_i = 38·9 %, Date: 27/7/66.
2 @ 0·010" thick lubricated membranes used at each end of sample on axial platens.
1 @ 0·010" thick lubricated membrane used on each face of I.S.C. belt platens.
Sample sheath 0·013" thick.

FIG. A11.2

Stresses, lbs/sq.ins.

180
160
140
120
100
80
60
40

Axial stress, σ_1'

I.S.C. belt stress, σ_2'

Cell pressure, σ_3'

20
0
-2
-4

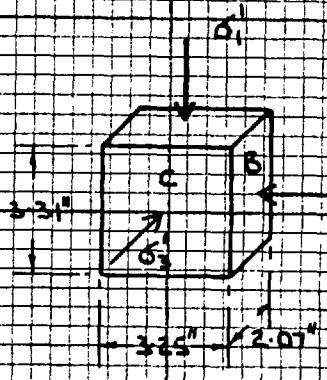
$\Delta V/V_c$

$\Delta B/B_c$

I.S.C. belt strain, $\Delta B/B_c$ %

-3.0
-2.0
-1.0
0
+1.0
+1.0

Volumetric strain, $\Delta V/V_c$ %



0 2 4 6 8 10 12

Axial strain, $\Delta H/H_c$ %

TEST ISC13 INDEPENDENT STRESS CONTROL

Ham River Sand, Batch #2, Bags #1&2
n_i = 39.1%, Date: 29/7/66.
2 lo·010" thick lubricated membranes used at each end of sample on axial plattens.
1 lo·010" thick lubricated membrane used on each face of I.S.C. belt plattens.
Sample sheath 0·013" thick.

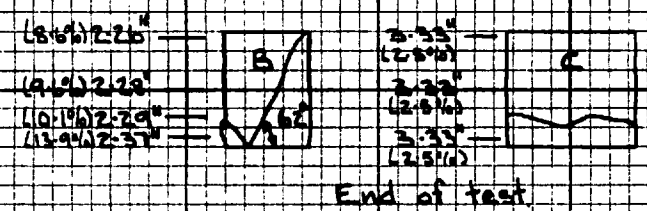
FIG. A11.3

Stresses, lbs/sq. ins.

180
160
140
120
100
80
60
40
20

I.S.C. belt stress, σ_3'

Cell pressure, σ_3'

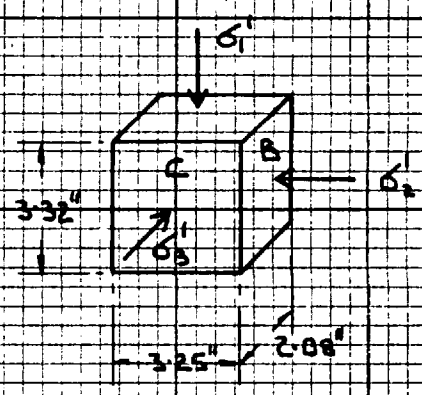


End of test

Volumetric strain, $\Delta V/V_c$ %

-4·0
-3·0
-2·0
-1·0
0
+1·0

$\Delta V/V_c$



I.S.C. belt strain, $\Delta B/B_c$ %

0
2
4

$\Delta B/B_c$

0 2 4 6 8 10 12

Axial strain, $\Delta H/H_c$ %

TEST ISC14. INDEPENDENT STRESS CONTROL.

Ham River Sand, Batch #2, Bags #1&2.
n_i = 39·6%, Date: 11/9/66.
2 @ 0·010" thick lubricated membranes used at each end of sample on axial platens.
11 @ 0·010" thick lubricated membrane used on each face of I.S.C. belt platens.
Sample sheath 0·013" thick.

FIG. AII.4

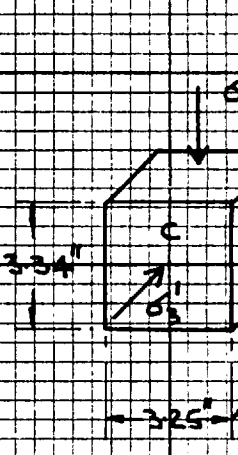
Axial stress, σ_1'

I.S.C. belt stress, σ_2'

Cell pressure, σ_3'

$\Delta V/V_c$

$\Delta B/B_c$



Stresses, lbs / sq. ins.

I.S.C. belt strain, $\Delta B/B_c$ %

Volumetric strain, $\Delta V/V_c$ %

Axial strain, $\Delta H/H_c$ %

TEST IS.C.15. INDEPENDENT STRESS CONTROL.

Ham River Sand, Batch #2, Bags #1&2.
n_i = 39.2 %, Date: 31/8/66.
2 @ 0.010" thick lubricated membranes used at each end of sample on axial plattens.
11 @ 0.010" thick lubricated membrane used on each face of I.S.C. belt plattens.
Sample sheath 0.013" thick.

FIG. A11.5

Axial stress, σ_1'

I.S.C. belt stress, σ_2'

Cell pressure, σ_3'

$\Delta V/V_c$

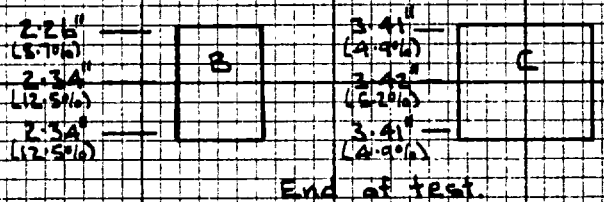
$\Delta B/B_c$

Stresses, lbs/sq. ins.

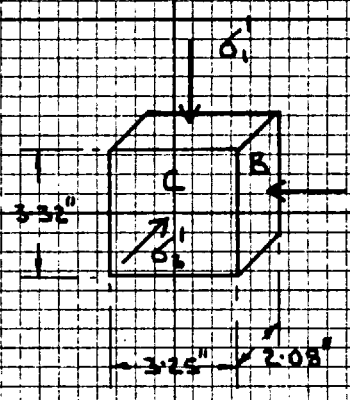
I.S.C. belt strain, $\Delta B/B_c$ %

Volumetric strain, $\Delta V/V_c$ %

Axial strain, $\Delta H/H_c$ %



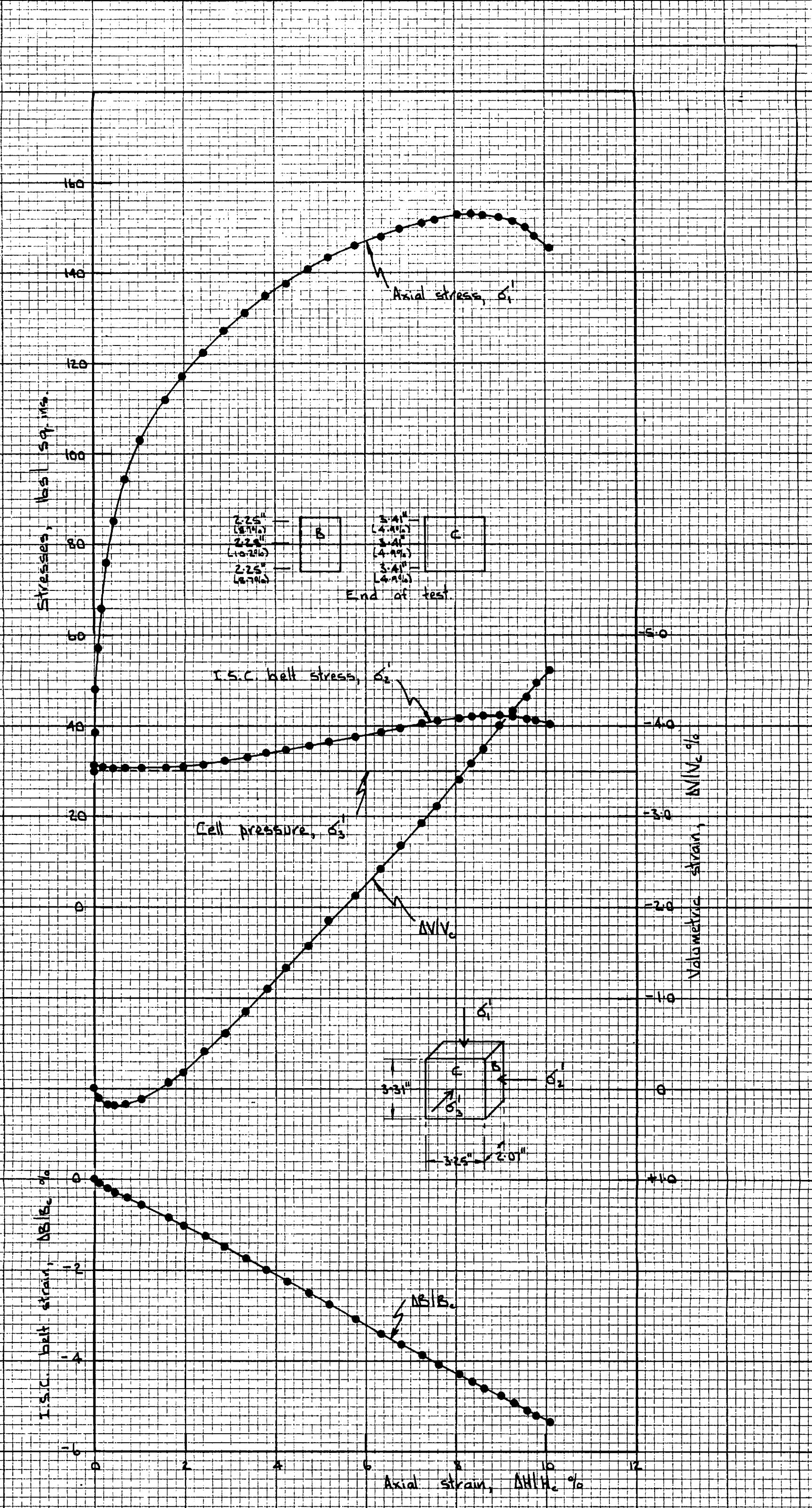
End of test.



TEST I5C16. INDEPENDENT STRESS CONTROL.

Ham River Sand, Batch #2, Bags #1&2.
n_i = 38·7%, Date: 5/9/66.
2/0·010" thick lubricated membranes used at each end of sample on axial plattens.
1/0·010" thick lubricated membrane used on each face of I.S.C. belt plattens.
Sample sheath 0·013" thick.

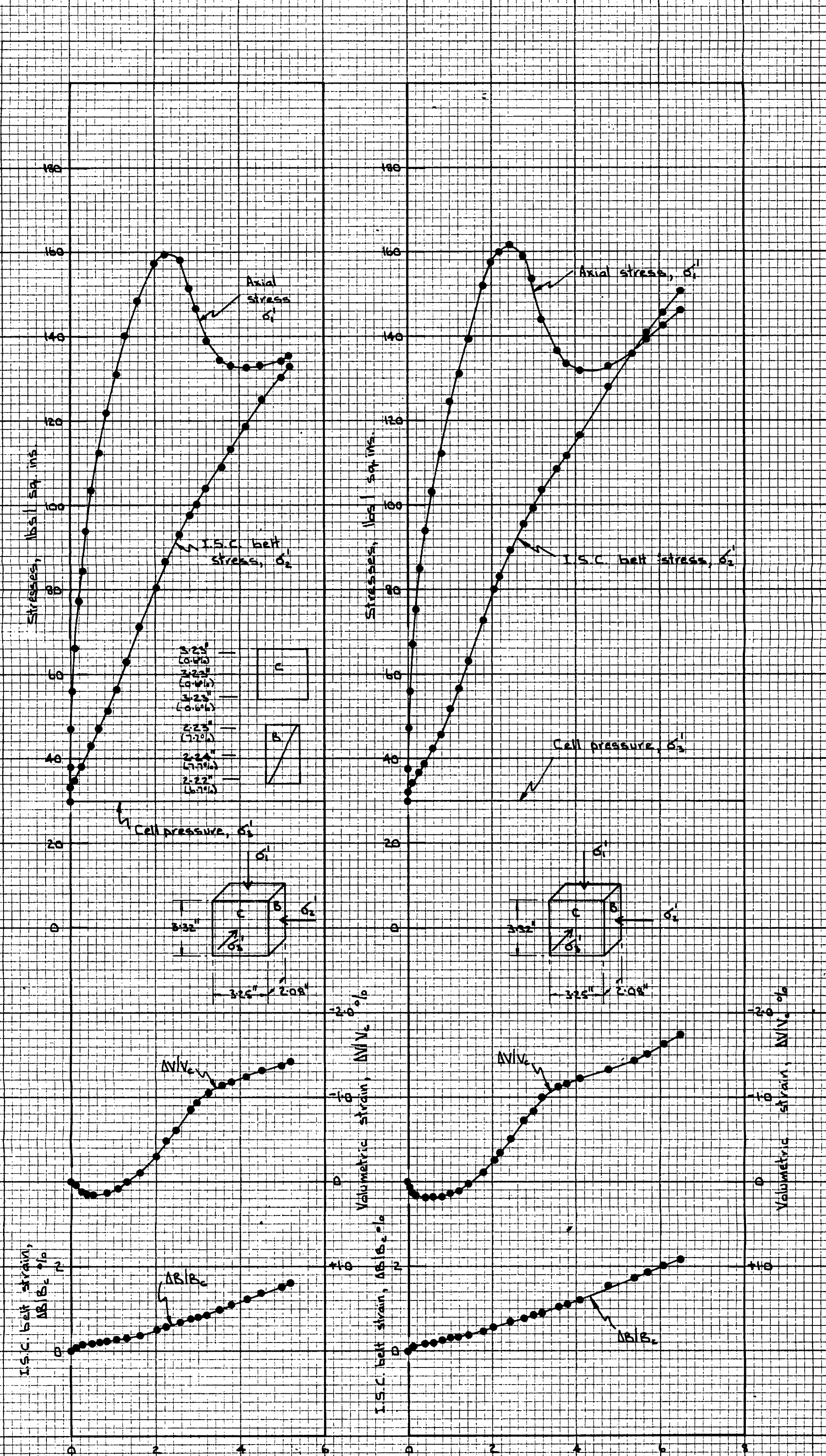
FIG. A11.6



TEST ISC17. INDEPENDENT STRESS CONTROL.

Ham River Sand, Batch #2, Bags #182.
n_i = 38·8%, Date: 2/10/66.
2 | 0·010" thick lubricated membranes used at each end of sample on axial platens.
1 | 0·010" thick lubricated membrane used on each face of I.S.C. belt platens.
Sample sheath 0·013" thick.

FIG. A11.7



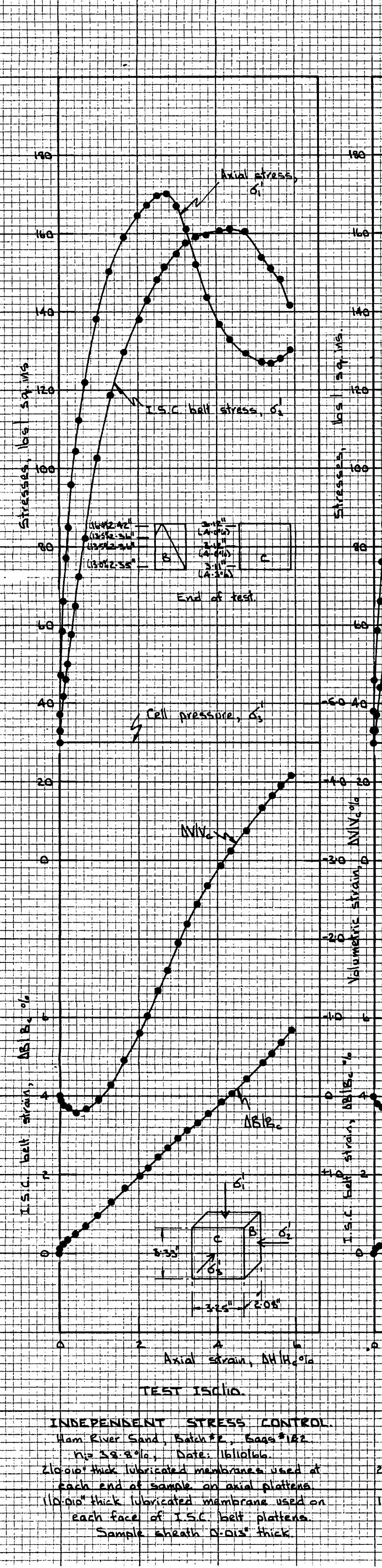
TEST ISC/8

INDEPENDENT STRESS CONTROL.
Ham River Sand, Batch*2, Bags*1&2.
n_i = 39·1%, Date: 9/10/66.
2 lo·010" thick lubricated membranes used at each end of sample on axial plattens.
1 lo·010" thick lubricated membrane used on each face of I.S.C. belt plattens.
Sample sheath 0·013" thick.

TEST ISC/9.

INDEPENDENT STRESS CONTROL.
Ham River Sand, Batch*2, Bags*1&2.
n_i = 38·7%, Date: 12/10/66.
2 lo·010" thick lubricated membranes used at each end of sample on axial plattens.
1 lo·010" thick lubricated membrane used on each face of I.S.C. belt plattens.
Sample sheath 0·013" thick.

FIG. AII. 8



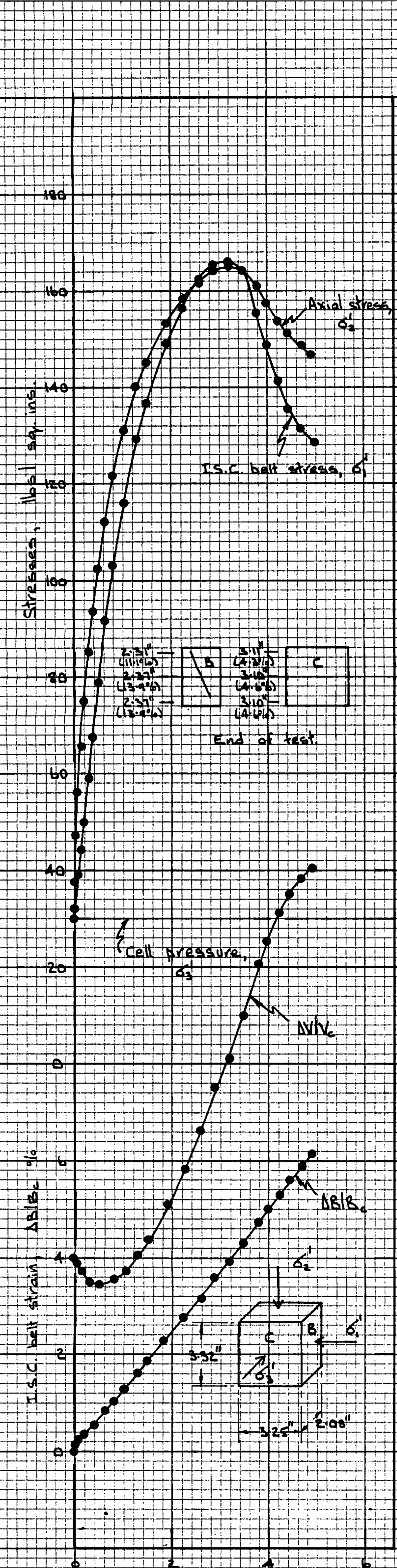
TEST ISC/10.

INDEPENDENT STRESS CONTROL.
Ham River Sand, Batch #2, Bags #1&2.
n_i = 38·8%, Date: 16/10/66.
2 @ 0·010" thick lubricated membranes used at each end of sample on axial platterns.
1 @ 0·010" thick lubricated membrane used on each face of I.S.C. belt platterns.
Sample sheath 0·013" thick.

TEST ISC/11.

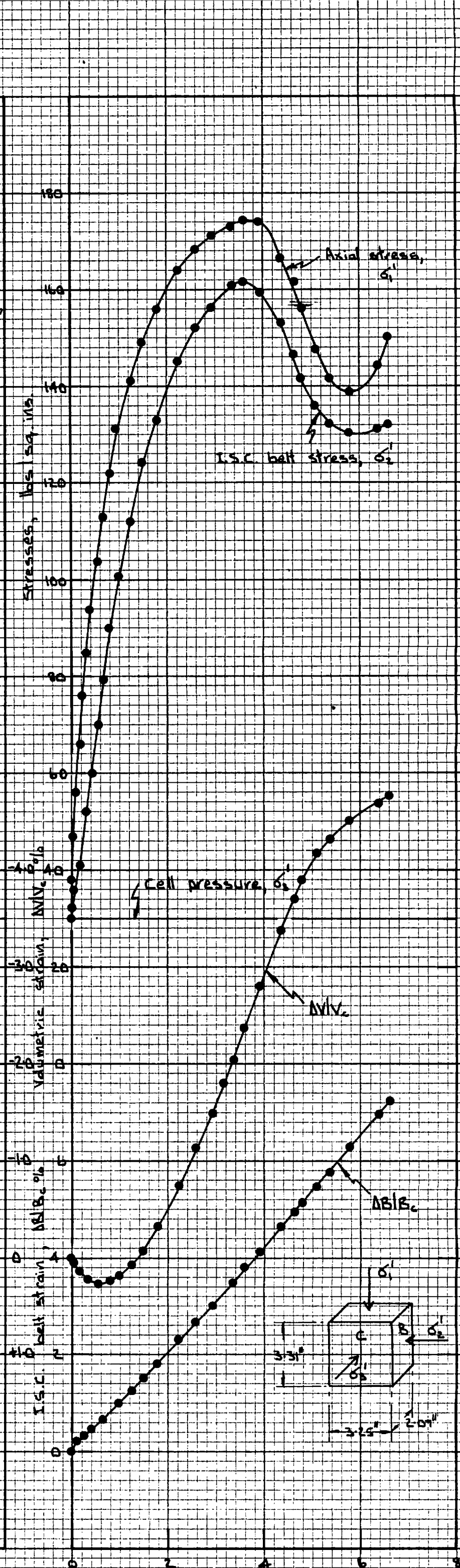
INDEPENDENT STRESS CONTROL.
Ham River Sand, Batch #2, Bags #1&2.
n_i = 38·7%, Date: 19/10/66.
2 @ 0·010" thick lubricated membranes used at each end of sample on axial platterns.
1 @ 0·010" thick lubricated membrane used on each face of I.S.C. belt platterns.
Sample sheath 0·013" thick.

FIG. A11.9



TEST ISC/15.

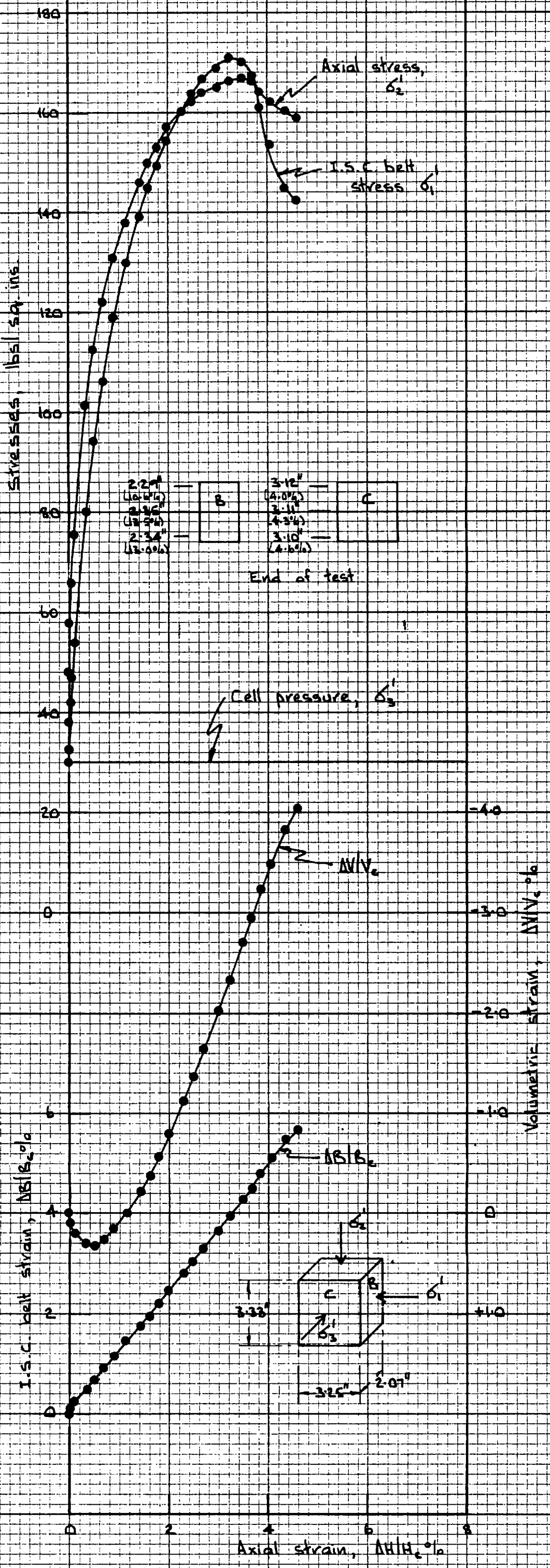
INDEPENDENT STRESS CONTROL.
Ham River Sand, Batch #2, Bags #1&2.
n_i = 39·8%, Date: 2/11/66.
2 lo·oio" thick lubricated membranes used at each end of sample on axial platens.
11 lo·oio" thick lubricated membrane used on each face of I.S.C. belt platens.
Sample sheath 0·013" thick.



TEST ISC/12.

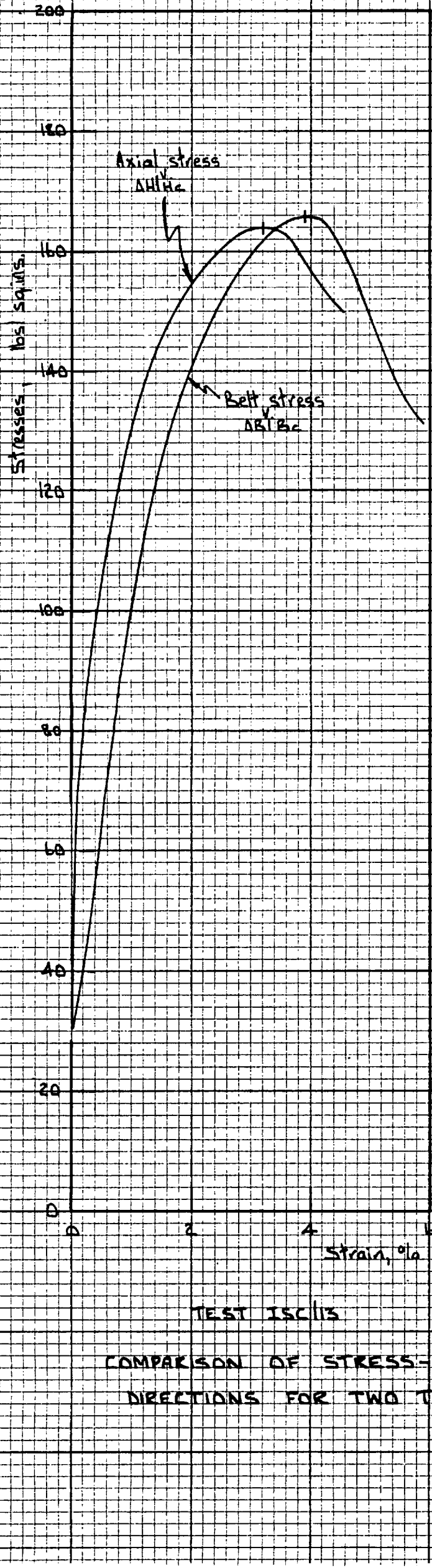
INDEPENDENT STRESS CONTROL.
Ham River Sand, Batch #2, Bags #1&2.
n_i = 39·0%, Date: 27/10/66.
2 lo·oio" thick lubricated membranes used at each end of sample on axial platens.
11 lo·oio" thick lubricated membrane used on each face of I.S.C. belt platens.
Sample sheath 0·013" thick.

FIG. AII.10

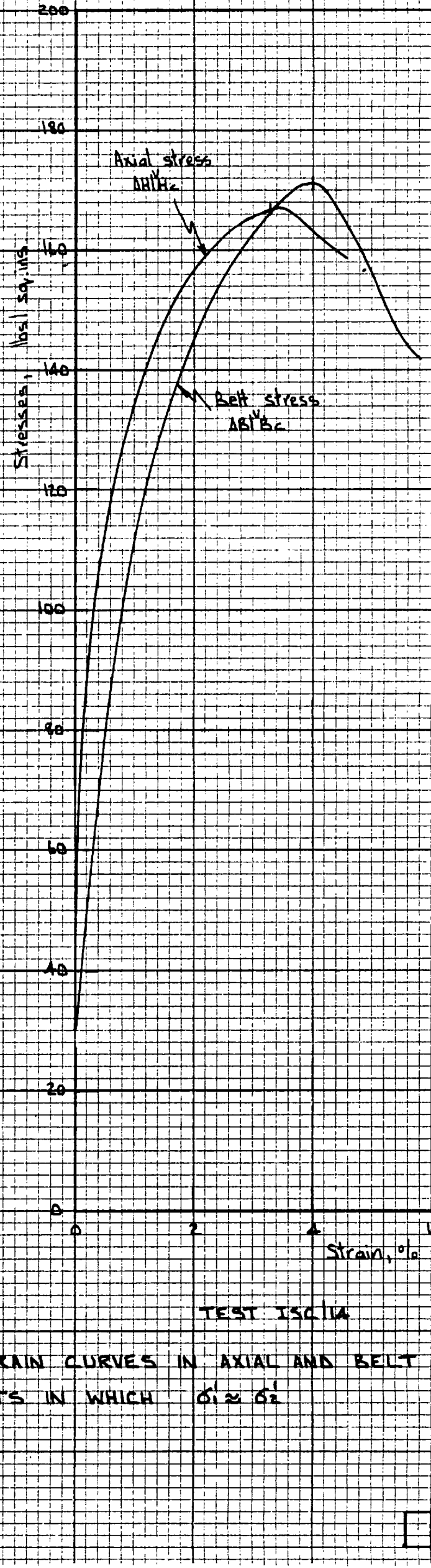


TEST ISC/14. INDEPENDENT STRESS CONTROL.
Ham River Sand, Batch #2, Bags #1&2.
n_i = 38.9%, Date: 9/11/66.
2/0.010" thick lubricated membranes used at each end of sample on axial platens.
11/0.010" thick lubricated membrane used on each face of I.S.C. belt platens.
Sample sheath 0.013" thick.

FIG. A11.11



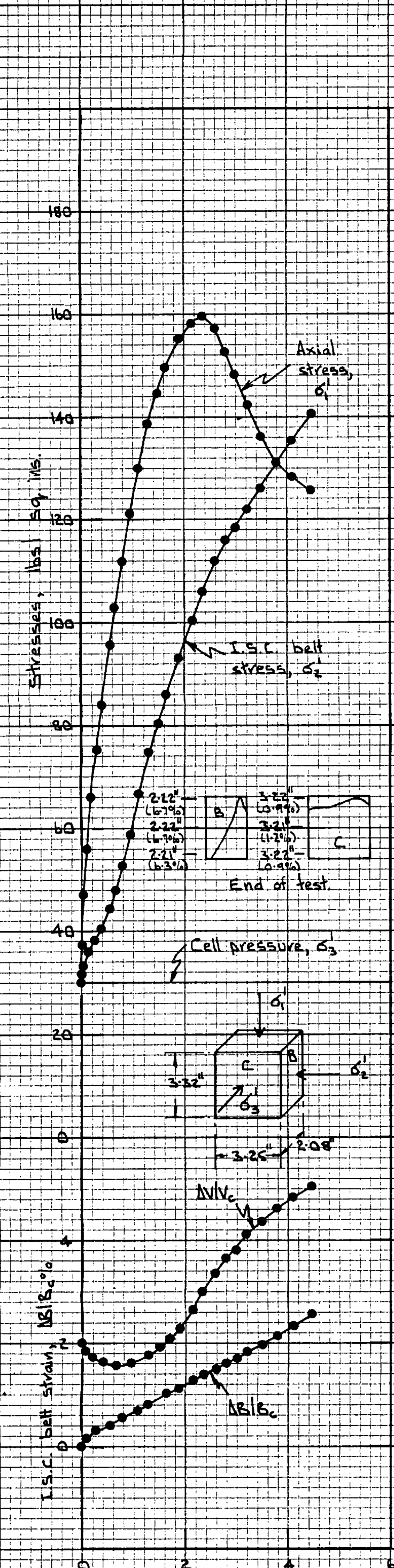
TEST ISC113



TEST ISC114

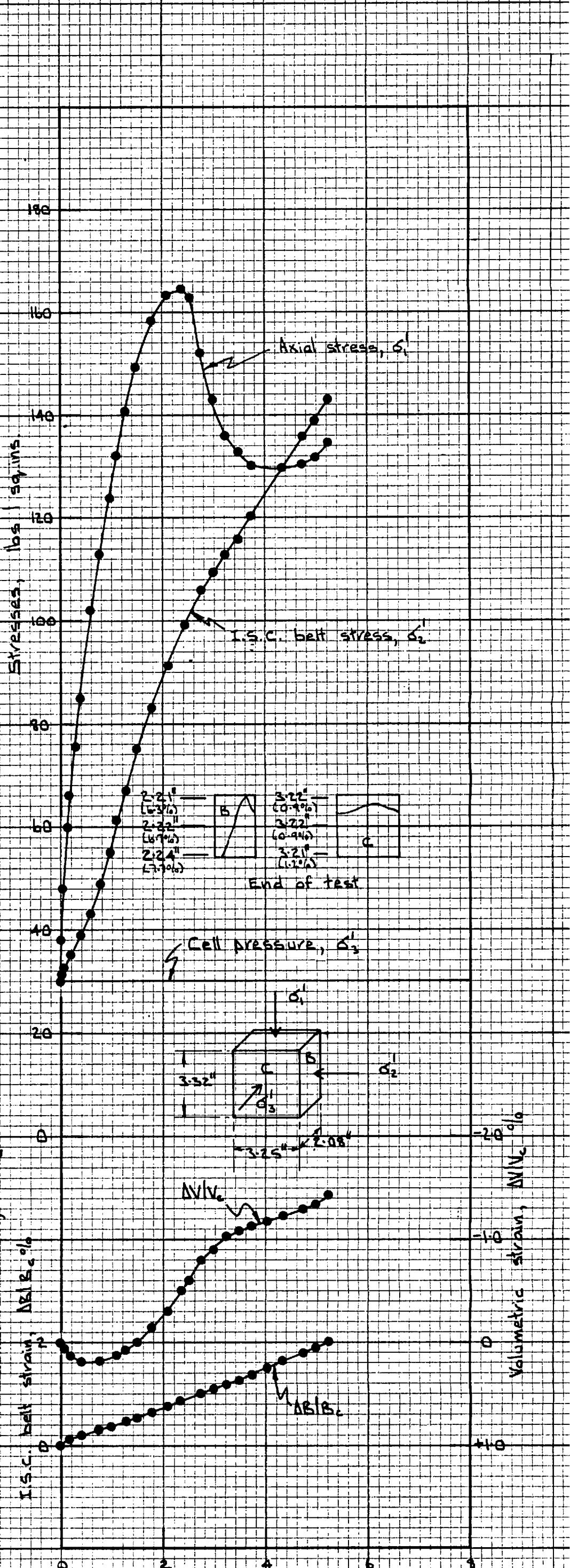
COMPARISON OF STRESS-STRAIN CURVES IN AXIAL AND BELT DIRECTIONS FOR TWO TESTS IN WHICH $\sigma_1' \approx \sigma_2'$

FIG. A11.12



TEST ISC115.

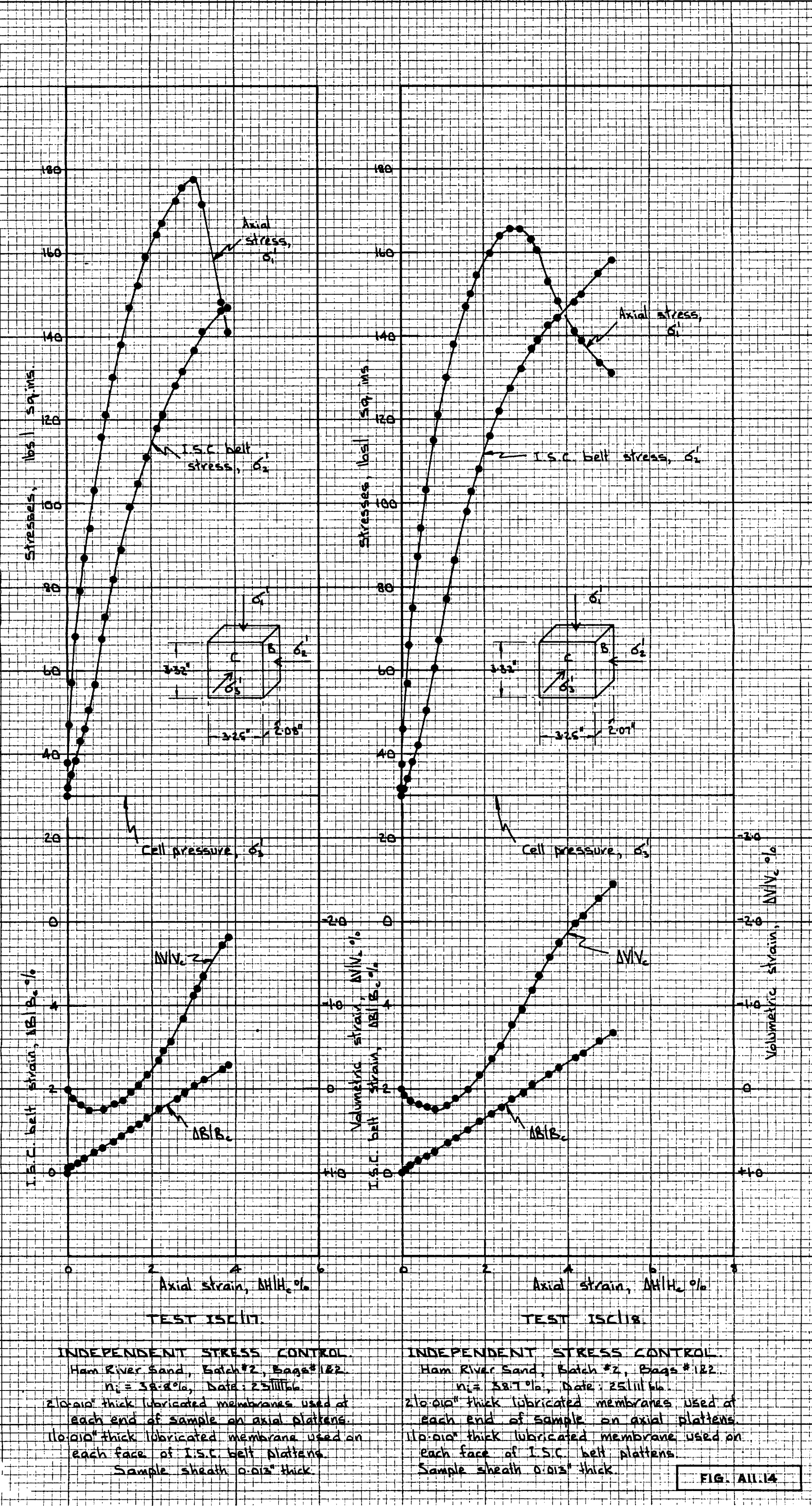
INDEPENDENT STRESS CONTROL.
Ham River Sand, Batch*2, Bags*1&2.
n_i = 39·1%, Date: 14/11/66.
2 @ 0·010" thick lubricated membranes used at each end of sample on axial platens.
1 @ 0·010" thick lubricated membrane used on each face of I.S.C. belt platens.
Sample sheath 0·013" thick.



TEST ISC116.

INDEPENDENT STRESS CONTROL.
Ham River Sand, Batch*2, Bags*1&2.
n_i = 39·0%, Date: 19/11/66.
2 @ 0·010" thick lubricated membranes used at each end of sample on axial platens.
1 @ 0·010" thick lubricated membrane used on each face of I.S.C. belt platens.
Sample sheath 0·013" thick.

FIG. A11.13



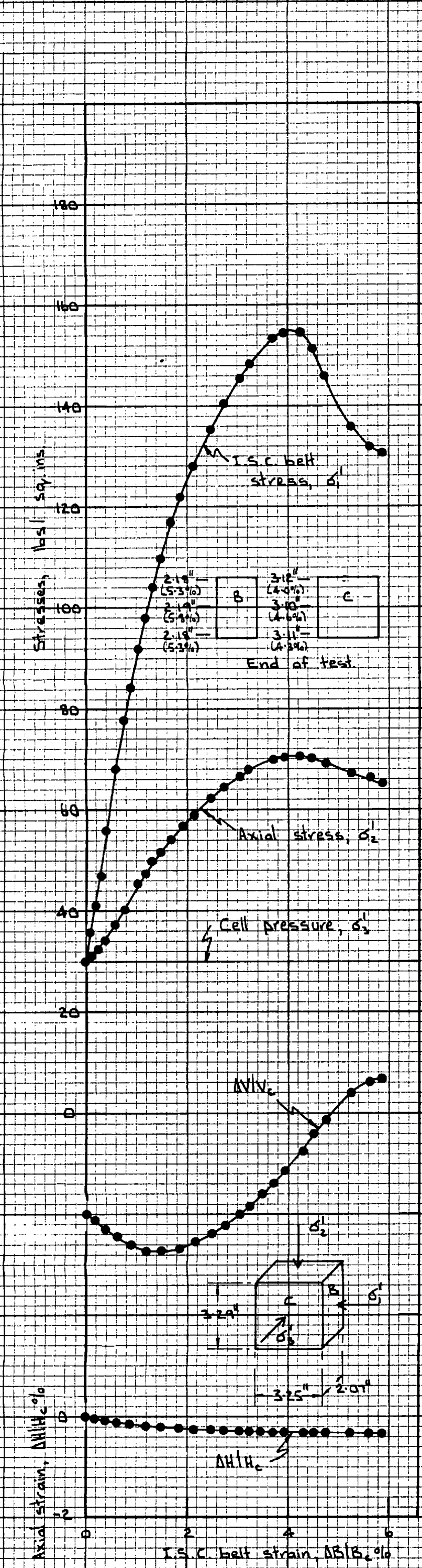
TEST ISC/17.

INDEPENDENT STRESS CONTROL.
Ham River Sand, Batch #2, Bags # 1&2.
n_i = 38·8%, Date: 23/III/66.
2/0·010" thick lubricated membranes used at each end of sample on axial platens.
1/0·010" thick lubricated membrane used on each face of I.S.C. belt platens.
Sample sheath 0·013" thick.

TEST ISC/18.

INDEPENDENT STRESS CONTROL.
Ham River Sand, Batch #2, Bags # 1&2.
n_i = 38·7%, Date: 25/III/66.
2/0·010" thick lubricated membranes used at each end of sample on axial platens.
1/0·010" thick lubricated membrane used on each face of I.S.C. belt platens.
Sample sheath 0·013" thick.

FIG. AII.14



TEST ISC/19.

INDEPENDENT STRESS CONTROL.

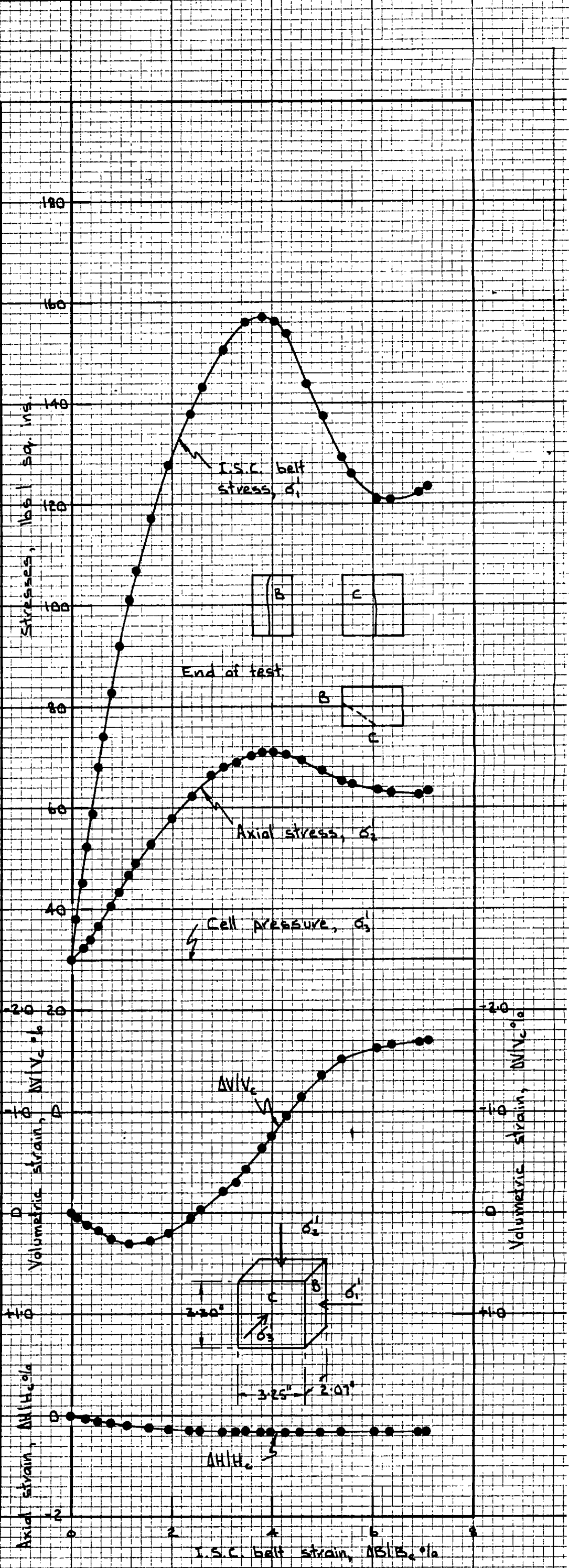
Ham River Sand, Batch #2, Bags #1&2.

n_i = 39·1%, Date: 28/11/66.

2/0·010" thick lubricated membranes used at each end of sample on axial platens.

1/0·010" thick lubricated membrane used on each face of I.S.C. belt platens.

Sample sheath 0·013" thick.



TEST ISC/20.

INDEPENDENT STRESS CONTROL.

Ham River Sand, Batch #2, Bags #1&2.

n_i = 38·6%, Date: 1/12/66.

2/0·010" thick lubricated membranes used at each end of sample on axial platens.

1/0·010" thick lubricated membrane used on each face of I.S.C. belt platens.

Sample sheath 0·013" thick.

FIG. A11.15

Axial stress, σ_1'

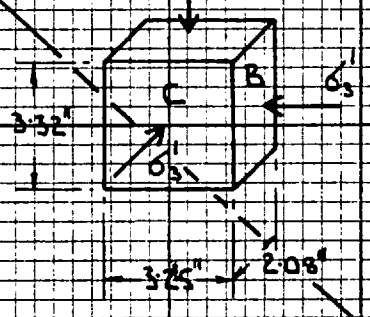
Cell pressure, σ_3'

$\Delta B/B_c = \Delta C/C_c$

$\Delta V/V_c$

B		C	
(5.8%) 2.20"		(6.9%) 3.47"	
(8.7%) 2.26"		(7.1%) 3.48"	
(8.7%) 2.26"		(8.3%) 3.52"	
(7.0%) 2.24"		(9.7%) 3.55"	

End of test



Stresses, lbs/sq ins.

Mean lateral strain, $\Delta B/B_c = \Delta C/C_c$ %

Volumetric strain, $\Delta V/V_c = \varepsilon_a$

Axial strain, $\Delta H/H_c$ %

TEST IC15. CUBOIDAL TRIAXIAL COMPRESSION.

Ham River Sand, Batch #2, Bags #1&2.
n_i = 38.4 %, Date: 31/2/66.
2 | 0.010" thick lubricated membranes used at each end of sample.
Sample sheath 0.015" thick.

FIG. A11.16

Stresses, lbs/sq.ins.

Axial stress, σ_1'

Cell pressure, σ_2'

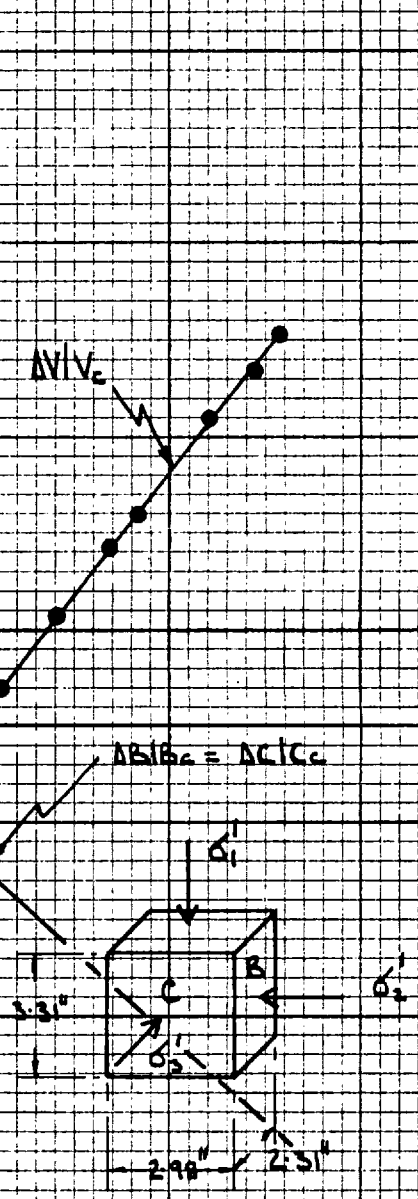
$\Delta V/V_c$

$\Delta B/B_c = \Delta C/C_c$

Mean lateral strain, $\Delta B/B_c = \Delta C/C_c$ %

Volumetric strain, $\Delta V/V_c$ %

Axial strain, $\Delta H/H_c$ %



TEST IC16 CUBOIDAL TRIAXIAL COMPRESSION.

Ham River Sand, Batch #2, Bags # 1&2.
n_i = 38·8 %, Date: 5/12/66.
2 [0·010" thick lubricated membranes used at each end of sample.
Sample sheath 0·013" thick.

FIG. A11.17